EXCITED STATE ACIDITY PROMOTED PHOTONITROSATION: SYNTHETIC AND MECHANISTIC STUDIES

by

Zhengzhi Wu

B.Sc. University of Science and Technology of China, 1968

M.Sc. Shanghai Institute of Organic Chemistry,

Academia Sinica, Shanghai China, 1981

A THESIS SUBMITTED IN PARTIAL FULFILLMENT OF

THE REQUIREMENTS FOR THE DEGREE OF

DOCTOR OF PHILOSOPHY

in the Department

of

Chemistry

Simon Fraser University

November 1986

APPROVAL

Name: Zhengzhi Wu

Degree: Doctor of Philosophy

Title of Thesis: **Excited State Acidity Promoted Photonitrosation: Synthetic and Mechanistic Studies**

Examining Committee: Chairman: Dr. F.W.B. Einstein

Dr. Y.L. Chow
Senior Supervisor

Dr. K.N. Slessor
Supervisory Committee

Dr. P.W. Percival
Supervisory Committee

Dr. M.L.W. Thewalt
Internal Examiner

Dr. R. Stewart
External Examiner
Department of Chemistry
University of British Columbia

Date Approved: December 22, 1986

PARTIAL COPYRIGHT LICENSE

I hereby grant to Simon Fraser University the right to lend my thesis, project or extended essay (the title of which is shown below) to users of the Simon Fraser University Library, and to make partial or single copies only for such users or in response to a request from the library of any other university, or other educational institution, on its own behalf or for one of its users. I further agree that permission for multiple copying of this work for scholarly purposes may be granted by me or the Dean of Graduate Studies. It is understood that copying or publication of this work for financial gain shall not be allowed without my written permission.

Title of Thesis/Project/Extended Essay

Excited State Acidity Promoted Photonitrosation: Synthetic and Mechanistic Studies

Author: _____
(signature)

Zhengzhi Wu
(name)

January 5, 1987
(date)

ABSTRACT

In the presence of hydrochloric acid, singlet pyrene sensitizes photodecomposition of proton-associated N-nitrosodimethylamine (NND) under nitrogen. In the same acidic medium but under oxygen, NND photolytically adds to 1-arylpropenes regiospecifically to give *erythro*- and *threo*-*a*-amino nitrates which can be reduced to give *a*-amino alcohols, or which can undergo substitution reactions.

Photoexcitation of naphthols and anthrols in the presence of NND in **neutral media** induces a novel photonitrosation of these phenols to give quinone monooximes. The mechanism of photonitrosation of 1-naphthol (1-NpOH) with NND was investigated. Excitation of NND failed to induce the photonitrosation of 1-NpOH, indicating that the ground state of 1-NpOH (pK_a = 9.2) is not acidic enough to form proton-associated NND (H^+...NND). The similarity in quenching rate constants obtained from measurements of 1-NpOH fluorescence lifetimes (k_q = 7.6 x 10^9 $M^{-1}s^{-1}$) and from measurements of quantum yields of the photonitrosation (k_q = 6.8 x 10^9 $M^{-1}s^{-1}$) strongly supports the view that the nitrosation is initiated by the singlet excited state of 1-NpOH. The quenching rate constant determined from 1-NpOH fluorescence intensity (k_q = 11 x 10^9 $M^{-1}s^{-1}$) is larger than those quoted above. The discrepancy is attributed in part to the formation of a ground state complex of 1-NpOH with NND. Deuteration of 1-NpOH at the oxygen did not change k_q significantly. The lack of isotope effect suggests that singlet excited 1-NpOH and NND interact at the encounter- controlled rate via a hydrogen bonded exciplex. Proton-acceptors, such as triethylamine, water and N,N-dimethylformamide, quenched the nitrosation by competing for the proton from singlet excited 1-NpOH. The quenching results together

with the lack of photonitrosation of 1-methoxynaphthalene with NND suggest that within the exciplex, singlet excited 1-NpOH ($pK_a(S_1)$ = 0.5) transfers a proton to NND to give H^+...NND. An energy migration from singlet excited 1-NpO^- to H^+...NND causes the latter to decompose to dimethylaminium and nitric oxide radicals. Electron transfer from 1-NpO^- to dimethylaminium radical gives 1-NpO$^\cdot$ which combines with nitric oxide to provide 1,4-naphthoquinone-4-oxime. Proton transfer was found to be substantially retarded by donor-type hydrogen bonding solvents, e.g. methanol and ethanol. A ground state complex of 1-NpOH with NND was detected by means of UV-visible absorption spectroscopy and ^{1}H-NMR, and was shown to be photostable. The photonitrosation of 1-anthrol with NND exhibited a similar pattern.

Photophysical studies of NND revealed a $S_o \rightarrow T_1$ (n,π^*) electronic transition in methylcyclohexane at 456 nm(ϵ = 0.064 $M^{-1}cm^{-1}$) and phosphorescence around 490-650 nm. The lowest triplet and singlet excited state energies were determined to be E_T = 58-59 kcal/mol and E_S = 72-73 kcal/mol.

TO MY PARENTS

TO JUNSHI, BICHENG AND BIZHENG

ACKNOWLEDGEMENT

I would like to thank my supervisor, Dr. Y.L. Chow, for his continual encouragement and guidance during the course of this study. I also thank the members of my supervisory committee, Dr. K.N. Slessor and Dr. P.W. Percival, for their valuable advice.

Sincere thanks are also due to the following persons:

Dr. A.G. Sherwood and Dr. B.M. Pinto for their helpful discussions, especially, Dr. A.G. Sherwood for use of his computer.

Dr. M.L.W. Thewalt and Dr. T.W. Steiner (Department of Physics, SFU) for doing time-resolved fluorimetry.

Dr. G.B. Porter (Department of Chemistry, University of British Columbia) for the use of his laser system.

Dr. G.E. Buono-core, Dr. B. Marciniak, Mr. H. Li and other members of Dr. Chow's group for their cooperation, discussion and fellowship.

Mr. M. Cackette for his help with computing.

The generous financial support from Simon Fraser University, the Department of Chemistry, and Dr. Y.L. Chow is greatfully acknowledged.

This research work was performed during a leave of absence from Shanghai Institute of Organic Chemistry, Academia Sinica, China.

TABLE OF CONTENTS

LIST OF TABLES

LIST OF FIGURES

LIST OF ABBREVIATIONS

1-AnOH	1-anthrol
9-AnOH	9-anthrol
CHDE	cyclohexadiene
EPO	epoxyethylbenzene
GSC	ground state complex
MCH	methylcyclohexane
NND	N,N-dimethylnitrosoamine
1-NpOD	O-deutero-1-naphthol
1-NpOH	1-naphthol
2-NpOH	2-naphthol
1-NpOMe	1-methoxynaphthalene
QC	quadricyclene

CHAPTER 1

INTRODUCTION

1.1 N-Nitrosodimethylamine

Photochemistry of N-nitrosodimethylamine (NND), the simplest chemically stable dialkylnitrosamine, has been extensively investigated.[1-4] The ground state electronic configuration of NND was assessed by SCF calculation[5] to possess a 48% contribution of the polar resonance form **1a**. Such a resonance contribution has been substantiated by electron diffraction studies[6] of NND and X-ray studies[7] of its cupric chloride complex, revealing the coplanarity of the C_2N_2O moiety and the partial double bond character of the N-N bond (1.3440 Å)[7]. The latter gives rise to the magnetic nonequivalence of the two methyl signals in the ^{1}H-NMR spectrum at 3.0 (*cis* to the nitroso oxygen) and 3.8 ppm (*trans* to the nitroso oxygen),[8] respectively, and the activation energy[9,10] for free rotation at the N-N bond was determined to be 23.4 kcal/mol. The bond dissociation energy of the N-N bond in NND is 40.7 kcal/mol.[10] The extensive contribution of the polar form **1a** causes the high electron density at the nitroso oxygen atom leading to protonation at the oxygen at higher concentrations of sulfuric acid (>2M).[2,11] At lower concentrations of the acid (<2M), the association through hydrogen bonding is the primary mode of interaction as shown in **2**.[1,2,4] The pK_a of protonated NND[12] is about -1.8, close to those of amides, e.g. the pK_a of $PhCONH_3^+$ is -2.[13]

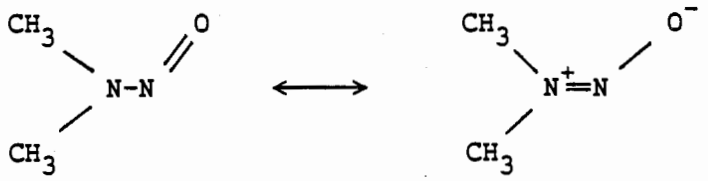

1 1a

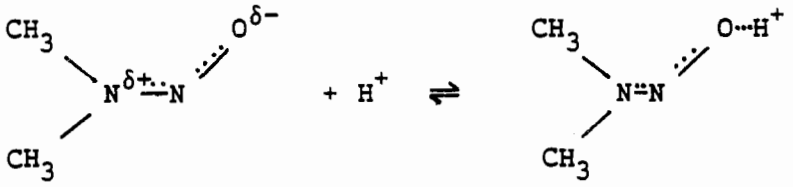

2

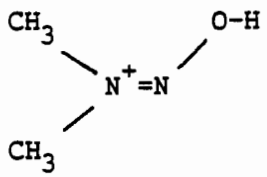

3

NND exhibits the n->π^* transition band at 350 nm ($\epsilon \simeq 100\ M^{-1}cm^{-1}$) and the π->π^* band at 230 nm ($\epsilon \simeq 6{,}000\ M^{-1}cm^{-1}$), but neither fluorescence nor phosphorescence is observed on excitation of these bands.[2] The lowest singlet and triplet excited energy levels ,E_S and E_T, of N-nitrosopiperidine (NNP), estimated from the onset (366 nm) of its absorption and quenching of triplet excited states of naphthalene and of 1,2'-binaphthyl generated by flash photolysis in acidic medium, are about 78 kcal/mol and 59 kcal/mol, respectively[15]. The corresponding values for NND should be close to those for NNP. The failure to observe emission from dialkylnitrosamines causes difficulties in elaborating their photochemical and photophysical behavior.

1.2. Photodecomposition of NND in Acidic Solutions

Photodecomposition of NND in solution at room temperature is strongly dependent on the acidity of the medium. At high concentrations of acid, e.g. 4M H_2SO_4, nitrosamines do not undergo photodecomposition,[17] presumably because of the formation of protonated nitrosamines which are not photolabile. On the other hand, at low concentrations of the acid (1-2M), the hydrogen-bonded complexes of nitrosamines are photoreactive, and have been studied extensively.[1,2,4,14-16] It has been established that the acidic complex decomposes from its singlet excited state to generate a transient aminium radical and nitric oxide[2, 14-16](Scheme 1-1). Aminium radicals, being electrophilic, efficiently initiate additions to various types of unsaturated carbon-carbon bonds, followed by scavenging of the C-radicals by nitric oxide or oxygen (if under oxygen atmosphere).[17-22] The addition has been shown to proceed by a stepwise radical mechanism (Scheme 1-1).[1,22]

Aminium radicals also electrophilically attack some fused aromatic hydrocarbons.[22] Anthracene, for example, being a typical singlet sensitizer (τ_s = 5 ns, E_s = 76.3 kcal/mol, Φ_f = 0.27)[23], sensitized the photodecomposition of NNP in acidic ethanol solution under nitrogen to give 9-piperidinoanthrone-10-oxime 4 in a 70% yield, as shown in Equation 1-1.[22] The process may be represented by the mechanism shown in Scheme 1-2,[22] where anthracene (ArH) acts as a singlet sensitizer as well as a substrate.

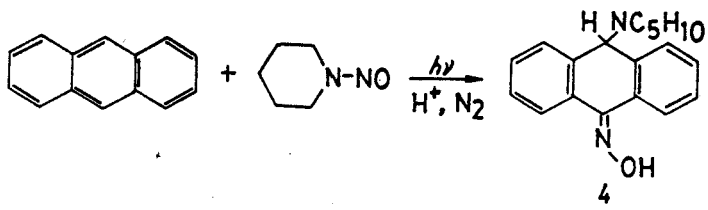

4

1-1

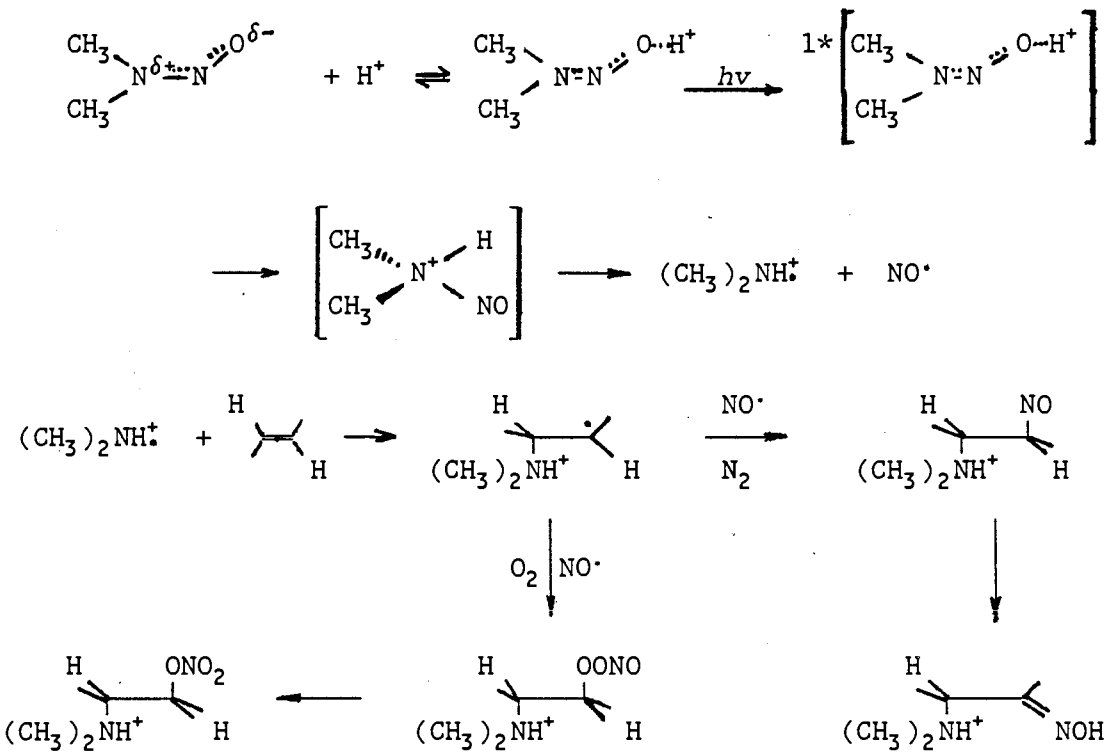

Scheme 1-1

In contrast to the photolability of NND in acidic media, NND is stable toward UV irradiation **in neutral solution**[24-27], except that NND undergoes *syn-anti* isomerization,[28] and undergoes decomposition, followed by fast recombination of the amino and NO radicals.[3] The photodecomposition of NND in neutral media has been a topic of continued interest for organic photochemists.

$$ArH + C_5H_{10}NN{=}O \xrightarrow[H^+]{h\nu} {}^{1*}ArH + C_5H_{10}NN{=}O\cdots H^+ \longrightarrow$$

$$ArH + {}^{1*}[C_5H_{10}NN{=}O\cdots H^+] \longrightarrow ArH + C_5H_{10}NH^{\cdot+} + NO^{\cdot} \longrightarrow 4$$

Scheme 1-2

1.3. Excited state Acidity of Naphthols

The acid-base properties of the excited states of aromatic compounds have been topics of great interests[29-34]. These properties are closely related to electronic structures of the excited states, which are considerably different from those of the ground states. A number of studies of acidity constants of the excited states, $pK_a(S_1)$ or $pK_a(T_1)$ of the aromatic compounds have been reported showing that the values are dramatically different from those in the ground states, $pK_a(S_o)$.[35-40] Some pK_a values are collected in Table 1-1:

Table 1-1 Ground and Excited State pK_a-Values for Some Aromatic Compounds[31]

Reaction	Molecules	$pK_a(S_o)$	$pK_a(S_1)$	$pK_a(T_1)$
$-OH+H_2O \rightleftharpoons -O^-+H_3O^+$	Phenol	10.0	4.0	8.5
	1-Naphthol	9.2	2.0	-
			0.5[c]	
	2-Naphthol	9.5	3.1	7.7
			2.5-2.8[d]	
$-NH_3^++H_2O \rightleftharpoons -NH_2+H_3O^+$	2-$NpNH_3^+$ [a]	4.1	-1.5	3.1
$-CO_2H+H_2O \rightleftharpoons -CO_2^-+H_3O^+$	1-NpCOOH [b]	3.7	10-12	4.6
$>C=O^+H+H_2O \rightleftharpoons >C=O+H_3O^+$	Acetophenone	-6.5	-4.7	1.0
	Benzophenone	-5.7	-4.2	-0.4

a. 2-Naphthylammonium. b. 1-Naphthoic acid.

c. Cited from the ref.48. d. Cited from the ref.29.

Examination of the data in Table 1-1 reveals the following features:

1. For phenols and the protonated aromatic amines, the lowest singlet excited state is much more acidic than the ground state by a factor of 10^5- 10^6.
2. Conversely, aromatic acids are much weaker in S_1 than in the ground state.
3. Aromatic carbonyl compounds become much stronger bases in S_1.

The pK_a values of excited states can be estimated using the Förster cycle,[29,30,35,36] fluorescence titration curves,[29,36] or triplet- triplet absorption titration curves.[41,42] These methods involve the assumption that proton transfer in the excited state is so fast that the acid-base equilibrium between the excited acid (e.g. phenol, HA^*) and its conjugate base (phenolate, A^{-*}) can be established during their excited lifetimes (Equation 1-2). The Förster cycle is the simplest and least time-consuming technique of the three methods.

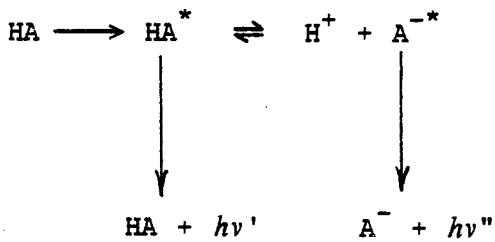

1-2

This method is based on determination of an energy gap between the ground and excited states for the acidic form and a gap for the basic form, of an aromatic compound molecule. In Figure 1-1, ΔH and ΔH^* are, respectively, the enthalpies of reactions in the ground and the excited states; ΔE_{HA} and ΔE_{A^-} are the energy differences between the two states of each species, whose values can be determined by absorption and emission spectroscopy. Equation 1-3 follows from Figure 1-1, assuming that the entropy of

dissociation is the same in both ground and excited states. Subsequently, Equation 1-4 is generated:

$$\Delta E_{HA} - \Delta E_{A} = \Delta H - \Delta H^{*} = \Delta G - \Delta G^{*} \qquad 1\text{-}3$$

$$pK_a(S_o) - pK_a(S_1) = h\Delta\nu/(2.303\ RT) \qquad 1\text{-}4$$

here R is the gas constant, h, Planck's constant, and T the temperature; $\Delta\nu$ is the difference in the frequency of absorption or emission of HA and A^- measured with the 0-0 bands.

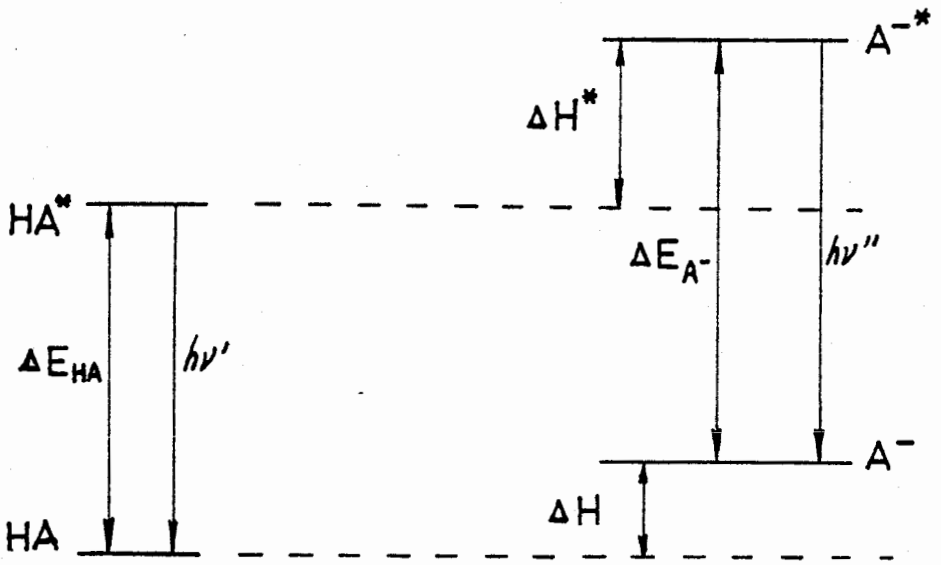

Figure 1-1 Förster cycle for deriving $pK_a(S_1)$ values for excited states.

Examination of Table 1-1 shows that for phenols, the order of pKa values is $pK_a(S_1) < pK_a(T_1) < pK_a(S_o)$. This sequence can be accounted for by resonance theory.[43] Using the phenol molecule as a model, the wavefunctions for its S_o and S_1 states can be approximated by mixing the wavefunctions corresponding to structures **4**, **5** and **6**.

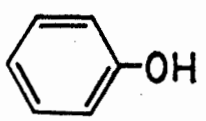

4

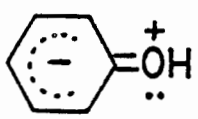

5

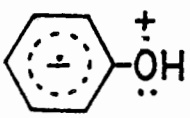

6

The important difference in S_1 and T_1 lies in the greatly enhanced contribution of structure **5** to the resonance hybrid constituting S_1, which leads to greatly increased positive charge on the oxygen atom and hence to greatly increased acidity of S_1. Structure **5**, which implies the transfer of a pair of electrons from the oxygen atom to the aromatic nucleus, does not contribute significantly to the T_1 state because spin correlation tends to keep electrons with parallel spins apart. For the same reason, structure **6** contributes mainly to the T_1 state. Hence the oxygen atom is less positively charged in T_1 than in S_1, leading to the observed sequence.

1.4 Reactions Promoted by Excited State Acids

A report[44] claiming that the enhanced acidity of the singlet excited state of 2-naphthol promotes the photodecomposition of nitrite ion via an excited state intermolecular proton transfer from 2-naphthol to nitrite ion has been disputed on the grounds of the low quantum yield value of 10^{-4} for the reaction.[45] Recently, however, the excited state intramolecular proton transfer leading to photohydration of o-hydroxy-phenylacetylene **7** to give o-hydroxyacetophenone was reported.[46] The pH-dependence of the relative quantum yields for the photohydration of **7** as compared to that for o-methoxyphenylacetylene **8** (Figure 1-2) indicates that the intramolecular proton transfer in S_1 is probably the key step in the photohydration as shown in Scheme 1-3. The curve for **7** exhibits an inflection point at *ca* pH 8 closely coinciding with the known value of $pK_a(S_o)$ = 8.6 for the ground state dissociation constant of **7**.

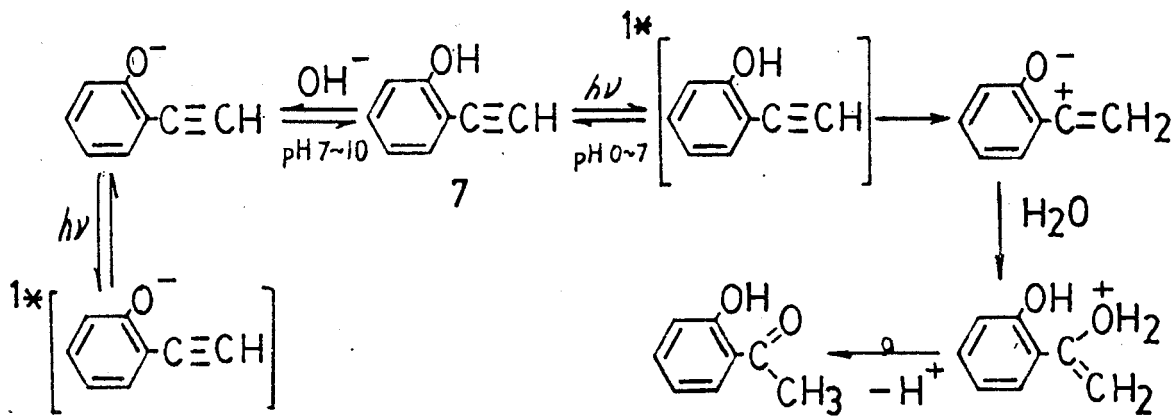

Scheme 1-3

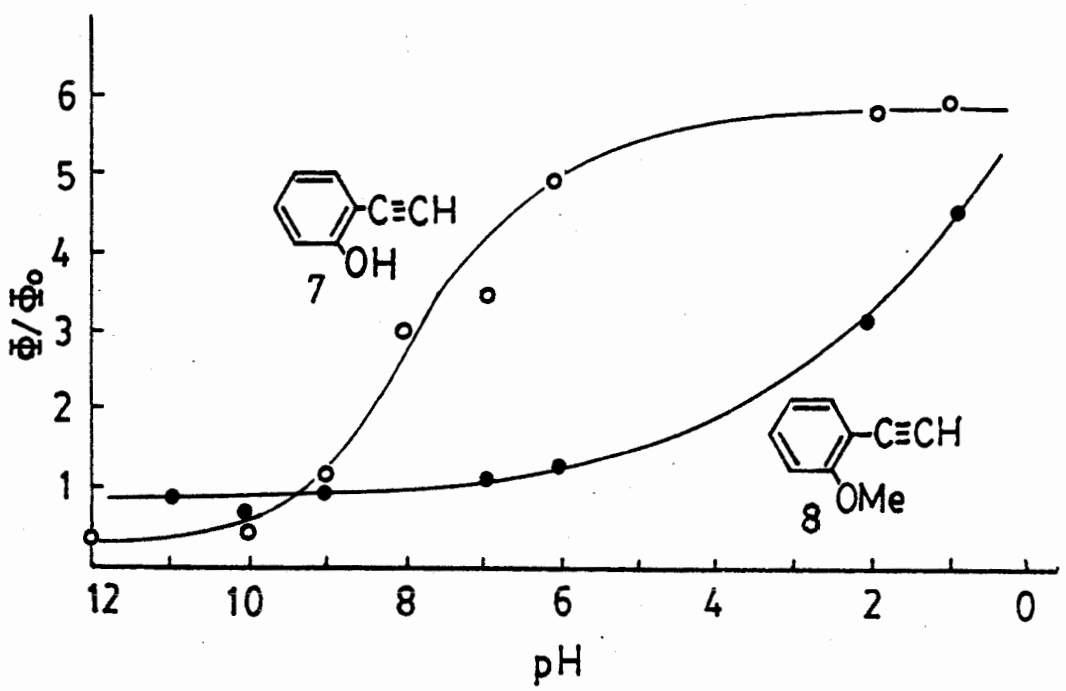

Figure 1-2 Plots of quantum yield ratio Φ/Φ_o against pH in the photohydration of **7** and **8** in aqueous acetonitrile, where Φ_o is the quantum yield of the product formation from **8** at pH 7.[46]

1.5 Research Proposal

The dramatically enhanced acidity of phenols in their singlet excited states, e.g. $pK_a(S_1)$ = 0.5 for 1-naphthol (1-NpOH),[48] leads us to speculate that the singlet excited 1-NpOH might function as a proton donor as well as an energy-transfer sensitizer to cause the sensitized photodecomposition of NND **in neutral media.** On the basis of this assumption, we have chosen several phenols such as naphthols and anthrols to sensitize photodecomposition of NND for the following reasons.

1. They possess low $pK_a(S_1)$ values (≤ 3), high singlet excited energies (72-91 kcal/mol), and long singlet excited state lifetimes (10-17 ns). (see Table 1-2).
2. These phenols would provide a less aromatic reaction site relative to benzene, whereby it might be possible to use them in a dual role of the sensitizer and the substrate in the investigation of the decomposition of NND.
3. They generally absorb light strongly in the 300-400 nm region,[23,47] providing the opportunity to excite phenols selectively.

Table 1-2 Spectroscopic Data[a] of Several Phenols (ArOH)

ArOH	E_S kcal/mol (nm)	Φ_f	τ_f (ns)	$pK_a(S_1)$	$E_S(ArO^-)$[f] kcal/mol (nm)
1-Naphthol	91.3	0.18	10.6	2.5	79
9	(313)			0.5[b]	(360)
2-Naphthol	86.7	0.27	13.3	2.8	77
10	(330)				(370)
2-Allyl-1-naphthol	88.0[f]	-	-	-	77
11	(325)				(370)
1-Allyl-2-naphthol	87.0[f]	-	-	-	77
12	(330)				(370)
1-Anthrol	72.0[c]	-	19[g]	-0.07[c]	62
13	(400)				(460)
9-Anthrol	72.0[f]	-	-	0.6[d]	60
14	(400)				(480)
9-Phenanthrol	73.4[f]	-	-	1.8[e]	64
15	(365)				(450)

a.-e. From references 23, 48, 49, 46, and 50, respectively.

f. These values were calculated from the overlapping wavelengths (the data in brackets) of absorption and fluorescence spectra for phenols in MeOH and phenolate in MeOH-KOH at room temperature, assuming that the Stoke's shifts were small.

g. Determined using a single photon counting technique (see CHAPTER 2).

The aims of this research project can be outlined as follows:

1. To identify the products from the sensitized photodecomposition of NND by some phenols **9-15** (Table 1-2).
2. To investigate the multiplicity of the reactive excited-state involved in the photochemical reaction by quenching and sensitization techniques, and by kinetic studies.
3. To investigate the solvent effects on the reaction quantum yield for the system of 1-NpOH and NND, and to determine the reaction quantum yields for other phenols at various concentrations of NND.
4. To investigate the kinetics of the sensitization process using static and dynamic fluorescence quenching techniques as well as quantum yield measurements.
5. To establish a sensitization mechanism of proton-transfer and energy-migration from singlet excited 1-NpOH to NND with quenching the reaction by some proton-acceptors.
6. To establish a general reaction pattern for the sensitized photodecomposition of NND.

Two matters related to this project were also investigated. One was to search for $S_o \rightarrow T_1$ spin-forbidden absorption together with phosphorescence of NND in order to determine its triplet energy level. Another was to investigate the applications of oxidative photoaddition of NND to 1-arylpropenes in acidic media .

CHAPTER 2

PHOTODECOMPOSITION OF N-NITROSODIMETHYLAMINE PROMOTED BY ENHANCED EXCITED STATE ACIDITY

2.1 Results

2.1.1 Photonitrosation of Phenols with NND; Preparation of Quinone Monooximes

Irradiation of a neutral solution containing the phenol (ArOH in Table 2-1) and NND at 15°C under nitrogen was investigated using a Pyrex filter to excite both the phenol and NND. The photolysis caused decomposition of NND to afford quinone monooximes (as shown in Table 2-1) and dimethylamine; this photoreaction is referred to as the photonitrosation of the phenol with NND. As the irradiation progressed, the photolysate generally turned dark brown except for the phenol **14**. Progress was followed by monitoring the concentration change of the phenol with GC or HPLC analysis. From the photolysate a relatively small quantity of an ether-insoluble black solid (*vide infra*) was obtained which was not investigated further. The ether-soluble fraction gave the quinone monooxime, unreacted phenol and NND. The quinone monooxime was isolated by column chromatography or recrystallization, or a combination of the both. These monooximes were identified by elemental analysis and spectroscopic data, and were confirmed by the comparison of their IR and ^{1}H NMR spectra with published spectra or with those of authentic samples. The presence of the quinone monooxime moiety was demonstrated by IR bands near 3100-3400(OH), 1620(C=O), 1580(C=N) and 980(N-OH) cm^{-1}.[51] The intensity and the exact position of the bands varied from case to case depending on the structures of quinone monooximes. Dimethylamine was identified by a preparation of the

N,N-dimethyl-4-nitrobenzamide derivative. In each case, a control experiment in the dark showed no chemical changes of either NND or the phenols. This ascertains that the nitrosation is indeed induced by photoexcitation.

Table 2-1 Photonitrosation of Phenols (ArOH) with NND in Dioxane

ArOH	Product	Yield (%)	Conversion of ArOH[a] (%)
1-Naphthol **9**	1,4-Naphthoquinone-4-oxime **16**	52	80
2-Naphthol **10**	1,2-Naphthoquinone-1-oxime **17**	60	36
2-Allyl-1-naphthol **11**[b]	2-Allyl-1,4-naphthoquinone-4-oxime **18**	45	74
1-Allyl-2-naphthol **12**	-[c]	-	-
1-Anthrol **13**	1,4-Anthraquinone-4-oxime **19**	53[a]	61
9-Anthrol **14**[b]	9,10-Anthraquinone-10-oxime **20**	84	100
9-Phenanthrol **15**[b]	9,10-Phenanthraquinone-10-oxime **21**	34[a]	100

a. The percentages were determined by GC and/or HPLC analysis with an internal standard.

b. The solvents were toluene (for **11**), THF (for **14**), and benzene (for **15**).

c. No photonitrosation was observed.

Photolysis of 1-Naphthol and NND

Photolysis of 1-naphthol (1-NpOH) and NND was carried out in dioxane, THF, acetonitrile, or methanol using a Pyrex filter at 15°C under N_2. HPLC analysis showed that the disappearance of 1-NpOH was faster in dioxane than in other solvents. Preparative-scale irradiation of 1-NpOH and NND in dioxane led to a photoproduct of 1,4-naphthoquinone-4-oxime (**16**) (yellow needles) as shown by the identical IR spectrum with that reported[51] (Equation 2-1).

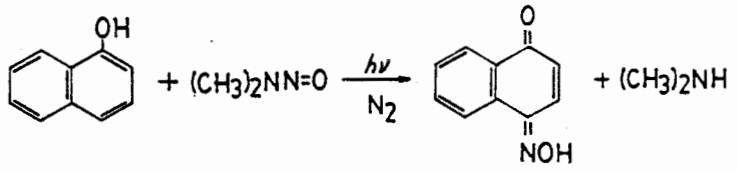

9 16 2-1

The material balance of the reaction (Equation 2-1) was determined by GC analysis, and plotted in Figure 2-1. Firstly, the concentration of **16** increased quickly during the first 2.5 h during which the photolysate turned dark-brown. The rate of the formation of **16** dropped off as the reaction proceeded. Secondly, the sums of [1-NpOH]+[**16**] at various intervals were always lower than the initial concentration of 1-NpOH (0.05 M) indicating the presence of unisolated minor products. The decrease of [1-NpOH] and the increase of [**16**] were nearly linear (i.e. a zero-order reaction) in the first hour of photolysis.

In the presence of hydrochloric acid, the similar photolysis of 1-NpOH and NND gave **16** and an unidentified compound with retention time (Rt) = 2.08 min. Similar photolysis of 1-NpOH and NND in dioxane but under O_2

(Equation 2-2) afforded 2-nitro-1-naphthol (5%) and an unknown compound (8%, Rt 11.4 min) in addition to **16** as shown by GC-MS analysis. 2-Nitro-1-naphthol was confirmed by GC peak-matching with an authentic sample. The conversion of 1-NpOH was estimated from the GC trace to be 24%, and the yield of **16** to be 60%.

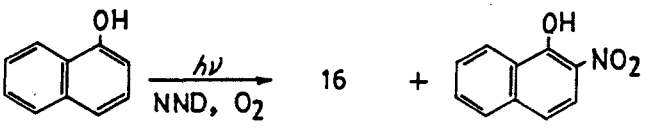

2-2

However, irradiation of 1-methoxynaphthalene (1-NpOMe) and NND in neutral THF or dioxane under conditions similar to those used for 1-NpOH caused no decomposition of NND and no photoproduct formation as shown by HPLC analysis. The singlet excited state properties of 1-NpOMe (E_s = 89.3 kcal/mol, Φ_f = 0.36 and τ_f = 13 ns)[23] are reasonably close to those of 1-NpOH (E_s = 91.3 kcal/mol, Φ_f = 0.18 and τ_f = 10.6 ns)[23] with the exception of the lack of a dissociable hydrogen. The absence of photonitrosation of 1-NpOMe with NND can be taken as an indication that excited state acidity is required in the decomposition of NND.

Photolysis of 2-Naphthol and NND

Irradiation of 2-naphthol (**10**) and NND in dioxane under conditions similar to those used for 1-NpOH except using a Corex filter, led to a photoproduct (Table 2-1), identified as 1,2-naphthoquinone-1-oxime **17** on the basis of spectroscopic data and elemental analysis. Its IR spectrum is identical with that reported[51]. The ^{1}H NMR spectrum shows a singlet at 17.52 ppm (D_2O exch.) indicating an intramolecular hydrogen-bonded hydroxy

group. Prolonged irradiation up to 76% conversion of 2-NpOH (for 16 h) yielded other by-products as shown by six minor peaks in the GC trace.

Similar irradiation of 2-NpOH and NND in dioxane with a Corex filter but under O_2 led to three more photoproducts besides **17**. The dark-brown photolysate was shown by GC-MS analysis to contain unknown A (31.3%, Rt 3.93 min, m/e 189 M^+), unknown B (16.1%, Rt 3.93, m/e 189 M^+), **17** (38.3%, Rt 4.42 min) and unknown C (14.2%, Rt 11.55 min, m/e 212 M^+).

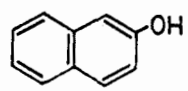

10

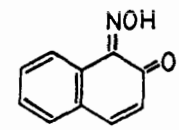

17

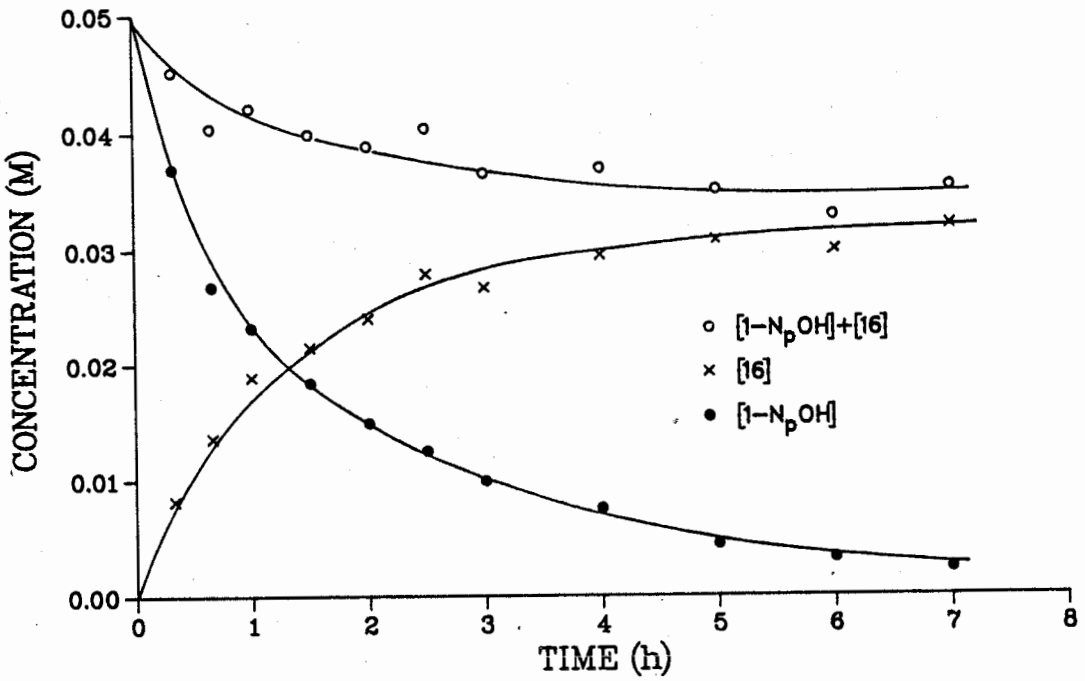

Figure 2-1 Material balance of photonitrosation of 1-NpOH with NND in dioxane at 15°C.

Photolysis of 2-Allyl-1-naphthol and NND

Irradiation of 2-allyl-1-naphthol (**11**) and NND in various solvents such as dioxane, THF, acetonitrile, toluene and methanol led to a single product as shown by GC. The disappearance of **11** in the first four solvents was shown to be much faster than in methanol, and the photolysates turned dark brown except in toluene (red-brown). Light brown crystals (mp 134-135°C) were obtained from the preparative photolysis in toluene under conditions similar to those used for the system of 1-NpOH and NND, and were assigned to 2-allyl-1,4-naphthoquinone-4-oxime **18** on the basis of spectroscopic data. The vinyl group was indicated by three vinylic proton signals at 5.19, 5.22 and 5.97 ppm with characteristic coupling pattern (Figure 2-2). Surprisingly, neither photocyclization product **22** nor photoadduct **23** of NND to the C=C bond in the allyl group (Equation 2-3) was detected. The former was observed by GC-FT-IR and GC-MS analyses in photolysis of **11** in benzene without NND under the same conditions as above.

The material balance during the photoreaction of **11** and NND in toluene is plotted in Figure 2-3 to show the similarity of the concentration curve shapes of **11** and **18** to those of 1-NpOH and **16** in Figure 2-1. It was noteworthy that while the formation of **18** ceased after one hour of irradiation, the decrease of **11** continued.

Attempted Photolysis of 1-Allyl-2-naphthol and NND

In contrast, prolonged irradiation of 1-allyl-2-naphthol (**12**) and NND for 16 h under conditions similar to those used for **11** in various solvents such as dioxane, THF, acetonitrile, toluene or methanol led to no photoproduct detectable by GC and HPLC analyses , even though the photolysates turned to light yellow and the amount of **12** decreased 3-7%

after irradiation. It is speculated that the failure of the photonitrosation of **12** might arise from the blockage of the C-1 position by the allyl group.

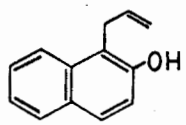

12

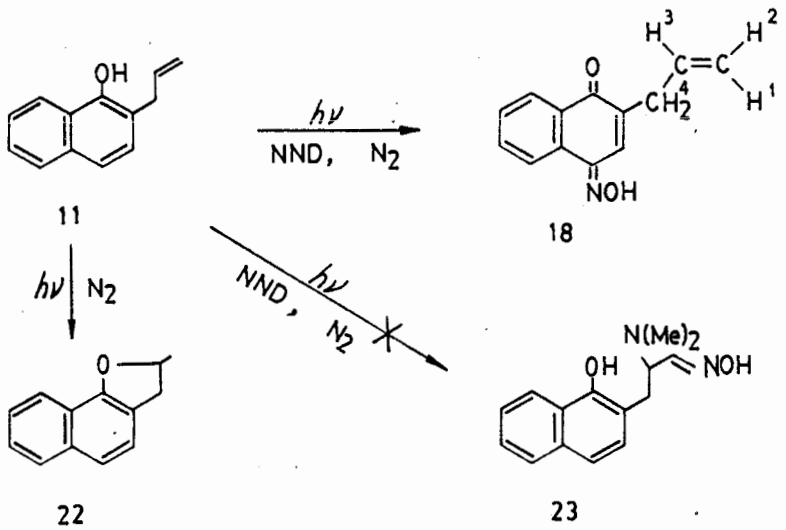

2-3

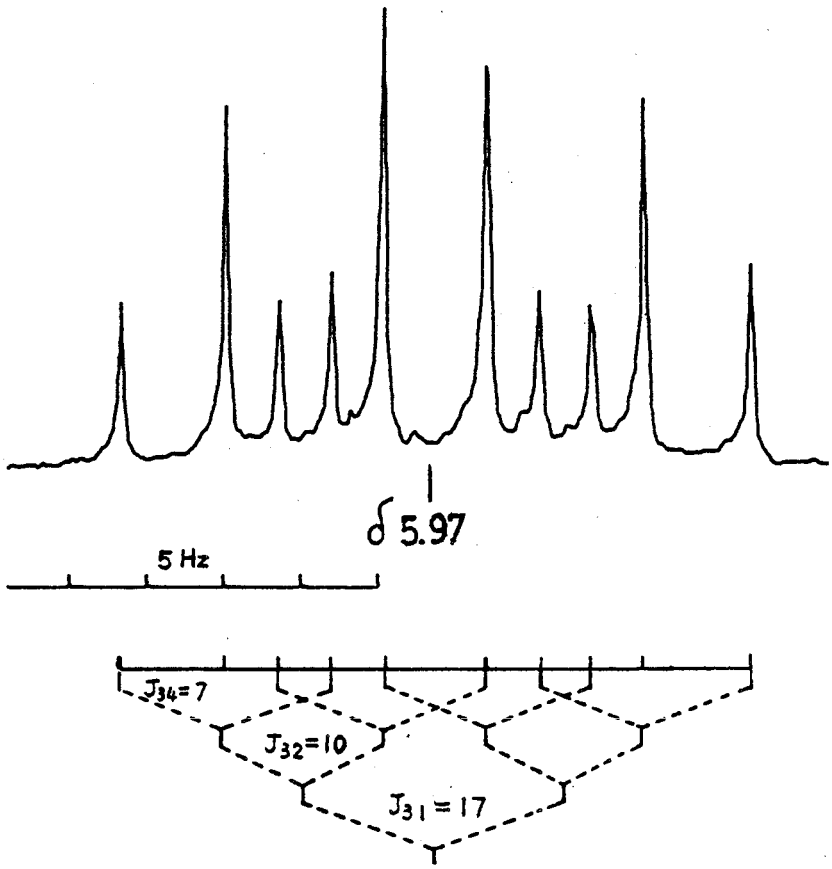

Figure 2-2 The NMR signal of H^3 in **18**.

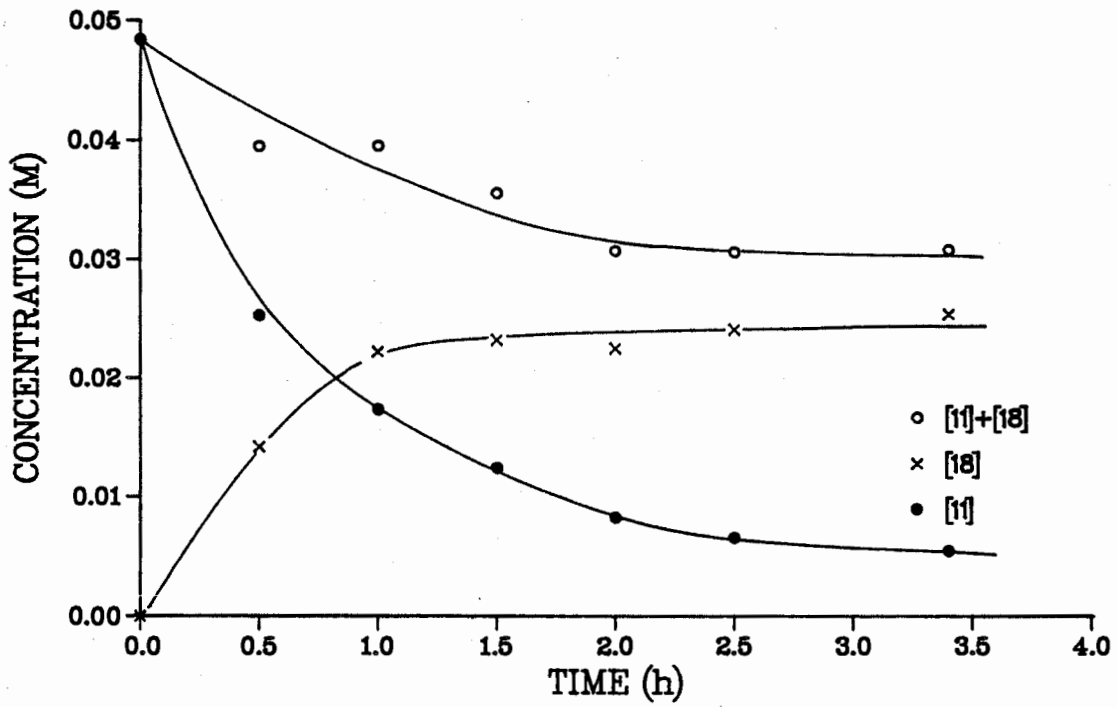

Figure 2-3 Material balance of photonitrosation of **11** with NND in toluene at 15°C.

Photolysis of 1-Anthrol and NND

Photoaddition of N-nitrosopiperidine to anthracene in an acidic medium has been previously shown in Equation 1-1 to give 9-piperidinoanthrone-10-oxime.[22] Preparative irradiation of 1-anthrol (**13**) and NND in dioxane gave orange crystals (Equation 2-4) which showed the expected IR absorptions and NMR signals for 1,4-anthraquinone-4-oxime (**19**). These data are similar to those of **16**. No detectable photoadduct from addition of NND to the 9,10- positions of the anthracene ring was found.

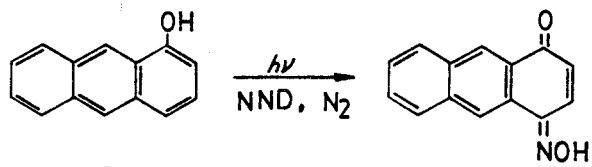

13 19 2-4

Photolysis of 9-Anthrol and NND

It was reported[52,53] that the keto-enol tautomeric reaction of anthrone and 9-anthrol in toluene was catalyzed by bases, e.g. triethylamine (TEA) or pyridine, and that the tautomeric equilibrium was also displaced to the side of the enol form by these bases. The absorption spectra of anthrone in THF in the absence and presence of NND (0.10 or 0.17 M) were determined, and shown in Figure 2-4. An absorption shoulder in the spectra of anthrone-NND in THF appears at 410 nm, and is assigned to the absorption of 9-anthrol based on the comparison of the spectra with those reported[52] for the mixture (anthrone and 9-anthrol) and for 9-anthrol.

Anthrone was used as a 9-anthrol source, because it is difficult to obtain pure 9-anthrol.[52] Irradiation of anthrone and NND in THF through a

Pyrex filter gave 9,10-anthraquinone-10-oxime **20**, according to spectroscopic data. The structure was confirmed by comparison of its IR and NMR data with those of an authentic sample. That the photonitrosation is initiated by 9-anthrol but not by anthrone was substantiated by selective irradiation of the former, using a filter solution to cut off light with wavelength <410 nm, since anthrone shows no absorption at wavelengths longer than 390 nm[52]. The photonitrosation reaction may be depicted by Equation 2-5.

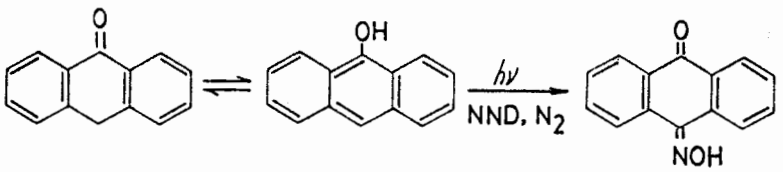

14 20 2-5

Photolysis of 9-Phenanthrol and NND

Preparative photolysis of 9-phenanthrol (**15**) and NND in benzene was carried out with RPR 300 nm lamps at 31°C to give orange crystals. The crystal was shown by ^{1}H-NMR to possess an intramolecular hydrogen bond with resonance at 17.06 ppm, and was assigned to 9,10-phenanthraquinone 10-oxime **21** according to the expected spectroscopic data. The assignment was confirmed by the identity of the spectra of **21** to those of an authentic sample.

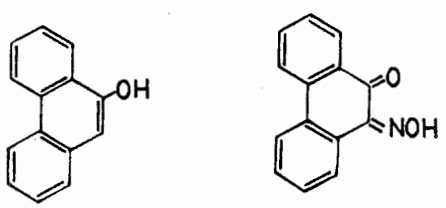

15 21

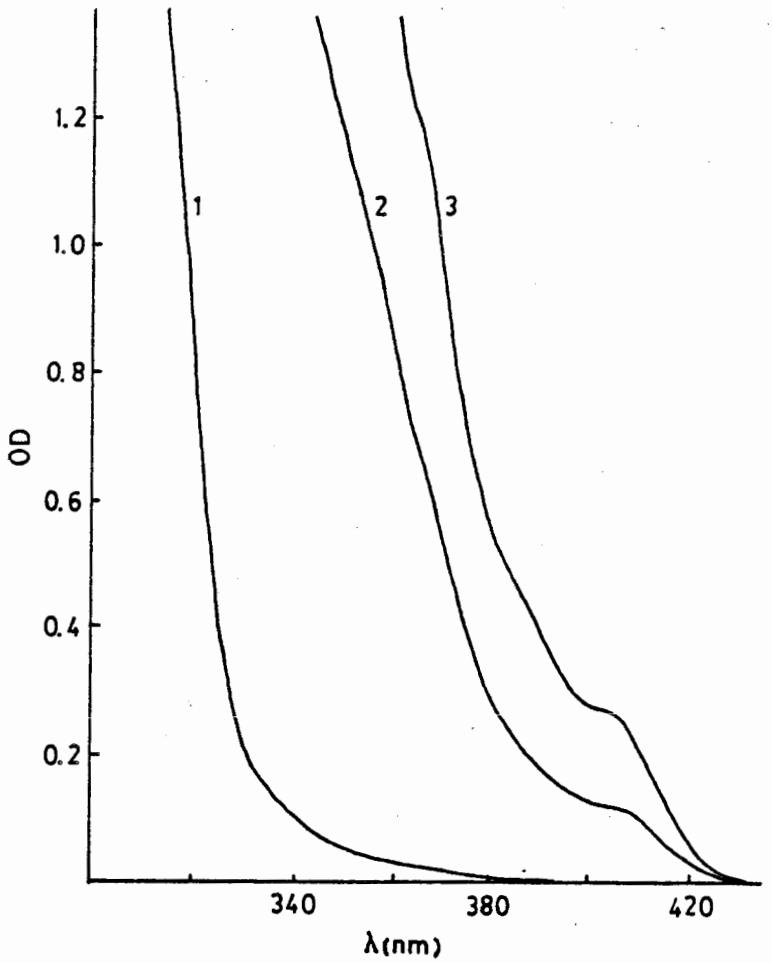

Figure 2-4 Absorption spectra of anthrone (0.005 M) in the absence and presence of NND in THF at 20°C; the curves 1, 2 and 3 contained [NND] of 0, 0.10 and 0.17 M, respectively. The absorption band at 407 nm in the curves 2 and 3 is due to 9-anthrol.

2.1.2 Wavelength-Dependent Irradiation

Irradiation of Phenols

The reactive state in photonitrosation was determined by selective excitation of 1-NpOH or NND at different wavelengths. The absorption spectrum of 0.025 M NND in dioxane shows a transparent window around 300 nm (curve 3 in Figure 2-5) where 1-NpOH absorbs strongly (ϵ_{300} = 3,600 $M^{-1}cm^{-1}$, in dioxane). The NND solution is photostable, showing no substantial change in absorption spectrum after irradiation through a Pyrex filter for 2.25 h (curve 4 in Figure 2-5). The NND solution was used as a filter to selectively excite 1-NpOH in the presence of NND in dioxane. The reaction afforded **16** in a 53% yield with a 40% conversion of 1-NpOH, as determined by GC analysis. As a control, a solution identical to the one above was irradiated under similar conditions except for use of a Pyrex filter. It gave **16** in 45% yield with 65% conversion of 1-NpOH. Therefore direct excitation of 1-NpOH undoubtedly leads to the photonitrosation.

Solutions of 1-NpOH (0.050 M) and NND (0.050 M) in dioxane, THF or methanol were irradiated at room temperature with an Excimer Laser (0.3 watt) at 308 nm, where 1-NpOH absorbed at least 99% of the laser emission:

$$\epsilon_{1\text{-NpOH}}/(\epsilon_{1\text{-NpOH}} + \epsilon_{NND}) = 3200/(3200 + 24) = 99.3\%$$

In dioxane, pulsing of 1-NpOH for ten minutes led to the formation of **16** in a 80% yield with a 11.5% conversion of 1-NpOH, and in THF, a 40% yield with a 9.2% conversion. In methanol, however, similar pulsing for twenty minutes gave no photoproduct.

Pulsing of 2-NpOH with NND in dioxane for 20 minutes under similar conditions gave the quinone monooxime **17** in a 53% yield with a 16.7% conversion of 2-NpOH, but similar solutions in THF or methanol yielded no monooxime **17**.

Irradiation of NND

Direct irradiation of NND (0.050 M, cut-off < 390 nm) in the presence of 1-NpOH (0.025 M, cut-off < 340 nm) through a GWA filter (cut off <340 nm, see Figure 5-2 in Experimental) for 6 h yielded no quinone monooxime **16** detectable by GC analysis. The result clearly indicates that the direct excitation of NND causes no photonitrosation. In other words, the NND decomposition is sensitized by an excited state of 1-NpOH.

2.1.3 Triplet Sensitization and Quenching Studies

To investigate the possibility of a triplet pathway in photonitrosation of 1-NpOH (E_T = 58.6 kcal/mol)[23], xanthone (E_T = 74.1 kcal/mol)[23] or 2-acetylnaphthone (E_T = 59.4 kcal/mol)[23] was used as a triplet sensitizer. In these experiments, enough sensitizer was added to a dioxane solution of 1-NpOH (0.025 M) and NND (0.025 M) to absorb larger than 90% of incident light(> 380 nm) by using a GWA filter. GC analysis of the photolysates gave no detectable product **16** in either case.

Furthermore, 1,3-cyclohexadiene (CHDE) which has E_S = 97 kcal/mol and E_T = 52.4 kcal/mol[23] failed to quench the photonitrosation in the concentration range of 0.001 - 0.009 M on irradiation with the 300 nm light source in THF at 31°C.

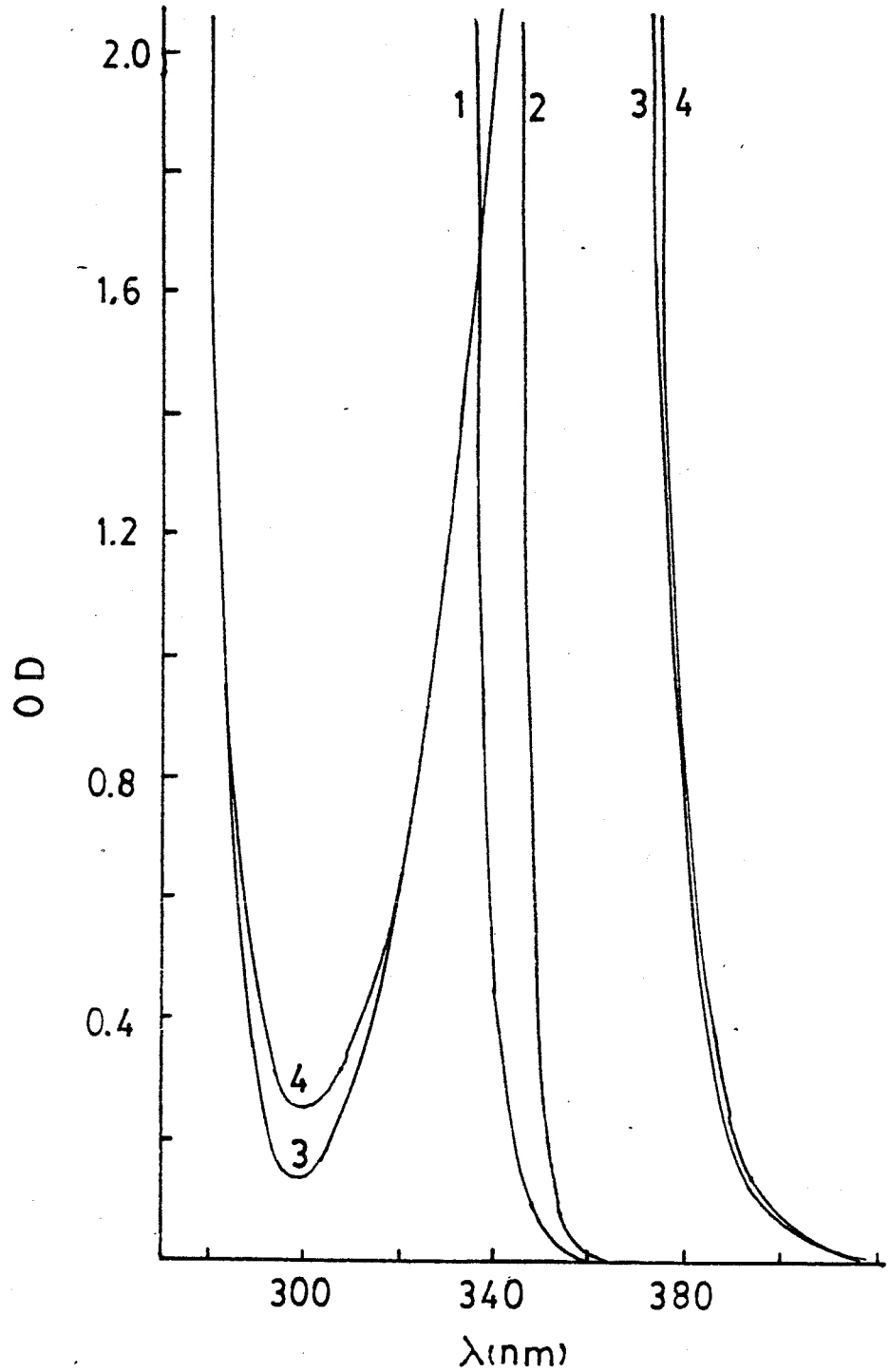

Figure 2-5 Absorption spectra of dioxane solutions of: (1) 1-NpOH (0.050M); (2) 2-NpOH (0.050 M); (3) and (4) NND (0.025 M), before and after irradiation, with a 450 watt Hanovia lamp for 2.25 h at 15°C.

Under these conditions, the quantum yield of **16** formation was determined as a function of the CHDE concentration, and shown to be virtually unchanged in the plot of $\Phi_{ox}^{\circ}/\Phi_{ox}$ against [CHDE] in Figure 2-6.

The failure of triplet sensitization and failure of quenching indicates that the photonitrosation of 1-NpOH with NND probably occurs from the singlet excited state of 1-naphthol (^{1*}1-NpOH) rather than from the triplet state. This suggestion is consistent with the fact that NND photodecomposition in acidic media occurs from its singlet excited state [1,2,4]. This is further confirmed by fluorescence intensity and lifetime quenching studies (*vide infra*).

2.1.4 Steady-State Fluorescence Quenching Studies

Since the emission of 1-NpOH around 345 nm overlaps with the absorption of NND (Figure 2-7), an internal "trivial quenching" process[54-56] can occur and can lead to spurious results using a routine illumination technique (Figure 5-6). Quenching of fluorescence intensity of 1-NpOH (0.0002 M) by NND (0.0002-0.0020 M) in methanol, acetonitrile or dioxane was determined using routine illumination technique at room temperature; one of them is shown in Figure 2-8. The Stern-Volmer correlations between I°/I and [NND], based on Equation 2-6, were calculated from least square analysis to give quenching rate constants k_q (x 10^{10} $M^{-1}s^{-1}$): 5.86 (in methanol, correlation coefficient, r = 0.997), 4.85 (in acetonitrile, r = 0.999) and 4.45 (in dioxane, r = 0.996).

$$\Phi_f^{\circ}/\Phi_f = (I^{\circ}/I)_{max} = 1 + k_q\tau_o[NND] \qquad 2\text{-}6$$

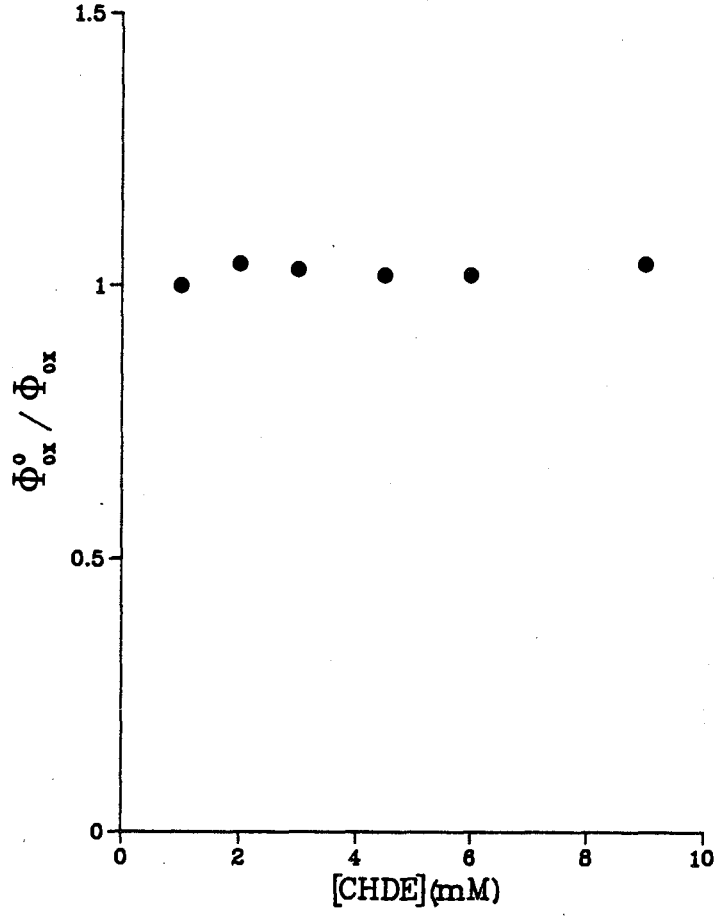

Figure 2-6 Relative quantum yields of **16**, $\Phi^{\circ}_{ox}/\Phi_{ox}$, in the photonitrosation of 1-NpOH and NND, where Φ°_{ox} and Φ_{ox} are quantum yields in the absence and presence of various concentrations of CHDE, respectively.

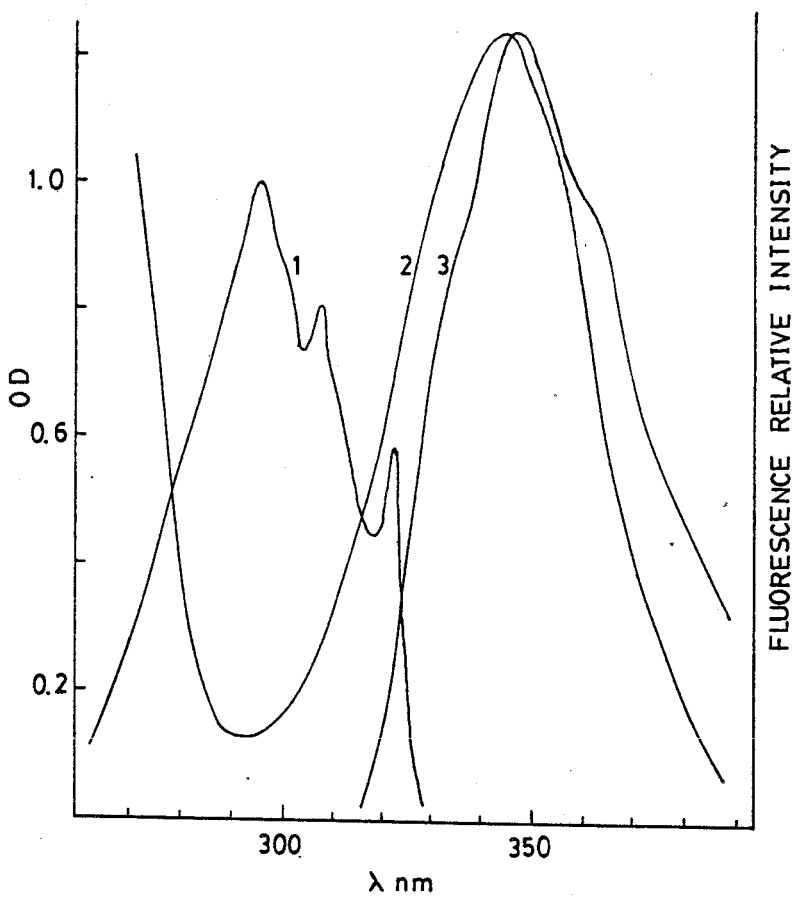

Figure 2-7 Absorption spectra of (1) 1-NpOH (0.0002 M) and (2) NND (0.012 M), and (3) fluorescence spectrum of 1-NpOH (0.0002 M) in methanol at 20°C.

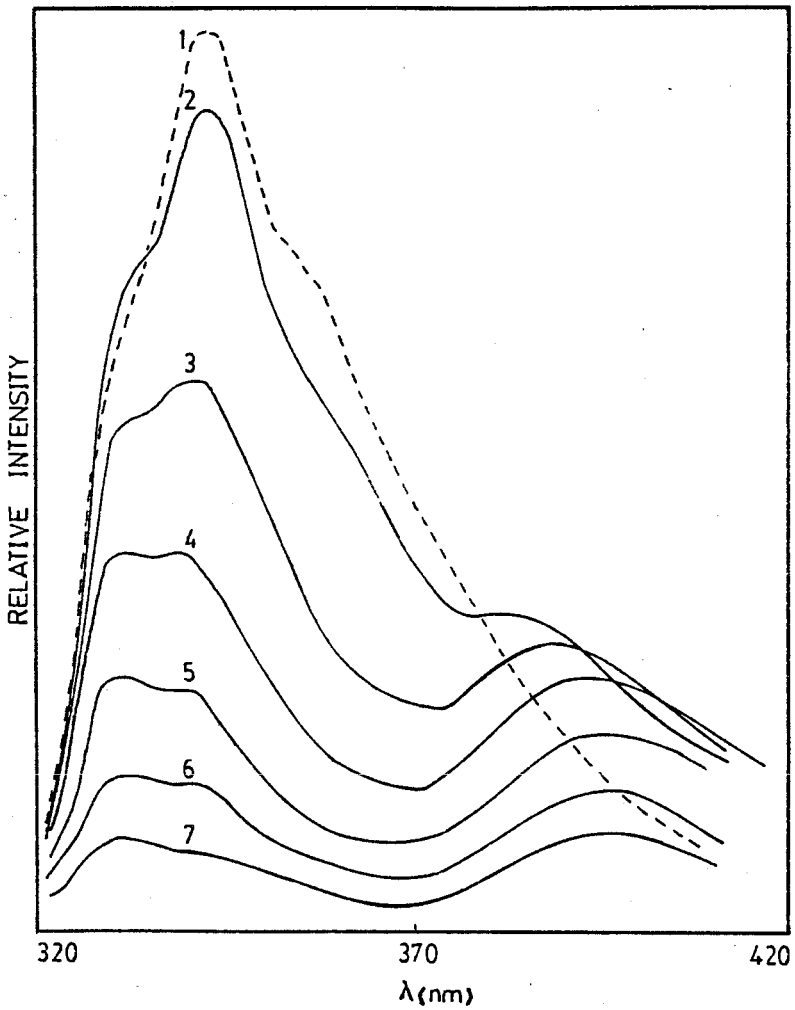

Figure 2-8 Quenching of 1-NpOH (0.0002 M) fluorescence in dioxane at 20°C by NND with excitation at 300 nm using the routine illumination technique: curves 1-7 contained [NND] of 0, 0.004, 0.008, 0.012, 0.016, 0.020 and 0.025 M, respectively.

In Equation 2-6, Φ_f° and Φ_f are the fluorescence quantum yields of 1-NpOH in the absence and presence of various concentrations of NND; I° and I are the fluorescence intensities at the maximum emission wavelength of 1-NpOH in the absence and presence of NND; τ_o is the fluorescence lifetime of 1-NpOH without NND. Obviously, the k_q values larger than the diffusion controlled rate constant must arise from the trivial quenching process. Furthermore, in a higher NND concentration range (0.004-0.025 M), quenching of 1-NpOH fluorescence with the routine illumination technique showed gradual shifts of the fluorescence band up to 390 nm (Figure 2-8). At [NND]=0.070-0.100 M, the main 1-NpOH fluorescence band at 340 nm disappeared and was replaced by a band at 390 nm (Figure 2-9). These observations led us to misinterpret the 390 nm band as emission from an exciplex of ^{1*}1-NpOH and NND.[57] These phenomena can be clearly attributed to reabsorption of the emission from ^{1*}1-NpOH by NND.

The front-face illumination technique can circumvent the "trivial quenching" process, since the path length of emitted light is almost negligible[54,55] (see Figure 5-6 in Experimental). The quenching of 1-NpOH fluorescence in dioxane by NND using the front-face illumination technique is shown in Figure 2-10. The Stern-Volmer plot of I^o/I against [NND] yielded a straight line (Figure 2-11) with the slope of $k_q\tau_o$ = 117 M^{-1}, and a k_q value of 11.0 x 10^9 $M^{-1}s^{-1}$ using τ_o = 10.7 ns in dioxane (*vide infra* Table 2-3).

No fluorescence of NND in dioxane was detected with excitation at either 280 nm or 340 nm. These observations are consistent with a previous report from our laboratory.[2] Nor was fluorescence of quinone monooxime **16** in dioxane detected with excitation at 300 nm.

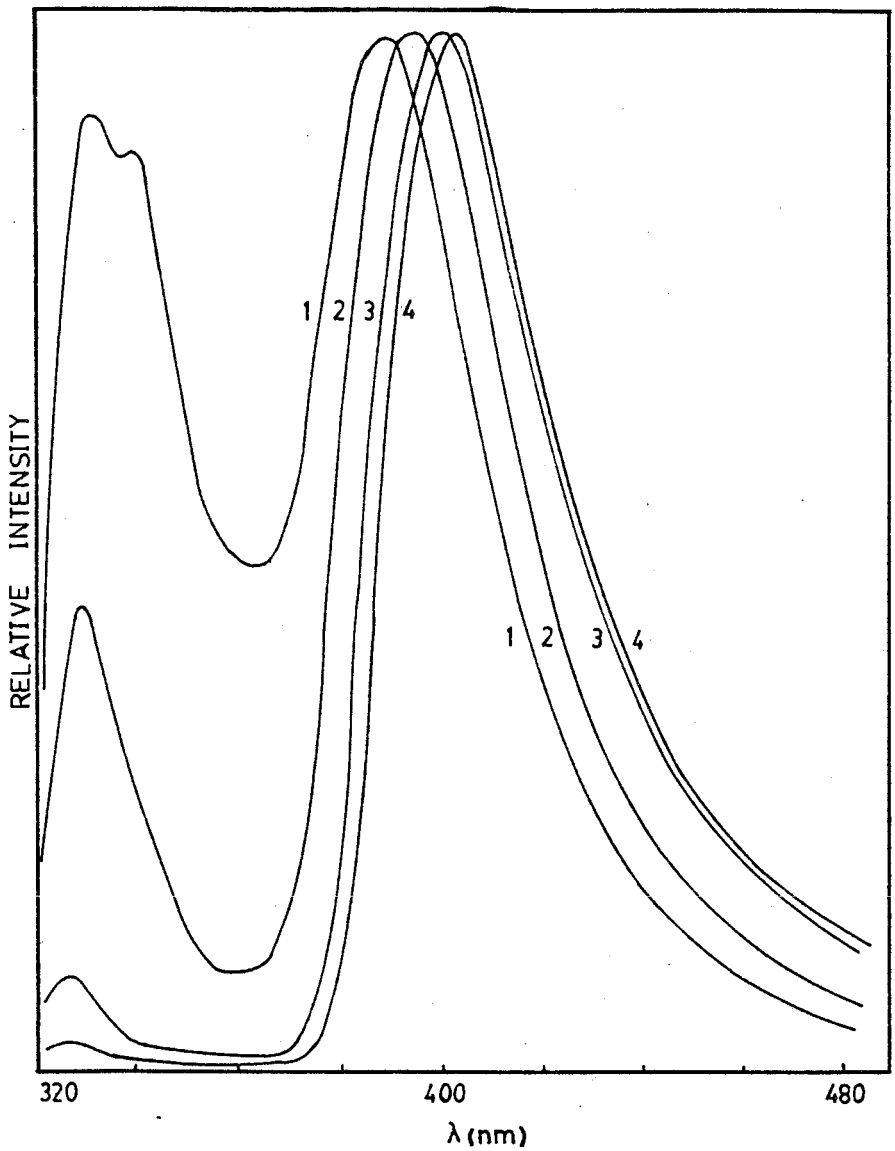

Figure 2-9 Fluorescence spectra of 1-NpOH (0.0002 M) in the presence of NND in acetonitrile at 20°C with excitation at 300 nm using the routine illumination technique; curves 1-4 contained [NND] of 0.01, 0.03, 0.07 and 0.10 M, respectively; curves 2-4 were normalized at 390-410 nm with respect to the curve 1.

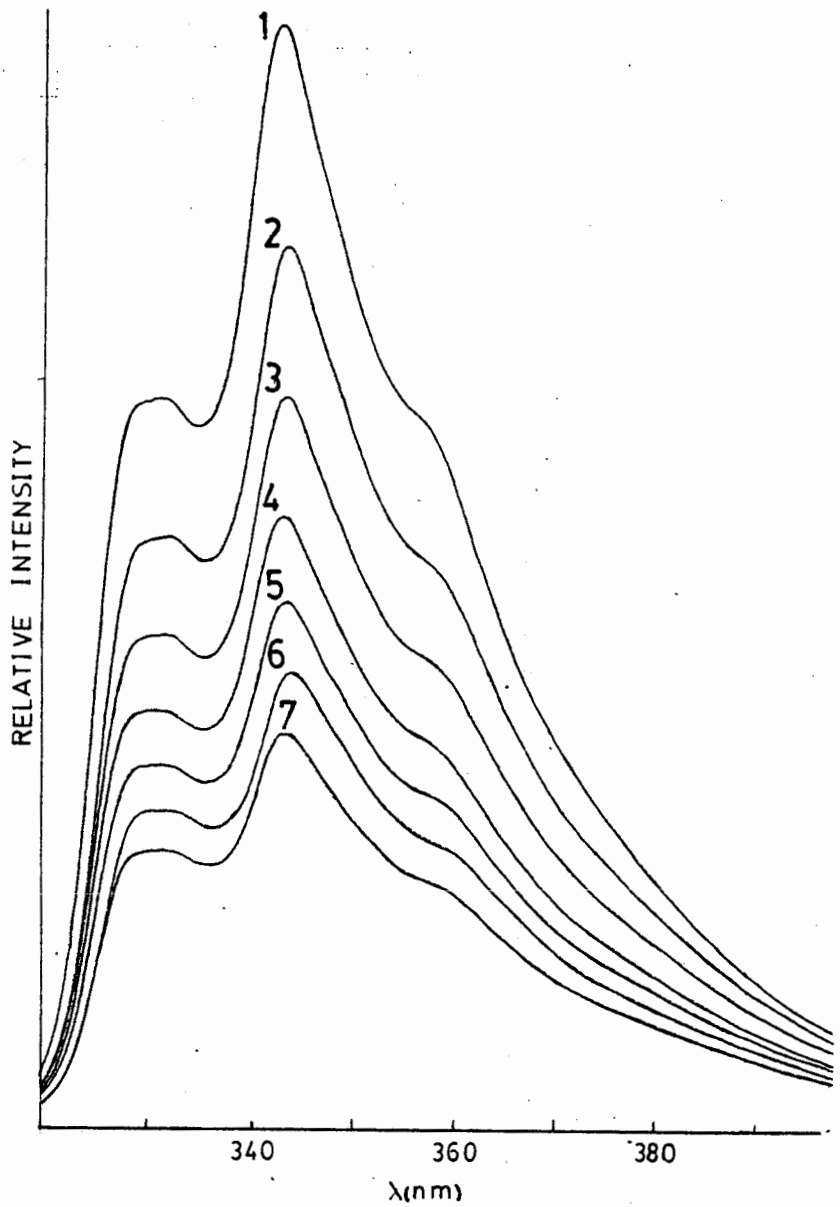

Figure 2-10 Quenching of 1-NpOH (0.002 M) fluorescence with NND in dioxane at 22°C with excitation at 300 nm using the front-face illumination technique; curves 1-7 contained [NND] of 0, 0.0025, 0.0050, 0.0075, 0.0100, 0.0125 and 0.0150 M.

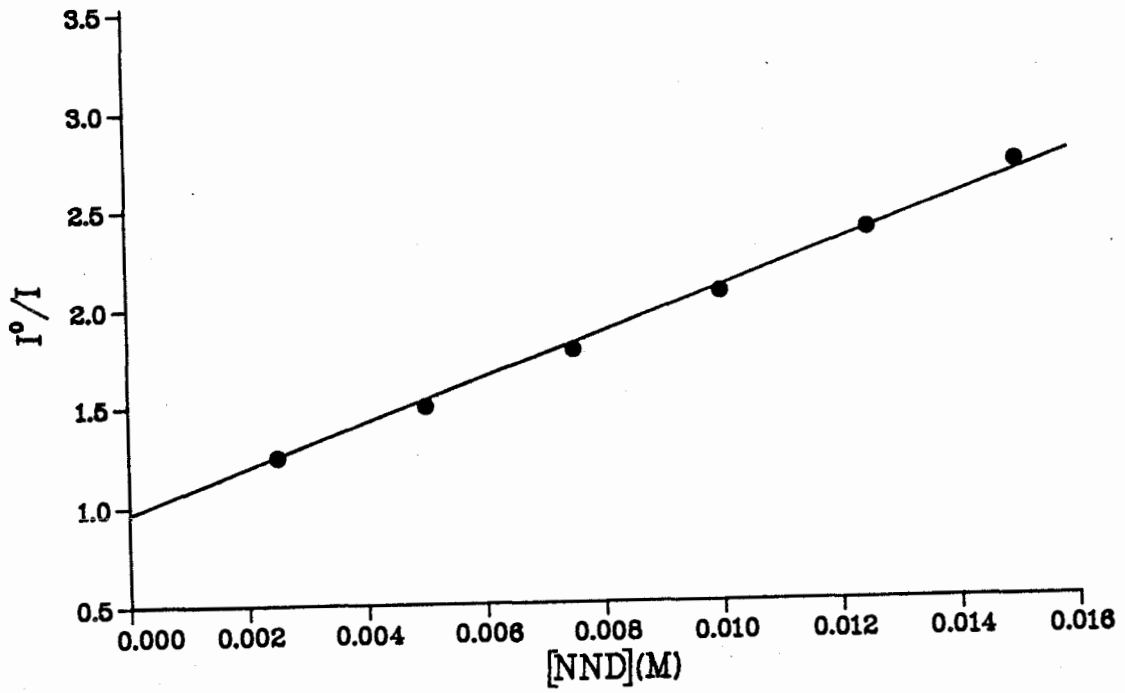

Figure 2-11 The Stern-Volmer plot of I°/I *vs* [NND] in dioxane at 22°C, the data of I°/I were measured at 342 nm from Figure 2-10.

Quenching of 1-anthrol (1-AnOH) fluorescence by NND was studied with the routine illumination technique, because the fluorescence of 1-AnOH lies around 400-600 nm (see Figure 2-23), well separated from the absorption band of NND.

At 77K, the fluorescence spectra of 1-AnOH (0.0002 M) in isopentane-methylcyclohexane (1:1, by volume) were recorded in the absence and presence of base, e.g. NND (0.013 M), TEA (0.150 M) or potassium hydroxide (0.002 M) as shown in Figure 2-12. The 1-AnOH fluorescence maximum at 440 nm is displaced to 456 nm by NND and to 520 nm by TEA or by potassium hydroxide, respectively. These observations are in agreement with those in a previous report[58] of the 77K fluorescence spectra of 1-NpOH in the presence of some bases, e.g. N,N-dimethylformamide (DMF), TEA or potassium hydroxide; the 1-NpOH fluorescence maximum at 340 nm in ether was shifted to 360 nm by DMF, to 400 nm by TEA and to 420 nm by potassium hydroxide. Since singlet excited 1-NpOH possesses enhanced acidity , the authors[58] suggested that the emission at 360 nm band was from the hydrogen-bonded exciplex between DMF and the fluorescent state of 1-NpOH (Equation 2-7), and that the emission at 400 nm band was from the excited state ion pair (Equation 2-8) which was formed from proton transfer from ^{1*}1-NpOH to TEA.

$$^{1*}\text{1-NpOH} + \text{DMF} \rightleftharpoons [^{1*}\text{1-NpOH}\cdots\text{DMF}] \qquad 2\text{-}7$$

$$^{1*}\text{1-NpOH} + \text{Et}_3\text{N} \rightleftharpoons [^{1*}\text{1-NpO}^- \ \text{Et}_3\text{NH}^+] \qquad 2\text{-}8$$

In analogy to the shifts of the 1-NpOH fluorescence maxima, those of 1-AnOH are interpreted by the same scheme, e.g. hydrogen-bonded exciplex with NND and an ion-pair with TEA. A shoulder around 440 nm in curve 2 in Figure 2-12 is assigned to the emission from the free 1-AnOH.

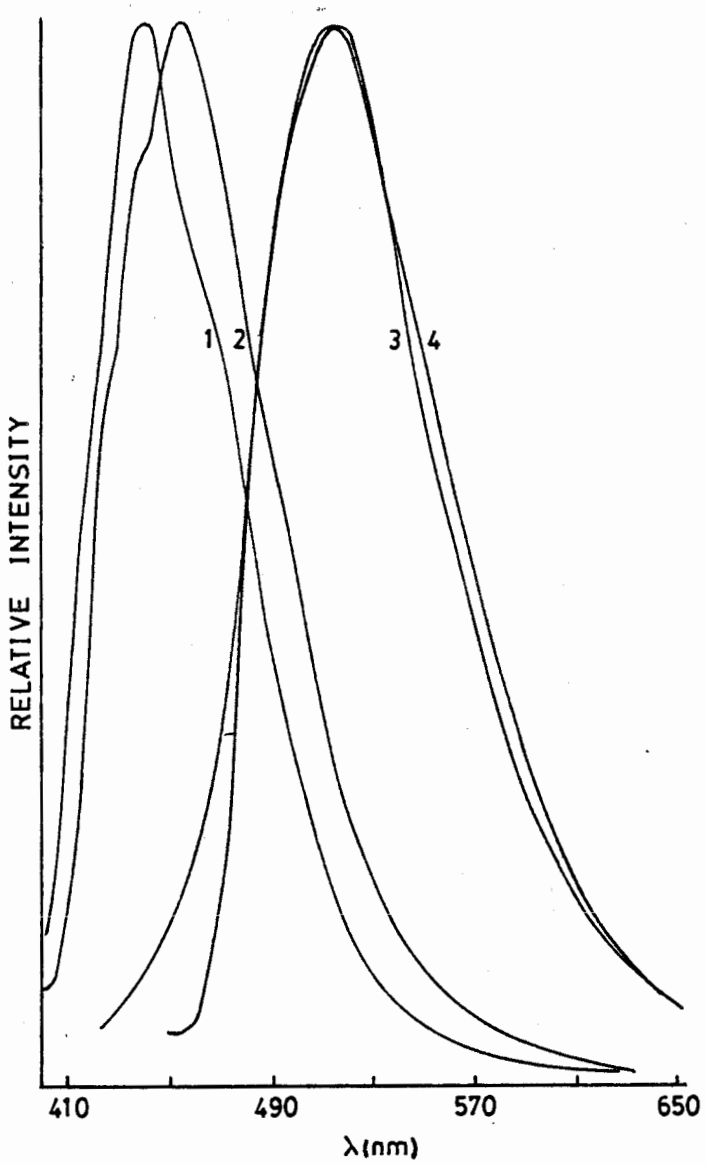

Figure 2-12 Fluorescence spectra of 1-AnOH (0.0002 M) in isopentane-methylcyclohexane (1:1, by volume) at 77K with excitation at 400 nm; curves 2, 3 and 4 contained [NND] = 0.013 M, [KOH] = 0.002 M (in ethanol-isopentane-methylcyclohexane, 1:2:2, by volume) and [TEA] = 0.150 M, respectively.

At room temperature, quenching of 1-AnOH (0.0002 M) fluorescence by NND (0.008-0.040 M) in various solvents e.g. THF, dioxane, acetonitrile, methanol or ethanol was determined using the routine illumination technique. The fluorescence maximum of 1-AnOH around 435-450 nm decreased with increasing NND concentration (Table 5-6). A typical run in THF is shown in Figure 2-13; the intensity ratio, I°/I, at the maximum emission wavelength of 442 nm was plotted against [NND] according to Equation 2-6 to give a straight line with a slope of $k_q\tau_o$ = 26.0 M^{-1} (Figure 2-14). The plots of I°/I against [NND] in other solvents also yielded straight lines with the slopes of $k_q\tau_o$ = 46.2 (in acetonitrile), 37.7 (in dioxane), 13.4 (in methanol) and 11.7 M^{-1} (in ethanol), as shown in Figure 2-14. Accordingly, solvents can affect this quenching process; hydroxylic solvents, in particular, can retard it.

Quenching of 1-AnOH fluorescence by NND in dioxane was examined at various temperatures from 10 to 50°C. The fluorescence intensity ratio of I°/I at 440 nm was determined as a function of [NND]. The corresponding Stern-Volmer plots of I°/I against [NND] yielded straight lines (Figure 2-15). The slopes increase with increasing temperature. It was reported[59] that the $k_q\tau_o$ value of dynamic fluorescence quenching increases with increasing temperature, whereas the value of static fluorescence quenching decreases. Thus, dynamic and static quenching can be distinguished by their temperature dependence. Remarkably, the positive temperature effect in quenching of 1-AnOH by NND indicates its character of dynamic quenching.

Using the lifetime of 1-AnOH in dioxane, τ_o = 19.1 ns (Table 2-6), the corresponding quenching rate constants were also calculated (in Table 2-2).

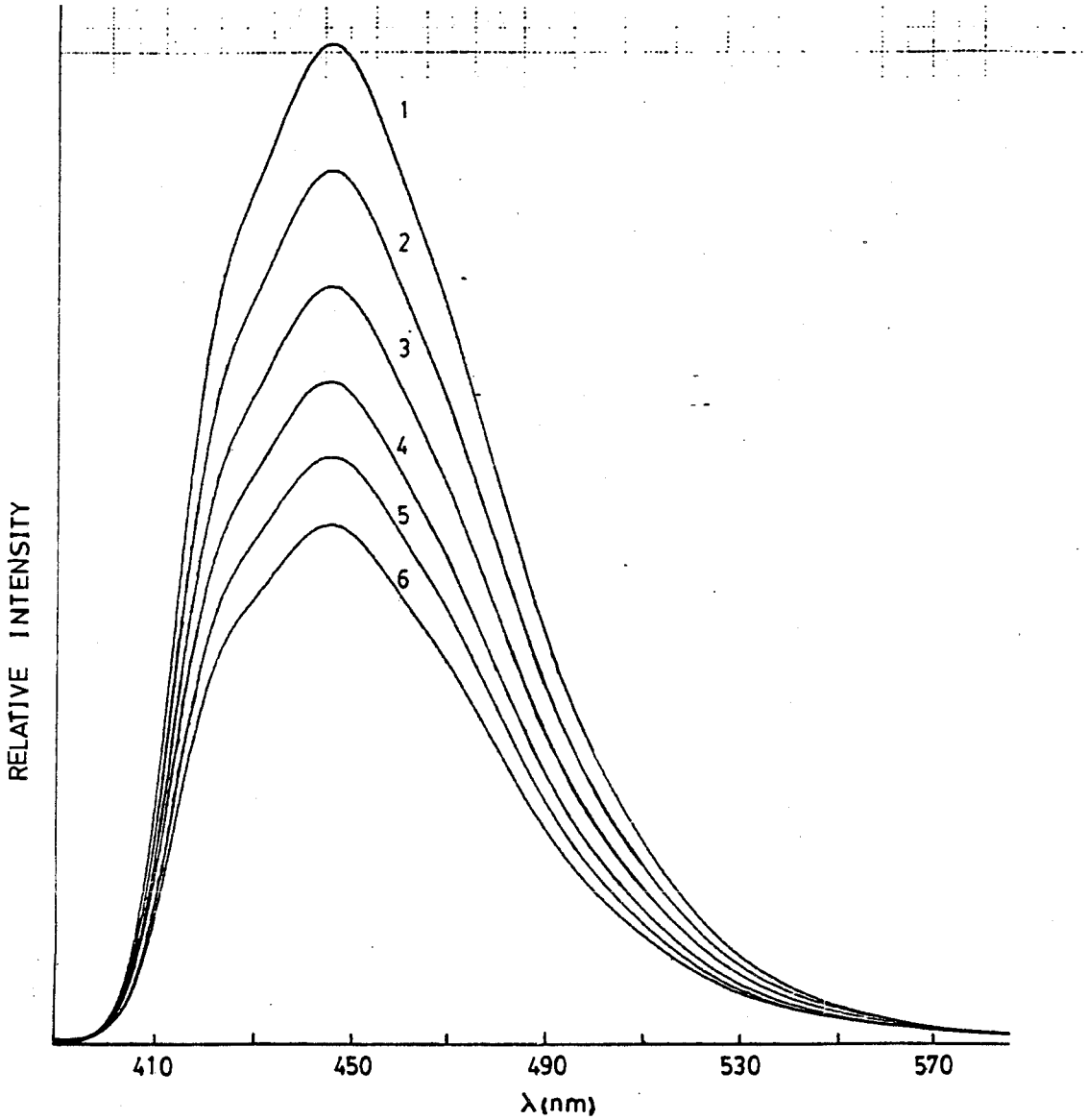

Figure 2-13 Quenching of 1-AnOH (0.0002 M) fluoresence by NND (0.007-0.0375 M) in THF at 22°C: the excitation wavelength was 400 nm with emission range from 390 to 620 nm, and curves 1-6 contained [NND] of 0, 0.0075, 0.0150, 0.0225, 0.0300 and 0.0375 M, respectively.

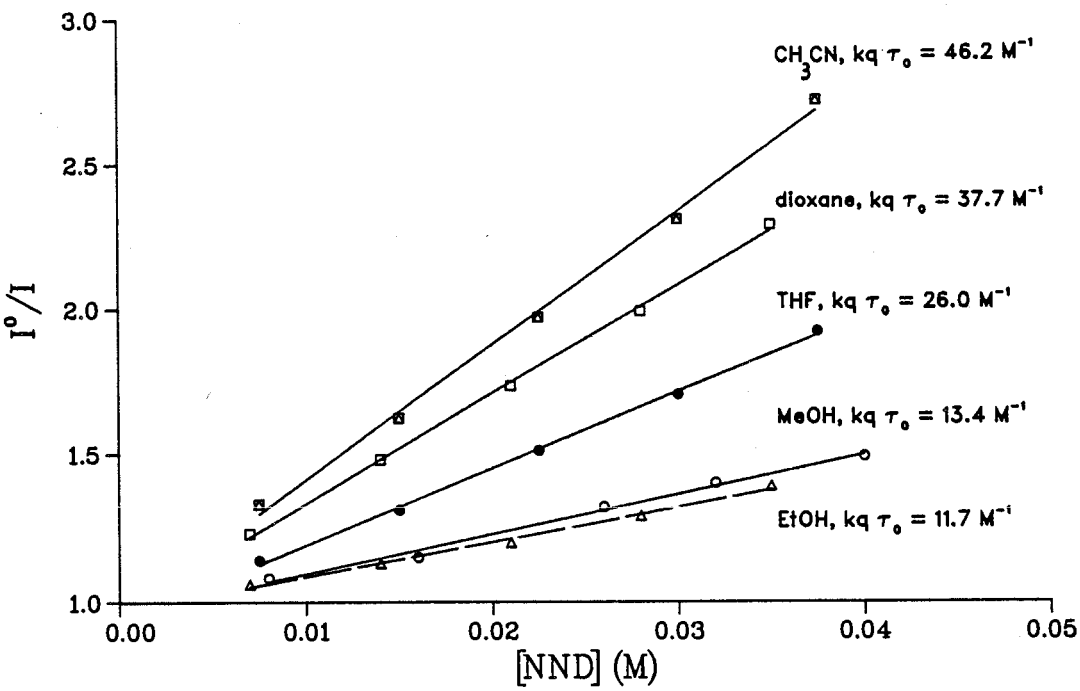

Figure 2-14 Stern-Volmer plots for quenching of 1-AnOH (0.0002 M) fluorescence by NND in various solvents at room temperature.

Table 2-2 Kinetic Parameters for Fluorescence Quenching of 1-AnOH by NND in Dioxane[a]

T (K)	$k_q\tau_o$ (M^{-1})	$k_q x10^{-9}$ ($M^{-1}s^{-1}$)	r
283	29.0 ± 0.6	1.52 ± 0.03	0.999
298	37.7 ± 0.8	1.97 ± 0.03	0.999
308	42.7 ± 0.8	2.24 ± 0.04	0.999
323	50.4 ± 1.3	2.64 ± 0.07	0.999

a. [1-AnOH] = 0.0002 M, [NND] = 0.007-0.035 M, λ_{ex} = 400 nm, λ_{em} = 440 nm, and τ_o = 19.1 ns.

The Arrhenius plot of logarithm of quenching rate constants *vs* 1/T yielded a straight line (Figure 2-16) with an activation energy of 2.54 kcal/mol and log A = 11.2 ; these values are consistent with those reported[60] (E_a = 2-3 kcal/mol and log A = 10-12) for the diffusion-controlled quenching process.

$$\log k_q = \log A - E_a/(2.303\ RT) \qquad 2\text{-}9$$

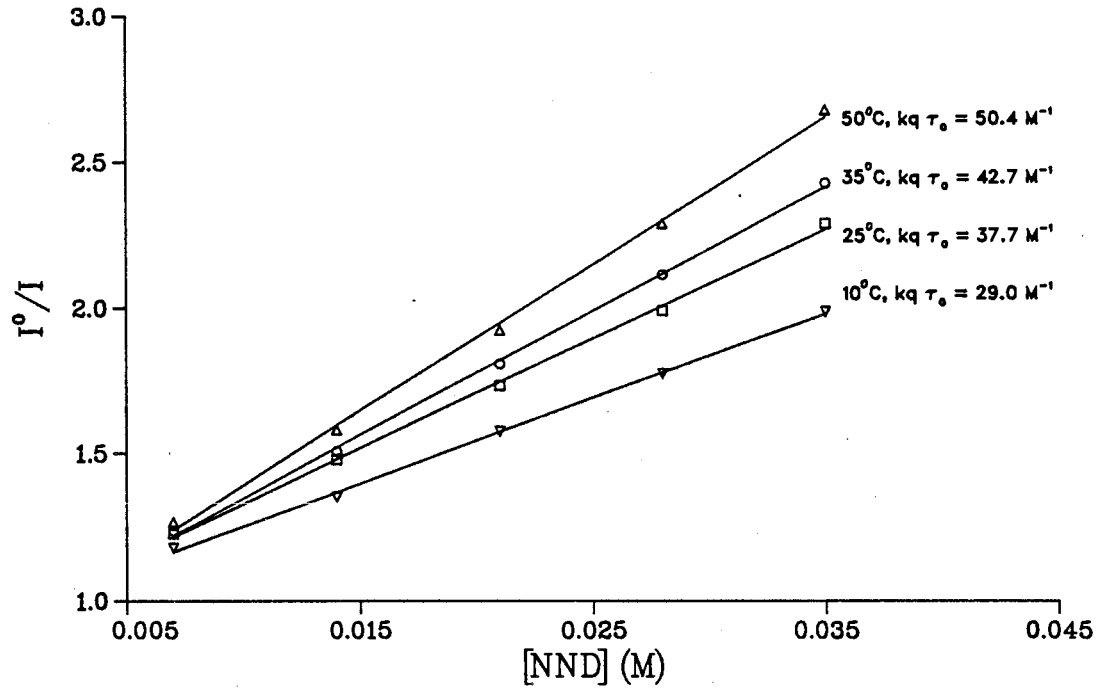

Figure 2-15 The Stern-Volmer plots of I^o/I *vs* [NND] for quenching of 1-AnOH (0.0002 M) fluorescence by NND in dioxane at various temperature.

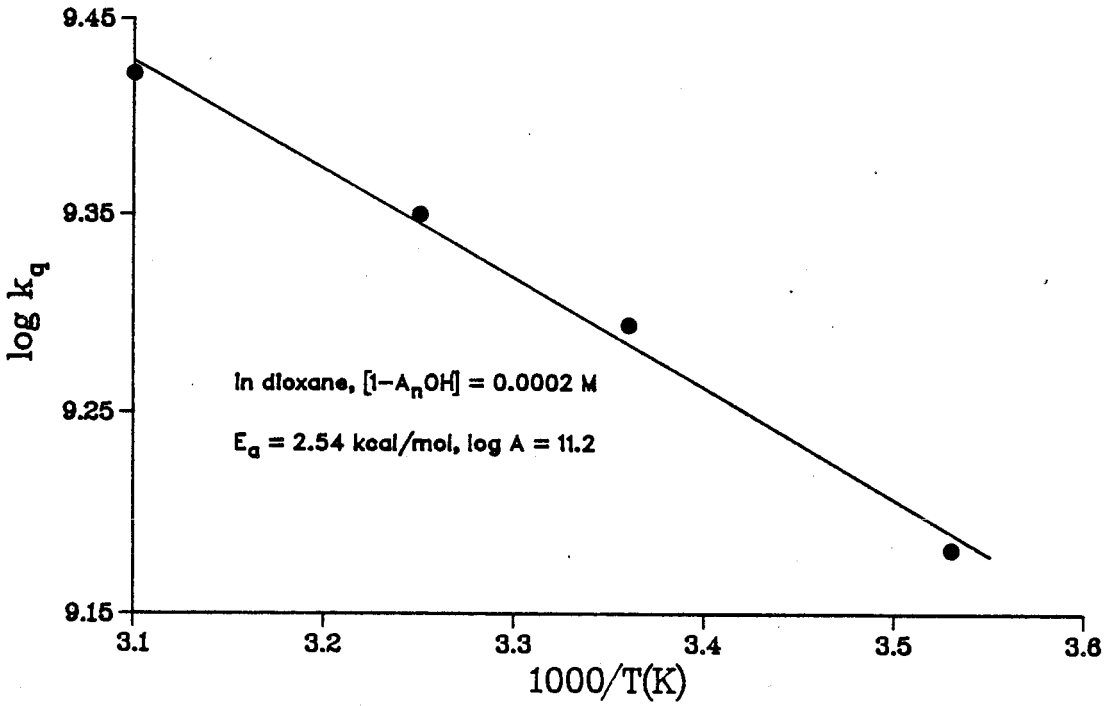

Figure 2-16 The Arrhenius plot of log kq *vs* 1/T for quenching of 1-AnOH fluorescence by NND in dioxane.

2.1.5 Time-Resolved Fluorescence Studies

Fluorescence lifetimes for 1-NpOH, O-deutero-1-naphthol (1-NpOD) and 1-AnOH in the absence (τ_o) and in the presence (τ) of the various concentrations of NND were determined with pulsed laser (a synchronously pumped, cavity-dumped and mode locked dye laser system) excitation at λ_{ex} = 300 nm and using the single-photon-counting method.[61,62] The apparatus was made available by the courtesy of Professor M.L.W. Thewalt. The data were treated with the Stern-Volmer equation to give quenching rate constants:

$$\tau_o/\tau = 1 + k_q\tau_o\,[NND] \qquad 2\text{-}10$$

In addition, transient fluorescence spectra were recorded at various delay times.

2.1.5.1 1-Naphthol

The steady-state fluorescence of 1-NpOH in methanol at room temperature was determined with an excitation wavelength of 300 nm and showed a maximum emission at 340 nm. Addition of 0.002 M potassium hydroxide as a proton acceptor shifted the emission maximum to 460 nm, which indicated that the origin of the emission was ^{1*}1-NpO$^-$ (see Figure 5-5, in Experimental). The transient fluorescence spectra (Figure 2-17) of 1-NpOH (0.0006 M) in acetonitrile were recorded at 20°C using laser excitation at 300 nm and scanning from 320 to 520 nm at various delay times (1-20 ns). These transient spectra show a similar shape to the steady-state fluorescence spectrum. Similar measurements in the presence of NND (0.006 M) in acetonitrile (Figure 2-18) and in the presence of NND (0.060 M) in THF (Figure 2-19) were examined.

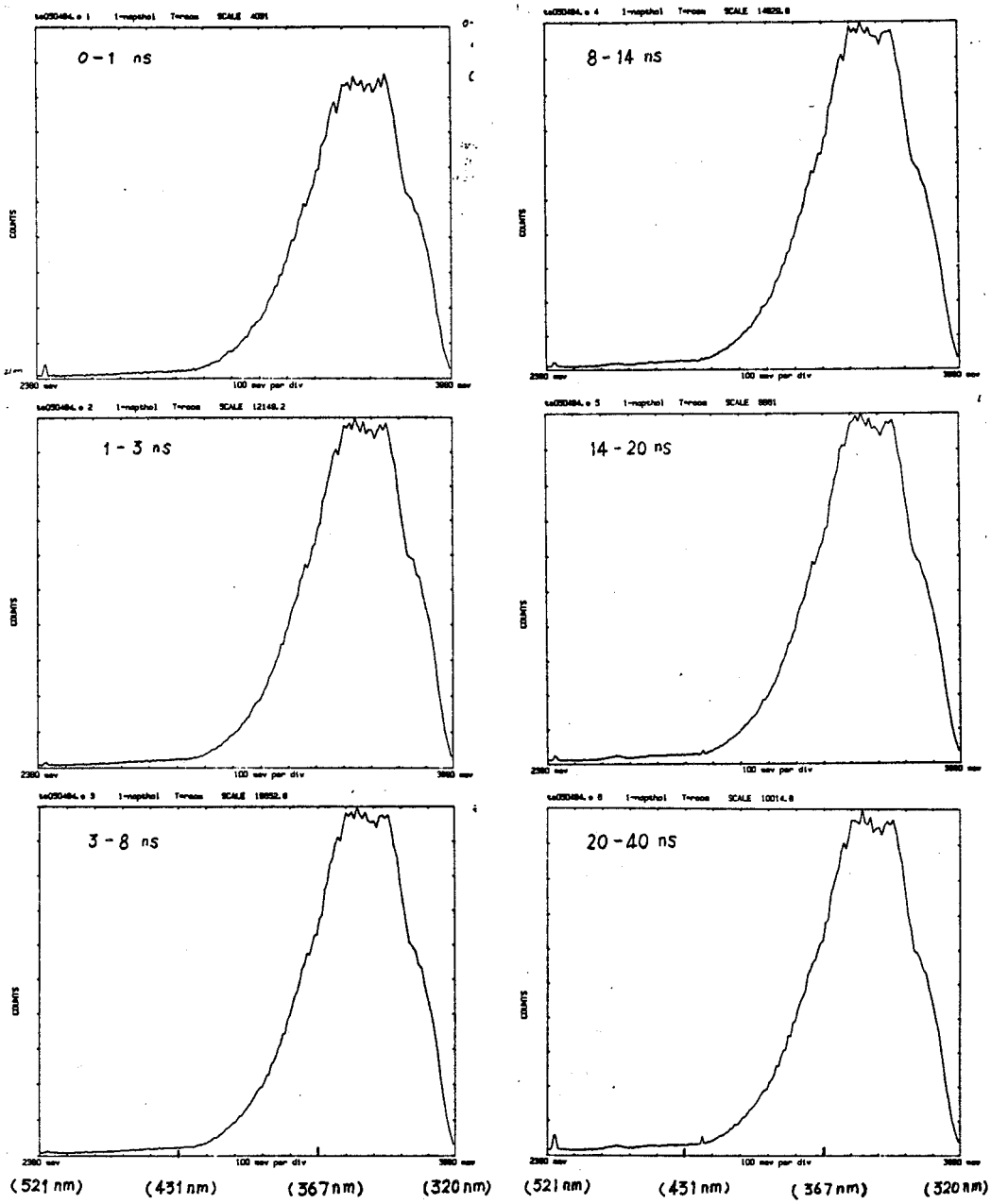

Figure 2-17 Transient fluorescence spectra of 1-NpOH (0.0006 M) in acetonitrile at room temperature; the excitation wavelength was 300 nm.

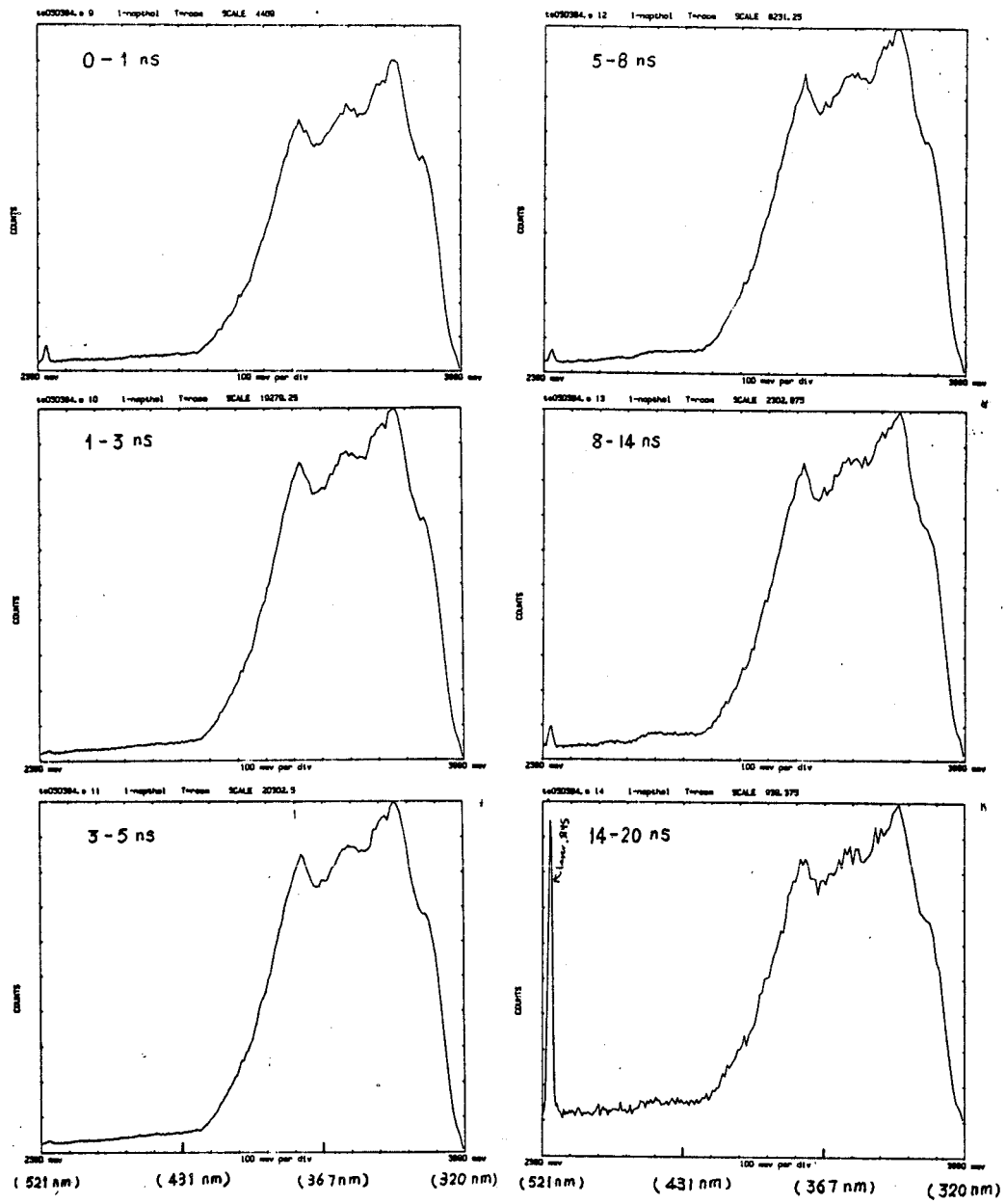

Figure 2-18 Transient fluorescence spectra of 1-NpOH (0.0006 M) in acetonitrile in the prescence of NND (0.006 M) at room temperature, the excitation wavelength was 300 nm.

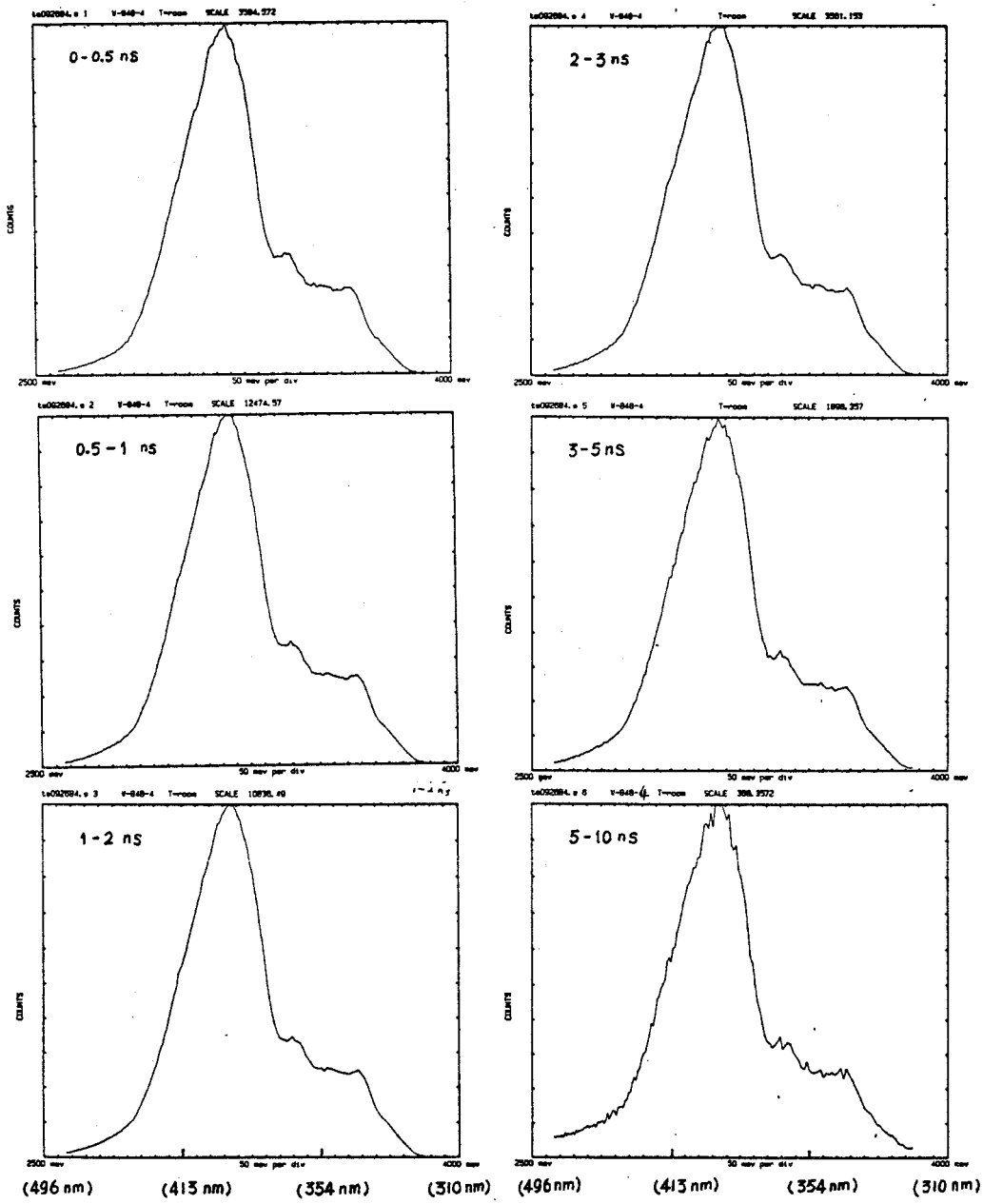

Figure 2-19 Transient fluorescence spectra of 1-NpOH (0.0006 M) in THF in the prescence of NND (0.060 M) at room temperature, the excitation wavelength was 300 nm.

Inspection of transient spectra in Figures 2-18 and 2-19 reveals no change in the spectral shape at various delay times. Furthermore, the shape of the emission spectra is unaffected by the lower concentration of NND (0.006 M),(see Figures 2-17 and 2-18), but distorted by the higher concentration of NND (0.060 M) (Figure 2-19). The spectra show an emission maximum at 390 nm and a shoulder at about 340 nm. This pattern is similar to that observed in the steady-state fluorescence spectra (Figure 2-9). The shoulder is caused by the distortion of the spectra, owing to reabsorption of emission at 340 nm by NND at its high concentration (see Figure 2-7).

The fluorescence lifetimes of 1-NpOH in dioxane at room temperature in the absence and presence of NND (0.0004-0.025 M) were determined at emission wavelengths of 330, 345 and 400 nm, respectively, with the excitation wavelength of 300 nm. The decay curves are single-exponential both in the absence and in the presence of various concentrations of NND, as shown in an example in Figure 2-20. The measured lifetimes are independent of the monitoring emission wavelength and decrease with increasing concentration of NND (Table 2-3). Based on Equation 2-10, the linear Stern-Volmer plot (Figure 2-21) of τ_o/τ at 345 nm against [NND] yielded a slope of 81 M^{-1} from which the quenching rate constant was calculated to be $k_q = 7.6 \times 10^9\ M^{-1}s^{-1}$. This k_q value is somewhat smaller than that obtained from fluorescence intensity quenching in the same solvent ($k_q = 11.0 \times 10^9\ M^{-1}s^{-1}$). This observation implies that the static quenching process is of minor importance (*vide infra*).

Table 2-3 Fluorescence Lifetimes of 1-NpOH (0.0002 M) in the Absence and Presence of Various Concentrations of NND at Various Emission Wavelengths[a]

[NND] x 10^3 (M)	τ (ns) 300 nm	345 nm	400 nm
0	10.60	10.70	10.70
0.4	10.10	10.20	10.10
1.2	9.17	9.36	9.01
2.0	8.90	8.80	8.30
4.0	7.15	6.94	7.02
8.0	6.48	6.45	6.33
12.0	5.10	5.10	5.05
16.0	4.55	4.50	4.43
20.0	4.05	4.06	3.90
25.0	3.47	3.42	3.27
$k_q\tau_o$ (M^{-1})	80±2	81±3	85±3
k_q x 10^{-9} ($M^{-1}s^{-1}$)	7.6±0.2	7.6±0.3	7.9±0.3
r	0.997	0.997	0.997

a. The samples were excited in dioxane solution at 300 nm at room temperature.

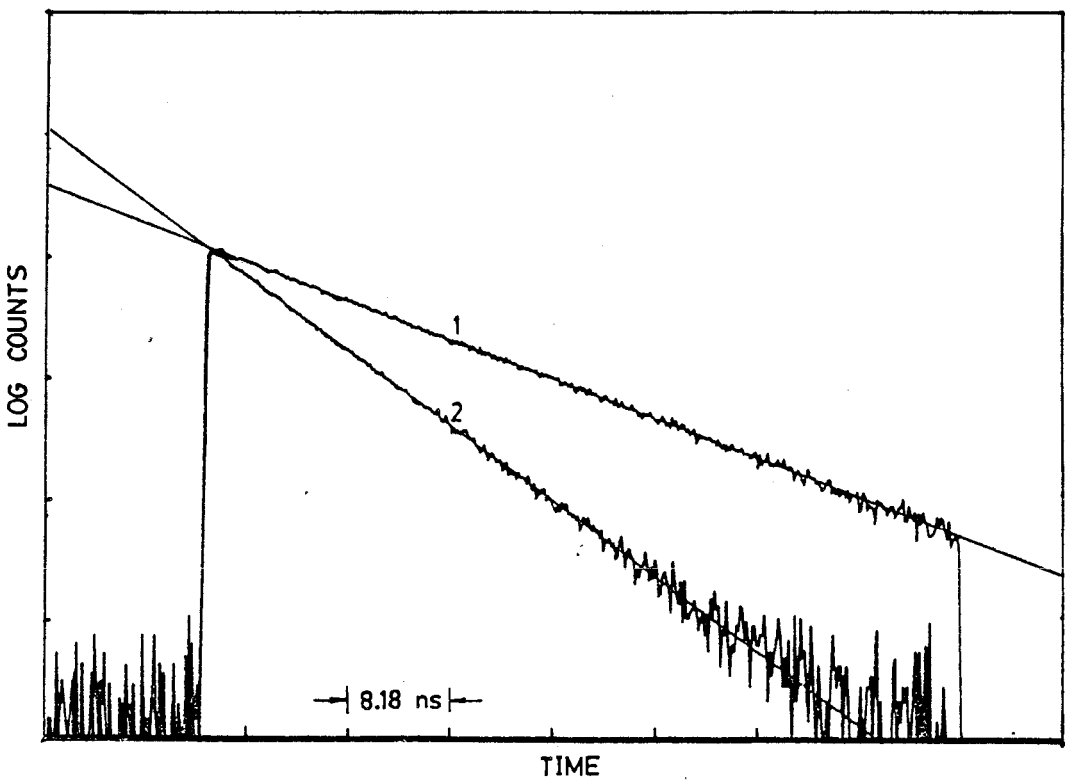

Figure 2-20 Decay curves of 1-NpOH (0.0002 M) in dioxane at room temperature in the absence (curve 1) and presence of NND (0.0012 M, curve 2); the sample solutions were excited at 300 nm and monitored at 345 nm.

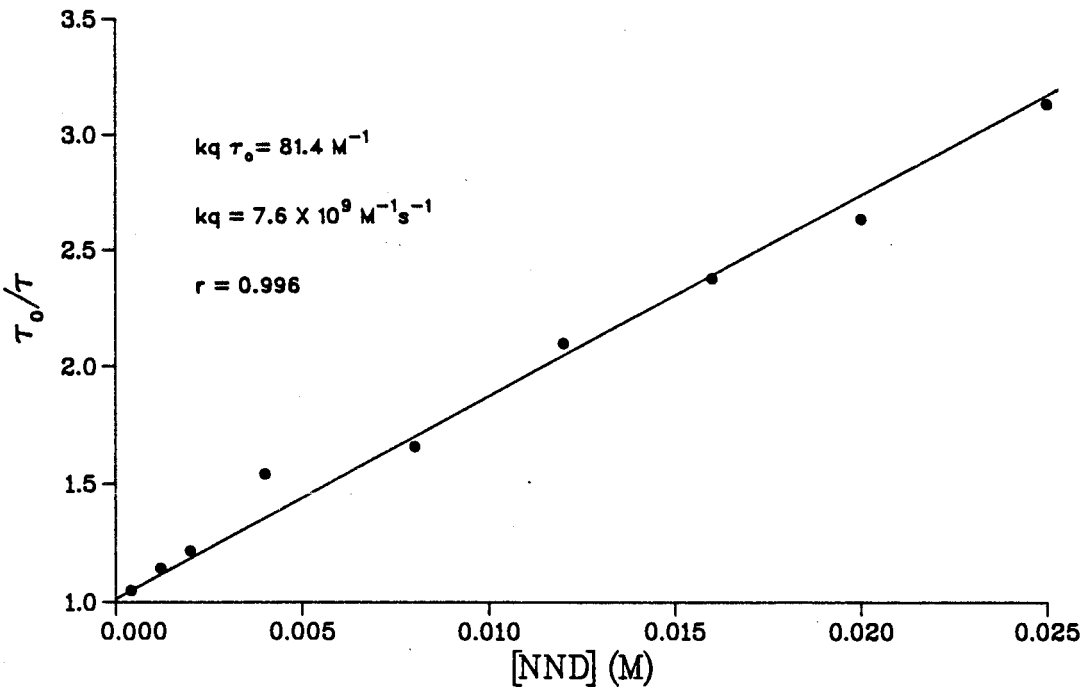

Figure 2-21 The Stern-Volmer plot of τ_o/τ *vs* [NND] for quenching of fluorescence lifetimes of 1-NpOH (0.0002 M) by NND in dioxane at room temperature.

Fluorescence lifetimes of 1-NpOH (0.0002 M) in methanol in the absence and presence of various concentrations (0.030-0.180 M) of 1,2-epoxyethylbenzene (EPO) were determined with excitation at 310 nm and monitoring at 355 nm. All decay curves are also single-exponential. The lifetimes (Table 2-4) are almost independent of the concentration of NND, although the quenching of 1-NpOH fluorescence by EPO was measured previously in our laboratory[63] to give $k_q = 1.4 \times 10^9\ M^{-1}s^{-1}$. Obviously, this indicates a static quenching character in the system of 1-NpOH and EPO.

Table 2-4 Fluorescence Lifetimes of 1-NpOH (0.0002 M) in Methanol in the Absence and in the Presence of EPO[a]

[EPO] M	τ[b] ns
0	7.69 ± 0.06
0.030	7.53 ± 0.16
0.050	7.59 ± 0.06
0.080	7.50 ± 0.07
0.130	7.46 ± 0.03
0.180	7.24 ± 0.06

a. The sample solutions were excited at 310 nm and monitored at 355 nm.

b. Each τ value was averaged from three runs.

The decrease of the 1-NpOH fluorescence lifetime with increasing [NND] implies that the quenching process is dynamic. Both the single-exponential decay curves and the transient fluorescence spectra at various delay times indicate the existence of a single emitting species of ^{1*}1-NpOH. In other words, neither ^{1*}1-NpO$^-$ (emitting at 460 nm in Figure 5-5) nor an exciplex of ^{1*}1-NpOH with NND is detectable by using time-resolved fluorimetry.

2.1.5.2 O-Deutero-1-naphthol

The transient fluorescence spectra (Figure 2-22) of 1-NpOD (0.00034 M) at various delay times (1-17 ns) in dioxane in the presence of NND (0.025 M) measured under conditions similar to those used with 1-NpOH show no change in spectral shape and no new emission at 460 nm from ^{1*}1-NpO$^-$. The fluorescence decays of 1-NpOD in the absence and presence of NND (0.0050-0.0250 M) also show the single-exponential pattern and about the same τ values as those of 1-NpOH (see Tables 2-3 and 2-5). The quenching rate constant of k_q = 8.1 x 10^9 $M^{-1}s^{-1}$ is close to that for the system of 1-NpOH and NND (7.6 x 10^9 $M^{-1}s^{-1}$), indicating no substantial deuterium isotopic effect.

2.1.5.3 1-Anthrol

A steady-state fluorescence spectrum of 1-AnOH in THF, recorded with excitation at 350 nm at room temperature, showed an emission maximum at 445 nm, which was shifted to 610-620 nm by the presence of potassium hydroxide (0.0020 M). This maximum is assigned to the emission from ^{1*}1-AnO$^-$ (Figure 2-23). Adding H_2O to the THF solution of 1-AnOH also generated the emission from ^{1*}1-AnO$^-$ (Curve 3 in Figure 2-23).

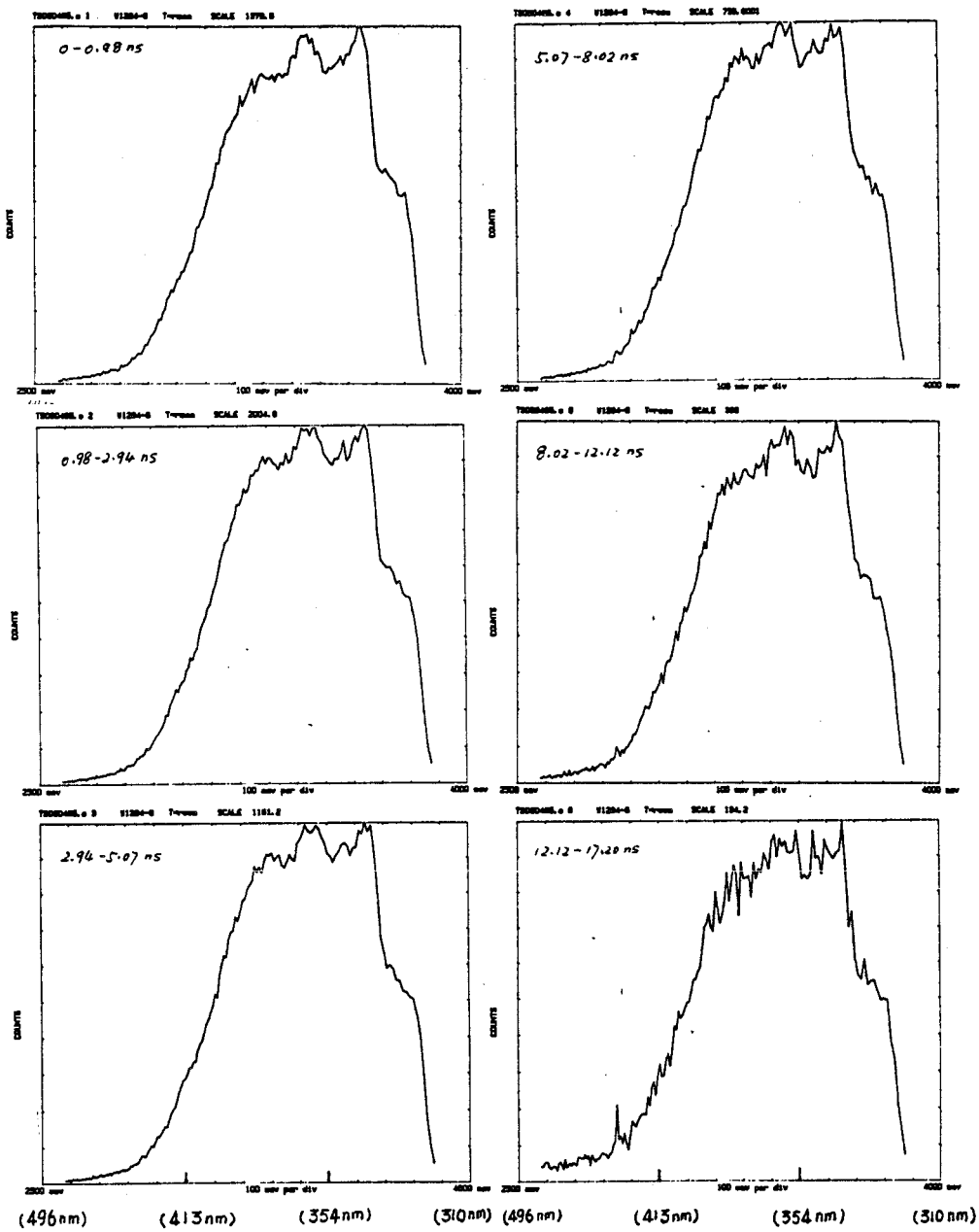

Figure 2-22 Transient fluorescence spectra of 1-NpOD (0.00034 M) in the presence of NND (0.0250 M) in dioxane at 20°C; each sample solution was excited at 300 nm and scanned from 320 nm to 480 nm.

Table 2-5 Fluorescence Lifetimes of 1-NpOD (0.00034M) in Dioxane in the Presence of Various Concentration of NND[a]

[NND] x 10^3 (M)	τ ns	τ_o/τ
0	11.15 (τ_o)	
5.0	7.64	1.15
10.0	5.83	1.91
15.0	4.77	2.33
20.0	3.98	2.79
25.0	3.39	3.27
$k_q\tau_o$ (M^{-1})		90 ± 1
k_q x 10^{-9} ($M^{-1}s^{-1}$)		8.1 ± 0.1
r		1.000

a.Each sample solution was excited at 300 nm and monitored at 345 nm at 20°C.

The transient fluorescence spectra of 1-AnOH (0.0002 M) with NND (0.025 M) in dioxane at various delay times (from 0-1.3 to 27-37 ns) were recorded using the same apparatus and conditions as those used for 1-NpOH except for scanning from 310 to 708 nm. The spectra show the emission of 1-AnOH around 413-460 nm, but no emission around 610 nm from ^{1*}1-AnO$^-$. Spectra for two delay times are shown in Figure 2-24.

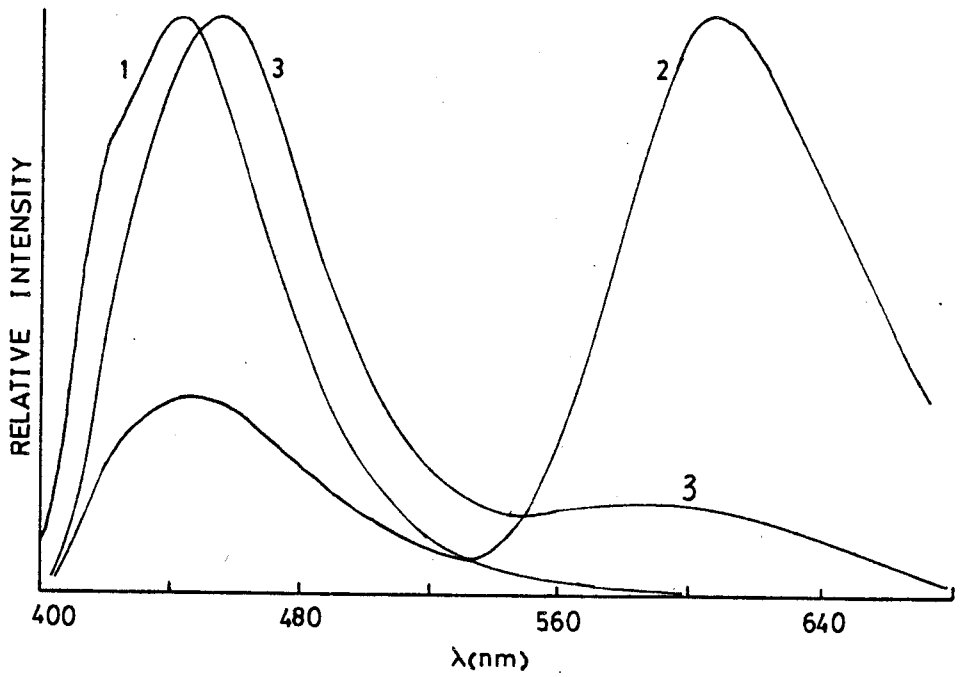

Figure 2-23 Fluorescence spectra of 1-AnOH (0.0001 M) in: (1) THF, (2) KOH (0.002 M)-THF, and (3) H_2O-THF (4:6, by volume), respectively, with excitation at 350 nm at room temperature; the maximum intensity of curves 2 and 3 was adjusted equal to that of curve 1.

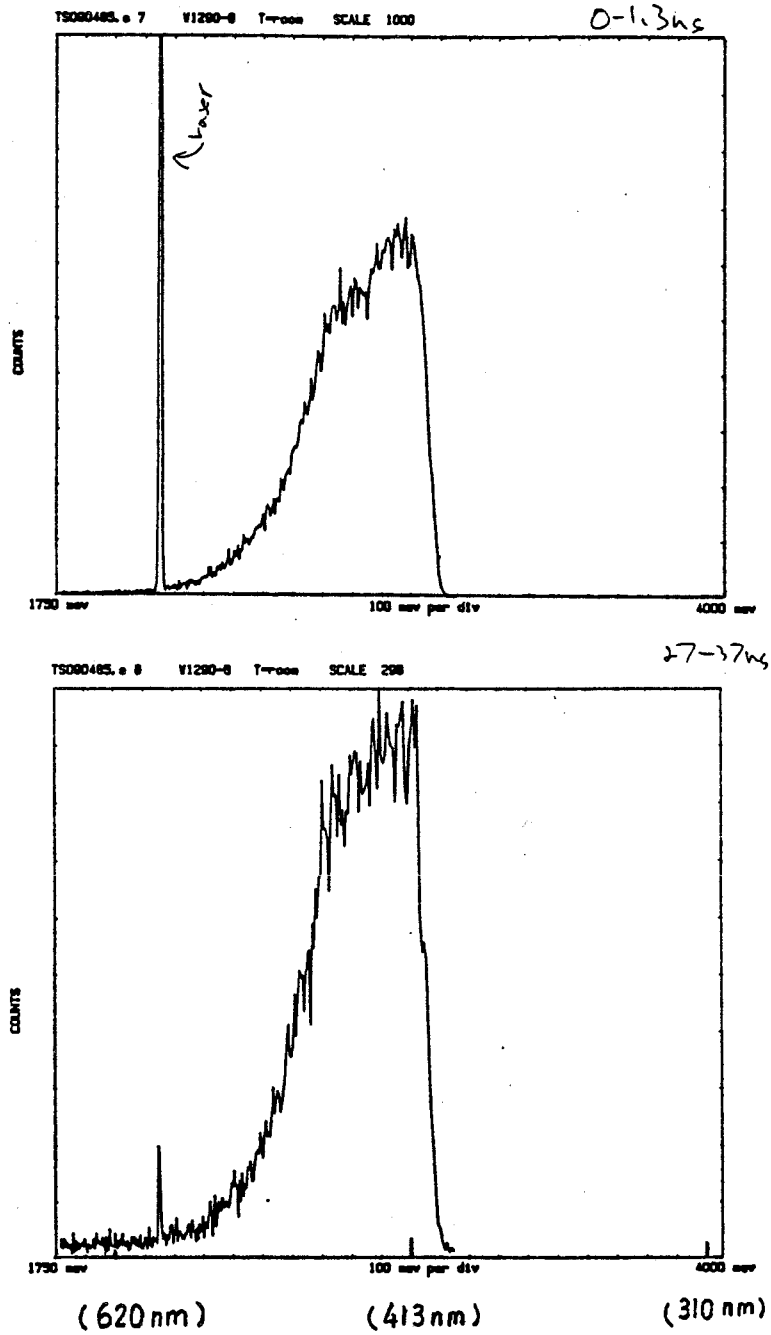

Figure 2-24 Transient fluorescence spectra of 1-AnOH (0.0002 M) in the presence of NND (0.025 M) in dioxane at 20°C; the sample solution was excited at 300 nm and scanned from 310 to 708 nm with delay times: (1) 0-1.3 ns, (2) 27-37 ns.

In the absence and presence of various concentrations of NND, fluorescence of 1-AnOH decayed with a single-exponential pattern (Figure 2-25), giving lifetimes (Table 2-6), from which the Stern-Volmer parameters of $k_q\tau_o$ = 24.4 M^{-1} and k_q = 1.28 x 10^9 $M^{-1}s^{-1}$ were obtained. These observations are similar to those for 1-NpOH. The lack of an emission band at 610 nm in the transient spectra together with the single-exponential decay pattern indicates that a single transient species of ^{1*}1-AnOH possesses a lifetime long enough to emit.

Table 2-6 Fluorescence Lifetimes of 1-AnOH (0.0002 M) in NND-Dioxane Solution[a]

[NND] x 10^3 (M)	τ ns	τ_o/τ
0.0	19.06 (τ_o)	
5.0	16.87	1.130
10.0	15.27	1.248
15.0	13.82	1.380
20.0	12.69	1.502
25.0	11.82	1.613
$k_q\tau_o$ (M^{-1})		24.4 ± 0.4
k_q x 10^{-9} ($M^{-1}s^{-1}$)		1.28 ± 0.02
r		0.996

a. Each sample solution was excited at 300 nm and monitored at 435 nm at 20°C.

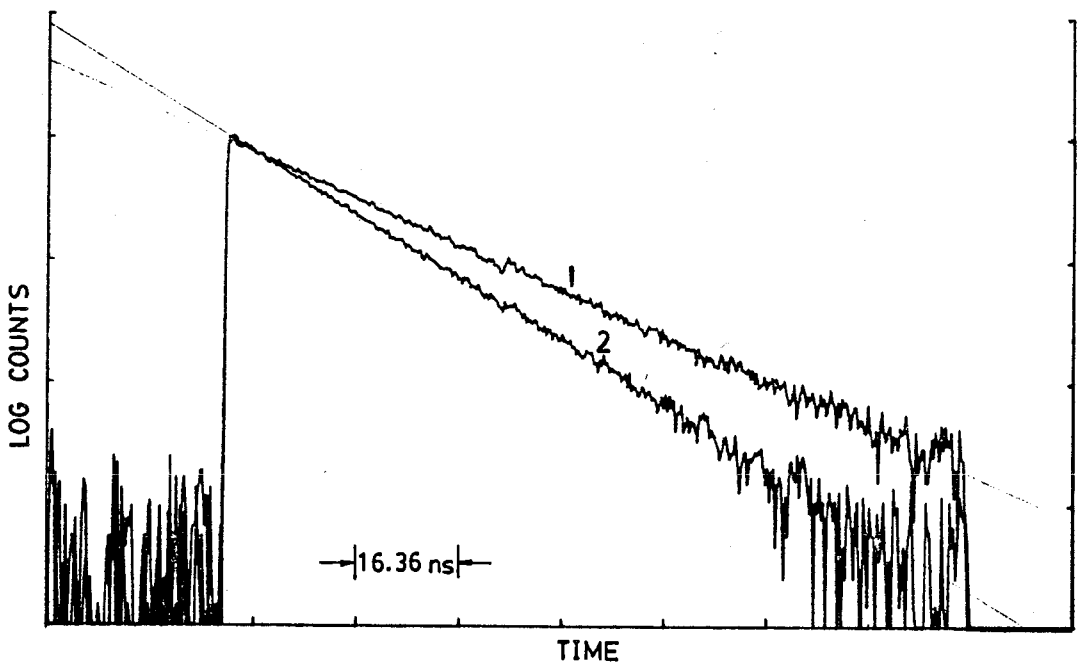

Figure 2-25 Fluorescence decay curves of 1-AnOH (0.0002 M) in the absence (1) and in the presence (2) of NND (0.0150 M) in dioxane at 20°C; each sample solution was excited at 300 nm and monitored at 435 nm.

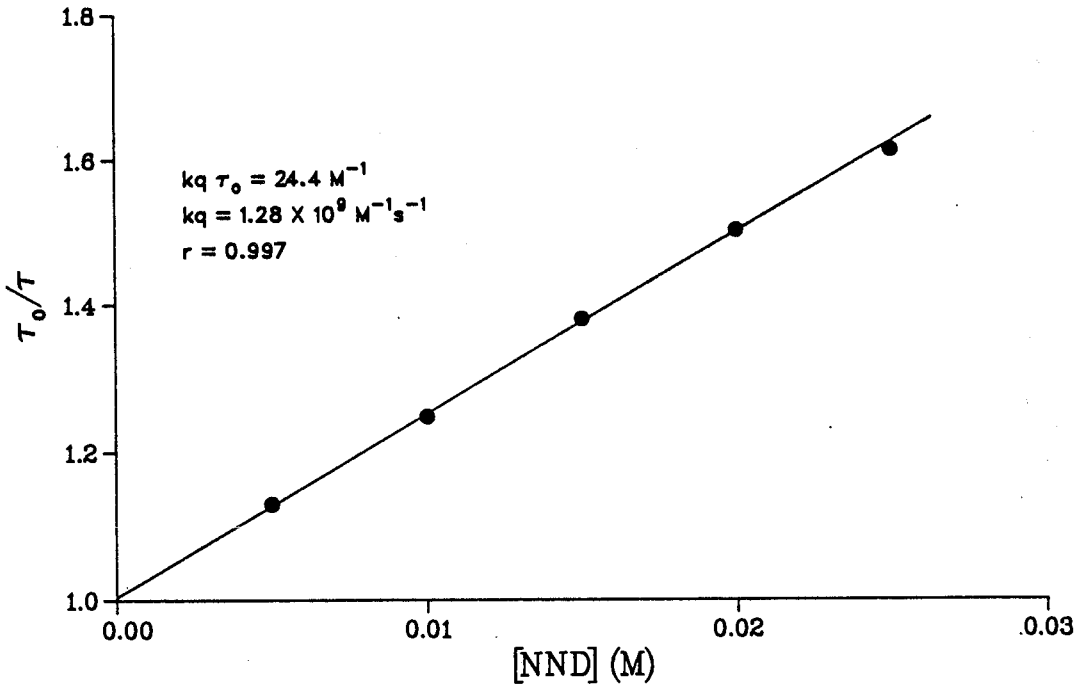

Figure 2-26 Stern-Volmer plot of τ_o/τ against [NND] for quenching of 1-AnOH fluorescence lifetime by NND in dioxane at 20°C.

2.1.6 Quantum Yield Determination

A basic reaction mechanism for the photonitrosation of 1-NpOH with NND is proposed in Scheme 2-1, based on the following findings: (i) photonitrosation leading to quinone monooxime **16**, (ii) dynamic quenching of 1-NpOH fluorescence by NND, (iii) singlet-exponential decay of 1-NpOH fluorescence in the presence of NND, (iv) neither triplet sensitization nor triplet quenching of the photonitrosation, (v) no photonitrosation by direct irradiation of NND, and (vi) no decomposition of NND by irradiation of 1-NpOMe.

$$\text{1-NpOH} \xrightarrow{h\nu,\ I} {}^{1*}\text{1-NpOH} \qquad \text{2-11}$$

$${}^{1*}\text{1-NpOH} \xrightarrow{k_f} \text{1-NpOH} + h\nu' \qquad \text{2-12}$$

$${}^{1*}\text{1-NpOH} \xrightarrow{k_{ic}} \text{1-NpOH} + \Delta \qquad \text{2-13}$$

$${}^{1*}\text{1-NpOH} \xrightarrow{k_{st}} {}^{3*}\text{1-NpOH} \qquad \text{2-14}$$

$${}^{1*}\text{1-NpOH} + \text{NND} \xrightarrow{k_q} C_1 \qquad \text{2-15}$$

$$C_1 \xrightarrow{k_p} \mathbf{16} + (\text{Me})_2\text{NH} \qquad \text{2-16}$$

$$C_1 \xrightarrow{k_{p'}} \text{by-product} \qquad \text{2-17}$$

$$C_1 \xrightarrow{k_b} \text{1-NpOH} + \text{NND} \qquad \text{2-18}$$

Scheme 2-1

In Scheme 2-1, C_1 is an exciplex assumed to be formed from the collisional interaction of ^{1*}1-NpOH with NND. C_1 could dissipate primarily by three pathways, *i.e.*, collapsing to the final products (Equation 2-16), to other unidentified by-products (Equation 2-17), or back to the starting materials (Equation 2-18). The kinetic equations 2-19 and 2-21 were derived from Scheme 2-1 using the steady state approximation (see Appendix I).

The quantum yield of NND disappearance, Φ_N, or of the formation of quinone monooxime **16**, Φ_{ox}, was determined as a function of NND concentration for the photonitrosation of 1-NpOH in various solvents. The Φ_N values were also determined for the other phenols in acetonitrile or dioxane.

$$1/\Phi_{ox} = 1/\beta + 1/\{\beta k_q \tau_o [NND]\} \qquad 2\text{-}19$$

where $\beta = \Phi_{ox}(lim) = k_p/(k_p + k_b + k_{p'})$ 2-20

$$1/\Phi_N = 1/\beta' + 1/\{\beta' k_q \tau_o [NND]\} \qquad 2\text{-}21$$

where $\beta' = \Phi_N(lim) = (k_p + k_{p'})/(k_p + k_b + k_{p'})$ 2-22

Combination of Equations 2-20 and 2-22 yields:

$$k_{p'}/k_p = \beta'/\beta - 1 \qquad 2\text{-}23$$

$$k_b/k_p = (1 - \beta')/\beta \qquad 2\text{-}24$$

If the proposed Scheme 2-1 is valid, a Stern-Volmer plot of either $1/\Phi_{ox}$ against 1/[NND] or $1/\Phi_N$ against 1/[NND] should be linear based on Equations 2-19 and 2-21. From each plot a common $k_q\tau_o$ value but different intercept should be obtained. The values of $\Phi_{ox}(lim)$, $\Phi_N(lim)$ and the ratios $(k_p:k_b:k_{p'})$ can be obtained accordingly.

2.1.6.1 Photonitrosation of 1-Naphthol

The Φ_{ox} value (Table 2-7) for the photonitrosation of 1-NpOH (0.050 M) in dioxane at 19°C was determined as a function of [NND] (0.005-0.050 M) using a 450 Watt Hanovia lamp as light source through a Pyrex filter. The light intensity was determined by the benzophenone-benzhydrol actinometer in benzene, which has a quantum yield of 0.74.[64] The incident light absorbed by 1-NpOH was corrected for that absorbed by NND. The Stern-Volmer plot (Figure 2-27) of $1/\Phi_{ox}$ against 1/[NND] yielded a straight line with slope and intercept of 0.154 M and 11.1, respectively, from which $k_q\tau_o$ and $\Phi_{ox}(lim)$ were calculated to be 72 M^{-1} and 0.091, based on Equations 2-19 and 2-20.

Table 2-7 Quantum Yields of 16 Formation in Photolysis of 1-NpOH (0.050 M) and NND in Dioxane at 19°C[a]

[NND] x 10^3 (M)	Φ_{ox}	1/[NND] (1/M)	$1/\Phi_{ox}$
5.8	0.0270	174	37.0
7.7	0.0315	130	31.8
9.6	0.0364	104	27.5
14.4	0.0449	69.4	22.3
19.2	0.0528	52.1	19.0
24.0	0.0559	41.7	17.9
28.8	0.0610	34.7	16.4
38.4	0.0680	26.0	14.7
48.0	0.0736	20.8	13.6

$k_q\tau_o$ (M^{-1})	72 ± 4
k_q x 10^{-9} ($M^{-1}s^{-1}$)[b]	6.8 ± 0.4
Φ_{ox}(lim)	0.091 ± 0.003
r	0.998

a. The sample solutions were irradiated under the same conditions with a 450 watt Hanovia lamp through a Pyrex filter for 100 min to cause 5-15% conversion of 1-NpOH.

b. τ_o = 10.6 ns from Table 2-3.

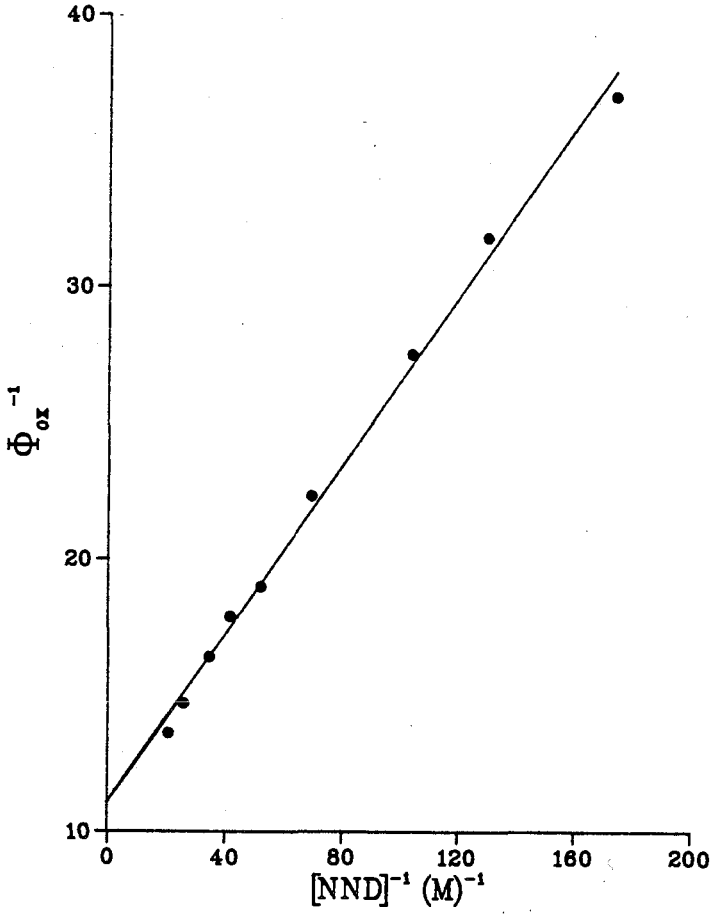

Figure 2-27 Plot of $1/\Phi_{ox}$ against 1/[NND] in dioxane according to Equation 2-19; slope = 0.154 ± 0.004 (M), intercept = 11.1 ± 0.4, and r = 0.998.

Determination of Φ_{ox} as a function of [NND] was also carried out in acetonitrile, benzene, toluene and methanol under the same conditions as in dioxane. The measured data are listed in Appendix II, and the calculated Stern-Volmer parameters are summarized in Table 2-8.

Table 2-8 The Stern-Volmer Parameters for the Photonitrosation of 1-NpOH with NND from Measurement of Φ_{ox} in Various Solvents at 19°C[a]

Solvent	$k_q\tau_o$ (M^{-1})	$k_q \times 10^{-9}$ ($M^{-1}s^{-1}$)	$(k_{p'}+k_b)/k_p$[c]	Φ_{ox}(lim)	r
Dioxane[b]	72 ± 4	6.8 ± 0.4	10.0 ± 0.3	0.091 ± 0.003	0.998
Acetonitrile[c]	81 ± 9	11.0 ± 1.0	11.5 ± 0.6	0.080 ± 0.004	0.993
Benzene[b]	33 ± 4	3.1 ± 0.4	21.7 ± 2.0	0.044 ± 0.004	0.998
Toluene[b]	45 ± 9	4.3 ± 0.8	30.3 ± 4.0	0.032 ± 0.004	0.993
Methanol[c]	85 ± 5	11.1 ± 0.6	58.8 ± 3.5	0.017 ± 0.001	0.996

a. [1-NpOH] = 0.050 M, [NND] = 0.008-0.050 M; the conversions of 1-NpOH were 5-15%.

b. τ_o = 10.6 ns[23] in nonpolar solvents.

c. τ_o = 7.7 ns. This was determined in methanol (Table 2-4) and assumed to be the same in acetonitrile.

d. $(k_{p'} + k_b)/k_p = (1/\beta) - 1$ (see Equation 2-20).

Quantum yields of Φ_{ox} and Φ_N for the photonitrosation of 1-NpOH with NND were determined in various solvents under conditions comparable to those used earlier, except that RPR-300 nm lamps were used as the light source at 31°C. The observed data are listed in Appendix II. Analysis of these data from Equations 2-19 and 2-21 yielded the Stern-Volmer constants, limiting quantum yields, quenching rate constants and rate constant ratios; all these data are listed in Table 2-9.

Table 2-9 Stern-Volmer Parameters for Photonitrosation of 1-NpOH with NND from Measurements of Both Φ_{ox} and Φ_N in Various Solvents[a]

Solvent	Φ_{ox}-monitoring			Φ_N-monitoring			
	$k_q\tau_o$ (M^{-1})	Φ_{ox}(lim)	r	$k_q\tau_o$ (M^{-1})	Φ_N(lim)	r	kp:kp':k_b[b]
Dioxane	74±7	0.08±0.01	0.997	93±9	0.15±0.01	0.996	1.0:0.9:11.0
MeCN	89±9	0.089±0.005	0.995	74±9	0.19±0.01	0.993	1.0:1.0:9.0
THF	69±9	0.094±0.006	0.993	60±5	0.24±0.01	0.999	1.0:1.6:8.0
EtOH	60±5	0.034±0.002	0.997	110±20	0.081±0.005	0.990	1.0:1.6:26.4
MeOH	82±13	0.020±0.002	0.991	-[c]	-	-	-

a. [1-NpOH] = 0.030 M, [NND] = 0.007-0.022 M, the conversions of 1-NpOH were 3-20% with irradiation at 300 nm at 31°C. See Table 2-8 for other parameters.

b. Calculated from Equations 2-23 and 2-24.

c. The change of [NND] during irradiation was too small to be determined.

Inspection of the data in Tables 2-8 and 2-9 suggests the following points: (i) The linear Stern-Volmer plots of both $1/\Phi_{ox}$ *vs* 1/[NND] and $1/\Phi_N$ *vs* 1/[NND] together with the similarity of $k_q\tau_o$ values measured from Φ_{ox} and from Φ_N in three solvents, dioxane, THF and acetonitrile, strongly support Scheme 2-1. (ii) The limiting quantum yields $\Phi_{ox}(lim)$ are sensitive to solvents and increase in the order : ethanol ≃ methanol < benzene ≃ toluene < dioxane ≃ acetonitrile ≃ THF. (iii) Photonitrosation is retarded by the hydroxylic solvents, such as methanol and ethanol, in relation to the other solvents.

2.1.6.2 Photonitrosation of O-Deutero-1-naphthol

For the system of 1-NpOD and NND, the quantum yield Φ_{ox} was determined in carefully dried dioxane as a function of [NND] under similar conditions to those used in the experiments of Table 2-9. The observed data listed in Table 2-10 are close to those obtained for 1-NpOH in Table 2-7; the Stern-Volmer parameters are, within experimental errors, the same as those measured for 1-NpOH in the same solvent (compare Tables 2-7, 2-9 and 2-10). This indicates the lack of deuterium isotope effects in photonitrosation of 1-NpOH.

2.1.6.3 Photonitrosation of the Other Phenols

The quantum yield, Φ_N, for photonitrosation of the other phenols was determined as a function of [NND] under similar conditions to those used in Table 2-9. The observed data are listed in Appendix III and the Stern-Volmer plots of $1/\Phi_N$ against 1/[NND] yielded straight lines with reasonably good correlations (r = 0.993-0.996), indicating that the mechanism proposed for the reaction of 1-NpOH and shown in Scheme 2-1 may

also operate in the reactions of these phenols. The calculated limiting quantum yields $\Phi_N(\text{lim})$, $k_q\tau_o$ and rate constant ratios $k_b/(k_p+k_{p'})$ from the slopes and intercepts are summarized in Table 2-11.

Table 2-10 Quantum Yields $\bar{\Phi}_{ox}$ for the Photonitrosation of 1-NpOD (0.030 M) with NND in Dioxane[a]

$[NND] \times 10^3$ (M)	1/[NND] (1/M)	Φ_{ox}	$1/\Phi_{ox}$
	Run No.1		
5.0	200	0.0246	40.6
7.5	133	0.0318	31.5
10.0	100	0.0383	26.1
12.5	80.0	0.0435	23.0
15.0	66.7	0.0465	21.5
17.5	57.0	0.0508	19.7
	Run No.2		
7.5	133	0.0400	25.0
10.0	100	0.0473	21.1
12.5	80.0	0.0530	18.9
15.0	66.7	0.0562	17.8
17.5	57.0	0.0614	16.3
20.0	50.0	0.0679	14.7

	Run No.1	Run No.2
$k_q\tau_o$ (M^{-1})	78 ± 4	80 ± 8
$k_q \times 10^{-9}$ ($M^{-1}s^{-1}$)	7.0 ± 0.4	7.1 ± 0.7
Φ_{ox}(lim)	0.087 ± 0.003	0.107 ± 0.006
r	0.999	0.997

a. Conversion of 1-NpOD was 5-12% at 31°C.

Table 2-11 Stern-Volmer Parameters for the Photonitrosation of Phenols (ArOH) with NND from Measurements of Φ_N[a]

ArOH (Solvent)	$kq\tau_o$ (M^{-1})	$k_b/(kp+kp')$	Φ_N(lim)	r
1-NpOH (Dioxane)	74 ± 7	5.7	0.15 ± 0.01	0.996
(MeCN)	89 ± 9	4.3	0.19 ± 0.01	0.993
2-NpOH (MeCN)	79 ± 10	13.2	0.071 ± 0.005	0.993
11 (MeCN)	59 ± 9	1.9	0.35 ± 0.04	0.994
1-AnOH (Dioxane)	34 ± 8	4.4	0.19 ± 0.04	0.993
9-AnOH (Dioxane)	79 ± 8	3.4	0.23 ± 0.01	0.996
15 (THF)	38 ± 6	4.7	0.18 ± 0.02	0.996

a. The sample solutions of [ArOH] = 0.030 M and [NND] = 0.007-0.020 M were irradiated at 300 nm at 31°C to cause 3-20% conversion of the phenols.

2.1.7 Quenching of Photonitrosation of 1-NpOH

In order to examine the crucial proton transfer process from ^{1*}1-NpOH to NND in photonitrosation, a proton acceptor (B), such as H_2O, TEA or DMF was used as a competing substrate (Equation 2-25):

$$C_1 \xleftarrow[\text{NND}]{k_q} {}^{1*}\text{1-NpOH} \xrightarrow[\text{B}]{k_c} {}^{1*}\text{1-NpO}^- + BH^+ \qquad 2\text{-}25$$

$$B = H_2O, \text{ TEA or DMF}$$

where k_q is the quenching rate constant for the exciplex C_1 formation from ^{1*}1-NpOH with NND and k_c that for a proton transfer process from ^{1*}1-NpOH to the base. It was expected that the quantum yield of the photonitrosation at a fixed concentration of NND should decrease as the concentration of B was increased. The k_c value was evaluated from Equation 2-26 (for derivation, see Appendix I):

$$\Phi_N^o/\Phi_N = \Phi_{ox}^o/\Phi_{ox} = 1 + k_c\tau[B] \qquad 2\text{-}26$$

where the superscript "^{o}" indicates the absence of the base, and τ is the lifetime of ^{1*}1-NpOH at a fixed concentration of NND, but in the absence of B.

2.1.7.1 Quenching by Water

Water is the most commonly used proton acceptor in studies of proton transfer from the singlet excited state phenols.[29,65-68] In fluorescence spectra (Figure 2-28) of 1-NpOH in dioxane-H_2O (25-40%), for example, two

bands appeared at 340 and 460 nm with an isosbestic point at 420 nm. With increasing H_2O percentage, the intensity at 340 nm for ^{1*}1-NpOH decreased, and that at 460 nm for ^{1*}1-NpO^- increased. This observation strongly supports the proton transfer process shown in Equation 2-27:

$$^{1*}\text{1-NpOH} + H_2O \rightleftharpoons [^{1*}\text{1-Np}O^- \quad H_3O^+] \qquad 2\text{-}27$$

$$\lambda_{em} = 340 \text{ nm} \qquad \lambda_{em} = 460 \text{ nm}$$

In the H_2O concentration range of 0.50 to 5.0 M, the quenching of 1-NpOH fluorescence in THF was recorded at 20°C as shown in Figure 2-29. The intensity was decreased, and the spectra were made more complex and broader by the presence of H_2O. The Stern-Volmer plot of the intensity ratio $I°/I$ against $[H_2O]$ yielded a straight line with a slope of $k_c(H_2O)\tau_o$ = 0.325 M^{-1} (Table 2- 11). The k_q value was evaluated to be about 3.5 x 10^7 $M^{-1}s^{-1}$, adopting the τ_o value of 9.3 ns which was determined in THF (see Section 5.7.3 in Experimental).

For the photonitrosation of 1-NpOH with NND in THF solution, the quantum yields, Φ_{ox} and Φ_N , were respectively determined as a function of $[H_2O]$ in the range of 0.50-5.00 M under the same conditions (Table 2-12), and treated according to Equation 2-26 to give slopes: $k_c(H_2O)\tau$ = 0.188 M^{-1} and 0.233 M^{-1}, respectively. These data led to $k_c(H_2O)$ values of 4.6 x 10^7 $M^{-1}s^{-1}$ and 5.7 x 10^7 $M^{-1}s^{-1}$, adopting the τ value of 4.1 ns which was determined in dioxane at [NND] = 0.020 M in Table 2-3, and assumed to be the same as in THF in the presence of 0.020 M NND. Accordingly, the $k_c(H_2O)$ value measured from the quenching of fluorescence intensity is consistent with that from quantum yield measurement.

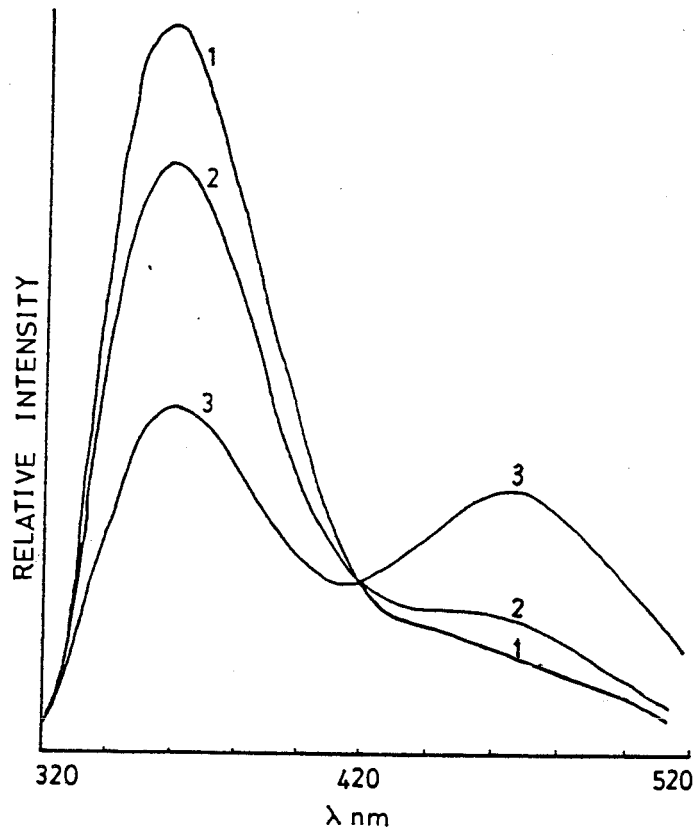

Figure 2-28 Fluorescence spectra of 1-NpOH (0.0002 M) in dioxane-H_2O; H_2O concentrations were 25% (14M), 30% (17M) and 40% (22M) for curves 1, 2 and 3, respectively.

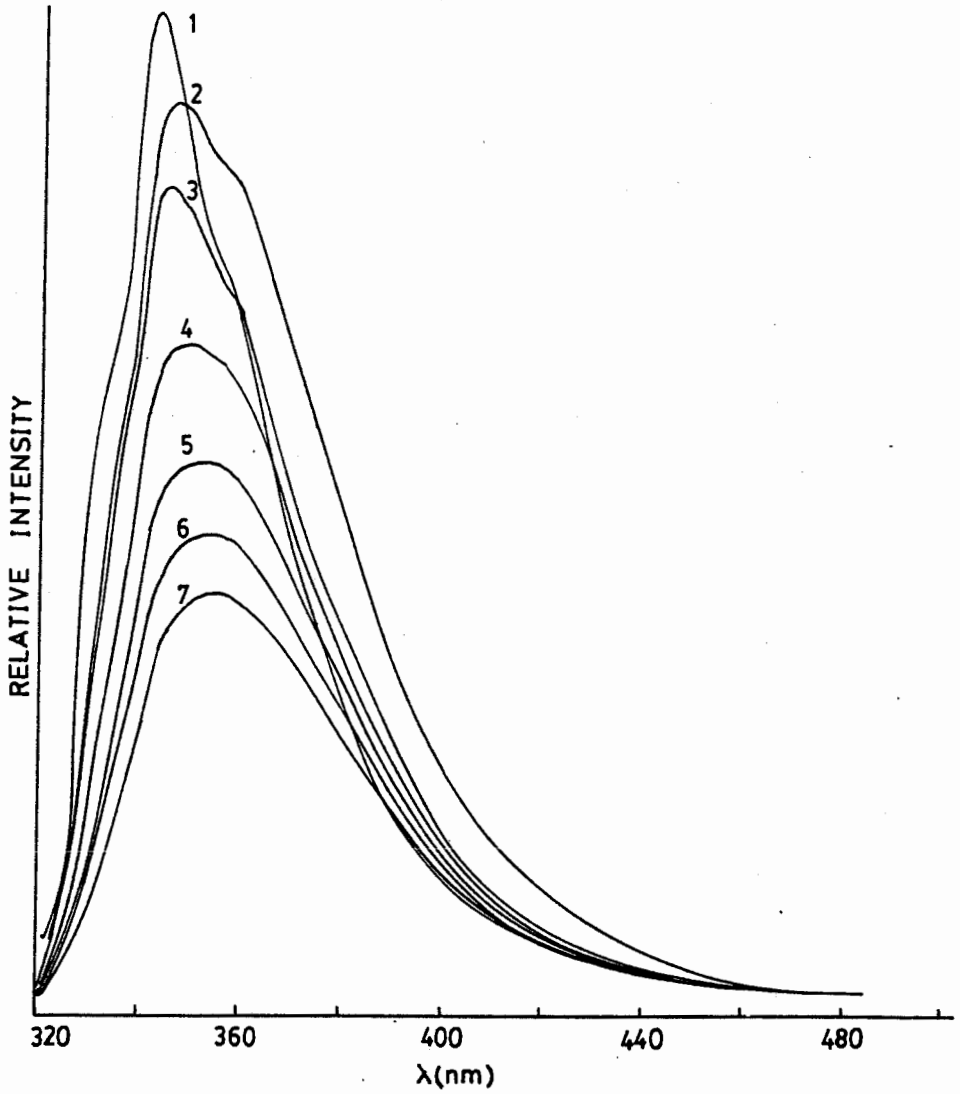

Figure 2-29 Fluorescence spectra of 1-NpOH (0.0002 M) in THF at room temperature in the absence and presence of H_2O with excitation wavelength at 300 nm; curves 1-7 contained [H_2O] of 0, 0.50, 1.00, 2.00, 3.00, 4.00 and 5.00 M, respectively.

Table 2-12 Effects of Water on Photonitrosation of 1-NpOH (0.030 M) with NND (0.020 M)[a] and on Fluorescence Intensity of 1-NpOH

$[H_2O]$ (M)	Φ_{ox}	Φ_{ox}^{o}/Φ_{ox}	Φ_N	$\Phi_N{}^{o}/\Phi_N$	I^{o}/I^{b}
0	0.0570		0.111		
0.50	0.0476	1.20	0.111	1.00	1.14
1.00	0.0441	1.29	0.100	1.11	1.22
2.00	0.0372	1.53	0.0870	1.28	1.57
3.00	0.0333	1.71	0.0717	1.55	1.93
4.00	0.0296	1.93	0.0652	1.70	2.27
5.00	0.0283	2.01	0.0544	2.04	2.54
$k_c(H_2O)\tau$ (M^{-1})	0.188 ± 0.011		0.233 ± 0.012		0.325 ± 0.010
$k_c \times 10^{-7}$ ($M^{-1}s^{-1}$)	4.6 ± 0.3		5.7 ± 0.3		3.5 ± 0.1
r	0.994		0.994		0.998

a. Each sample solution in THF was irradiated with RPR lamps at 300 nm at 31°C for 20 min to cause 6-13% conversion of 1-NpOH.

b. The excitation wavelength was 300 nm, and the monitoring one was 340nm in THF at room temperature in the absence of NND.

2.1.7.2 Quenching by TEA

It is well known that TEA adiabatically quenches the fluorescence of naphthols by a proton transfer mechanism.[58,69-71] 2-Naphtholate anion fluorescence at 445 nm , for example, was detected in acetonitrile solution of 2-NpOH and TEA by both static and time-resolved fluorimetry.[69] The fluorescence quenching experiments for the systems 1-NpOH/TEA and 2-NpOH/TEA

were carried out in acetonitrile at room temperature with an excitation wavelength of 300 nm. In the former system (Figure 2-30), with increasing the concentration of TEA, the fluorescence intensity at 350 nm (1-NpOH) decreased and a new broad emission band, assigned to emission from 1-naphtholate (1-NpO$^-$), appeared around 460-480 nm with an isosbestic point at 440 nm (compare with Figure 5-5). The Stern-Volmer plot of I°/I *vs* [TEA] at 350 nm gave $k_q\tau_o$ = 31.6 M^{-1} with r = 0.992. The system of 2-NpOH/TEA provided similar results (see Figure 5-7 in Experimental).

The quantum yield (Φ_{ox}) of the photonitrosation of 1-NpOH (0.030 M) with NND (0.020 M) in dioxane was determined as a function of [TEA]. With increasing concentration of TEA, the Φ_{ox} value first decreased then leveled off as shown in the plot of $\Phi_{ox}^\circ/\Phi_{ox}$ against [TEA] in the insert of Figure 2-31. The Stern-Volmer correlation for the initial part of quenching gave $k_c(TEA)\tau$ = 3.08 M^{-1}. In the same solvent, quenching of 1-NpOH (0.0002 M) fluorescence without NND by TEA was also determined at 18°C, showing no new emission around 460 nm, and the pertinent data are summarized in the same table for comparison with the quenching of photonitrosation. The two k_c values obtained under these conditions show substantial discrepancy (Table 2-13).

2.1.7.3 Quenching by DMF

The emission of the hydrogen-bonded exciplex between ^{1*}1-NpOH and DMF at 360 nm was detected at 77 K.[58] The nature of phenol-DMF and phenol-NND ground state hydrogen-bonded complexes was also investigated by IR spectroscopy giving equilibrium constants K = 60 M^{-1} and 13.5 M^{-1}, respectively, at 25°C in carbon tetrachloride.[72]

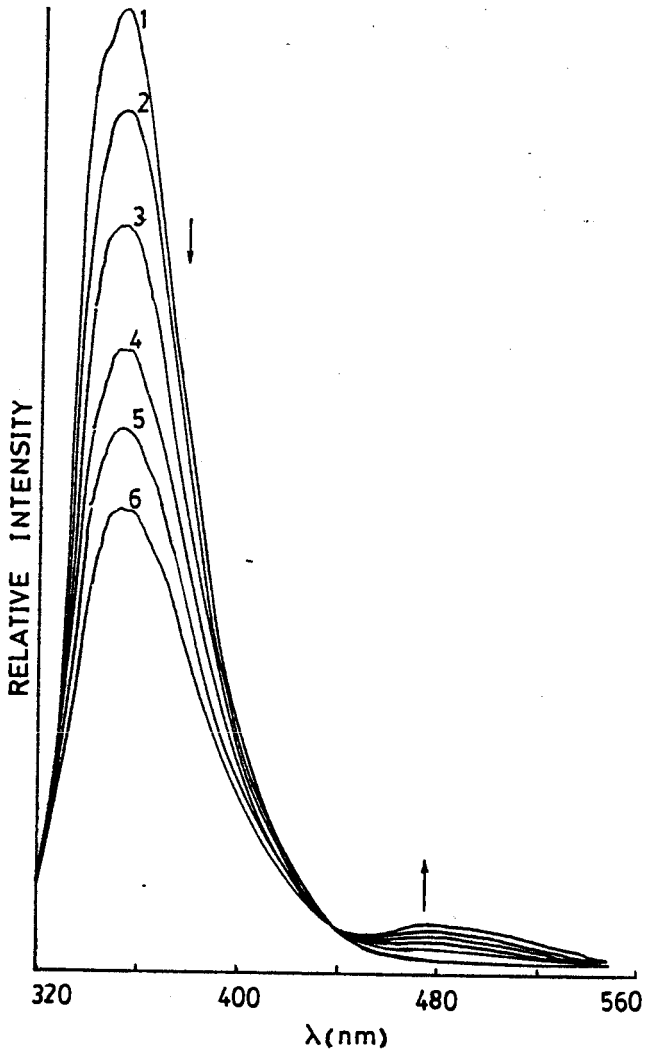

Figure 2-30 Fluorescence spectra of 1-NpOH (0.0002 M) in acetonitrile at room temperature in the absence and presence of TEA; curves 1-6 contained [TEA] of 0, 0.004, 0.010, 0.016, 0.024 and 0.036 M.

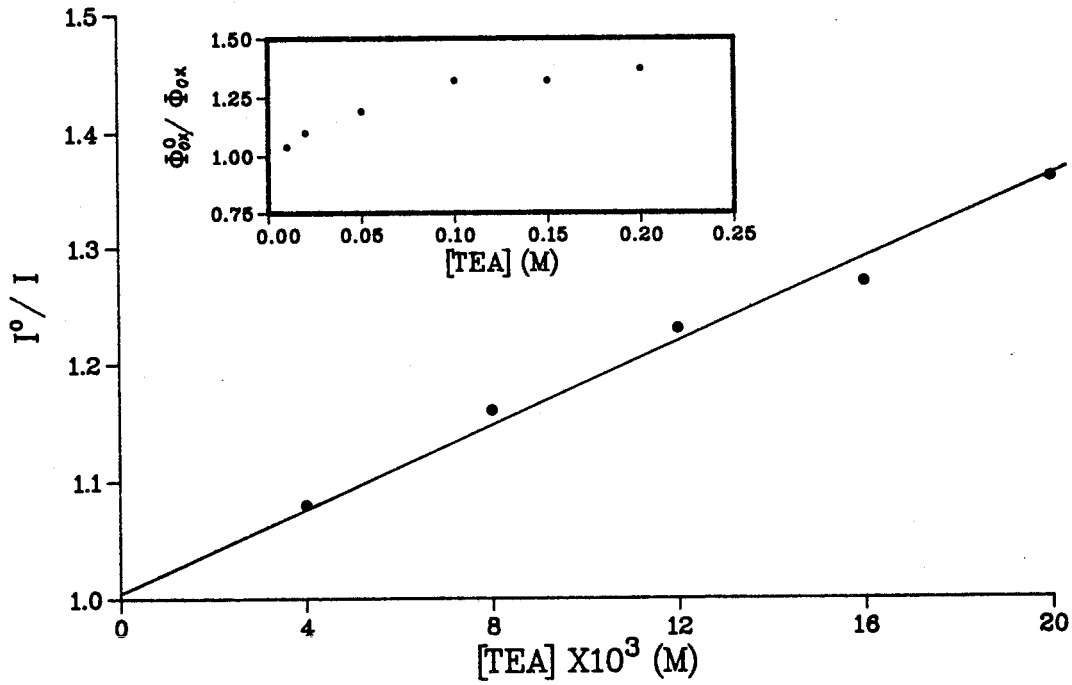

Figure 2-31 Quenching of 1-NpOH (0.0002 M) fluorescence by TEA (0.004-0.020 M) in dioxane at 18°C; the insert is the quenching of photonitrosation of 1-NpOH (0.030 M) with NND (0.020 M) by TEA (0.010-0.200 M).

Table 2-13 Effects of TEA on Photonitrosation of 1-NpOH (0.030 M) with NND (0.020 M)[a] and on Fluorescence Intensity of 1-NpOH

[TEA] (M)	Φ_{ox}[a]	$\Phi^{\circ}_{ox}/\Phi_{ox}$	[TEA] (M)	I°/I[c]
0	0.0438		0	
0.010	0.0418	1.04	0.004	1.08
0.020	0.0405	1.08	0.008	1.16
0.050	0.0370	1.18	0.012	1.23
0.100	0.0331	1.32	0.016	1.28
0.150	0.0331	1.32	0.020	1.36
0.200	0.0318	1.37		
$k_c(TEA)\tau$ (M^{-1})		3.08 ± 0.01[b]		17.0 ± 0.7
$k_c(TEA)$ x 10^{-8} ($M^{-1}s^{-1}$)		7.5 ± 0.2		16.0 ± 0.6
r		0.994		0.995

a. Each sample solution in dioxane was irradiated under the same conditions, with a 450 Watt Hanovia lamp through a Pyrex filter at 18°C for 120 min to cause 5-15% conversion of 1-NpOH.

b. The correlation was established from the first four data, and τ value was determined to be 4.1 ns at [NND] = 0.020 M (see Table 2-3)

c. [1-NpOH] = 0.0002 M, the excitation wavelength was 300 nm and the monitoring one was 344 nm in the absence of NND at 20°C.

The quantum yield, Φ_{ox}, for the photonitrosation of 1-NpOH (0.030 M) with NND (0.010 M) in dioxane was determined as a function of [DMF] (0-1.3 M) at 31°C. Quenching of 1-NpOH (0.0004 M) fluorescence by DMF (0.030-0.300 M) was also measured in the same solvent at 20°C, as shown in Table 2-14.

Table 2-14 Effects of DMF on Photonitrosation of 1-NpOH (0.030 M) with NND (0.010 M) and on Fluorescence of 1-NpOH in Dioxane

[DMF] (M)	Φ_{ox}[a]	$\Phi_{ox}^{\circ}/\Phi_{ox}$	[DMF] (M)	I°/I[b]
0	0.0429		0.030	1.46
0.10	0.0364	1.18	0.060	1.68
0.40	0.0346	1.24	0.120	2.39
0.70	0.0316	1.35	0.180	3.08
1.00	0.0292	1.47	0.240	3.47
1.30	0.0271	1.58	0.300	4.19
$k_c(DMF)\tau$ (M^{-1})[c]		0.34 ± 0.02		10.1 ± 0.3
$k_c(DMF) \times 10^{-7}$ ($M^{-1}s^{-1}$)		6.0 ± 0.4		94 ± 3
r		0.994		0.997

a. Each sample solution was irradiated under the same conditions by RPR lamps at 300 nm at 31°C for 20 min to cause 5-15% conversion of 1-NpOH.

b. The excitation wavelength was 300 nm and the monitoring one was 344 nm in the absence of NND at room temperature.

c. The τ value was determined to be 5.7 ns at [NND] = 0.010 M in dioxane (Table 2-3).

DMF quenches fluorescence of 1-NpOH fifteen times more efficiently than it quenches photonitrosation. This might be attributed to the reported tendency for DMF to form a ground state complex with 1-NpOH, leading to efficient quenching of 1-NpOH fluorescence.

2.1.7.4 Quenching by Quadricyclene

Murov and Hammond[73] reported that quadricyclene (QC) is a very effective quencher of fluorescence of aromatic hydrocarbons. The quenching was suggested to proceed via an electron-transfer process.[74] Fluorescence of 1-NpOH (0.0002 M) was quenched by QC (0.020-0.100 M) in THF at room temperature with a reasonably good Stern-Volmer correlation to give $k_q\tau_o$ = 2.30 M^{-1} and k_q = 2.47 x 10^8 $M^{-1}s^{-1}$ (the τ_o value was determined to be 9.3 ns in THF). However, the quantum yields Φ_N for photonitrosation of 1-NpOH (0.030 M) with NND (0.0075 M) in THF were not significantly changed in the range of [QC] = 0.10-0.32 M (Table 2-15). Failure of quenching of photonitrosation by QC can be rationalized in terms of the assumption that QC acts only as an electron donor[74] but not as a proton acceptor in the quenching process.

2.1.8 Ground State Complex of 1-NpOH with NND

2.1.8.1 Studies by UV-Vis Absorption Spectroscopy

Ground state complexes of naphthol with TEA[75,76] formed by H-bonding have been investigated by UV spectroscopy. The association constant K for the complex [1-NpOH···TEA] in heptane at 25°C was evaluated to be 112-129 M^{-1},[75] according to Equation 2-28[76]:

$$K = \frac{C_A(OD^\circ - OD') + C_A'(OD - OD^\circ)}{C_A C_A'(OD' - OD)} \qquad 2\text{-}28$$

Table 2-15 Effects of QC on Photonitrosation of 1-NpOH (0.030 M) with NND (0.0075 M) and on Fluorescence of 1-NpOH (0.0002 M) in THF

[QC] (M)	Φ_N[a]	Φ_N°/Φ_N	[QC] (M)	I°/I[b]
0	0.0697			
0.10	0.0693	1.01	0.020	1.04
0.16	0.0670	1.04	0.040	1.10
0.20	0.0676	1.03	0.060	1.13
0.24	0.0659	1.06	0.080	1.18
0.28	0.0668	1.04	0.100	1.23
0.32	0.0629	1.10		
$k_c(QC)\tau_o$ (M^{-1})		0		2.3
$k_c(QC)$ x 10^{-8} ($M^{-1}s^{-1}$)		0		2.47
r				0.996

a. Each sample solution was irradiated under the same conditions by RPR lamps at 31°C for 21 min to cause 3-10% conversion of 1-NpOH.

b. The excitation wavelength was 323 nm, and the monitoring one was 342 nm in the absence of NND at room temperature.

where OD°, OD and OD' are the absorbances at a fixed wavelength for three solutions containing proton-acceptor concentrations of zero, C_A and C_A', respectively, at a fixed concentration of a proton donor.

Differential absorption spectra (Figure 2-32) of a solution of 1-NpOH and NND in dioxane were recorded at 20°C against a reference which was a double-compartment cell, each one containing double the concentration of 1-NpOH and NND as in the sample cell (see Figure 5-9, in Experimental). The OD and OD'values were obtained at various wavelengths, and K was calculated from Equation 2-28 (Table 2-16); an average K value from the measurements at the various wavelengths and two concentration sets is 7.3 ± 1.0 M^{-1}. The reasonable constancy of K values in the various concentrations of NND may be taken as an indication that the 1:1 ground state complex of 1-NpOH···NND is formed (*vide infra*).

Table 2-16 Association Constants (K) for the Complex of 1-NpOH (0.0003 M) and NND at its Various Concentrations in Dioxane at 20°C

Monitoring	OD		OD'	K(M^{-1})	
wavelength(nm)	[NND](M):0.030	0.050	0.150	0.030-0.150	0.050-0.150
398	0.0058	0.0095	0.0180	5.5	8.2
400	0.0053	0.0084	0.0160	6.5	8.0
402	0.0050	0.0080	0.0150	6.7	8.5
K(average)= 7.3±1.0(M^{-1})				6.2	8.3

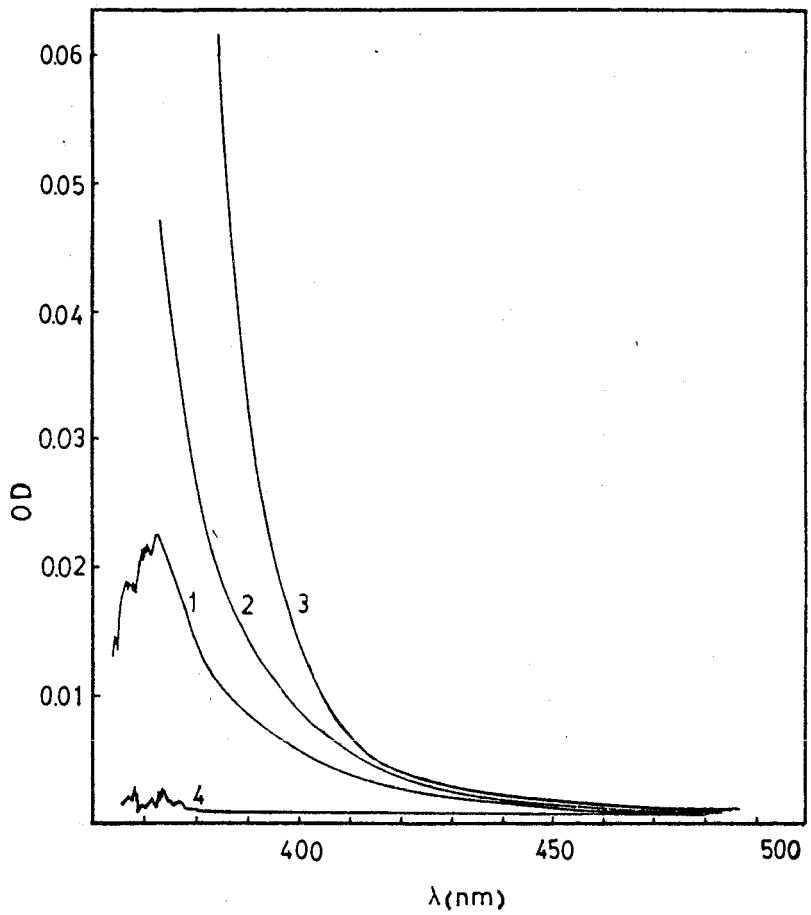

Figure 2-32 Differential absorption spectra of 1-NpOH (0.0003 M) and NND in dioxane at 20°C; curves 1-3 contained [NND] of 0.03, 0.05 and 0.15 M, respectively. The base lines were recorded when a sample cell contained the same solutions as in a reference cell. The curve 4 was an example of these base-lines, (see Figure 5-9 in EXPERIMENTAL).

A ground state complex of 1-AnOH with NND was also studied by absorption spectroscopy. Absorption spectra of 1-AnOH (0.0001 M), NND (0.080 M) and the mixture of 1-AnOH (0.0001 M) with NND (0.010-0.080 M) in cyclohexane were recorded at 21°C. No absorption beyond 510 nm appears for either 1-AnOH (0.0001 M) or NND (0.080 M) solution (Figure 2-33). For the mixtures of 1-AnOH (0.0001 M) and NND (0.010-0.080 M), however, the absorption in the 450 nm region increases, and a new broad band appears at 530 nm. The absorbance at 530 nm increases with increasing NND concentration (Figure 2-33). The 530 nm band could be assigned to the absorption of the ground state complex, [1-AnOH···NND]. The absorbances at 530 nm were determined as a function of [NND], as shown in Table 2-17.

Table 2-17 Absorbances of the Complex of 1-AnOH (0.0001 M) with NND (0.010-0.080 M) in Cyclohexane at 21°C

[NND] (M)	1/[NND] (1/M)	OD (at 530 nm)	1/OD
0.010	100	0.0013	769
0.020	50	0.0023	435
0.040	25	0.0045	222
0.060	26.7	0.0058	172
0.080	12.5	0.0093	108
$K\ (M^{-1})$		5.1 ± 0.2	

Based on Equation 2-29,[77] a linear regression analysis of 1/OD and 1/[NND] yielded the slope = 7.42 M and intercept = 38.1 with r = 0.998; the K

value was calculated from the ratio of intercept/slope to be 5.1 M^{-1}.

$$1/OD = \{\epsilon_c l[1\text{-AnOH}]\}^{-1} + \{\epsilon_c l[1\text{-AnOH}][NND]K\}^{-1} \qquad 2\text{-}29$$

Here OD is the absorbance of the complex at 530 nm, ϵ_c is the corresponding extinction coefficient, l is the optical length, and K is association constant for the complex.

2.1.8.2 ^{1}H-NMR Studies of the Ground State Complex

Studies of ground state complexes by ^{1}H-NMR spectroscopy can provide the association constants and allow interpretations of complex geometry.[78-82] Formation of complexes of nitrosamines with aromatic molecules has been demonstrated by ^{1}H-NMR spectra[8,83,84] and the geometry of the complex has been suggested to be a "face to face sandwich" type association in which the in-plane benzene axis is parallel to the N-N bond of nitrosamine.[83]

The NMR resonances[8] of the two magnetically nonequivalent methyl groups of NND (*cis* and *trans*) shift upfield in the presence of 1-NpOH in carbon tetrachloride at 20°C; the signal of the *trans* methyl group shifts upfield faster than that of the *cis* group with increasing [1-NpOH] as shown in Figure 2-34. The difference, $\Delta\delta$, is defined in Equation 2-30.

cis (δ, 3.0 ppm)

trans (δ, 3.8 ppm)

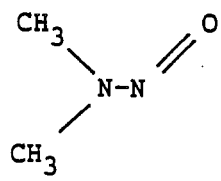

$$\Delta\delta = \delta(CCl_4) - \delta(CCl_4\text{-NpOH}) \qquad 2\text{-}30$$

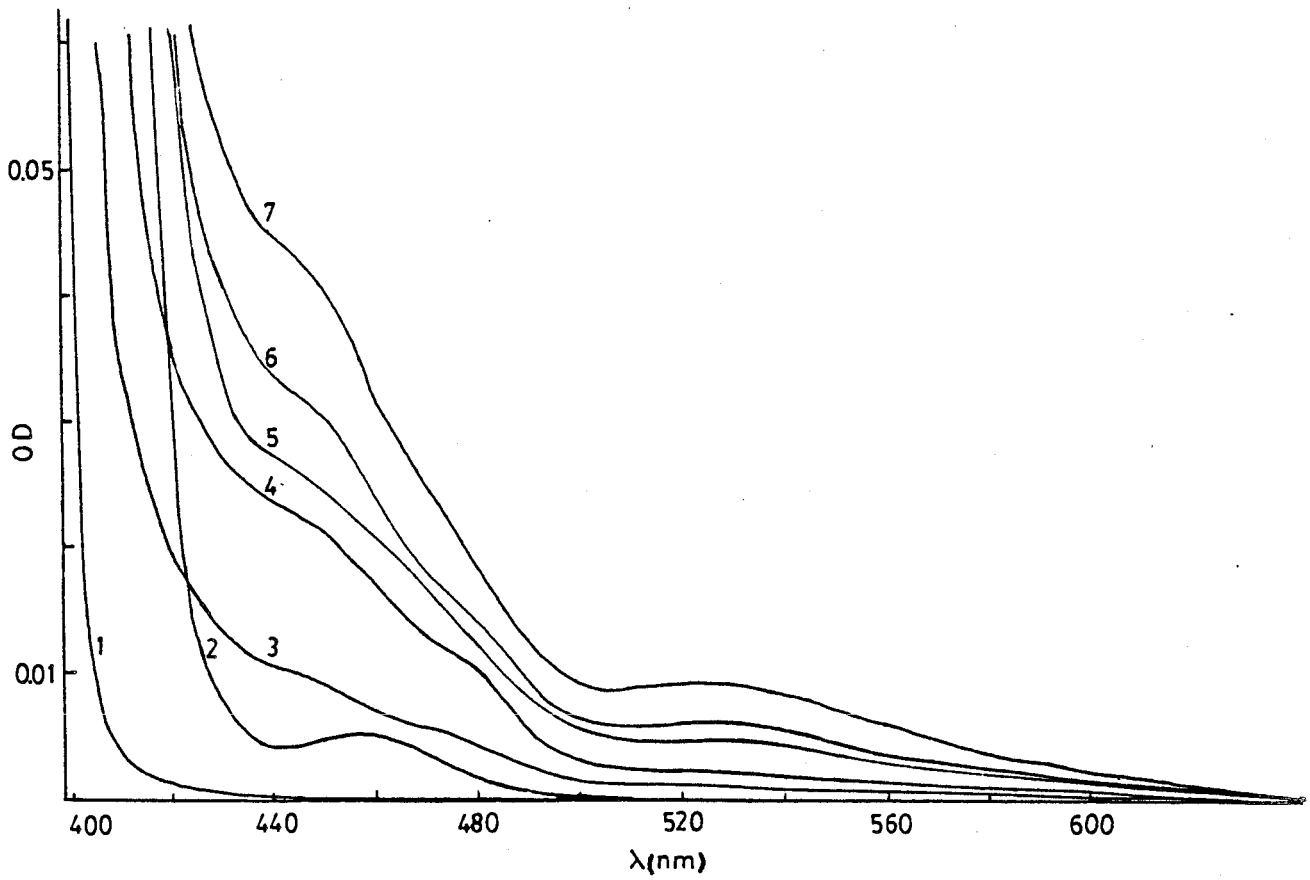

Figure 2-33 Absorption spectra of (1) 1-AnOH (0.0001 M), (2) NND (0.080 M) and (3)-(7) the mixtures of 1-AnOH (0.0001 M) and NND in cyclohexane at 21°C; curves (3)-(7) contained [NND] of 0.010, 0.020, 0.040, 0.060, and 0.080 M, respectively; the curve 2 shows a weak band at 455 nm, which was further investigated in Chapter 3.

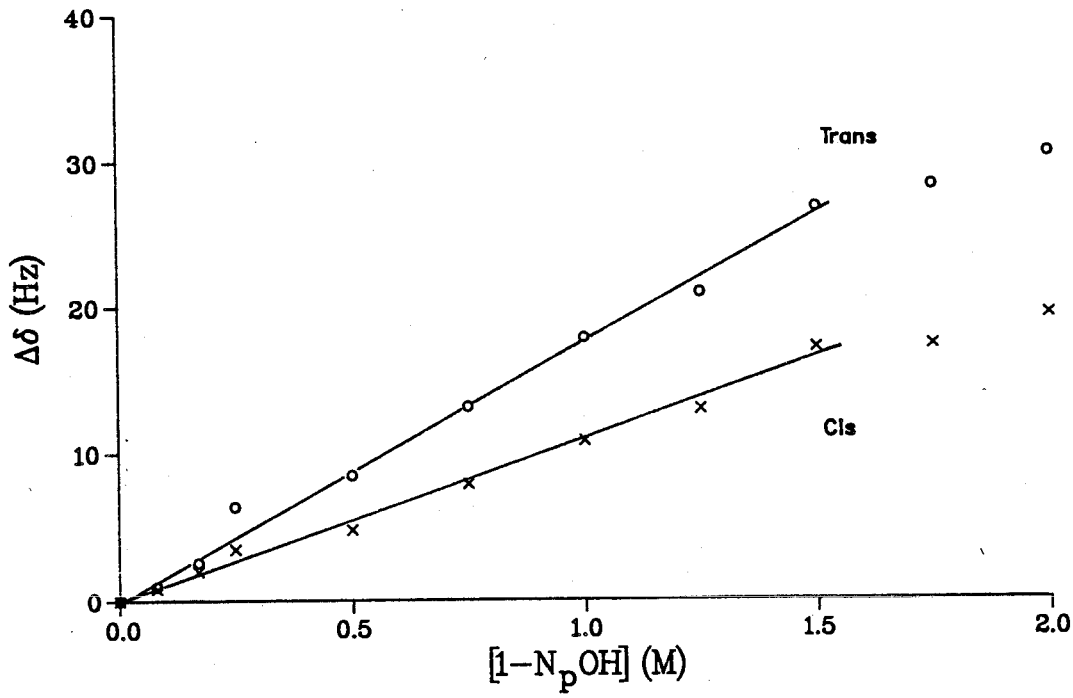

Figure 2-34 Plots of chemical shift differences $\Delta\delta$ for methyl groups of NND against [1-NpOH] in CCl_4 at 20°C.

Chemical shifts of the aromatic ring protons of 1-NpOH (0.070 M) were determined in the absence and presence of increasing NND concentrations (0.081-0.649 M) in CCl_4-$CDCl_3$ (7:3, by volume) solution at 20°C. The chemical shifts (in ppm) are assigned according to Lucchini's report:[85]

(8.1)

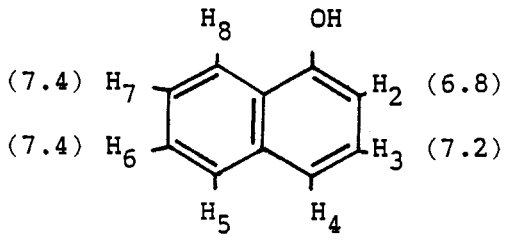

Chemical shift differences, $\Delta\delta$, (defined in Figure 2-35) for each proton in 1-NpOH with increasing [NND] are tabulated in Table 2-18 and plotted in Figure 2-36. The shifts are upfield for protons H_3 to H_7 and downfield for protons H_2 and H_8. The other chemical shift difference, Δ_o in Figure 2-35, is defined as the difference for each proton between uncomplexed 1-NpOH (δ) and the complexed one (δ_c) in the 1:1 complex with NND; the Δ_o value can be determined from Equation 2-31[80] on the assumption that 1:1 complex is formed, as in determination of an equilibrium constant of K.

$$1/\Delta\delta = 1/K \bullet 1/\Delta_o \bullet 1/[NND] + 1/\Delta_o \qquad 2\text{-}31$$

The plots of $1/\Delta\delta$ against 1/[NND] for each proton from H_3 to H_7 yielded straight lines (Figure 2-37) to afford Δ_o and K values, listed in Table 2-19.

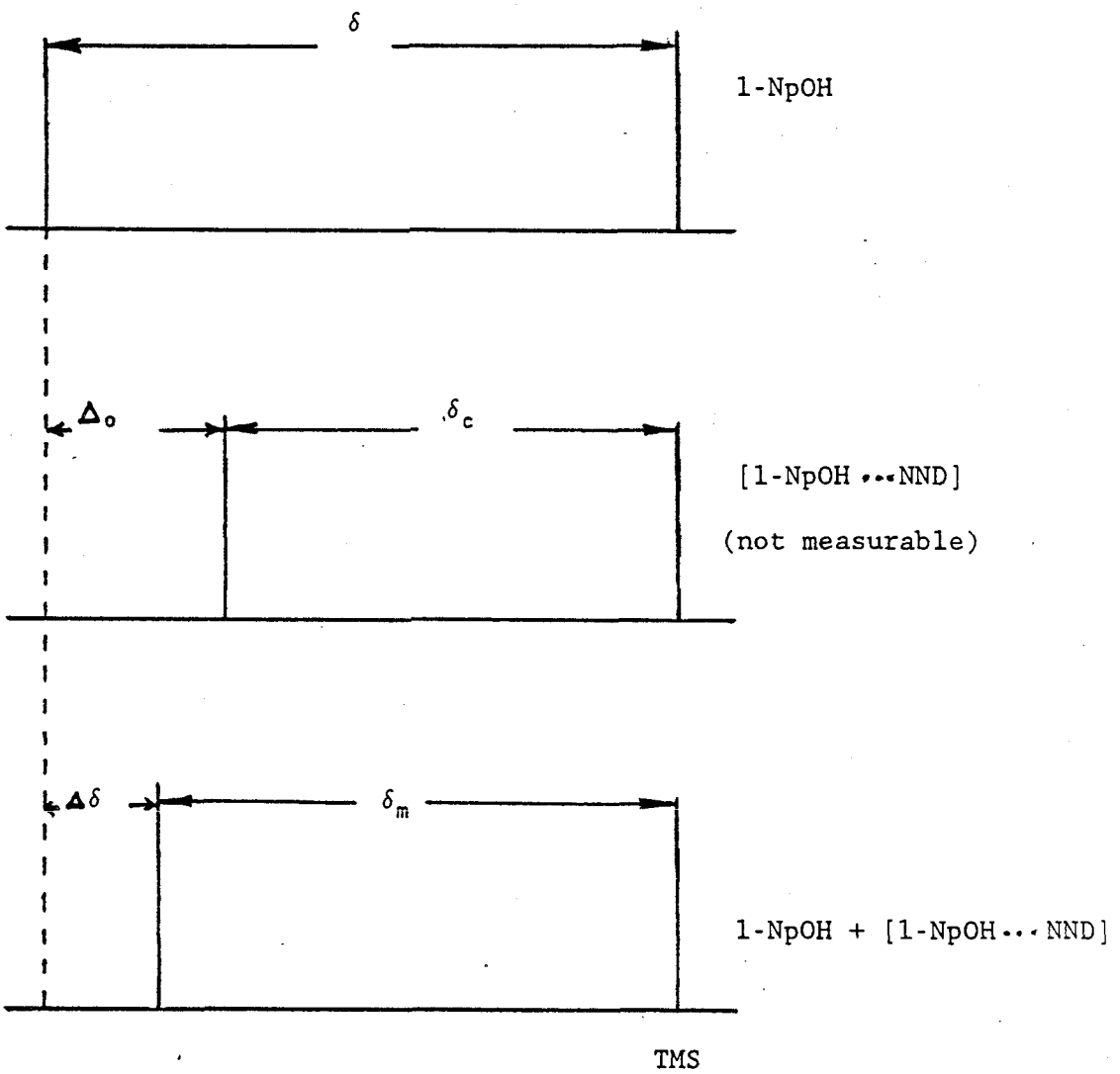

Figure 2-35 Definition of chemical shift variables; δ and δ_c are the chemical shifts of aromatic protons in the "free" 1-NpOH and in the 1:1 complex of (1-NpOH···NND), respectively; δ_m is the observed chemical shift for the equilibrium mixture. Thus the equations, $\Delta\delta = \delta - \delta_m$ and $\Delta_o = \delta - \delta_c$, are established.

Table 2-18 The $\Delta\delta$ Values in Hz for Each Aromatic Proton in 1-NpOH (0.070 M) in the Presence of Various Concentrations of NND[a]

[NND] (M)	H_2[b]	H_3	H_4	H_5	H_6	H_7	H_8[b]
0.081	-17.6	8.0	18.4	10.4	12.0	12.0	-15.0
0.162	-22.0	15.2	32.4	19.6	20.0	24.0	-19.0
0.324	-21.2	27.2	50.4	33.6	32.0	36.0	-15.0
0.486	-14.4	38.8	65.2	45.2	44.0	48.0	-6.0
0.649	-11.6	44.4	71.6	50.4	52.0	53.0	-2.0

a. ^{1}H-NMR spectra of 1-NpOH in the absence and presence of increasing [NND] were recorded in CCl_4-$CDCl_3$ (7:3, by volume) at 20°C using Bruker WM-400 (MHz) spectrometer.

b. Moved downfield.

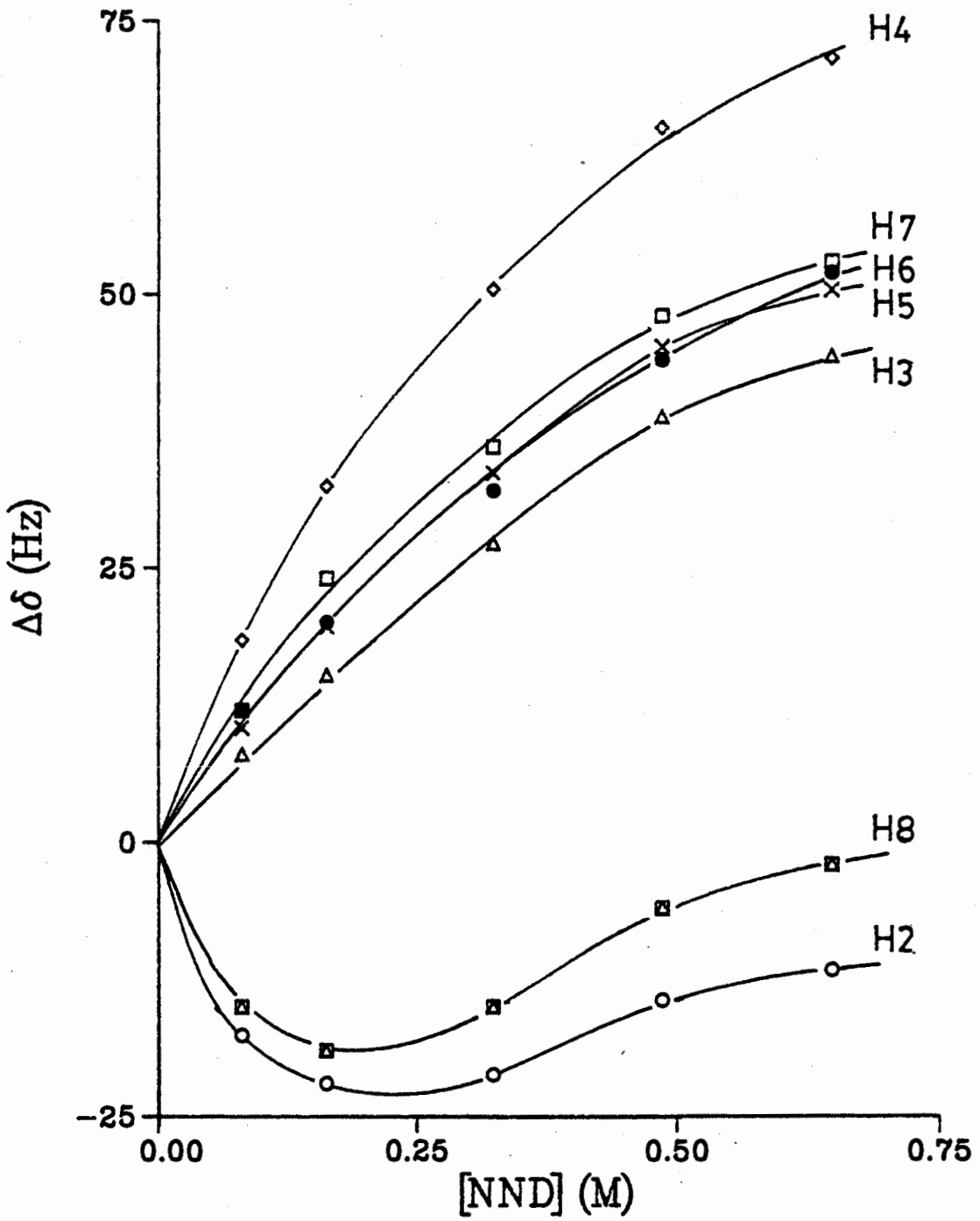

Figure 2-36 Plots of Δδ against [NND] for H_2-H_8 protons in 1-NpOH in CCl_4-$CDCl_3$ (7:3, by volume) at 20°C.

Table 2-19 Association Constant K and Δ_o Values for Protons H_3-H_7 in 1:1 Complex of 1-NpOH···NND

1/[NND] (M^{-1})	1/Δδ (1/Hz)				
	H_3	H_4	H_5	H_6	H_7
12.4	0.125	0.0544	0.0962	0.0833	0.0833
6.17	0.0658	0.0309	0.0510	0.0500	0.0417
3.09	0.0368	0.0198	0.0298	0.0313	0.0278
2.06	0.0258	0.0153	0.0221	0.0277	0.0208
1.54	0.0225	0.0140	0.0198	0.0192	0.0189
Δ_o(Hz)	139	125	125	73.4	116
K(M^{-1})[a]	1.32	2.14	1.13	2.40	1.46
r	1.000	1.000	1.000	0.998	0.997

a. The association constant K was averaged from these five data to be K = 1.7 ± 0.5 M^{-1} in CCl_4-$CDCl_3$ (7:3, by volume) at 20°C.

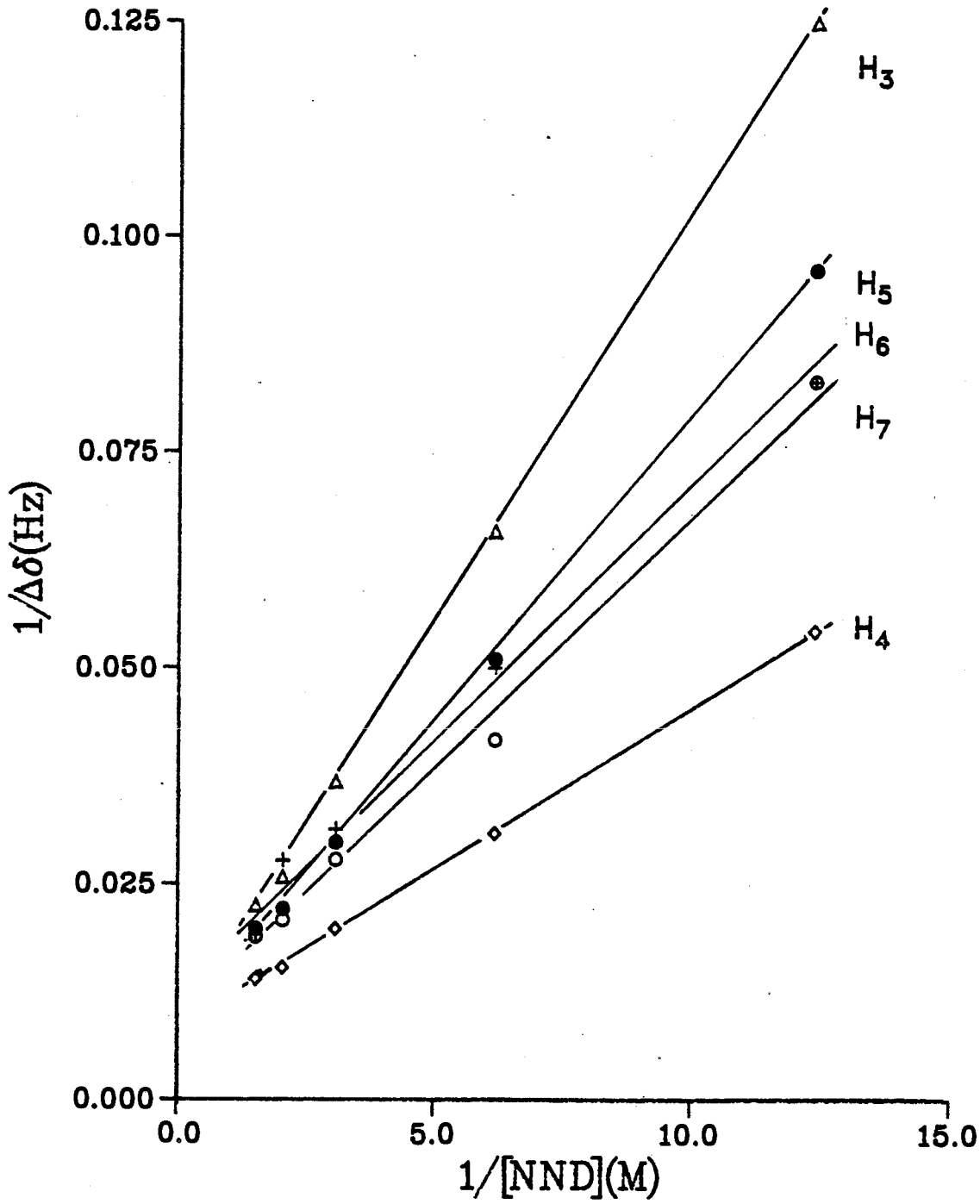

Figure 2-37 Plots of $1/\Delta\delta$ against 1/[NND] for each proton of H_3-H_7 in 1-NpOH.

The K values obtained from monitoring the various protons vary slightly (1.13-2.14 M^{-1}) giving an average of 1.7 ± 0.5 M^{-1}. The linear plots of $1/\Delta\delta$ against 1/[NND] (Figure 2-37) together with the constancy of K values indicates that the assumption of a 1:1 complex of 1-NpOH···NND is valid. That the Δ_o values vary in order $H_3 > H_4 \simeq H_5 > H_7 > H_6$ shows that these protons interact with NND in the complex to unequal extents. The chemical shift difference ($\Delta\delta$) curves of H_2 and H_8 in Figure 2-36 are more complex than the others. The complexity is at present unexplained. Control experiments showed that without NND the chemical shifts of the aromatic protons varied less than 4 Hz, as [1-NpOH] was changed from 0.017 to 0.070 M. These observations exclude the possibility that the effect on the chemical shifts arises from association between 1-NpOH molecules.

2.1.8.3 Excitation of the Ground State Complex 1-NpOH···NND

As shown in Figure 2-32 the ground state complex (GSC) of 1-NpOH···NND absorbs in the 370 - 410 nm region, which is above the absorption range (Figure 2-7) of either 1-NpOH (0.0002 M) or NND (0.012 M). On excitation of an acetonitrile solution containing 1-NpOH (0.0002 M) and NND (0.012 M) at 370 nm, a broad fluorescent band 430 - 600 nm peaking at 480 nm was recorded (Figure 2-38). No fluorescence, however, was detected in this region for either 1-NpOH or NND under the same conditions (Figure 2-38). The new fluorescent band could be assigned to an "excited state complex" derived from direct excitation of GSC, as shown in Scheme 2-2.

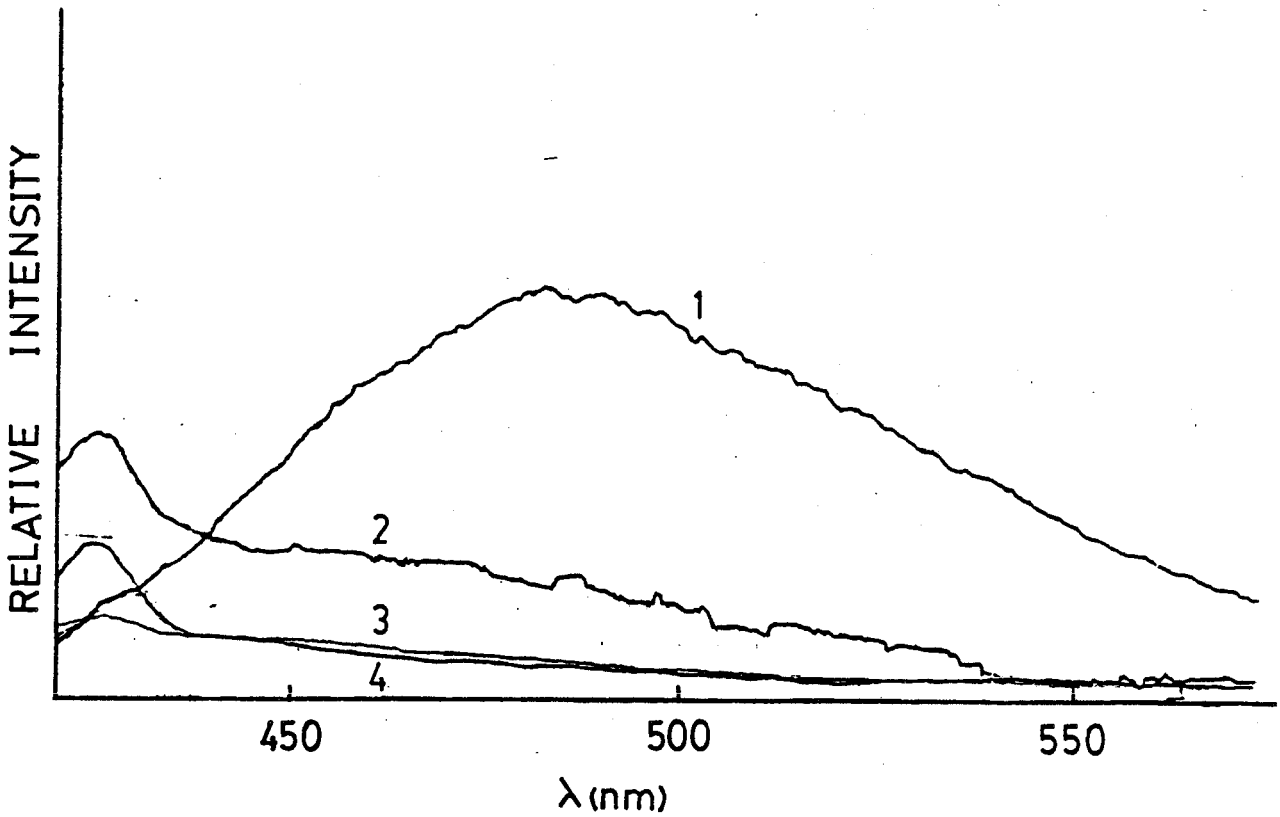

Figure 2-38 Fluorescence spectra of the ground state complex 1-NpOH···NND in acetonitrile at room temperature with excitation wavelength of 370 nm; curve 1, [1-NpOH] = 0.0002 M and [NND] = 0.012 M; curve 2, [1-NpOH] = 0.0002 M; curve 3, [NND] = 0.012 M; curve 4, solvent only.

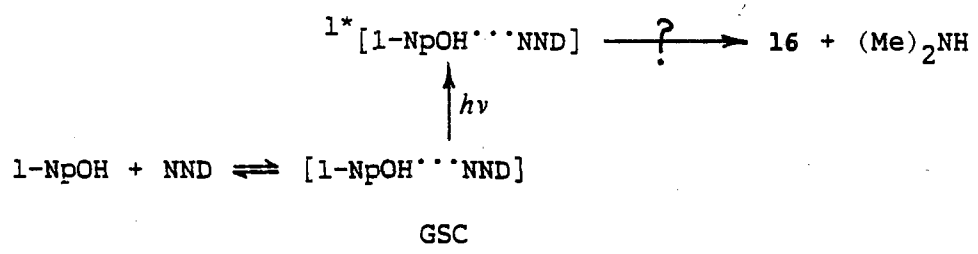

Scheme 2-2

The direct irradiation of GSC in acetonitrile or dioxane solution of 1-NpOH (0.030 M) and NND (0.027 or 0.054 M) using a GWV filter (cut-off < 380 nm) for 31.5 h caused the formation of a trace amount of quinone monooxime **16** (<0.0007 M on the basis of barely detectable peaks in HPLC analysis). The quantum yields of **16**, using the potassium ferrioxalate actinometer[23], were estimated to be 0.0005 to 0.0008, depending on the initial concentrations of NND. No peak of **16** was detectable by GC. Since the concentration changes of NND during irradiation were too small to be accurately determined by HPLC, the quantum yield of NND disappearance, Φ_N, was estimated for only one run to be 0.0015 (Table 2-20). The negligibly small quantum yields (Φ_{ox}) suggest that **16** is not generated by the direct irradiation of GSC. **This confirms the point that the photonitrosation results from the dynamic collision of ^{1*}1-NpOH with NND.**

Table 2-20 Quantum Yields Φ_{ox} under Irradiation of GSC at 19°C

Solvent	$[1\text{-NpOH}]_o$[a] (M)	$[NND]_o$[a] (M)	$[16]\times10^4$ (M)	$\Phi_{ox} \times10^4$
Dioxane	0.030	0.027	4.28	5.23
Dioxane	0.030	0.054	6.80	8.31
Acetonitrile	0.030	0.027	4.51	5.50
Acetonitrile[b]	0.030	0.054	6.50	7.90

a. Before irradiation.

b. Φ_N = 0.0015.

2.2 Discussion

2.2.1 Mechanism of Photonitrosation

Photonitrosation of naphthols and anthrols with NND has been shown to be a novel and general reaction when these phenolic compounds are photoexcited, although phenol itself has been shown not to undergo photonitrosation. Failure to promote the nitrosation by excitation of NND clearly indicates that the ground state of 1-NpOH (pKa = 9.2) is not acidic enough to hydrogen-bond with NND, and therefore can cause no decomposition of NND.[1,2,4,14] For the system of 1-NpOH and NND, the similarity of k_q values from quenching of fluorescence lifetime (k_q = 7.6 x 10^9 $M^{-1}s^{-1}$) and from quantum yield measurements for photonitrosation (k_q = 6.8 x 10^9 $M^{-1}s^{-1}$) strongly supports the view that the photonitrosation is initiated by collision of singlet excited state of 1-NpOH and NND. The k_q value from quenching of fluorescence intensity (k_q = 11.0 x 10^9 $M^{-1}s^{-1}$) is somewhat larger than those quoted above. The difference is due to the formation of the GSC of 1-NpOH with NND. Indeed, this k_q value is contributed by both dynamic and static quenching (*vide infra*). The failure of triplet sensitization by xanthone and by 2-acetonaphthone and the failure of quenching of this reaction by 1,3-cyclohexadiene also suggest that the singlet excited state of 1-NpOH is involved in the photonitrosation. The basic mechanism proposed in Scheme 2-1 agrees with the kinetic results obtained from quantum yield measurements, i.e., the consistent $k_q\tau_o$ values (Table 2-9) provided by plots of $1/\Phi_{ox}$ *vs* 1/[NND] and $1/\Phi_N$ *vs* 1/[NND]. The photonitrosation of 1-NpOH with NND is used as a model for the discussion below.

In Scheme 2-1 we assume that the hydrogen-bonded exciplex (C_1), i.e. [^{1*}1-NpOH$\cdot\cdot\cdot$NND] is formed by a collisional process. The crucial question to be answered is " By what mechanism does the exciplex lead to the final products?". Several possible pathways (Schemes 2-3 to 2-6) will be discussed in an effort to answer this question. However, it must be emphasized that simple energy transfer from ^{1*}1-NpOH to NND cannot be used to explain photodecomposition of NND, since the singlet excited state of NND without an associated proton cannot decompose and would decay to the ground state.[1,2,14]

A straightforward interpretation might be a direct hydrogen-atom transfer process from ^{1*}1-NpOH to NND as shown in Scheme 2-3.

$$[^{1*}\text{1-NpO-H}\cdot\cdot\cdot\text{O=N-N(Me)}_2] \longrightarrow [\text{1-NpO}\cdot \ \text{NO}\cdot] + (\text{Me})_2\text{NH}$$

$$\downarrow$$

16

Scheme 2-3

This radical mechanism is, however, inadmissible on the grounds that singlet excited ^{1*}1-NpOH is not a hydrogen-atom donor while the triplet excited state of 1-NpOH (^{3*}1-NpOH) is.[49, 86-89] Recently, Shizuka[89] reported that ^{3*}1-NpOH produced by benzophenone triplet sensitization can effectively transfer a hydrogen-atom to ground state benzophenone through formation of a triplet exciplex of [^{3*}1-NpOH$\cdot\cdot\cdot$O=C(Ph)$_2$], to give a 1-naphthoxy radical 1-NpO$\cdot$ and a ketyl radical (Ph)$_2\dot{C}$-OH (Scheme 2-4). In the present case, since the photonitrosation of 1-NpOH is unambiguously initiated from its singlet excited state, and since the triplet sensitization causes no reaction, the radical mechanism can be positively excluded.

$$^{3*}\text{1-NpOH} + (\text{Ph})_2\text{C=O} \longrightarrow [^{3*}\text{1-NpOH}\cdots\text{O=C(Ph)}_2] \longrightarrow$$

$$\text{1-Np}\dot{\text{O}} + (\text{Ph})_2\dot{\text{C}}\text{-OH} \longrightarrow \text{REACTION PRODUCTS}$$

Scheme 2-4

Alternatively, a sensitization mechanism by electron transfer might be used to explain photonitrosation. The possibility of electron transfer from ^{1*}1-NpOH to NND (or from NND to ^{1*}1-NpOH) can be examined with reference to the Weller equation:[90-92]

$$\Delta G_{et} = 23.1\ (E_{ox} - E_{red}) - E_{0-0}(\text{1-NpOH}) \qquad 2\text{-}32$$

where ΔG_{et} is a free energy for an electron transfer; E_{ox} and E_{red} are the oxidation and reduction potentials for the species being oxidized and for the species being reduced , respectively; E_{0-0}(1-NpOH) is the singlet excitation energy of 1-NpOH.

First, electron transfer from ^{1*}1-NpOH to NND is considered; the calculated ΔG_{et} value is -25.8 kcal/mol, when E_{ox}(1-NpOH) = 1.25 v,[93] E_{red}(NND) = -1.584 v[94] and E_{0-0}(1-NpOH) = 91.3 kcal/mol[23]. The large negative ΔG_{et} indicates the high possibility of electron transfer from ^{1*}1-NpOH to NND within the exciplex. Therefore, a mechanism of an electron transfer followed by proton transfer can be considered, and quinone monooxime **16** could be formed by the mechanism proposed in Scheme 2-5.

Unfortunately, this Scheme cannot be used to explain why a hydroxylic solvent, e.g. methanol or ethanol, retards the photonitrosation of 1-NpOH and why a proton-acceptor, e.g. water, TEA or DMF, quenches the reaction.

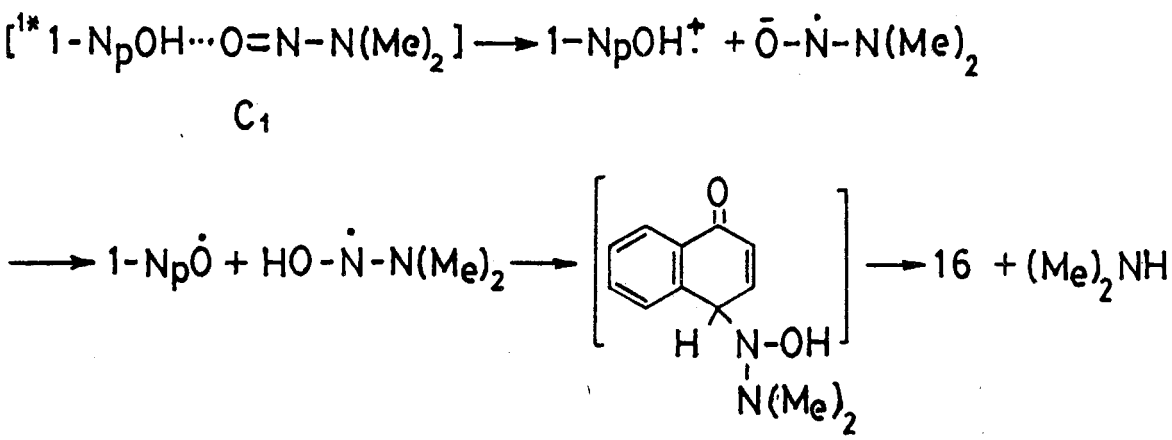

Scheme 2-5

Secondly, the Weller equation for electron transfer from NND to ^{1*}1-NpOH gives a positive ΔG_{et} = 6.88 kcal/mol, using values of E_{ox}(NND) = 2.05 v,[95] E_{red}(1-NpOH) = -2.2 v,[93] and E_{0-0}(1-NpOH) = 91.3 kcal/mol[23]. This suggests the lack of an electron transfer from NND to ^{1*}1-NpOH.

The foregoing discussion indicates that a new mechanism should be postulated to explain the sensitized photodecomposition of NND within the exciplex. The following findings allow us to propose a mechanism involving a proton transfer from ^{1*}1-NpOH to NND followed by energy migration, as shown in Scheme 2-6:

1. All these phenolic compounds possess tremendously enhanced acidity in their singlet excited states ranging $pK_a(S_1)$ = -0.07 to 2.8 (Table 1-2). This should be a driving force for proton transfer to NND.
2. Although 1-methoxynaphthalene (1-NpOMe) is an effective singlet sensitizer [E_S(1-NpOMe) = 89.3 kcal/mol,[23] E_S(NND) = 72 kcal/mol[2]], it does not induce the photodecomposition of NND, because of the lack of a labile proton.

3. The photodecomposition of NND occurs from the singlet excited state of proton-associated NND.[1,2,4,14-16]

4. Water, TEA and DMF quench photonitrosation of 1-NpOH by accepting a proton from ^{1*}1-NpOH in competition with NND.

In Scheme 2-6, the k_H step, i.e. proton-transfer from ^{1*}1-NpOH to NND within the exciplex C_1, must take place prior to the intramolecular energy migration in the k_E step. The singlet excited state of proton-associated NND rapidly decomposes in the k_D step by the mechanism proposed in Scheme 1-1[1,2] to dimethylaminium and nitric oxide radicals. The former converts subsequently to dimethylamine by accepting an electron from 1-NpO$^-$ in the k_e step leading to 1-NpO$^\cdot$; the latter combines with 1-NpO$^\cdot$ to form the quinone monooxime **16** as shown in the k_{co} step. From the exciplex C_1 the other two collapsing processes lead to by-products in the k_p, step and to the starting materials by a normal energy transfer in the k_b step. Direct excitation of GSC does not lead to **16** as demonstrated. Since fluorescence decay measurements on 1-NpOH in the presence of NND indicate that the decays are single-exponential, the "feedback" step, k_{-q} , is negligible.[149,150]

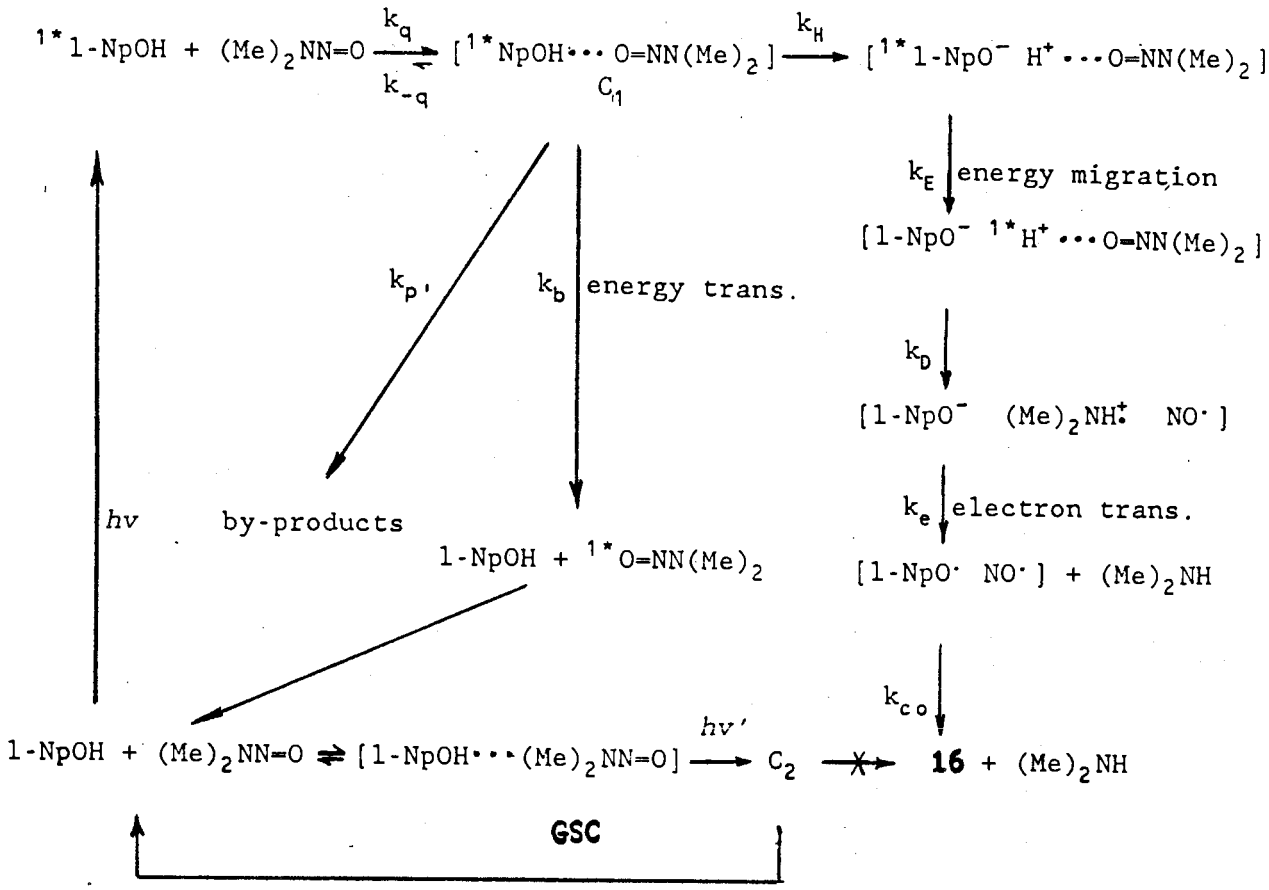
^{1*}1-NpOH + $(Me)_2NN{=}O$
k_q
k_{-q}
$[^{1*}NpOH\cdots O{=}NN(Me)_2]$
C_1
k_H
$[^{1*}1\text{-}NpO^-\ H^+\cdots O{=}NN(Me)_2]$
k_E energy migration
$[1\text{-}NpO^-\ ^{1*}H^+\cdots O{=}NN(Me)_2]$
$k_{p'}$
k_b energy trans.
k_D
$[1\text{-}NpO^-\ (Me)_2NH^+\cdot\ NO\cdot]$
k_e electron trans.
$[1\text{-}NpO\cdot\ NO\cdot] + (Me)_2NH$
k_{co}
hv
by-products
1-NpOH + $^{1*}O{=}NN(Me)_2$
1-NpOH + $(Me)_2NN{=}O \rightleftharpoons [1\text{-}NpOH\cdots(Me)_2NN{=}O]$
hv'
C_2
16 + $(Me)_2NH$
GSC

Scheme 2-6

2.2.2 Exciplex C_1 Formation

A simple mechanism for a proton transfer in solution is Eigen's three steps proposal,[96,97] as shown in Scheme 2-7.

$$AH^+ + B^- \underset{k_{-1}}{\overset{k_1}{\rightleftharpoons}} [AH^+ \cdots B^-] \underset{k_{-2}}{\overset{k_2}{\rightleftharpoons}} [A \cdots HB] \underset{k_{-3}}{\overset{k_3}{\rightleftharpoons}} A + HB$$

encounter $\qquad$ H^+-transfer $\qquad$ separation

Scheme 2-7

Of special interest in the Scheme 2-7 is k_2, the rate constant of proton transfer. It is now apparent that direct measurement of k_2 independent of the other five contributing steps, i.e., k_1, k_{-1}, k_{-2}, k_3 and k_{-3}, is exceedingly difficult.[97] In particular, the coupling of the various steps is troublesome when $\Delta G^{\ddagger}$ for proton transfer is $\simeq 0$, i.e., k_2 is much faster than k_1, and the rate-determining step is the formation of an encounter complex.[99]

Several findings in the reaction of ^{1*}1-NpOH with NND also suggest that the rate-determining step is the formation of the exciplex. For example, the agreement of quenching rate constants determined from quenching of fluorescence lifetime (k_q = 7.6 x 10^9 $M^{-1}s^{-1}$) with that determined from quantum yield measurements (k_q = 6.8 x 10^9 $M^{-1}s^{-1}$) implies that the rate determining step is the dynamic quenching of ^{1*}1-NpOH by NND, leading to the exciplex formation. This conclusion is confirmed by the lack of a deuterium isotope-effect,

$k_q(H)/k_q(D) \simeq 1$ (Table 2-21), which indicates no substantial proton migration in the rate determining step.

Table 2-21 Comparison of Stern-Volmer Parameters in Photonitrosation of 1-NpOH and of 1-NpOD in Dioxane at 31°C

Substance	τ_o (ns)	$k_q \times 10^{-9}$ ($M^{-1}s^{-1}$)	Φ_{ox}(lim)	r
1-NpOH	10.6	6.8	0.078	0.996
1-NpOD	11.2	7.0	0.087	0.999
		7.1	0.101	0.995

The single-exponential decay curve of 1-NpOH in the presence of NND and the failure to detect emission from ^{1*}1-NpO$^-$ (at 460 nm) indicate that the acid-base equilibrium between ^{1*}1-NpOH and ^{1*}1-NpO$^-$ cannot be established within their lifetimes, owing to various reasons (*vide infra*), and that the reverse step (k_{-q}) in Scheme 2-6 is insignificant.

The k_q values shown in Table 2-8 are dependent on solvent viscosity. For example, when the solvent is changed from acetonitrile (η = 0.36 cp/20°C,[23] k_q = 11.0 x 10^9 $M^{-1}s^{-1}$) to toluene (η = 0.59 cp/20°C,[23] k_q = 4.3 x 10^9 $M^{-1}s^{-1}$) and to benzene (η= 0.65 cp/20°C,[23] k_q = 3.1 x 10^9 $M^{-1}s^{-1}$), the k_q value decreases in the order of the increasing viscosity. The dependence of the k_q value on the solvent viscosity is a feature of a dynamic quenching process.[59] The k_q value of 6.8 x 10^9 $M^{-1}s^{-1}$ in dioxane, however, is larger than that in toluene, in spite of the fact that its viscosity (η = 1.54 cp/20°C) is greater than that of toluene.

Thus the formation of hydrogen-bonded exciplex C_1 in encounter step (k_q) is the rate-determining one in photonitrosation. The rate constants for each of the subsequent steps (k_H, k_p, and k_b) from the exciplex C_1 must be larger than that for the k_q step, since they occur within an ordered exciplex.

2.2.3 Dual Proton- and Energy-Transfer

In Scheme 2-1 (section **2.1.6**), three competitive steps to collapse the hydrogen-bonded exciplex C_1 are described as oxime formation (k_p), by-product formation ($k_{p'}$) and re-formation of the starting materials (k_b). In Scheme 2-6, we further propose that the k_p step consists of a series of consecutive steps i.e. k_H, k_E, k_D, k_e and k_{co}. In order to simplify the dicussion of some effects on the proton transfer step, we assume $k_p \simeq k_{p'}$ (see in Table 2-9) , therefore, $k_b/(k_p + k_{p'}) \simeq k_b/2k_p$. Since the ratio of $k_b/(k_p + k_{p'})$ is measurable, this assumption provides a way to quantitatively elucidate the following effects on the proton transfer step.

The hydroxy-group location, C-1 or C-2 position, in the naphthalene ring strongly affects photonitrosation. Table 2-11 shows $k_b/k_p \simeq 8.6$ and $\Phi_N(\text{lim}) \simeq 0.19$ for 1-NpOH in acetonitrile, and $k_b/k_p \simeq 26.4$ and $\Phi_N(\text{lim}) \simeq 0.071$ for 2-NpOH in the same solvent. This significant difference can be rationalized in terms of the difference of the electron density distribution in their lowest singlet excited states. The singlet excited states of naphthols most likely possess a high degree of charge-transfer (CT) character.[31,32,34,100] Since the CT character of ^{1*}2-NpOH (dipole moment, 3.5D)[152] is weaker than that of ^{1*}1-NpOH (dipole moment, 5.8D)[152,65,66] the rate constant of proton transfer from ^{1*}2-NpOH to a proton-acceptor must be smaller than that from ^{1*}1-NpOH. The rate constants of proton transfer to

water from ^{1*}1-NpOH (2.1×10^{10} s^{-1}) and ^{1*}2-NpOH (7.5×10^{7} s^{-1}), for example, were determined by Clark[65] using picosecond time-resolved spectroscopy. This difference was also explained with the difference of their CT characters.[65]

The determination of quantum yield (Φ_{ox}) as a function of [NND] shows the solvent dependence of Φ_{ox}(lim) in the following order (Table 2-8): dioxane [Φ_{ox}(lim) = 0.091] > MeCN (0.080) > benzene (0.044) > toluene (0.032) > MeOH (0.017). The calculated ratios of k_b/k_p for these solvents are in the opposite order (Table 2-8): dioxane (k_b/k_p = 9.0) < MeCN (10.5) < benzene (20.7) < toluene (29.3) < MeOH (57.8). This ratio k_b/k_p might provide some information about the proton transfer process. The largest k_b/k_p value in MeOH, for example, shows that hydrogen bonding interacton between NND and MeOH molecules[101] retards NND to accept a proton from ^{1*}1-NpOH, resulting in depopulation of the exciplex C_1 via a normal energy transfer leading to the starting materials. The smallest k_b/k_p in dioxane or in THF ($k_b/k_p \simeq 8.0$, from Table 2-9), therefore, it means that proton transfer is fast in these solvents. A hydrogen-bonding acceptor solvent such as dioxane or THF favors the proton transfer step, but a hydrogen-bonding donor solvent such as MeOH or EtOH retards the step.

2.2.4 Electron Transfer from 1-NpO$^-$ to $(Me)_2NH^{+\cdot}$

As aminium radicals are good electrophiles, they readily attack C=C bonds[1,2,4](Scheme 1-1) or aromatic rings[22] (Scheme 1-2). Since both dimethylaminium radical and 1-naphtholate have high and opposite charges, the normal course of the reaction is assumed to be an electron transfer to form $(Me)_2NH$ and 1-naphthoxy radical; the latter couples with NO$^\cdot$ to give **16** (see Scheme 2-6). The failure of $(Me)_2NH^{+\cdot}$ to attack the C=C bond in the

photonitrosation of 2-allyl-1-naphthol **11** suggests that the electrophilic radical attack is not as efficient as electron transfer, and thereby **23** (Equation 2-3 in section **2.1.1**) is not formed.

2.2.5 Ground State Complex

Electronic absorption and ^{1}H-NMR spectroscopic studies of 1-NpOH in the presence of NND show ground state complex (GSC) formation with K = 7.3 ± 1.0 (M^{-1}) in dioxane at 20°C. Since direct excitation of the GSC absorption band in MeCN causes insignificant photonitrosation (Φ_{ox} = 5-8 x 10^{-4}), but generates fluorescene at 430-600 nm, a second exciplex C_2 (see Scheme 2-6) formed from excitation of GSC must be proposed. This exciplex C_2 differs from C_1, which is generated by dynamic collision of ^{1*}1-NpOH and NND and undergoes the nitrosation process.

The different behavior of the two exciplexes leads us to seek explanations from their geometries, since they possess finite structures and lifetimes, and since they do not interconvert within the lifetimes. A "sandwich" geometry is commonly accepted[102] in aromatic hydrocarbon-diene exciplexes[103-107] and in pyrene- N,N-dimethylaniline exciplexes[108]. In the system of 1-NpOH and NND, the exciplex C_2 should inherit the GSC geometric structure[109]. If the structure is inappropriate for proton transfer, energy transfer should prevail within its lifetime, and no photonitrosation can occur. Two geometric structures are proposed as shown in Figure 2-39. In each exciplex, the optimum geometric structure should allow maximum π-orbital overlap[102] between the naphthalene ring and the partial double bond of N-N-O. Note that the GSC does not involve hydrogen-bonding in contrast to the GSC of phenols with bases such as TEA. [69-71] In the GSC, the NO group direction should orient opposite to the C-OH axis in 1-NpOH to

allow the dipole-dipole interaction between 1-NpOH and NND, and the ring is attracted by the positive charge on the nitrogen of amino group and repelled by the negative charge on the oxygen of nitroso group (see Figure 2-39). In the exciplex C_1, however, the NO group should orient parallel to OH group in ^{1*}1-NpOH to favor the formation of a hydrogen bond of $OH\cdots O{=}NN(Me)_2$. The suggested different orientation of NO group in C_2 from that in C_1 is based on the tremendous enhancement of acidity in ^{1*}1-NpOH [$pK_a(S_1) = 0.5$][48] with respect to that in 1-NpOH [$pK_a(S_o) = 9.2$][23]. The lack of hydrogen bonding in the GSC is suggested to be a rationale for its photostability, because proton transfer occurs along a preexisting hydrogen bond.[151]

exciplex C_1 exciplex C_2 (GSC)

Figure 2-39 Proposed "sandwich" structures of exciplexes C_1 and C_2.

The following observations from ^{1}H-NMR studies of the GSC amply support the proposed structure. (i) Figure 2-34 shows that with increasing [1-NpOH] the resonances of the protons in a *trans* methyl group in NND shift to high field more rapidly than those of the corresponding *cis* protons. This is consistent with the fact that the *trans* protons are closer to

naphthalene ring than the *cis* ones in the GSC, as shown in the Figure 2-39. This observation is in agreement with the systems of benzene-NND[8] and benzene-DMF[110]. In both cases the faster high-field shift of the resonances of *trans* protons over those of the *cis* ones with increasing the concentration of benzene suggests stereospecific association between the benzene ring and NND (or DMF), whereby the the ring is also attracted by the positive charge on the nitrogen and repelled by the negative charge on the oxygen.[106] (ii) The linear plots in Figure 2-37 indicate the formation of the 1:1 GSC, i.e. 1-NpOH···NND based on the assumption[78-80] in the derivation of Equation 2-31. This conclusion is also supported by the constancy of the K value measured by UV-Vis absorption spectroscopy in various concentrations of NND (Table 2-16). (iii) Figure 2-36 shows that with increasing [NND] the resonances of H_3-H_7 in the ring of 1-NpOH shift to higher field, they might be located in the shielding zone of the N=N bond as shown in Figure 2-39.

2.2.6 System of 1-AnOH and NND

The following observations suggest that photonitrosation of 1-AnOH with NND essentially follows a similar mechanism to that for the system of 1-NpOH and NND.

(i) The measurements of quenching of 1-AnOH fluorescence intensity (Table 2-2) and lifetime (Figure 2-16), and of quantum yield Φ_N (Table 2-11) provided consistent k_q values (in dioxane at 20-31°C) as shown in Table 2-22; this indicates that photonitrosation of 1-AnOH is also initiated from ^{1*}1-AnOH and also encounter-controlled.

Table 2-22 Comparison of $k_q\tau_o$ and k_q for System of 1-AnOH and NND in Dioxane from Various Measurement Approaches

Measurement approach	t (°C)	$k_q\tau_o$ (M^{-1})	k_q x 10^{-9} ($M^{-1}s^{-1}$)	r
I^o/I - [NND]	25	37.7	1.97	0.999
τ_o/τ - [NND]	20	24.4	1.28	0.999
$1/\Phi_N$ - 1/[NND]	31	33.6	1.76	0.995

(ii)The single-exponential decay of ^{1*}1-AnOH in the presence of NND shows that the reverse reaction from the exciplex, [^{1*}1-AnOH$\cdots$O=NN(Me)$_2$], (like the step of k_{-q} in Scheme 2-6) is negligible. This observation together with undetectable emission from ^{1*}1-AnO$^-$ by time-resolved fluorimetry means that the acid-base equilibrium of ^{1*}1-AnOH $\rightleftharpoons$ ^{1*}1-AnO$^-$ + H^+ can not be established during their lifetimes, owing to rapid excited energy migration from ^{1*}1-AnO$^-$ to proton-associated NND.

(iii) Figure 2-16 shows a positive temperature effect on the k_q values for quenching of 1-AnOH fluorescence by NND in dioxane, providing E_a = 2.54 kcal/mol and log A = 11.2, which are in agreement with E_a = 2-3 kcal/mol and log A = 10-12, for encounter-controlled quenching processes[60].

(iv) Figure 2-14 shows that the $k_q\tau_o$ value decreases as the solvent is changed from acetonitrile ($k_q\tau_o$ = 46.2 M^{-1}) to methanol (13.4 M^{-1}). The difference between the $k_q\tau_o$ values suggests that the quenching of 1-AnOH fluorescence involves an exciplex having hydrogen-bonding, because methanol as a hydrogen-bonding donor solvent can retard the exciplex formation via hydrogen-bonding interaction between methanol and NND molecules.[101]

(v) The electronic absorption spectroscopic studies of 1-AnOH in the presence of various concentrations of NND (Figure 2-33 and Table 2-17) show the electronic absorption of the ground state complex, (1-AnOH···NND), at 530 nm in cyclohexane. A linear plot of 1/OD against 1/[NND] gave K = 5.4 M^{-1} for the 1:1 complex at 20°C. The K value was also calculated to be 13.3 M^{-1} in dioxane at the same temperature according to Equation 2-33:[111]

$$I^o/I = \{1+k_q\tau_o[NND]\}\{1+K[NND]\} \simeq 1+(k_q\tau_o+K)[NND] \qquad 2\text{-}33$$

which involves two terms of dynamic and static quenching processes; $k_q\tau_o$ is a Stern-Volmer constant in dynamic quenching (i.e. equal to the value measured from quenching of 1-AnOH fluorescence lifetime in Table 2-22); the term involving K arises from static quenching. Since quenching of 1-AnOH fluorescence intensity includes both dynamic and static quenching processes, the observed slope from the plot of I^o/I against [NND] is equal to $k_q\tau_o$ + K = 37.7 M^{-1}, where $k_q\tau_o$ = 24.4 M^{-1}, thus K = 13.3 M^{-1}.

2.2.7 Conclusions and Further Research Proposals

The investigation of the mechanism for photonitrosation of 1-NpOH with NND provides an application of excited state acid to promote an irreversible organic reaction. The following conclusions are drawn from the work presented in this Chapter:

(i) Photoexcitation of naphthols and anthrols in the presence of NND in neutral media causes decomposition of NND and nitrosation of these phenolic compounds to give the corresponding quinone monooximes.

(ii) Photonitrosation of 1-NpOH (or 1-AnOH) is initiated by its singlet excited state, and is encounter-controlled leading to a hydrogen-bonded exciplex C_1 in which proton transfer occurs from ^{1*}1-NpOH (or ^{1*}1-AnOH) to NND followed by excited energy migration from ^{1*}1-NpO$^-$ to proton-associated NND.

(iii) A hydrogen-bonding donor solvent such as methanol or ethanol can retard the photonitrosation; a hydrogen-bonding acceptor solvent such as dioxane or THF can assist the reaction.

(iv) Direct photoexcitation of a 1:1 ground state complex, [1-NpOH$\cdots$NND], cannot lead to the photoproduct **16** but to an exciplex C_2 which emits at 480 nm. The configuration of the ground state complex is suggested to involve dipole-dipole interaction other than hydrogen-bonding, which is suggested to be involved in the exciplex C_1. Thus two distinctive exciplexes C_1 and C_2 can be generated under excitation at different wavelengths.

(v) The position of OH group on the naphthalene ring substantially affects the photonitrosation, and the reaction quantum yield for 1-NpOH is

larger than that for 2-NpOH.

Photonitrosation of the phenolic compounds with NND opens a new field of nitrosamine photochemistry, in which photodecomposition of NND takes place in a neutral medium. This is different from the previous studies on acid- promoted photodecomposition of nitrosamines,[1,2,14-22] and will be of significance for further studies on nitrosamine photochemistry in the presence of some biological systems.

Further research proposals on this subject are listed as follows:

a. It is worthwhile to investigate photodecomposition of NND promoted by nonsubstituted and substituted phenols. The quantum yields of NND disappearance in the presence of nonsubstituted phenol ($\Phi_N°$) and subustituted phenols (Φ_N) will be determined in THF. The plot of $\log(\Phi_N/\Phi_N°)$ against $pK_a(S_1)$ for these phenols is expected to be a straight line with a negative slope, because the stronger the acidity of the substituted phenol, the higher the Φ_N is. The observation will be reasonable evidence for the excited-state proton transfer mechanism. The following phenols $[pK_a(S_1)]$[30,31] will be employed: C_6H_5OH (4.0), *m*-$Cl-C_6H_4OH$ (3.0), *p*-$Cl-C_6H_4OH$ (3.5), *m*-$Br-C_6H_4OH$ (2.8), *m*-$CH_3O-C_6H_4OH$ (2.7), *p*-$CH_3O-C_6H_4OH$ (4.7) and *p*-$C_2H_5O-C_6H_4OH$ (5.3).

b. Extrapolation of photonitrosation to some biological substances is an attractive topic. *α*-Tocopherol as a wellknown biological antioxidant[112,113] protects tissues and lipids from oxidative degradation[114], and is smoothly photooxidized in the presence of a dye sensitizer.[115] Since *α*-tocopherol contains a phenol ring, it might undergo photonitrosation with NND to give an expected product as in Equation 2-34.

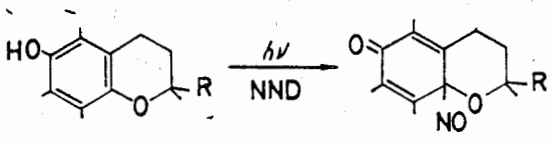

2-34

c. An intramolecular proton transfer reaction in singlet excited states of some phenolic compounds is also an intriguing topic.[32,46] The photolysis of 2-allylphenol was observed to lead to mixture of cyclized products as shown in Equation 2-35.[116,117] The reaction was initially thought to involve protonation of the double bond by the moderately acidic phenol excited state[116], but the quantum yield of the reaction does not appear to correlate with $pK_a(S_1)$[118] and an electron-transfer mechanism is now preferred.[119] In the case of 2-allyl-1-naphthol **11**, however, since the singlet excited acidity of 1-naphthol [$pK_a(S_1) = 0.5$][48] is much stronger than that of phenol [$pK_a(S_1) = 4.0$][30], it is reasonable to propose an intramolecular proton transfer to the double bond in the singlet excited state, leading to photocyclization (Scheme 2-7). The preliminary result of photolysis of **11** in benzene (Equation 2-3) leads us to design the following experiments to support the proposed mechanism: quenching of the photocyclization by some base such as TEA or DMF, quenching of fluorescence of **11** by these bases, detecting the excited state zwitterion **24** by using time-resolved fluorimetry, and studies of solvent effects on the reaction. These experiments will be carried out with a methodology similar to that used for the system of 1-NpOH and NND.

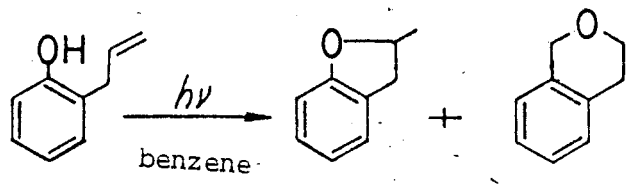

2-35

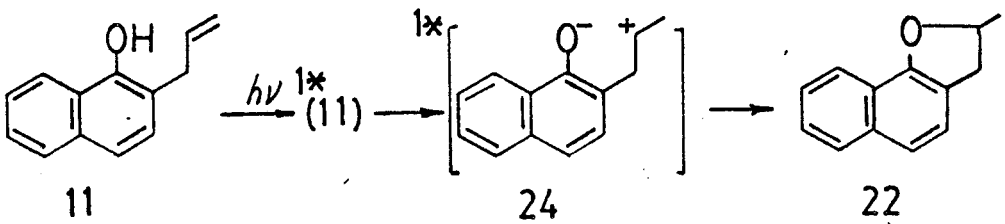

Scheme 2-8

CHAPTER 3

ON THE TRIPLET EXCITED STATE OF N-NITROSODIMETHYLAMINE

3.1 Results

3.1.1 S_o -> T_1 Absorption Spectra

The electronic absorption spectra of NND at the concentrations of 0.0002 and 0.010 M in methylcyclohexane (MCH) at room temperature showed maxima at 234 nm (ϵ = 6000 $M^{-1}cm^{-1}$) and 342 nm (ϵ = 130 $M^{-1}cm^{-1}$) for the π->π^* and n->π^* electronic transitions which have been well studied.[120] At [NND] = 0.10 M, it also showed a new absorption band at 456 nm with a low ϵ value of 0.064 $M^{-1}cm^{-1}$ (Figure 3-1). The spectra of various concentrations of NND in Figure 3-2 demonstrate that the absorbance at 456 nm obeys Beer's Law (Table 3-1). Therefore, the absorption is a genuine electronic transition, but not due to the formation of the dimer of NND.

Table 3-1 OD Values at Various Concentrations of NND in MCH[a]

[NND] (M)	OD (at 456 nm)
0.040	0.0023
0.080	0.0048
0.120	0.0073
0.160	0.0100
0.200	0.0125

a. ϵ = 0.064 ± 0.001 ($M^{-1}cm^{-1}$), r = 1.000.

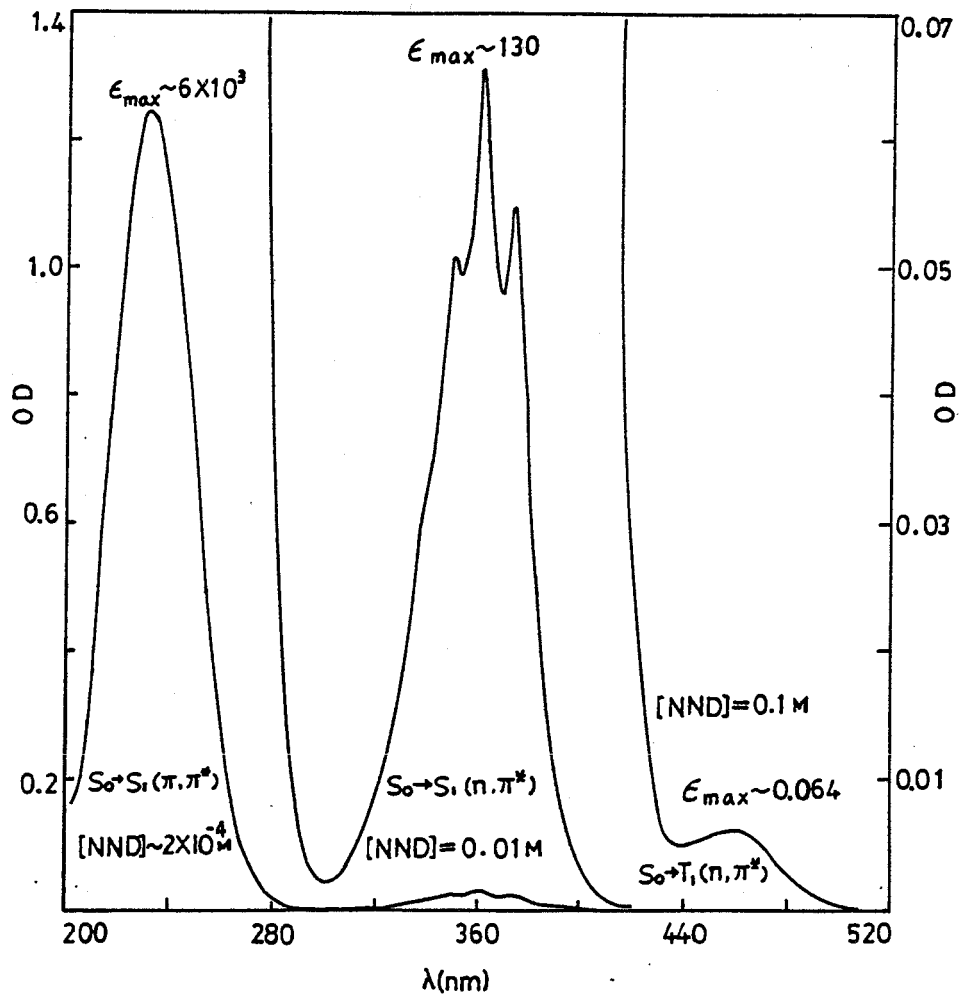

Figure 3-1 Electronic absorption spectra of NND in MCH at room temperature.

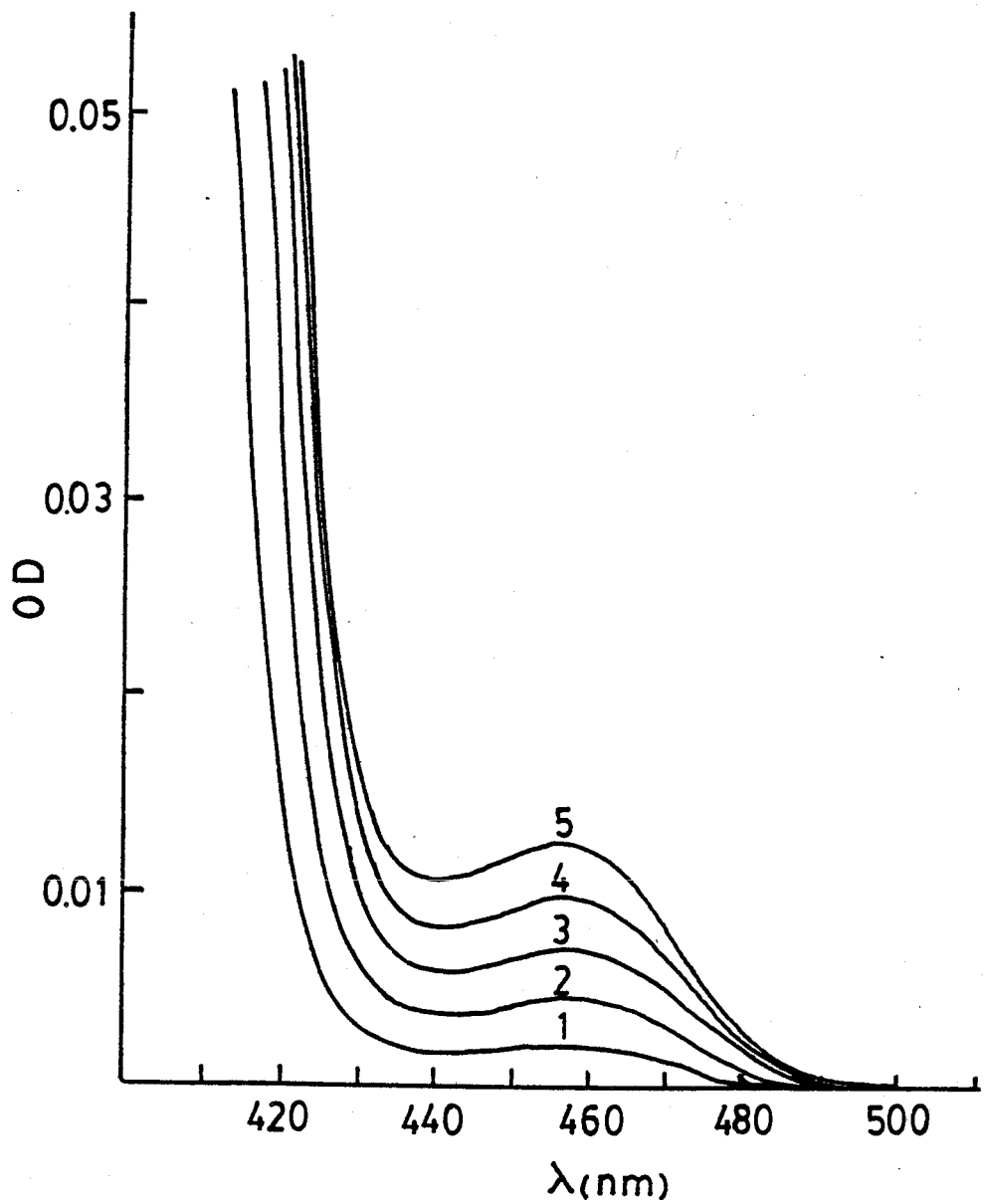

Figure 3-2 S_o-> T_1 absorption spectra of NND at various concentrations in MCH; curves 1-5 contained [NND] of 0.04, 0.08, 0.12, 0.16 and 0.20 M, respectively.

The electronic absorption spectra of NND (0.20 M) in various solvents, such as toluene, THF, methylene chloride, methanol, acetonitrile and water, at room temperature are shown in Figure 3-3. With increasing polarity of the solvent, the maximum of the band shifts to shorter wavelengths (Table 3-2). The blue shift together with ϵ = 0.064 indicates that this absorption must arise from the $S_o \rightarrow T_1$ (n, π^*) electronic transition.[121]

Table 3-2 Wavelengths of the Maxima in the $S_o \rightarrow T_1$ Absorption of NND in Various Solvents

Solvent	MCH	Toluene	THF	CH_2Cl_2	MeOH	MeCN	H_2O
λ_{max}(nm)	456	452	448	442	440[a]	436	424[a]
$\epsilon_{20°C}$[b]	2.02	2.38	7.58	8.93	32.7	37.5	80.2

a. Absorption shoulders.

b. Dielectric constants cited from the ref. 23.

$S_o \rightarrow T_1$ electronic absorption spectra of NND in the concentration region of 0.040-0.200 M in some heavy-atom solvents such as iodoethane, 1,2-dibromoethane, 1,1-dibromoethane and bromobenzene are shown in Figure 3-4, and their pertinent data, in Table 3-3. The external heavy-atom effect on the $S_o \rightarrow T_1$ transition is a criterion for assignment of the electronic transition to (n, π^*) or (π, π^*); for the (n, π^*) transition, the heavy-atom solvents can greatly enhance the $S_o \rightarrow T_1$ absorption, but not for the (π, π^*) one.[122,123] The slight increase (10 - 80%) of the extinction coefficient in changing solvent from methylcyclohexane to brominated or iodinated hydrocarbons agrees with the assignment of a (n,π^*) character for

the S_o-> T_1 electronic transition.

Table 3-3 OD Values of the Maxima in the S_o -> T_1 Absorption of NND (0.040-0.200 M) in Some Heavy-Atom Solvents[a]

[NND] (M)	OD		
	CH_3CH_2I (444 nm)	$BrCH_2CH_2Br$ (442 nm)	PhBr (448 nm)
0.040	0.0052	0.0028	0.0030
0.080	0.0080	0.0051	0.0065
0.120	0.0117	0.0087	0.0092
0.160	-	0.0111	0.0119
0.200	0.0182	0.0140	0.0147
ϵ ($M^{-1}cm^{-1}$)	0.082 ± 0.002	0.071 ± 0.003	0.072 ± 0.002
r	0.999	0.998	0.999

a. The OD values for NND in 1,1-dibromoethane at 442 nm were determined to be 0.0076 and 0.0113, when [NND] = 0.060 M and 0.100 M, respectively; ϵ was calculated to be 0.12 ± 0.01 ($M^{-1}cm^{-1}$).

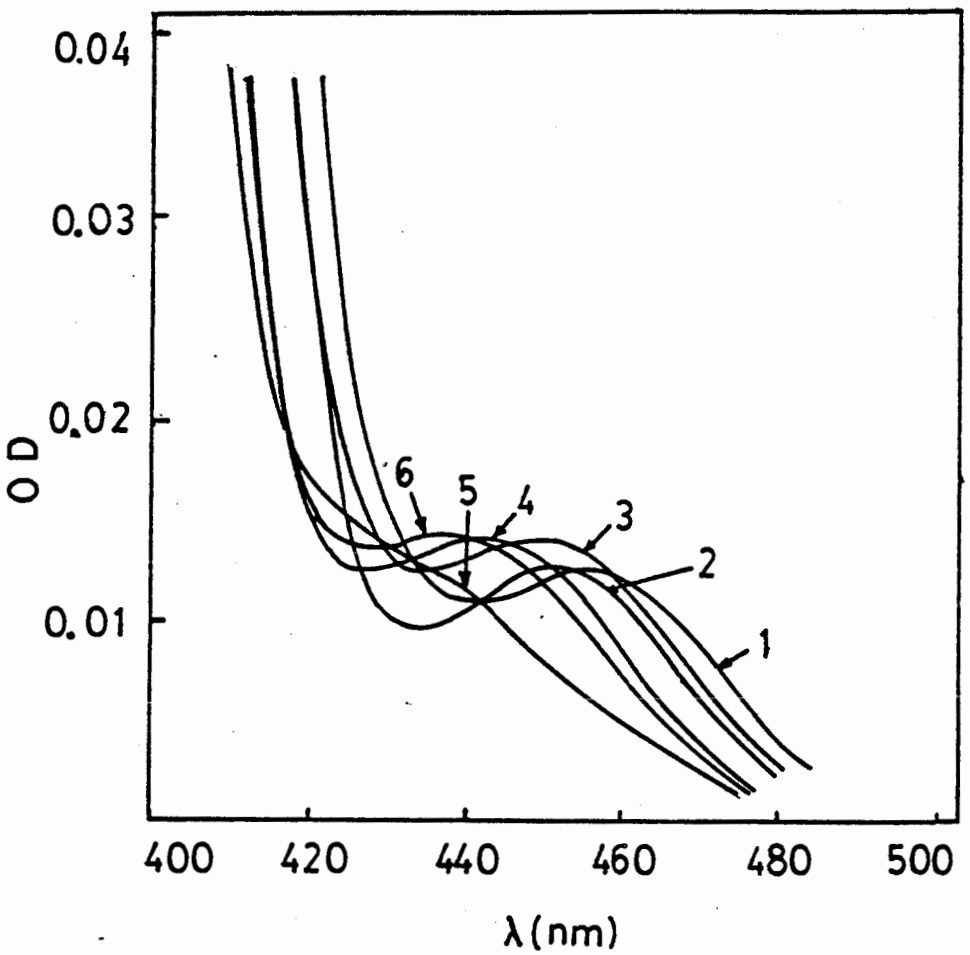

Figure 3-3 S_o-> T_1 absorption spectra of NND (0.20 M) in various solvents: 1, MCH; 2, toluene; 3, THF; 4, methylene chloride; 5, methanol; 6, acetonitrile.

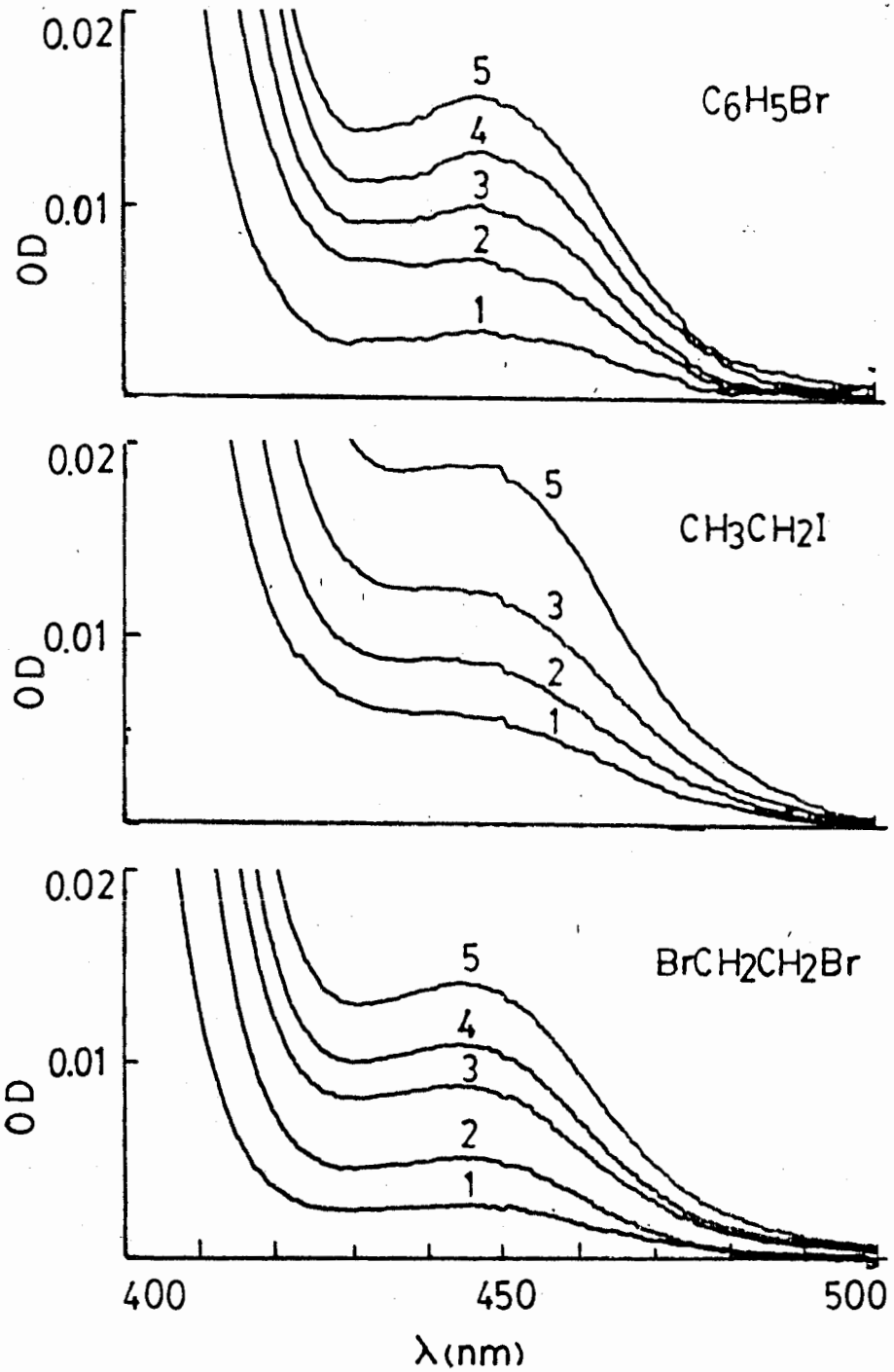

Figure 3-4 S_o-> T_1 absorption spectra of NND in heavy-atom solvents; curves 1-5 contained [NND] of 0.040, 0.080, 0.120, 0.160 and 0.200 M, respectively.

3.1.2 Phosphorescence of NND

In EPA glass (ether/isopentane/ethanol, 5/5/2, by volume) at 77 K, phosphorescence of NND centered at 550 nm was detected on excitation of its $S_o \rightarrow T_1$ transition band at 440 nm (Figure 3-5), but not observed on excitation of the $S_o \rightarrow S_n$ transition bands at 250 and 330 nm. Under similar conditions a phosphorescence excitation spectrum of NND was recorded by monitoring at 530 nm (Figure 3-5). This indicates an absorption in the 400-480 nm region which is very similar to the $S_o \rightarrow T_1$ (n, π^*) absorption in Figure 3-1. The lowest triplet excited state energy level (E_T) of NND was evaluated to be 58 kcal/mol (490-495 nm) from the $S_o \rightarrow T_1$ transition band in the electronic absorption and phosphorescence spectra.

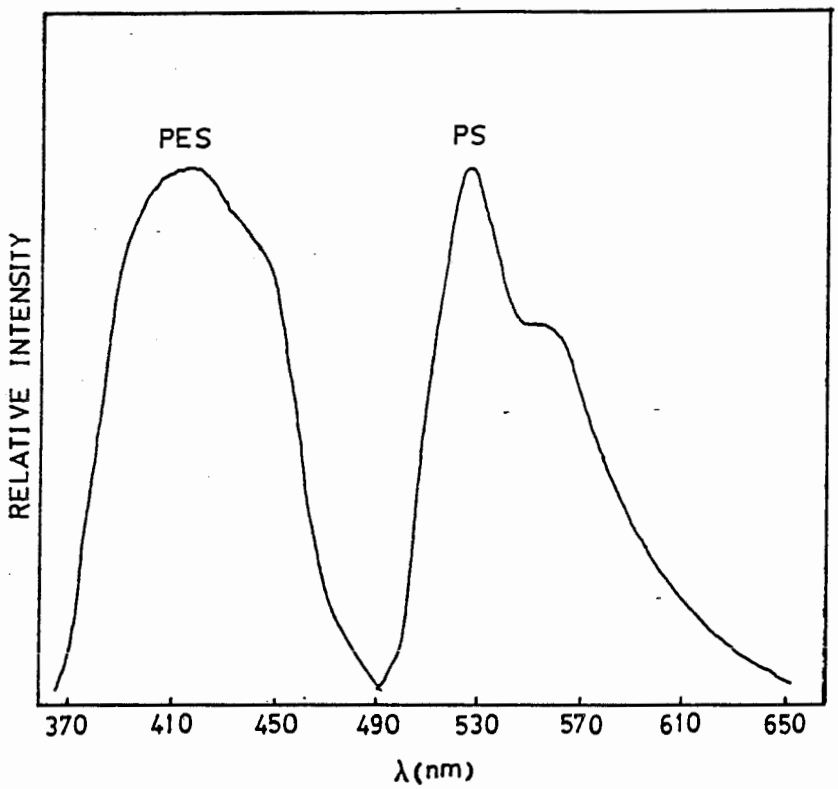

Figure 3-5 Phosphorescence spectrum (PS) and phosphorescence excitation spectrum (PES) of 0.33 M NND in EPA at 77 K; the excitation wavelength was 440 nm, and the PES was monitored at 530 nm.

3.1.3 Quenching Studies

Fluorescence spectra of some selected aromatic hydrocarbons such as anthracene, 9,10-dimethylanthracene, perylene and tetracene were measured in the absence and presence of NND in methanol using routine illumination technique. The excitation wavelength was normally selected around 400-440 nm where NND does not absorb at all. For anthracene, however, the excitation wavelength was 375 nm. Since NND also weakly absorbs at 375 nm, the observed fluorescence intensity ratios, $I°/I$, at 396 nm from Figure 3-6 were corrected as listed in Table 3-4. The correlation of $(I°/I)_{corr}$ with [NND] yielded the Stern-Volmer constant $k_q\tau_o$ = 115 M^{-1} with r = 0.998, and the quenching rate constant was calculated to be 21.7 x 10^9 ($M^{-1}s^{-1}$) when τ_o = 5.3 ns.[23]

Quenching of fluorescence of 9,10-dimethylanthracene (Figure 3-7) and quenching of fluorescence of perylene, by NND in methanol were observed. The Stern-Volmer constants and k_q values were calculated by a usual manner, and are summarized in Table 3-5. No quenching of fluorescence of tetracene was observed (Figure 3-8). The gradual deviation in the quenching rate constants of 9,10-dimethylanthracene and perylene from the near diffusion-controlled value indicates that the singlet-state energy E_s of NND could be 72 - 73 kcal/mol, based on the Sandros' plot [123]. This value agrees well with that estimated from the "onset" of the S_o-> S_1 (n, π^*) transition band (at about 395 nm, see Figure 3-1).

Attempts to populate the triplet excited state of NND by benzophenone and 2-acetonaphthone sensitization in EEI (ether/ethanol/iodoethane, 2/2/1, by volume) glass were not successful, probably owing to strong overlap of both emissions from sensitizer and NND, although the phosphorescence intensity was quenched by NND, as shown in Figures 3-9 and 3-10.

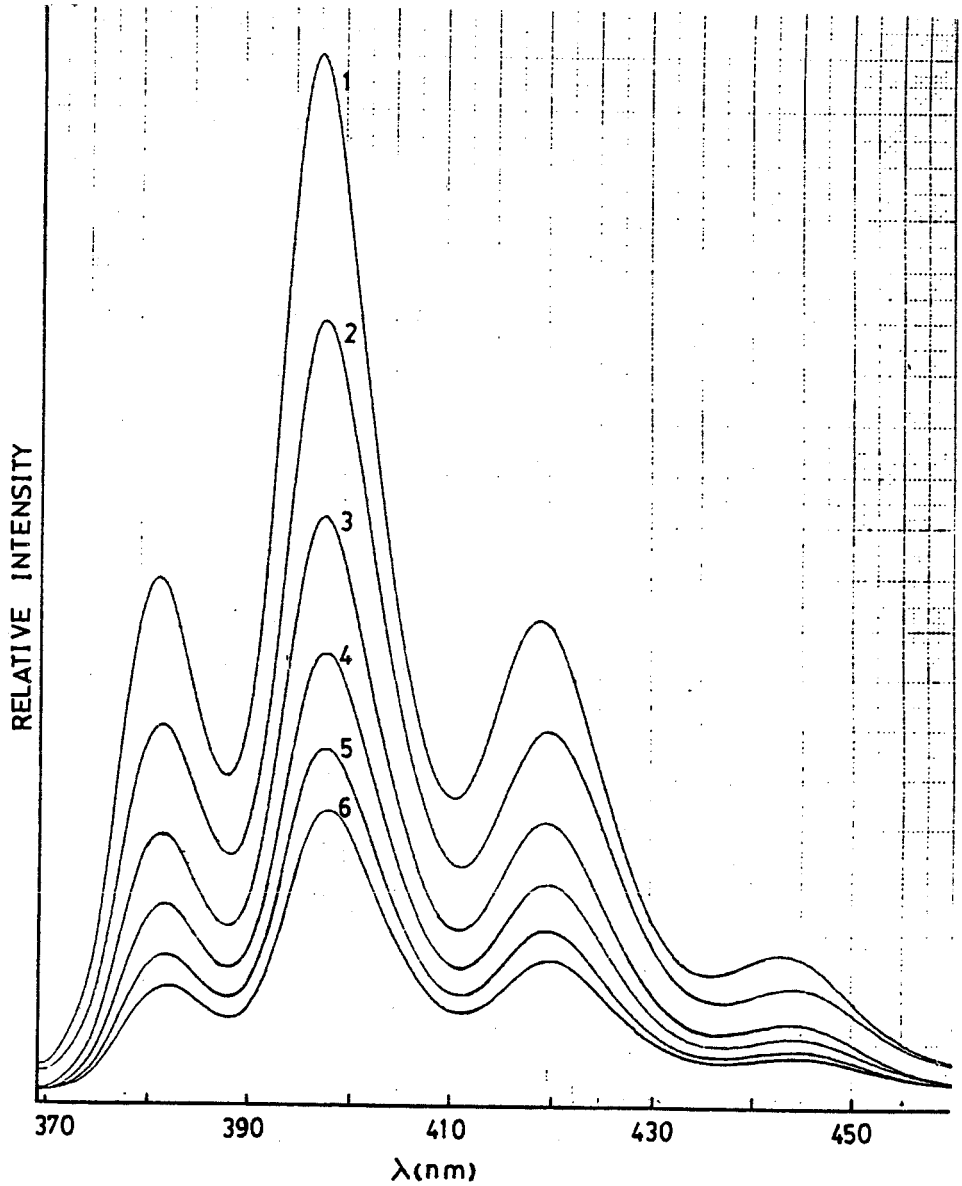

Figure 3-6 Fluorescence spectra of 0.0002 M anthracene in methanol in the absence and presence of various concentrations of NND with excitation at 375 nm at 22°C; curves 1-6 contained [NND] of 0, 0.004, 0.008, 0.012, 0.016 and 0.020 M, respectively.

Table 3-4 Relative Fluorescence Intensities of Anthracene at 396 nm in the Presence of NND in Methanol at 22°C

[NND] (M)	I°/I	A[a]	$(I^\circ/I)_{corr}$[b]
0.0040	1.33	0.962	1.28
0.0080	1.79	0.928	1.66
0.0120	2.35	0.895	2.10
0.0160	3.03	0.865	2.62
0.0200	3.70	0.837	3.10
$k_q\tau_o$ (M^{-1})			115
$k_q \times 10^{-9}$ ($M^{-1}s^{-1}$)			21.7
r			0.998

a. Calibration factor,[124] (see p194 in Experimental).

b. $(I^\circ/I)_{corr} = (I^\circ/I)A$

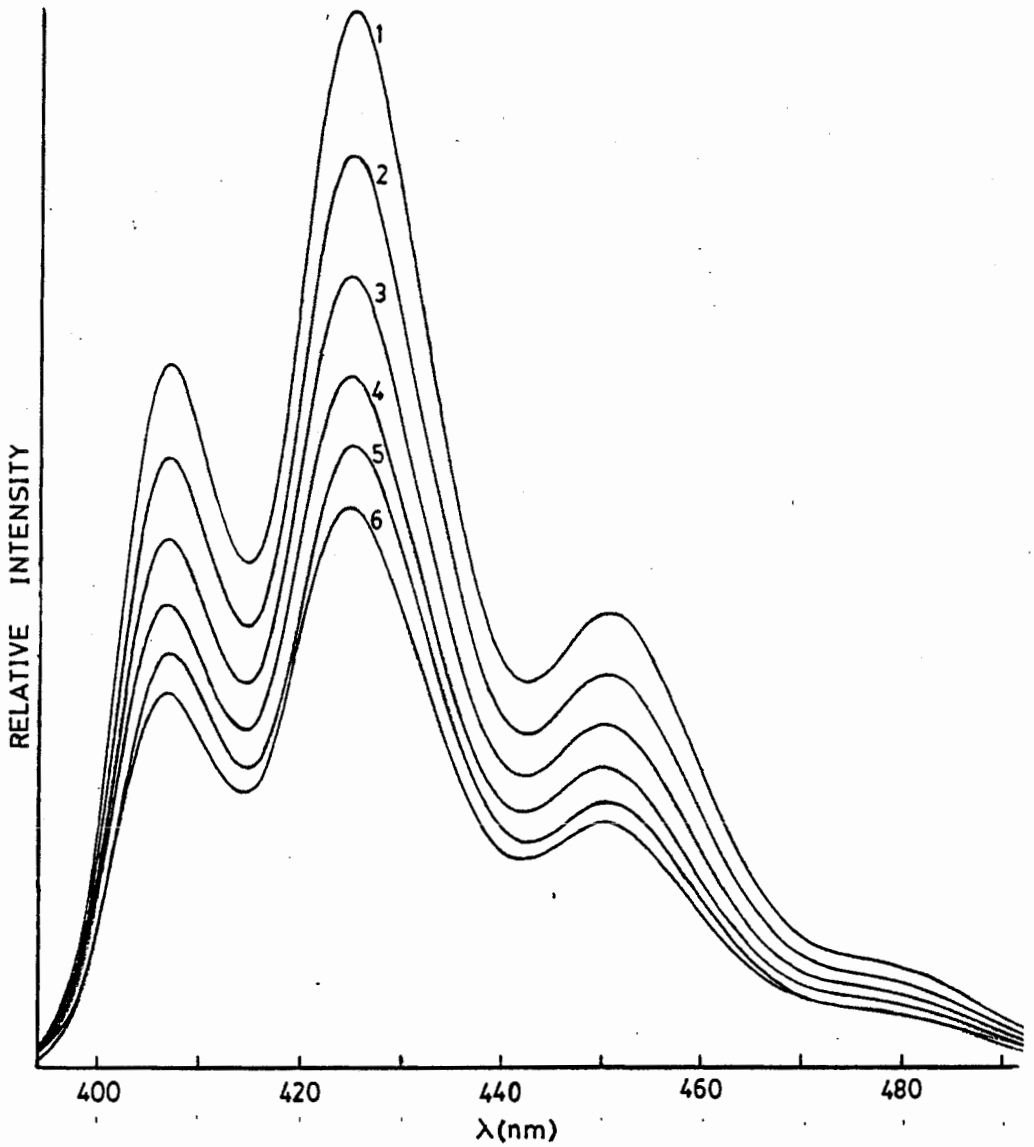

Figure 3-7 Fluorescence spectra of 0.0002 M 9,10-dimethylanthracene in methanol in the absence and presence of various concentrations of NND with excitation at 400 nm at 22°C; curves 1-6 contained [NND] of 0, 0.007, 0.014, 0.021, 0.028, and 0.035, respectively.

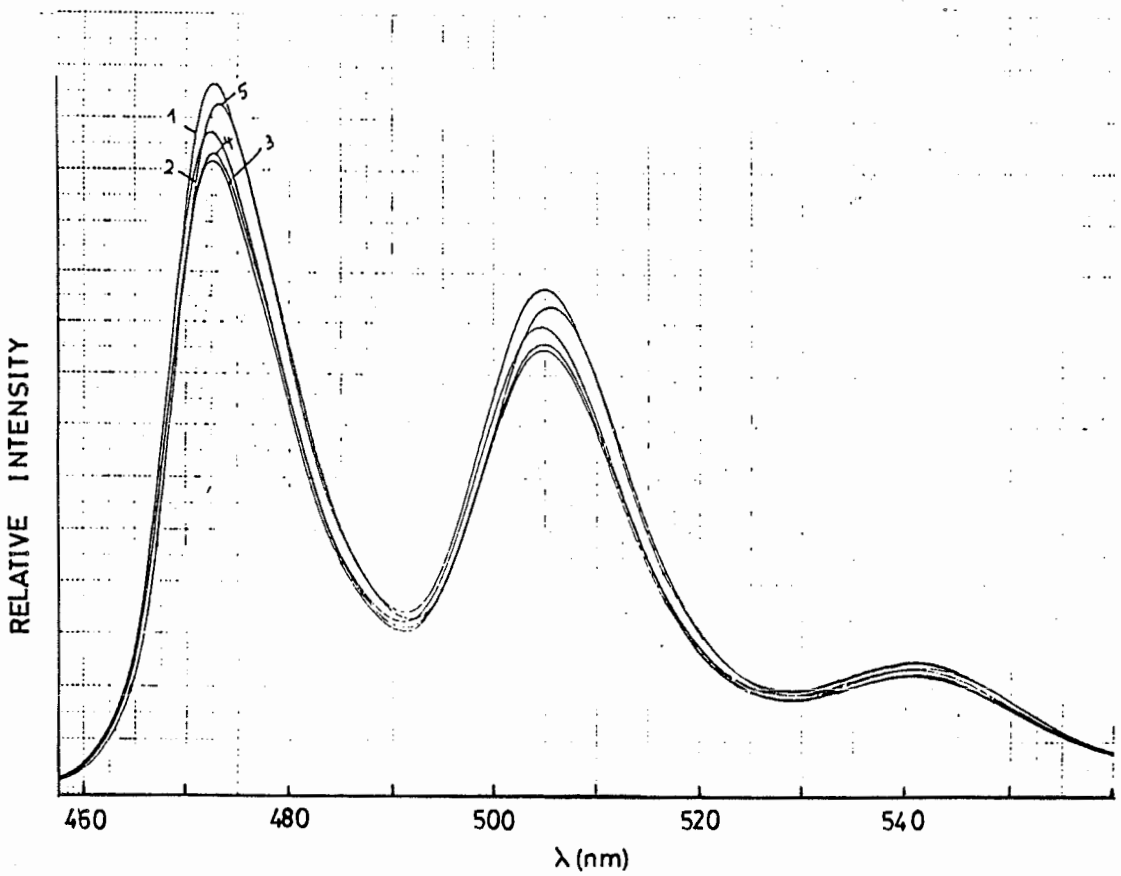

Figure 3-8 Fluorescence spectra of 0.00006 M tetracene in methanol in the absence and presence of various concentrations of NND with excitation at 440 nm at 22°C; the curves 1-5 contained [NND] of 0, 0.020, 0.030, 0.040 and 0.060 M, respectively.

Table 3-5 Quenching of Aromatic Hydrocarbon Fluorescence by NND in Methanol at 22°C

ArH	E_S[a] (kcal/mol)	λ_{ex} (nm)	λ_{em}^{max} (nm)	$k_q \times 10^{-9}$ ($M^{-1}s^{-1}$)	[NND]$\times 10^3$ (M)[b] r
anthracene	76.3	375	396	21.7	4 - 20
					0.998
9,10-dimethylanthracene	71.8	400	425	1.53	7 - 35
					1.000
perylene	65.8	430	465	0.185	10 - 60
					0.993
tetracene	60.7	440	473	c	20 - 60

a. Cited from ref. 23.

b. The NND concentration range used.

c. No quenching of fluorescence.

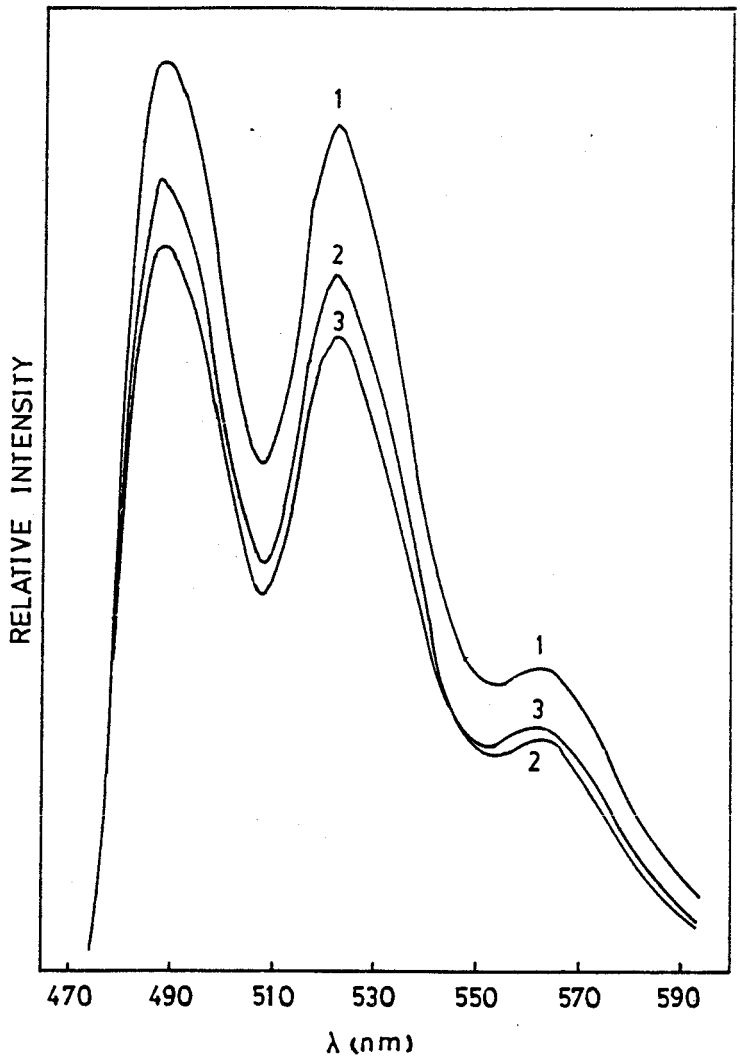

Figure 3-9 The changes of phosphorescence spectra of 2-acetonaphthone (0.002 M) in EEI (ether/ethanol/iodoethane) glass in the presence of NND at 77 K; curves 1-3 contained [NND] of 0, 0.0048 and 0.0096 M, respectively; and 2-acetonaphthone was excited at 320 nm.

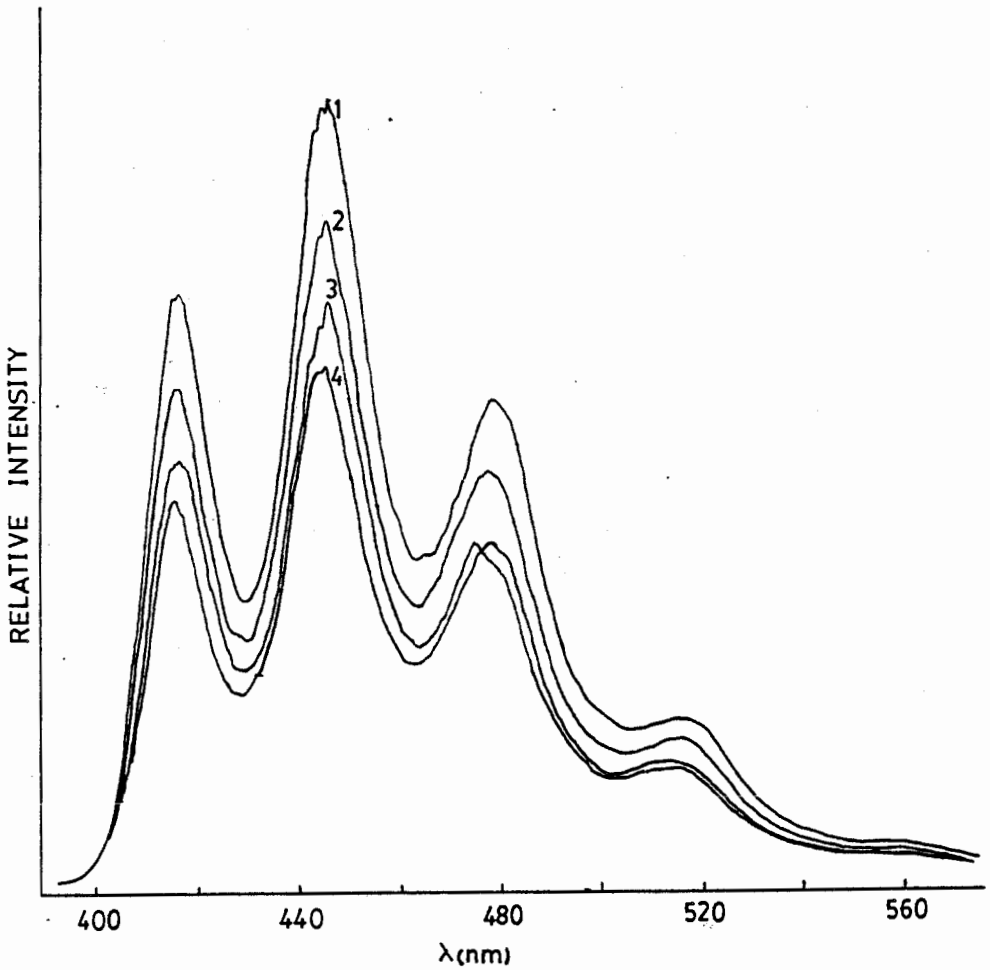

Figure 3-10 The changes of phosphorescence spectra of 0.0011 M benzophenone in EPA (ether/isopentane/ethanol) glass in the presence of NND at 77 K; the curves 1-4 contained [NND] of 0, 0.003, 0.006 and 0.009 M, respectively; benzophenone was excited at 300 nm.

3.2 Discussion

The first example of a spin-forbidden radiative transition of nitrosamines has been discovered by the detection of the $S_o \rightarrow T_1$ absorption and of phosphorescence of NND. It has been shown that[121,122] non-heavy-atom-containing molecules possessing a "pure" π,π^* configuration in the T_1 state, have values of ϵ_{max} ($S_o \rightarrow T_1$) in the order of 10^{-5} to 10^{-6}, show a "red-shift" in polar solvents, and are sensitive to heavy-atom solvent effects; those possessing a "pure" n,π^* configuration in the excited state have ϵ_{max} ($S_o \rightarrow T_1$) in the order of 10^{-1} to 10^{-2}, show a "blue-shift", and are insensitive to heavy-atom solvent effects. Therefore, the $S_o \rightarrow T_1$ transition of NND is suggested to be (n,π^*), since the transition is insensitive to external heavy-atom effects (see Table 3-3), shows a "blue-shift" in polar solvents, (Figure 3-3), and has the value of ϵ_{max} = 0.064 $M^{-1}s^{-1}$. This unperturbed absorption is more readily detected than that for N-oxide quinoline, which was observed under a high pressure of oxygen,[125-127] and than that for cyclic azoalkane[128], which showed a $S_o \rightarrow T_1$ absorption at 430 nm with ϵ_{max} = 0.01 $M^{-1}cm^{-1}$ using a 10 cm path-length cuvette.

The energy level of the lowest triplet excited state of NND was determined to be E_T = 58 - 59 kcal/mol, from both absorption and phosphorescence spectroscopy. Sensitization experiments conducted on N-nitrosopiperidine allowed E_T for that compound to be placed around 59 kcal/mol.[15] The calculated E_T value of NND is 62.1 kcal/mol.[129] The E_S value of NND was determined to be 72 - 73 kcal/mol from fluorescence quenching results in Table 3-5. The calculated energy gap between S_1 and T_1 is 14 kcal/mol.

Failure to observe fluorescence and phosphorescence emission on excitation of $S_o \rightarrow S_1$ hints that the spectroscopic S_1 state must depopulate rapidly by channels (e.g. chemical dissociation) other than intersystem crossing. Recently, Huber and his co-workers[3,130] have demonstrated that the excitation of the 363.5 nm band **in the gas phase** caused NND to dissociate from the its lowest singlet state to dimethylamine radical and nitric oxide (Equation 3-2) with $\Phi = 1.03$ and $k_2 > 8.5 \times 10^9\ s^{-1}$. Subsequently, the two radicals recombine very efficiently to NND (Equation 3-3). The lifetime of the singlet excited state was estimated to be < 0.12 ns according to the k_2 value. This means that the singlet excited state of NND decomposes so fast that the intersystem crossing (Equation 3-4) cannot substantially compete with Equation 3-2 to generate the phosphorescing triplet excited state.

The reversible photodissociation of NND established by Huber[3,130] together with what has been learned in this Chapter, allows us to present the following reaction scheme to describe the photochemical and photophysical behavior of NND in neutral media.[131]

$$(Me)_2N\text{-}NO \xrightarrow{h\nu} {}^{1*}(Me)_2N\text{-}NO \qquad 3\text{-}1$$

$${}^{1*}(Me)_2N\text{-}NO \xrightarrow{k_2} (Me)_2N^{\bullet} + NO^{\bullet} \qquad 3\text{-}2$$

$$(Me)_2N^{\bullet} + NO^{\bullet} \longrightarrow (Me)_2N\text{-}NO \qquad 3\text{-}3$$

$${}^{1*}(Me)_2N\text{-}NO \longrightarrow {}^{3*}(Me)_2N\text{-}NO \qquad 3\text{-}4$$

$$(Me)_2N\text{-}NO \xrightarrow{h\nu'} {}^{3*}(Me)_2N\text{-}NO \qquad 3\text{-}5$$

$${}^{3*}(Me)_2N\text{-}NO \longrightarrow (Me)_2N\text{-}NO + h\nu' \qquad 3\text{-}6$$

Scheme 3-1

CHAPTER 4

PHOTOADDITION OF NND TO PYRENE AND 1-PHENYLPROPENES IN ACIDIC MEDIA

4.1 Results

4.1.1 Sensitized Photoaddition of NND to Pyrene

As mentioned in the Introduction, certain fused aromatic hydrocarbons, e.g. anthracene (Equation 1-1), act as singlet sensitizers as well as substrates to induce addition of nitrosamines giving amino nitroso adducts in acidic media.[22] It was reported that pyrene (E_S = 77 kcal/mol, τ_s = 450 ns, Φ_f = 0.58)[23] sensitized photoaddition of N-nitrosopiperidine in acidic methanol solution to give 4-piperidinopyrene in 52% yield.[22]

Photolysis of pyrene and NND in acidic methanol under N_2 at 0-5°C rapidly caused the formation of dark photolysate, and could not be carried to completion. The OD ratio of 0.034 M NND to 0.043 M pyrene in methanol at 343 nm was determined to be 0.025, so that more than 95% of the incident light was absorbed by pyrene when a Pyrex filter was employed. A photoproduct was isolated as greenish-yellow needles in 28% yield together with some recovered pyrene. The photoproduct was shown by ^{1}H-NMR and ^{13}C-NMR to possess a dimethylaminium chloride moiety with the resonances at 2.50 and 45.9 ppm, respectively, and this was confirmed by IR absorption at 2350 cm^{-1} [$-(Me)_2NH^+Cl^-$]. The corresponding free base, dimethylaminopyrene, was obtained by neutralization, and shown by decoupled ^{1}H-NMR spectra (Figure 4-1) to possess a dimethylamino group at C-1 rather than C-4 or C-2, because of no singlet signal in the spectrum. The product must be 1-dimethylaminopyrene **25**. The pathway of the addition is suggested in Scheme 4-1, based on previous reports.[22, 132]

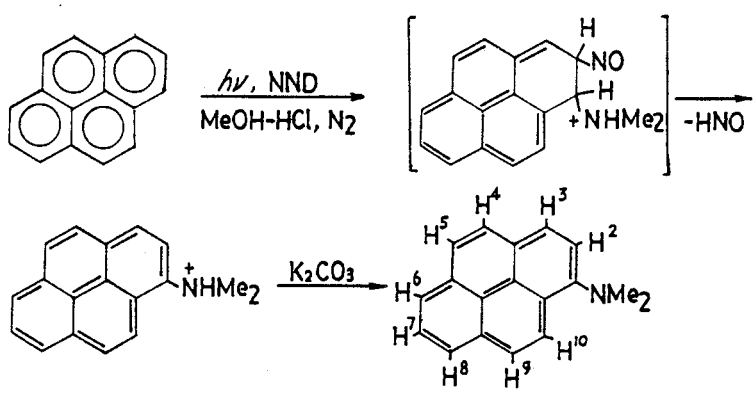
hν, NND
MeOH-HCl, N2
H
NO
H
+NHMe2
-HNO
+NHMe2
K2CO3
H4
H3
H5
H2
H6
NMe2
H7
H10
H8
H9

25

Scheme 4-1

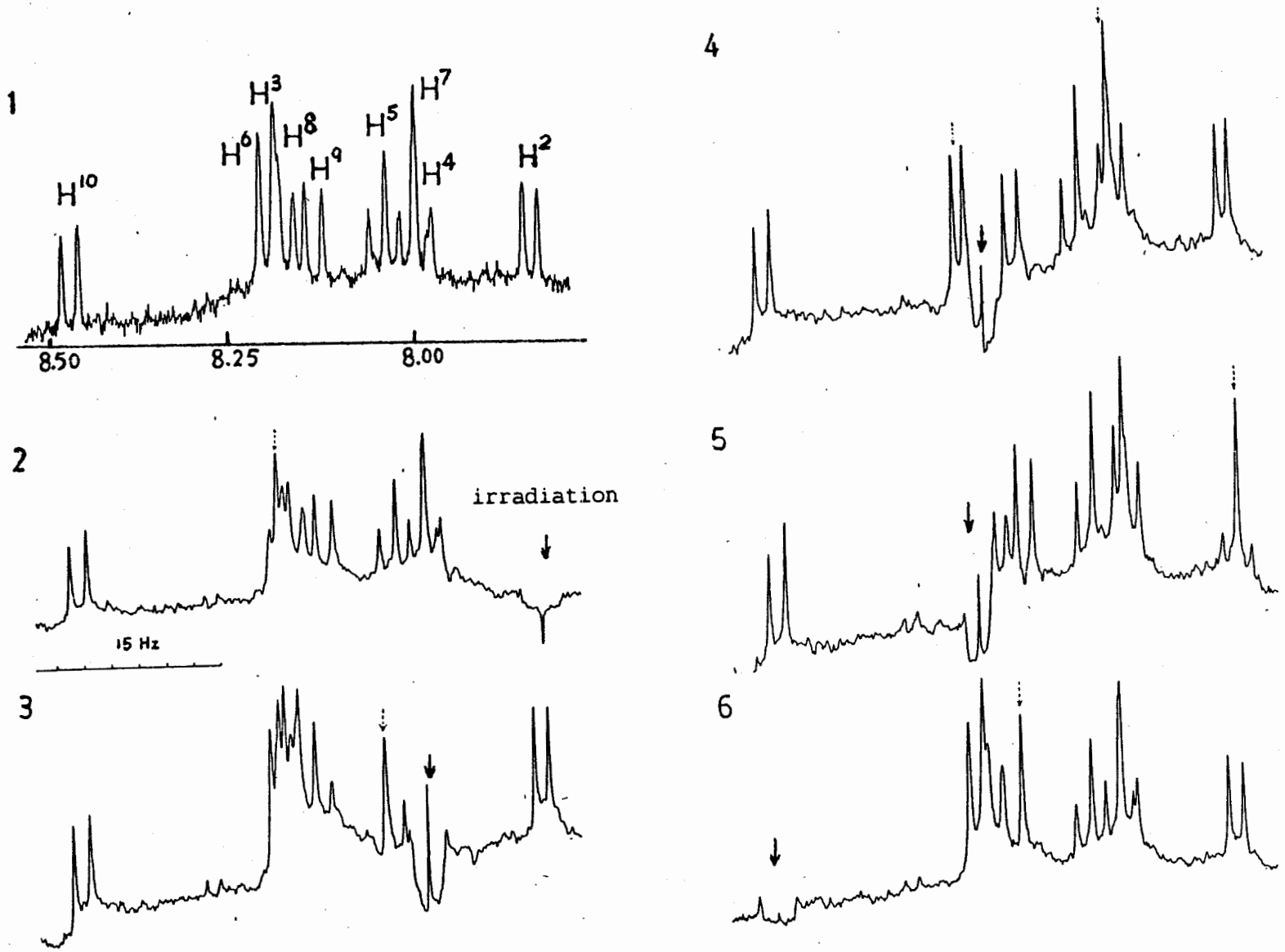

Figure 4-1 Partial NMR spectrum of **25**. (2)(5) H^2 and H^3 decoupled, (3) H^4 and H^5 decoupled, (4) H^6, H^7 and H^8 decoupled, (6) H^9 and H^{10} decoupled.

4.1.2 Oxidative Photoaddition of NND to (*E*)-1-Arylpropenes

The oxidative photoadditions of nitrosamines to olefins and some aromatic hydrocarbons in acidic media have been investigated in detail in our laboratory.[1,2,14,22,133,134] The addition has been shown in Scheme 1-1 (see Introduction) to proceed by stepwise radical attack of an aminium radical, followed by attack of oxygen with an anti-geometry.[21,133,134] The following experiments are some applications of the oxidative photoaddition in the preparation of ephedrine-like compounds.

The oxidative photoaddition of NND to (*E*)-1-arylpropene, in the presence of hydrochloric acid, was carried out in methanol under oxygen purging, and the progress of the photoreaction was monitored using UV spectroscopy by following the disappearance of the 330-nm absorption (NND $n\rightarrow\pi^*$ transition). The crude products were separated into "acidic-neutral" fraction and basic fraction. The former fraction was generally a complex mixture and was not investigated further. The basic fraction contained α-amino nitrates and other amine derivatives and was reduced with lithium aluminium hydride (LAH) to afford crude α-amino alcohols, which were isolated by chromatography.

The oxidative photoaddition to (*E*)-1-(4-methoxyphenyl)propene **26** and subsequent LAH reduction afforded 1-(4-methoxyphenyl)-1-methoxy-2-(dimethylamino)propane (**27**, 24%) and *threo*- and *erythro*-1-(4-methoxyphenyl)-2-(dimethylamino)-1-propanol (**28a** and **28b**) in 28 and 15% yield, respectively, as shown in Equation 4-1. The presence of a dimethylamino group in these products was confirmed by ^{1}H-NMR singlet signals in the 2.2 - 2.5 ppm region and by the Bohlman bands in the 2800 - 2700 cm^{-1} region.

The presence of a nitrate group in the crude photoproducts was readily shown by strong IR peaks at about 1675, 1250 and 860 cm^{-1}. The methoxy compound **27** was also present in these crude products as indicated by the presence of a NMR singlet at 3.13 ppm assigned to the benzylic OMe group.

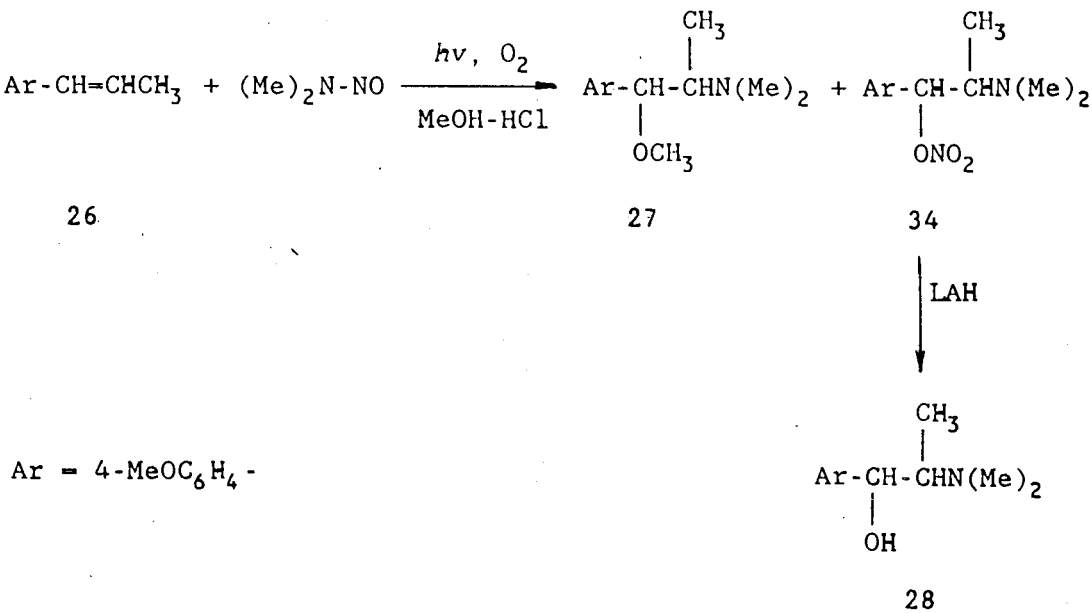

26 27 34 28

4-1

The structures of these compounds were supported by their NMR, IR and MS spectral data and also by elemental analysis (see Experimental). The two α-amino alcohols **28a** and **28b** exhibited rather similar spectral data with the exception of the coupling pattern of the NMR doublet of the benzylic proton, which was used to assign the diastereoisomers on the basis of the conformational analysis discussed below. The α-alcohol **28a** shows this proton coupled with the C-2 methine proton (J=10 Hz) and is assigned as the *threo* isomer.[135,136] Similarly, **28b** shows this proton in the corresponding vicinal interaction with J=3 Hz and is assigned as the *erythro* isomer.[135,136]

Two sets of three conformational isomers for the *threo*- and *erythro*-amino alcohols, **28a** and **28b**, respectively, are depicted in Figure 4-2 where X = H, R = 4-$MeOC_6H_4$ and R^1 = CH_3. Since the contribution of three conformers to each compound is determined by two opposing forces, e.g.

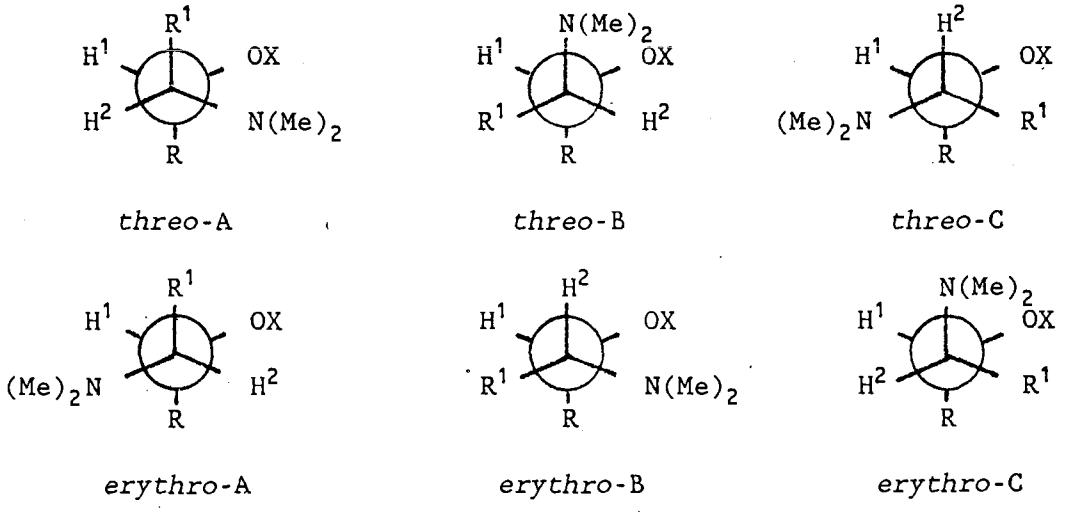

Figure 4-2 The conformational isomers of *threo* and *erythro* compounds in **28** and **30** (X = H).

the non-bonded repulsion of substituents and stabilization by hydrogen bonding, *threo*-B (with a *trans* interaction for H^1 and H^2) and *erythro*-B (or C, with a *gauche* interaction for H^1 and H^2) are expected to be more stable than the other conformers in each series. These considerations have led us to assign **28a** ($J_{1,2}$ = 10 Hz) to the *threo* isomer and **28b** ($J_{1,2}$ = 3 Hz) to the *erythro* isomer. These assignments are in line with those of some diastereoisomeric *a*-amino alcohols reported previously.[21,133,134] The methoxy amine **27** shows the corresponding coupling constant $J_{1,2}$ = 10 Hz as **28a**, but its stereochemistry could not be assigned with confidence owing to the absence of the other isomer. The similarity of the coupling constant does not necessarily imply the same stereochemistry as **28a**, since intramolecular hydrogen bonding no longer exists (*vide infra*).

The oxidative photoaddition of NND to (*E*)-3-phenyl-2-propenol **29** and subsequent LAH reduction under similar conditions gave *threo*- and *erythro*-1-phenyl-2-(dimethylamino)-1,3-propanediol (**30a** and **30b**) in 42 and 16% yield, respectively, in addition to 3-phenyl-2,3-bis(dimethylamino)-1-propanol **31** with 14% yield (Equation 4-2). The structure of **31** was readily deduced from the spectral data and elemental analysis, particularly from the NMR singlets at 2.12 and 2.15 ppm for the two $-N(Me)_2$ groups, and from the doublet at 3.77 ppm (J = 11 Hz) for the benzylic proton. The amino diols **30a** and **30b** show close similarity in their spectral data, except for the doublet at 4.43 ppm ($J_{1,2}$ = 10 Hz) of **30a** and that at 5.04ppm ($J_{1,2}$ = 3 Hz) of **30b** for the benzylic proton. The difference in the coupling constants closely resembles that of the **28a-28b** pair. Assuming the influence of hydrogen bonding from the terminal CH_2OH group to the conformational isomers depicted in Figure 4-2 (X = H, R = C_6H_5, R^1 = CH_2OH) is common and comparable in both the isomeric series, **30a** and **30b** are assigned with *threo* and *erythro* configurations, respectively, on the basis of an argument similar to that

used for **28** (*vide supra*). The *threo* isomer **30a** has *threo*-B as the most stable conformation with the *anti*-orientation of H^1 and H^2; the *erythro* isomer **30b** has *erythro*-B (or -C) as stable conformations with a *gauche*-orientation of H^1 and H^2.

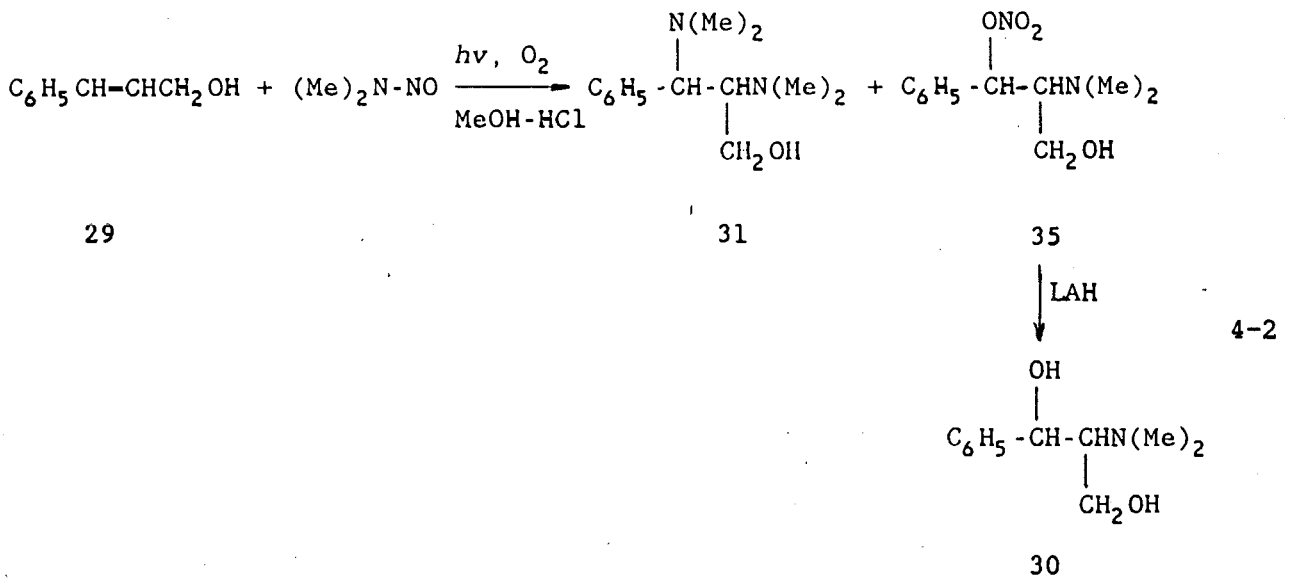

The oxidative photoaddition of NND to (*E*)-1-(3-methoxy-4-hydroxyphenyl)propene **32** gave a large quantity of the "acidic-neutral" fraction which exhibited a complex GC pattern. The minor basic fraction showed no IR absorption for the nitrate group and was chromatographed to afford 1-(3-methoxy-4-hydroxyphenyl)-1-methoxy-2-(dimethylamino)propene **33** in 16% yield (Equation 4-3). The pattern of the NMR spectrum above 6 ppm of **33** closely resembles that of **27**, including the two methoxy singlets at 3.2 and 3.8 ppm and a doublet at 3.85 ppm (J = 8 Hz) for the benzylic proton. The MS spectra of the two methoxy amines also exhibited corresponding fragments at the excepted mass numbers in comparable intensities. This information leaves no doubt as to the structure **33** for the compound.

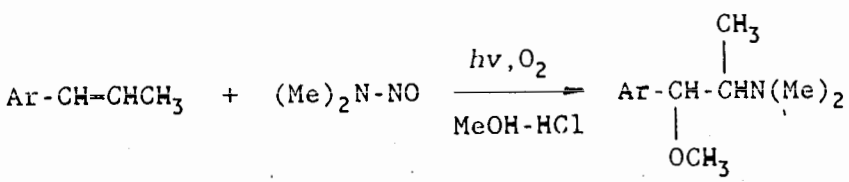

32 33 4-3

Ar = 3-MeO-4-OHC_6H_3-

4.2 Discussion

The sensitized photoaddition of NND to pyrene in acidic solution is suggested to follow the mechanism depicted in Scheme 4-1. Dimethylaminium and nitric oxide radicals are generated from sensitized photodecompoition of NND by the singlet excited pyrene. The former radical $(Me)_2NH^{\cdot+}$ electrophilically attacks pyrene at the C-1 position, followed by scavenging of the C-2 radical by nitric oxide to form the C-nitroso intermediate, which eliminates HNO to give the final product. Mechanistically, the elimination could occur either by acid catalysis or sensitized photolysis.[22] The driving force for the elimination may be ascribed to the tendency to achieve aromaticity. This reaction also re-confirms the requirement of an acidic medium for photodecomposition of NND.

The oxidative photoaddition of NND to phenylpropenes occurs with a high degree of regiospecificity to give the expected *α*-amino nitrates **34** and **35** in addition to by-products of *α*-methoxy amines **27** and **33** and diamine **31**. By analogy to previous reports[21,22,133] these by-products are assumed to be formed from the nitrates by intramolecular amine-group-participated substitution reaction, e.g. **34->36** and beyond as shown in Scheme 4-2. Undoubtedly, an electron-rich aryl group facilitates the formation of **27** and **33**, presumably by stabilizing the developing benzylic carbenium ions **36**. The nitrate **34**, derived from arylpropene **32**, is prone to undergoing such substitution and cannot be obtained, probably owing to the facile dissociation of the nitrate group assisted by the resonance effects of the 4-hydroxy-3-methoxyphenyl group. Such substitution does not occur with *α*-amino nitrate **35** under the acidic conditions used during the photoreaction, since the phenyl group without an electron-donating group presumably does not promote the benzylic carbenium ion formation. It is

suspected that diamine **31** is formed by a similar sequence of substitution reactions when the crude product, after the evaporation of methanol, is rendered basic in aqueous solution; the liberated dimethylamine then acts as a nucleophile to give diamine **31**. While its formation is most likely associated with certain effects of the terminal OH group in **35**, the detailed mechanism is unclear. The by-products, **27**, **31** and **33** all exhibit a large coupling constant of two tertiary hydrogens ($J_{1,2}$ = 8-11 Hz in Figure 4-2) and probably possess the *erythro* configuration on the basis of the mechanistic considerations discussed below.

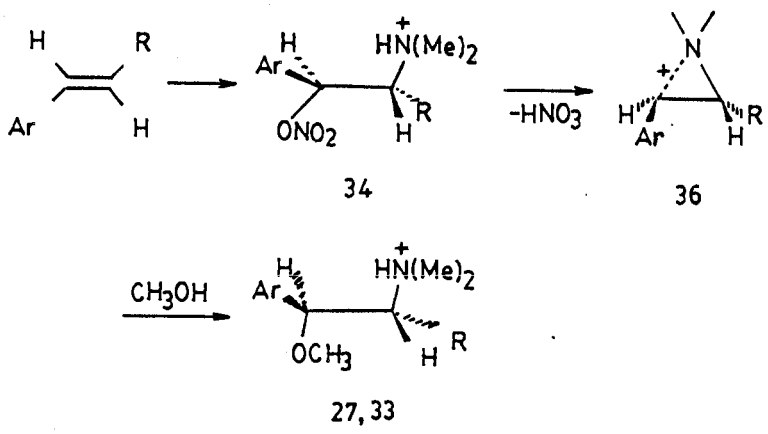

Scheme 4-2

Since all propenes used in this study have the (*E*)-configuration as shown by their ^{1}H-NMR coupling constants (J ≃ 16 Hz, see Experimental) of olefinic protons, the primary photoaddition products, nitrates **34** and **35**, must contain major fractions of the *erythro* isomer owing to the lower energy requirement in the *anti*-addition to (*E*)-alkenes.[137] Indeed, it has been shown[133] that the *erythro* isomer is the major product obtained under ordinary photoaddition conditions. The *erythro* isomers of **34** and **35** are

also more facile than the corresponding *threo* isomers in undergoing the amine-group-participated solvolysis, on the basis of energetic considerations in the transition state,[137] to give **27**, **31** and **33** via the aziridinium ion **36** with a net retention of stereochemistry; i.e., **27**, **31** and **33** are most likely to have the *erythro* configuration. The preferential solvolysis of the *erythro* isomrs of **34** and **35** is thought to be responsible for the unusually low yields of the *erythro* *a*-amino alcohols **28b** and **30b**. Lower yields of the *erythro* isomers compared to those of the *threo* isomers of *a*-amino alcohols have been observed in the similar oxidative photoaddition to (*E*, *E*, *E*)-1,5,9- cyclododeca-triene.[21] Since the by-products **27**, **31** and **33** no longer have the ability to participate in the hydrogen bonding depicted in Figure 4-2 [OX = OMe or $N(Me)_2$], the conformer *erythro*-A should be the most stable of the three on the basis of non-bonded repulsion of the substituent.[137] The observed large $J_{1,2} \simeq 10$ Hz is in agreement with the *anti*-orientation[135,136] of H^1 and H^2 in the *erythro*-A.

The low yield of the oxidative photoaddition to propene **32** may be due to the presence of the 4-hydroxy group. No satisfactory explanation, however, can be suggested at present for this phenomenon.

CHAPTER 5

EXPERIMENTAL

5.1 General Conditions

Unless otherwise specified, the following experimental conditions prevailed. Melting points (mp) were determined on a Fisher-Johns apparatus, and are uncorrected. Infrared spectra (IR) were recorded with a Perkin-Elmer 559B spectrophotometer using neat liquid film, nujol mull or KBr pellet. Ultraviolet and visible spectra (UV) were taken with a Varian Cary 210 spectrophotometer. Mass spectra (MS) and gas-chromatography-mass spectra (GC-MS) were obtained on a Hewlett-Packard 5985 GC-MS system either by electron ionization (at 70 ev) or by chemical ionization. Proton nuclear magnetic resonance (^{1}H-NMR) spectra were recorded with a EM-360, Bruker WM-400, or Bruker SY-100 spectrometer in $CDCl_3$ solution using tetramethylsilane (TMS) as a relative standard. Chemical shifts are reported in δ values in ppm and coupling constants (J) in Hz. The coupling patterns are presented as s (singlet), d (doublet), t (triplet), q (quartet) and m (multiplet). D_2O exchangeable protons are indicated by "D_2O exch". The chemical shifts of ^{13}C-NMR spectra are also reported as δ values in ppm relative to TMS. Elemental analyses were carried out by Mr. M.K. Yang using a Carlo Erba Model-1106 Elemental Analyzer. Gas chromatography (GC) analyses were performed on a Hewlett-Packard 5790A chromatograph (FID), equipped with an OV-1 capillary column and a Hewlett-Packard 3390A chart integrator. Retention times (Rt) are reported in minutes (min). High pressure liquid chromatography (HPLC) analyses were performed on a Waters Associates HPLC system, equipped with a Bondapak C_{18} column and a Waters Associates Model-440 UV detector at 254 or 340 nm.

The mobile phase was MeOH/H_2O = 7:3, by volume. Phosphorescence and fluorescence spectra were taken with a Perkin-Elmer MPF 44B spectrophotometer. Emission spectra were uncorrected. A general deaerating method for a sample solution in a test-tube or a fluorescence cuvette was performed by sealing the tube with a septum and bubbling oxygen-free nitrogen through the solution for at least 10 min.

5.2 Chemicals and Apparatus

For the preparative photochemical reactions, reagent grade solvents were distilled prior to use. Methanol and ethanol were distilled from magnesium. THF and dioxane were distilled from sodium-benzophenone.

For spectroscopy, commercial spectroscopic grade solvents were used as supplied: toluene (Fisher), acetonitrile (BDH), methylene chloride (Fisher), methanol (Fisher), and ethanol (Fisher). Water was HPLC grade (Fisher). Dioxane (Fisher) and THF (AnalaR) were analytical grade and were distilled from sodium-benzophenone prior to use. Methylcyclohexane (BDH) and isopentane (Mallinckrodt) were carefully purified according to standard methods.[138] Iodoethane (Aldrich), 1,2-dibromoethane (Aldrich), 1,1-dibromoethane (Aldrich) and bromobenzene (Aldrich) were freshly distilled twice prior to use.

NND was prepared according to the procedure described elsewhere[139], and purified by vacuum distillation twice. It should be noted that nitrosamines are powerful carcinogens[141] and appropriate caution was exercised on handling in the laboratory.

O-Deutero-1-naphthol (1-NpOD) was prepared by repetitive exchange of the hydroxylic proton by shaking with D_2O using the following procedure. All the glassware to be used was thoroughly flame-dried, and placed in a nitrogen glove box. A dried ether (Fisher) solution (10 ml) of freshly

sublimed 1-NpOH (500 mg) was washed with 3 ml D_2O (MSD), followed by re-washing with 1.5 ml D_2O five times. The ether solution was dried with magnesium sulfate. Both washing and drying procedures were carried out under nitrogen. The dried solution was evaporated under vacuum to afford 310 mg 1-NpOD, which was analyzed by IR (nujol) to be 87% pure (Figure 5-1).

Quadricyclene (QC) was prepared according to the method described by Smith.[140] To a 175 ml cylindrical vessel (Pyrex glass) with a magnetic stirrer and a reflux condenser, were added acetophenone (5 ml), norbornadiene (Aldrich, 25.62 g, 278 mmol) and ether (100 ml). The mixture was irradiated with a 450 Watt Hanovia lamp at running-tap-water temperature for 14 h. Ether was removed under reduced pressure, and the residue was distilled at 43°C/10 mm to give 13.4 g colorless liquid (QC): ^{1}H-NMR ($CDCl_3$), δ 1.34(m, 2H), 1.49(m, 4H) and 2.01 (m, 2H).

Commercially available reagent grade 1-naphthol (Anachemia), 2-naphthol (Anachemia), anthrone (Fisher), 9-phenanthrol (Aldrich), anthracene (Matheson), 9,10-dimethylanthracene (Aldrich), benzophenone (Fisher), xanthone (Aldrich), benzhydrol (Matheson), pyrene (Aldrich) and perylene (Aldrich) were purified by recrystallization, vacuum sublimation or a combination of the both. 1-Methoxynaphthalene (Aldrich) was purified by vacuum distillation. Tetracene was provided by Dr. R.W. Yip, National Research Council. 1-(4-Methoxyphenyl)propene (Eastman), 3-phenyl-2-propenol (Matheson) and 1-(4-hydroxy-3-methoxyphenyl)propene (Eastman) were commercially available, and were distilled under high vacuum or recrystallized prior to use.

Nitrogen gas (Union Carbide) was purified by scrubbling through a Fieser solution[142], through concentrated sulfuric acid, and then through potassium hydroxide pellets.

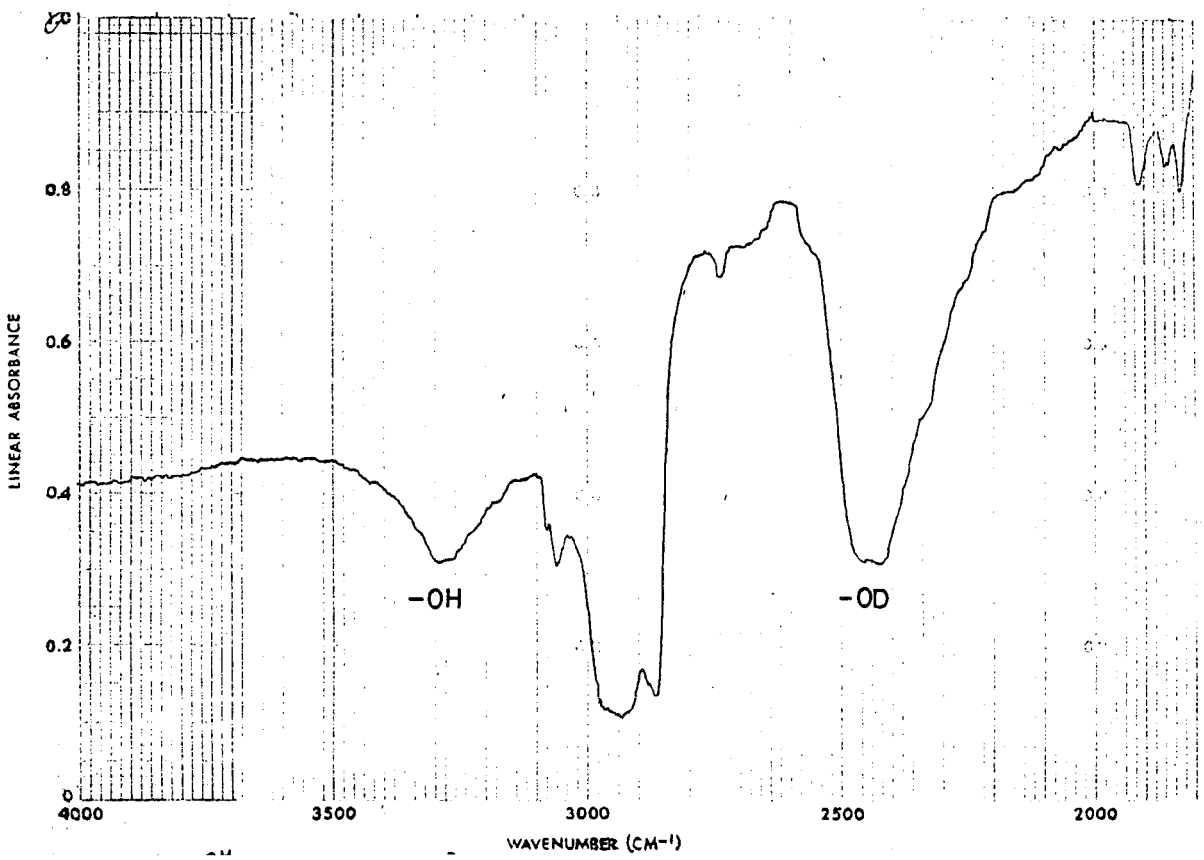

Figure 5-1 IR spectrum of O-deutero-1-naphthol in nujol.

5.3 Photolysis Apparatus

Three different types of photolysis apparatus were employed in the preparative experiments.

Apparatus I

This apparatus consisted of a flat cylindrical reaction vessel (40 ml) (Pyrex glass) fitted with a condenser and a side arm (gas inlet). A gas trap was also fitted on the top of the condenser to allow gas inside the apparatus to escape. The light source was generally a 450 Watt Hanovia medium pressure mercury lamp (679A 36) inserted into a quartz water-cooled jacket. Both the vessel and light source were immersed in running tap water, and the vessel was placed at a distance of about 1-2 cm from the light source. This apparatus was generally used for preparative photonitrosation.

Apparatus II

This apparatus consisted of a long cylindrical reaction vessel (3 x20 cm, quartz glass) fitted with a Teflon stopcock in order to seal the sample solution. The vessel was inserted into the center of a Rayonet Photochemical Reactor equipped with RPR 300 nm lamps (16 x 23 Watt) and a fan to circulate the air providing constant temperature at 31 ± 1°C.

Apparatus III

This apparatus consisted of a large cylindrical reaction vessel (180 ml or 320 ml, Pyrex glass) fitted with a side arm, into which a condenser was inserted. A Pyrex water-cooled lamp housing was inserted into the vessel. Gas was bubbled into the photolysate through a gas inlet tube. The reaction solution was magnetically stirred while the solution was irradiated. The light source was a 200 Watt Hanovia medium pressure mercury

lamp (654A 36). The whole apparatus was immersed in running tap water or ice-water. This apparatus was mainly used for oxidative photoaddition of NND to 1-arylpropenes.

5.4 Preparative Photonitrosation

5.4.1 General Procedures

Unless otherwise specified, the following procedures were followed. A solution of NND and a phenolic compound was placed in the vessel of Apparatus I which was cooled with a water-bath. The solution was purged with oxygen-free nitrogen for at least 15 min prior to irradiation. During irradiation, a sample of the photolysate was withdrawn at intervals for GC or HPLC analysis. A zero hour sample was kept in the dark at the same temperature and analyzed by GC or HPLC as a control. When the photolysate turned red-brown, the irradiation was stopped. The solvent was evaporated under reduced pressure, and the residue was separated into a small amount of an ether-insoluble black solid and ether-soluble fraction. The former was filtered from the ethereal solution of the residue, and was not investigated further. The latter was washed with a 5% aqueous NaOH solution (2 x 10 ml). The combined basic phase was neutralized immediately with acetic acid to pH 7 and the precipitate was filtered and purified by recrystallization to afford the photoproduct, quinone monooxime. The % yields of the quinone monooximes were calculated on the basis of on the phenolic compounds.

Figure 5-2 shows the transmission curves of the filters (Pyrex, Corex, GWA, and GWV) and the filter solution of sodium nitrite/potassium biphthalate/sodium hydroxide[143]. All these filters and filter solutions were used selectively in preparative and mechanistic studies of photonitrosation.

The ^{1}H-NMR, IR, MS and UV spectral data for the pertinent quinone monooximes are listed in Tables 5-1, 5-2, 5-3 and 5-4, respectively.

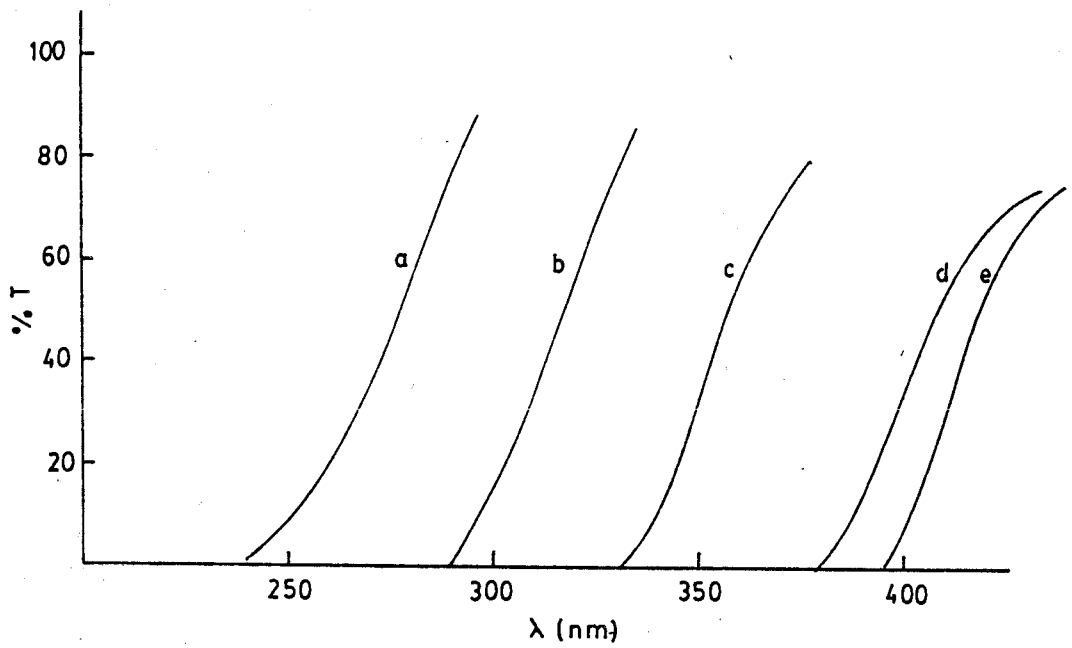

Figure 5-2 Transmission curves of filters and filter solution: (a) Corex,(b) Pyrex, (c) GWA, (d) GWV and (e) sodium nitrite/potassium biphthalate/sodium hydroxide.

5.4.2 Photolysis of 1-NpOH and NND

1-NpOH (30 mg, 0.2 mmol) and NND (45 mg, 0.6mmol) were dissolved in 5 ml aliquots of THF, dioxane, methanol or acetonitrile in Pyrex tubes (1.1 x 12 cm). Each solution was deaerated and subsequently irradiated using a 450 Watt Hanovia lamp at running water temperature for 3 h. The photolysates turned reddish brown. HPLC analysis (C_{18} column, mobile phase of MeOH-H_2O in 7:3 by volume) of these photolysates showed a product peak (Rt 3.16 min), 1-NpOH (Rt 5.21 min) and NND (Rt 2.98 min). The % yields of the product were calculated to be 52.2% in THF, 66% in dioxane, 32% in methanol and 49% in acetonitrile.

Preparative Photolysis

A solution of 1-NpOH (288 mg, 2 mmol) and NND (520 mg, 7mmol) in 40 ml freshly dried dioxane in the reaction vessel of Apparatus I was irradiated with a 450 Watt Hanovia lamp under nitrogen at 0-5°C for 3 h. The red-brown photolysate was shown by GC (OV-1 capillary column at 180°C) to contain two components: 1-NpOH (Rt 2.56 min) and a product (Rt 6.55 min) in the peak-area ratio of 1 : 2.47. The solvent was removed under reduced pressure, and the dark-red residue was dissolved in 25 ml ether. The ether-insoluble fraction was filtered as black solid (15 mg): IR (nujol) 1620 (m), 1370 (s), 1150 (m), 940 (s), 850 (m) and 750 (s) cm^{-1}. The ether-soluble fraction was washed with 5% NaOH aqueous solution (2 x 10 ml). The combined washing was neutralized by acetic acid to give the brown precipitate as a crude product (180 mg, isolated yield of 52%) which was further purified by recrystallization from MeOH-H_2O twice to afford yellow needles (82 mg): 1,4-naphthoquinone-4-oxime **16**, mp 189-191°C (decomp). Anal. calcd. for $C_{10}H_7NO_2$ (173): C 69.36; H 4.05; N 8.09; found:

C 69.09; H 3.71; N 7.92. The spectral data are listed in Tables 5-1 to 5-4.

Material Balance

For the material balance plots of Figure 2-1, a solution of 1-NpOH (288 mg, 2 mmol) and NND (740mg, 10 mmol) in 40 ml dioxane was irradiated under similar conditions. After irradiation for 3 h, the photolysate became red-brown. At intervals, a sample solution was withdrawn with a microliter syringe and analyzed by GC with 1-nitronaphthalene as an internal standard. GC traces showed three peaks at 2.54 min (1-NpOH), 3.37 min (the standard) and 6.56 min (**16**). The relative response factors (f) for 1-NpOH and **16** with respect to the standard were determined to be 0.87 and 0.65 using the plots of A_S/A_I against [S]/[I] based on Equation 5-1:

$$A_S/A_I = f \{[S]/[I]\} \qquad 5\text{-}1$$

where A_S and A_I are the peak areas of the sample and the internal standard, respectively; [S] and [I] are the concentrations of the sample and the standard, respectively.

In the Presence of O_2

A solution of 1-NpOH (36 mg, 0.25 mmol) and NND (38 mg, 0.51 mmol) in 5-ml dioxane was irradiated under oxygen at 15°C for 3 h. The dark-brown photolysate was shown by GC-MS to contain four compounds; 1-NpOH Rt 2.57 min, m/e 144 M^+), 2-nitro-1-naphthol (Rt 4.58 min; m/e 189 M^+, 172 M-OH, 143 M-NO_2), **16** (Rt 6.61 min; m/e 212 M^+) and an unknown compound A (Rt 11.46 min; m/e 212 M^+) in the peak-area ratio of 2.51 : 1.00 : 13.9 : 1.60. 2-Nitro-1-naphthol was identified by the matching of its GC peak with that of an authentic sample. The yields of 2-nitro-1-naphthol, **16** and the unknown A were calculated to be 5, 67 and 8%.

In the Presence of HCl

A solution (Sample A) of 1-NpOH (36 mg, 0.25mmol) and NND (92.5 mg, 1.25 mmol) in 5 ml dioxane in the presence of HCl (0.3 N) was irradiated with a 450 Watt Hanovia lamp through a Pyrex filter under nitrogen at 15°C for 3 h. A solution (Sample B), containing the same ingredients without the acid, was irradiated under similar conditions as a comparison. Both Sample A and B turned red-brown. After evaporation of the solvent from the photolysate A, the residue was dissolved in 5 ml water, and the aqueous solution was extracted with ether (2 x 4 ml). The ether extract was shown by GC-MS to contain three compounds: an unknown (Rt 2.08 min; m/e 158 M^+, 130, 104, and 76), 1-NpOH (Rt 2.57 min; m/e 144 M^+) and **16** (Rt 6.57 min; m/e 173 M^+, 157 and 115) in the peak-area ratio of 1.0 : 11.8 : 2.7. The extracted aqueous solution was neutralized by Na_2CO_3 to pH 8, and was then extracted with methylene chloride only to give 1-NpOH (Rt 2.57 min) . The photolysate B was shown by GC to contain two compounds : 1-NpOH (Rt 2.57 min) and **16** (Rt 6.56 min) in the ratio of 1 : 1.5.

5.4.3 Photolysis of 2-NpOH and NND

A solution of 2-NpOH (288mg, 2mmol) and NND (720mg, 10mmol) in 40 ml dioxane was placed in a quartz flat cylindrical vessel. The colorless solution was irradiated through a Corex filter under N_2 at running tap water temperature for 5 h. The GC trace of the dark red-brown photolysate showed four peaks at Rt 2.66, 3.02, 4.00 and 4.49 min in the peak-area ratio of 23.0 : 1.5 : 10.4 : 1.0. GC-MS identified the peak at 2.66 min as 2-NpOH (m/e 144 M^+) and that at 4.00 min as 1,2-naphthoquinone-1-oxime **17** (m/e 173 M^+, 156 M-OH, 143 M-NO). The photolysate was treated in the usual manner to afford 10 mg of black solid and an ether extract. The latter was washed with saturated NaCl aqueous solution (2 x 10 ml) to remove the

excess NND, then dried and evaporated to give a dark-red mixture (240 mg), which was chromatographed on silica gel (60-200 mesh) eluting with 5% ethylacetate/petroleum ether (30-60°C) to give two fractions. The first provided brown crystals (68 mg in 60% yield based on the reacted 2-NpOH) which were recrystallized from MeOH-H_2O, then from benzene/petroleum ether (30-60°C) to give **17** as brown prisms: mp 107-108°C; anal. calcd. for $C_{10}H_7NO_2$ (173): C 69.36; H 4.05; N 8.09; found C 69.24; H 4.07; N 7.98. The spectral data are listed in Tables 5-1 to 5-4. The second fraction provided 2-NpOH (103 mg).

5.4.4 Photolysis of 2-Allyl-1-naphthol (11) and NND

Preparation of 11

2-Allyl-1-naphthol **11** was prepared from 1-NpOH and allylbromide (Aldrich) via substitution and Claisen rearrangement by a known procedure.[144] The substitution product, 1-alloxynaphthalene, was a colorless oil; bp 85-90°C/0.05 mm (lit.[144] 60°C/0.01 mm); IR (neat): 3060(w), 1580(s) 1508(m), 1400(s), 1270(s), 1240(m), 1100(s), 795(s) and 775(s) cm^{-1}. The compound **11** was white needles: mp 33-34°C (lit.[144] 35-36°C); IR (Nujol): 3500(br s), 3050(m), 1635(m), 1574(s), 1388(s), 1267(m), 1240(m), 1070(m) 995(m), 920(m), 807(s) and 754(s) cm^{-1}. ^{1}H-NMR (400 MHz, $CDCl_3$) δ 3.60(m, 2H, J = 6 Hz), 5.26(m, 2H), 6.10(twelve lines, 1H, Figure 2-2), 6.55(s, 1H, D_2O exch), 7.25-8.18 (m, 6H). UV(CH_2Cl_2) 296 nm(ϵ = 5300), 310 nm (ϵ = 3300) and 324 nm (ϵ = 2400).

Photolysis of 11 and NND

A solution of **11** (230 mg, 1.25 mmol) and NND (450 mg, 6.08 mmol) in 25 ml toluene was irradiated through a Pyrex filter in Apparatus I under nitrogen at about 15°C. After irradiation for 1 h the photolysate turned

brown, and was showed by GC (OV-1 capillary column, at 190°C) to contain two compounds: **11** (Rt 3.45 min) and the product (Rt 10.21 min) in the peak-area ratio of 1 : 0.7. After irradiation for 3 h the dark brown photolysate was treated, following the general procedure, to give 170 mg crude product as brown crystals mp 86-91°C, which was recrystallized from toluene-petroleum ether (30-60°C) as light brown crystals (87 mg, isolated yield of 45%) of 2-allyl-1,4-naphthoquinone-4-oxime **18**: mp 134-135°C. Anal. calcd. for $C_{13}H_{11}NO_2$ (213): C, 73.24; H, 5.16; N, 6.57; found: C, 73.17; H, 5.29; N, 6.51. The spectral data are listed in Tables 5-1 to 5-4.

Photolysis of 11

A solution of **11** (23 mg, 0.125 mmol) in 2.5-ml benzene placed in a quartz tube (1.0 x 10 cm) was irradiated in a Royanet Photochemical Reactor with 300-nm lamps (16 x 21 Watt) for 15 h at 31°C. The GC trace (OV-1 capillary column at 190°C) of the yellow photolysate indicated two peaks: for **11** (Rt 3.48 min) and for a product (Rt 3.05 min) in the ratio of 1.0:0.27. The product was not isolated and possibly assigned to (2,3-dihydro-2-methyl)-5,6-naphthofuran **22** based on its GC-FT-IR and GC-MS. IR: 3063(m), 1578(m), 1458(m), 1383(s), 1279(s, Ar-O-C), 1072(s), 893(m, C-O-C, for five membered ether ring) and 797cm^{-1}; MS, m/e (%) 184(100), 169(45), 141(50), 128(33) and 115(25).

Material Balance

A 25-ml toluene solution containing **11** (230mg, 1.25mmol) and NND (450 mg, 6.08 mmol) was irradiated in Apparatus I under N_2 at 15°C. Every 30 min, a sample of the solution was withdrawn with a microliter syringe and analyzed by GC with anthracene as an internal

standard. The GC traces indicated three peaks: for **11**, Rt 3.45 min, for anthracene, Rt 4.61 min and for **18**, Rt 10.26 min. The relative response factors for **11** and **18** with respect to the standard were determined to be 0.93 and 0.69, respectively, from Equation 5-1. The concentration changes of both **11** and **18** during the irradiation are shown in Figure 2-3.

5.4.5 Attempted Photolysis of 1-Allyl-2-Naphthol and NND

1-Allyl-2-naphthol (**12**) was prepared from 2-NpOH and allylbromide by substitution and the Claisen rearrangement by a known procedure.[144] The substitution product of 2-alloxynaphthalene was a colorless oil, bp 55-60°C/0.01 mm (lit.[144] 130-134°C/0.6 mm). IR (neat): 3060(w), 1633(s), 1602(m), 1510(m), 1270(m), 1000(m), 840(s), 810(w) and 748(m) cm^{-1}. The product from rearrangement was purified by recrystallization from petroleum ether (bp 30-60°C) to give the product **12** as colorless prisms, mp 53°C (lit.[144] 56°C). IR(nujol): 3500(br), 3080(m), 1660(s), 1600(m), 1516(s), 1460(w), 1440(m), 1395(m), 1350(m), 1265(s), 1200(m), 986(m), 970(m), 918(m), 812(s) and 750(s) cm^{-1}; ^{1}H-NMR (400 MHz, $CDCl_3$) δ 3.85(d, 2H, J = 7 Hz), 5.07-5.10 (m, 2H), 5.30(s, 1H, D_2O exch.), 6.08(m, 1H), 7.13(d, 1H, J = 8 Hz), 7.35 (t, 1H, J = 7 Hz), 7.48(t, 1H, J = 7 Hz), 7.70(d, 1H, J = 8 Hz), 7.80(d, 1H, J = 7Hz), 7.90(d, 1H, J = 7 Hz); UV(dioxane): 268(ϵ 3980), 279(ϵ 5100), 290(ϵ 4380), 323(ϵ 2440) and 335 nm(ϵ 2820).

A series of solutions containing **12** (23 mg, 0.125 mmol) and NND (45 mg, 0.610 mmol) in 2.5 ml of dioxane, THF, methanol, acetonitrile and toluene was irradiated in Pyrex tubes under nitrogen at 15°C. After irradiation for 10 h, the photolysates turned slighly yellow, and were shown by GC (OV-1 capillary column, at 190°C) to contain two peaks: for **12**

(Rt 3.56 min) and for the internal standard of anthracene (Rt 4.62 min). The peak-area ratios of 12 and the standard were shown to be changed by 3-7%, during irradiation.

5.4.6 Photolysis of 1-Anthrol and NND

Preparation of 1-Anthrol (1-AnOH)

1-AnOH was prepared according to the method of Ferrero and Conzetti[145] by reduction of sodium 9,10-anthraquinone-1-sulfonate (BDH) with zinc to sodium anthracene-1-sulfonate which was heated with potassium hydroxide under nitrogen at 280-300°C for 1.5 h. The reduction product was yellow crystals: IR(nujol), 1620(w) 1530(w) 1375(m) 1160(br, s) 1050(m) 875(m) and 730(m) cm^{-1}.

The crude product of 1-AnOH was purified by recrystallization from ethanol-water, followed by sublimation under vacuum to give brown needles; mp 155-156°C; IR(nujol): 3300(br), 1630(m), 1560(w), 1412(w), 1380(m), 1290(s), 1200(w), 1145(m), 885(m), 865(w), 790(w) and 732(s) cm^{-1}; ^{1}H-NMR (400 MHz, $CDCl_3$): δ 5.47(s, 1H, D_2O exch), 6.78(d, 1H, J = 8 Hz), 7.30(m, 1H), 7.48(m, 2H), 7.36(d, 1H, J = 8 Hz), 8.00-8.05(m, 2H), 8.40(s, 1H) and 8.98(s, 1H); UV(dioxane): 355(shoulder, ε 4000), 361(ε 4600), 373 (ε 4870) and 393 nm (ε 3700).

Photolysis of 1-AnOH and NND

A 25-ml dioxane solution containing 1-AnOH (194 mg, 1 mmol) and NND (300 mg, 4.05 mmol) in Apparatus I was irradiated with a 200 Watt Hanovia lamp (654 A 36) through a Pyrex filter under nitrogen at about 15°C. After irradiation for 14 h, the red-brown photolysate was shown, by HPLC analysis (C_{18} column, MeOH/H_2O = 60/40, by volume, UV detector at 340 nm), to contain four components: NND (Rt 3.04 min), product 1 (Rt 12.12 min),

product 2 (Rt 14.06 min), and 1-AnOH (Rt 15.52 min), in addition to an internal standard of 1-NpOH at Rt 6.72 min. HPLC traces showed that the peak area ratios of 1-AnOH to the standard were 1.35, 1.10 and 1.06 after irradiation for 14, 20 and 23 h, respectively, The photolysate was treated according to the general procedure. The ether-insoluble fraction was filtered as black solid (90 mg) and the ether-soluble fraction afforded the brown solid (43 mg), which was further recrystallized from MeOH-H_2O to give orange crystals (13 mg): 1,4-anthraquinone-4-oxime **19**, mp 174-176°C (decomp); anal. calcd. for $C_{14}H_9NO_2$ (223): C, 75.34; H, 4.04; N, 6.28; found: C, 75.46; H, 4.03; N, 5.93. The spectral data are listed in Tables 5-1 to 5-4.

5.4.7 Photolysis of 9-Anthrol and NND

A solution of anthrone (388 mg, 2 mmol) and NND (400 mg, 5.4 mmol) in 35-ml THF in Appratus I was irradiated through a Pyrex filter under nitrogen at about 15°C for three hours. The yellow photolysate was treated according to the general procedure. No ether-insoluble fraction was observed. The ether-soluble fraction afforded 460 mg of a yellow solid, which was recrystallized from ethanol-water to give yellowish crystals (373 mg, 84%), identified as 9,10-anthraquinone-10-oxime **20**, mp 228-230°C (decomp); anal. calcd. for $C_{14}H_{19}NO_2$ (223), C, 75.34; H, 4.04; N, 6.28; found C,75.14; N, 4.02; H, 5.99.

Preparation of Authentical Sample of 20

An authentic sample of **20** was prepared by oximation of 9,10-anthraquinone with hydroxyamine hydrochloride in pyridine according to a known procedure.[146] The authentic compound was obtained in 91% yield as yellowish-white crystals, mp 226°C (decomp). The spectral data are also

listed in Tables 5-1 to 5-3 for comparison with **20**.

Photolysis with a Sodium Nitrite-Sodium Hydrogen Phthalate Filter Solution

A solution of anthrone (388 mg, 2 mmol) and NND (510 mg, 6.9 mmol) in 35-ml THF in Apparatus I was irradiated with a 200 Watt Hanovia lamp through a sodium nitrite-sodium hydrogen phthalate filter solution which did not transmit light below 400 nm[143], as shown in Figure 5-2. The whole of Apparatus I was immersed in the filter solution; after irradiation for 6 h, HPLC analysis of the yellowish photolysate showed peaks corresponding to **20** (Rt 4.86 min, in 93% yield) and the starting material (in 17% conversion). The absorption of the filter solution at 410 nm was changed from OD = 0.15 to 0.32, during irradiation for 6 h.

Preparation of the Filter Solution[143]

A saturated solution (250 ml) of sodium nitrite in distilled water was added to a solution of 5 g of sodium hydrogen phthalate in 1 l of distilled water with uniform stirring. This solution was brought to pH 12 by addition of dilute sodium hydroxide aqueous solution.

5.4.8 Photolysis of 9-Phenanthrol and NND

A solution of 9-phenanthrol (120 mg, 0.062 mmol) and NND (89 mg, 1.2 mmol) in 25-ml benzene in Apparatus II was irradiated with RPR 300-nm lamps (21 Watt x 16) under nitrogen at 31°C. After irradiation for 8 h, the photolysate was worked up in the usual manner to give a black solid (15 mg) and an ether solution, which was washed with saturated NaCl aqueous solution (2 x 10 ml) to remove excess NND. The residue, a red-brown solid (80 mg) obtained from the ether solution was chromatographed

with the eluent of 0-20% ethylacetate-hexane (silica gel 60-200 mesh) to give 9,10-phenanthaquinone-10-oxime **21** as orange crystals (26 mg, in 20% yield): mp 157-158°C; anal. calcd. for $C_{14}H_9NO_2$ (223), C, 75.34; H, 4.04; N, 6.28; found, C, 75.52; H, 3.76; N, 6.55. The spectral data are listed in Tables 5-1 to 5-4.

Preparation of an Authentic Sample of 21

An authentic sample of **21** was prepared by oximation of 9,10-phenanthaquinone with hydroxyamine hydrochloride in pyridine according to a known procedure[146] to give orange crystals in 70% yield: mp 157-158°C. The spectral data are also listed in Tables for comparison with **21**.

Table 5-1 ^{1}H-NMR Data of Quinone Monooximes[a]

Compound	Data
16	6.67(d, 1H, J = 11 Hz) 7.58(t, 1H, J = 8 Hz) 7.64(t, 1H, J = 8 Hz) 8.02(d, 1H, J = 11 Hz) 8.17(t, 2H, J = 8 Hz) 8.41(s, 1H, D_2O exch)
17	6.57(d, 1H, J = 10 Hz) 7.74(d, 1H, J = 10 Hz) 7.52-7.56(m, 3H) 8.37(d, 1H, J = 8 Hz) 17.52(s, 1H, D_2O exch)
18	3.35-3.37(m, 2H) 5.19(m, 1H) 5.22(m, 1H) 5.97(m, 1H) 7.58(m, 2H) 7.83(s, 1H) 8.18(m, 2H) 8.33(s, 1H, D_2O exch)
19	6.74(d, 1H, J = 10 Hz) 7.57(t, 1H, J = 9 Hz) 7.63(t, 1H, J = 9 Hz) 7.97(d, 1H, J = 9 Hz) 8.06(d, 1H, J = 9 Hz) 8.11(d, 1H, J = 10 Hz) 8.22(s, 1H, D_2O exch) 8.69(s, 1H) 8.74(s, 1H)
20	7.59(t, 1H, J = 8 Hz) 7.65(t, 2H, J = 8 Hz) 7.73(t, 1H, J = 8 Hz) 8.20(d, 1H, J = 8 Hz) 8.27(d, 1H, J = 8 Hz) 8.43(d, 1H, J = 8 Hz) 8.69(s, 1H, D_2O exch) 9.02(d, 1H, J = 8 Hz)

Table 5-1 (Cont'd)

20[b]	7.58(t, 1H, J = 8 Hz) 7.67(t, 2H, J = 8 Hz) 7.74(t, 1H, J = 8 Hz) 8.20(d, 1H, J = 8 Hz) 8.27(d, 1H, J = 8 Hz) 8.43(d, 1H, J = 8 Hz) 8.72(s, 1H, D_2O exch) 9.03(d, 1H, J = 8 Hz)
21	7.52(m, 3H) 7.80(t, 1H, J = 8 Hz) 8.13(d, 1H, J = 8 Hz) 8.20(d, 1H, J = 8 Hz) 8.35(d, 1H, J = 8 Hz) 8.43(d, 1H, J = 8 Hz) 17.06(s, 1H, D_2O exch)
21[b]	7.48-7.80(m, 4H) 8.13-8.43(m, 4H) 17.06(s, 1H, D_2O exch)

a. In $CDCl_3$.

b. Authentic samples.

Table 5-2 IR (Nujol) Data of Quinone Monooximes

Compound	ν_{max} in cm^{-1}					
16	3160(br)	3070(br)	1627(s)	1573(m)	1443(m)	1340(m)
	1320(m)	1160(w)	1095(m)	978(s)	850(m)	800(w)
	760(s)					
17	3440(br)	1620(s)	1525(m)	1455(m)	1406(w)	1377(m)
	1333(w)	1260(w)	1218(m)	1075(s)	965(m)	855(s)
	768(m)	760(m)	720(m)			
18	3260(br)	1635(s)	1600(s)	1435(m)	1380(m)	1345(m)
	1315(w)	1305(w)	1265(w)	985(s)	975(s)	768(s)
19	3220(br)	3130(br)	1645(m)	1620(s)	1585(m)	1465(s)
	1380(m)	1320(m)	1030(w)	970(m)	845(m)	760(m)
20	3270(br)	1648(s)	1595(m)	1465(m)	1323(s)	1315(s)
	1175(w)	1020(m)	940(w)	780(w)	680(m)	

Table 5-2 (Cont'd)

20[a]	3270(br)	1648(s)	1595(m)	1465(m)	1325(s)	1315(s)
	1175(w)	1022(m)	940(m)	780(w)	680(m)	
21	3440(br)	1635(w)	1600(m)	1535(s)	1455(m)	1280(m)
(KBr)	1120(m)	990(s)	845(m)	765(s)	725(s)	
21[a]	3440(br)	1640(w)	1600(s)	1525(s)	1450(m)	1275(s)
(KBr)	1120(m)	990(s)	845(w)	760(s)	725(s)	

a. Authentic samples.

Table 5-3 Mass Spectral Data of Quinone Monooximes

Compound	m/e (%, fragment)			
16	173(100, M^+)	143(10,M-NO)	115(54)	
17	173(100, M^+)	156(60, M-OH)	143(10, M-NO)	
	128(48)	115(64)		
18	213(23, M^+)	196(100, M-OH)	182(23, M-NO)	130(60)
19	223(100, M^+)	206(45, M-OH)	193(10, M-NO)	177(8)
	165(22)			
20	223(100, M^+)	193(25, M-NO)	177(10)	165(20)
20[a]	223(100, M^+)	206(8, M-OH)	193(25, M-NO)	
21	223(70, M^+)	206(100, M-OH)	178(50)	165(60)
	151(40)			

a. An authentic sample.

Table 5-4 UV Data of Quinone Monooximes[a]

Compound	Maximum Wavelengths in nm (ϵ)		
16	214(22,000)	282(24,000)	345(13,000)
17	215(26,300)	261(15,700)	368(6,000)
18[b]	285(14,300)	339(7,500)	
19[b]	290(39,700)	297(41,800)	412(6,100)
20	231(37,000)	244-250(18,000)	
	279(16,000)	340-350(5,200)	
21	254(41,000)	306(shoulder, 6200)	
	385(6,000)	414(2,600)	

a. In methanol.

b. In dioxane.

5.4.9 Attempted Photolysis of 1-Methoxynaphthalene and NND

Three solutions were prepared in quartz tubes (1.1 x 12 cm):

No.1, a 5-ml dioxane solution containing 1-methoxynaphthalene (1-NpOMe, 24 mg, 0.15 mmol) and NND (7.4 mg, 0.10 mmol).

No.2, a 5-ml THF solution containing 1-NpOMe (24 mg, 0.15 mmol) and NND (7.4 mg, 0.10 mmol).

No.3, a 5-ml THF solution containing 1-NpOH (21.6 mg, 0.15 mmol) and NND (7.4 mg, 0.10 mmol). Each solution was deaerated by bubbling nitrogen through the solution for 10 min, and then irradiated in a Rayonet Photochemical Reactor with 300-nm lamps (21 Watt x 16) at 31°C, for 2.5 h for No.1 and No.2, and for 0.5 h for No.3. HPLC analysis (C_{18} column, MeOH/H_2O = 70/30, by volume) of the colorless photolysates of both No.1 and No.2 with 1-nitronaphthalene as an internal standard showed three peaks: for NND Rt 2.75 min, for the standard Rt 8.43 min and for 1-NpOMe Rt 11.92 min. Before and after irradiation the peak-area ratios of 1-NpOMe and NND with respect to the standard changed, for No.1, from 1.43 and 1.77 to 1.40 and 1.74, and for No.2, from 1.49 and 1.74 to 1.59 and 1.72. Within the experimental error (< 7%), no significant change in the concentration of either 1-NpOMe or NND was found during irradiation. Similar analysis of the brown photolysate of No.3 showed a new peak at 4.83 min for **16** in a 60% yield and a 21% conversion of NND.

5.5 Wavelength-Dependent Irradiation of 1-NpOH and NND

Irradiation of 1-NpOH

A cylindrical quartz tube (1.1 x 12 cm) containing a solution of 1-NpOH (18 mg, 0.125 mmol) and NND (9.3 mg, 0.125 mmol) in 5-ml dioxane was placed in contact with a flat quartz vessel containing a filter solution of NND (74 mg, 1.0 mmol) in 40-ml dioxane. The two vessels were wrapped with heavy aluminum foil, leaving a window (1.0 x 4.0 cm) for irradiation as shown in Figure 5-3. The sample solution was degassed and then irradiated with a 450 Watt Hanovia lamp through the filter solution at about 15°C for 2.5 h. GC trace (OV-1 capillary column at 180°C) of the yellow photolysate indicated quinone monooxime **16** formation in 53% yield with a 40% conversion of 1-NpOH.

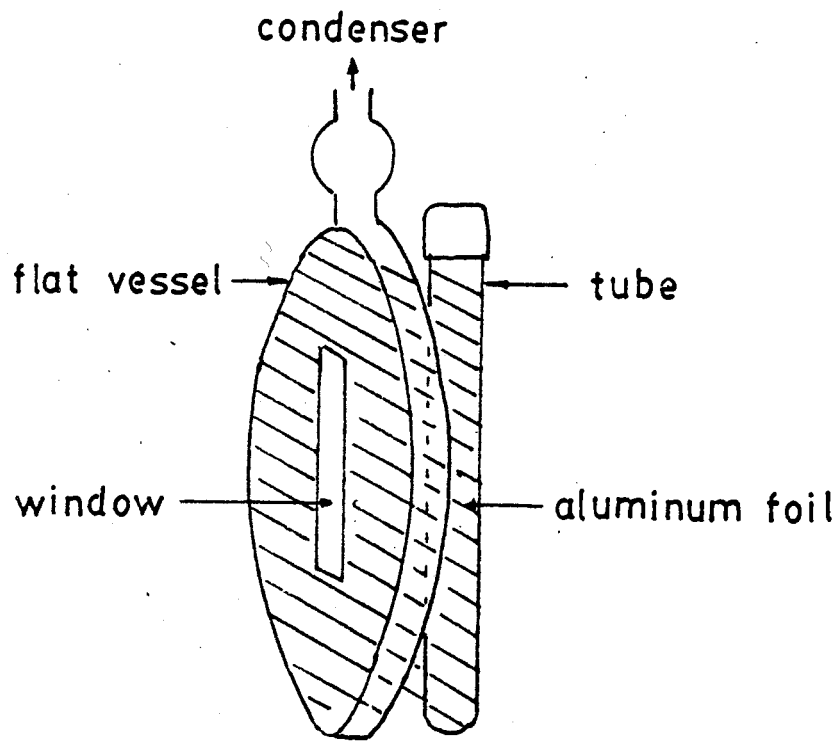

Figure 5-3 Assembly for photoexcitation of 1-NpOH.

Irradiation of NND

A 5-ml dioxane solution of 1-NpOH (18mg, 0.125mmol) and NND (18mg, 0.24 mmol) was degassed and then irradiated with a 200 Watt Hanovia lamp through a GWA filter (cut-off<350 nm) at 15°C for 6 h. GC analysis (OV-1 capillary column at 180°C) before and after irradiation showed two peaks at Rt 2.48 min of 1-NpOH and at Rt 3.29 min of the standard (1-nitronaphthalene) with the same peak-area ratio of 0.33:1.0.

The same solution was irradiated under similar conditions except for a Pyrex filter (cut-off < 280 nm). GC analysis of the brownish photolysate showed peaks at Rt 2.43 min for 1-NpOH, Rt 3.22 min for the standard and Rt 6.32 min for the product **16** in the peak-area ratio of 0.12:1.0:0.10. The yield of **16** was calculated to be 35%.

Laser Photolysis

These experiments were performed in Professor G.B. Porter's laboratory, Department of Chemistry, University of British Columbia. The laser pulses (pulse wavelength at 308 nm, pulse width about 8-12 ns, and maximum pulse energy of 80 mJ) were generated from a Lumonics TE-861-T_3 Excimer Laser with HCl, H_2 and Xe as the operating gas mixture. The pulse frequency was adjusted to give 0.3 Watt. The sample solution in a quartz tube (1.1 x 12 cm) was sealed with a septum and purged with nitrogen through an inlet needle for 10 min. The sample tube was placed on an optical bench as shown in Figure 5-4 for irradiation.

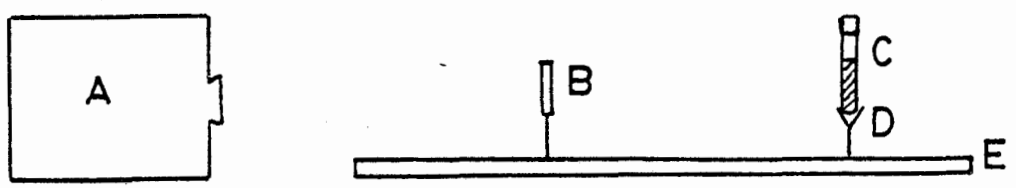

Figure 5-4 An optical bench, **A** Lumonics Excimer Laser,
B focussing lens, **C** sample tube,
D tube holder.

1-NpOH

The following sample solutions were prepared in quartz tubes:

No.1, a 7.5-ml dioxane solution containing 1-NpOH (54mg, 0.375mmol) and NND (54mg, 0.730mmol);

No.2, a 1.2-ml THF solution containing 1-NpOH (9mg, 0.0625mmol) and NND (30mg, 0.208mmol);

No.3, a 1.2-ml methanol solution containing 1-NpOH (9mg, 0.0625mmol) and NND (30 mg, 0.208 mmol).

The deaerated solutions were irradiated with laser pulses at 30-35°C for 10 min (No.1) and 20 min (No.2 and No.3). GC analysis of light brown photolysate of No.1 showed three peaks for 1-NpOH at Rt 2.55 min, an unknown compound at Rt 3.05 min and **16** at Rt 6.55 min in the ratio of 40:1.0:4.1. The conversion of 1-NpOH and the yield of **16** were determined to be 11.5% and 80%, respectively. Similar analysis of brownish photolysate of No.2 also showed three peaks for 1-NpOH at Rt 2.56 min, an unknown compound at Rt 2.67 min, and **16** at Rt 6.67 min in the peak-area ratio of 28.8:1.8:1.0. The conversion of 1-NpOH and the yield of **16** were determined to be 9.2% and 38%, respectively. GC analysis of yellowish photolysate of No.3, showed only one peak for 1-NpOH at Rt 2.57 min.

2-NpOH

The following three sample solutions were prepared in quartz tubes,

No.1, a 7.5-ml dioxane solution containing 2-NpOH (54 mg, 0.375mmol) and NND (54 mg, 0.730 mmol);

No.2, a 1.2-ml THF containing 2-NpOH (9mg, 0.0625mmol) and NND (30 mg, 0.208 mmol);

No.3, a 1.2-ml methanol solution containing 2-NpOH (9mg, 0.0625mmol)

and NND (30mg, 0.208mmol).

Each of the deaerated sample solutions was irradiated with laser pulses at 30-35°C for 20 min. GC analysis (OV-1 capillary column at 180°C) of the brown photolysate in Tube No.1, showed four peaks, 2-NpOH at Rt 2.60 min, unknown A at 2.95 min, unknown B at 3.12 min and **17** at 3.91 min. The peak-area ratio was 34.9:2.3:1.0:3.7 respectively. The conversion of 2-NpOH and the yield of **17** were determined to be 16.7% and 53%, repectively. The similar analysis of No.2 and No.3 each showed only one peak for 2-NpOH at Rt 2.60 min.

5.6 Triplet Sensitization and Quenching

5.6.1. Sensitization by Xanthone and 2-Acetonaphthone

A 5-ml dioxane solution of 1-NpOH (18 mg, 0.125 mmol), NND (10 mg, 0.135 mmol) and xanthone (196 mg, 1 mmol) was sealed in a quartz tube (1.1 x 12 cm) with a septum. The solution was purged by nitrogen and then irradiated with a 200 Watt Hanovia lamp through a GWA filter (cut-off<350 nm, Figure 5-2) at 15°C for 6 h. GC analysis (OV-1 capillary column at 180°C) of the photolysate showed that the peak-area ratios of 1-NpOH and the standard (1-nitronaphthalene) were 0.35 and 0.31, before and after irradiation, respectively. No peak at Rt 6.55 min for the compound **16** was detected.

Under conditions similar to those described above, a 5-ml dioxane solution containing 1-NpOH (18 mg, 0.125 mmol), NND (10 mg, 0.135 mmol) and 2-acetonaphthone (85 mg, 0.5 mmol) was irradiated for 6h. GC analysis of the yellowish photolysate showed that the peak-area ratios of 1-NpOH and the standard were 0.42 and 0.40, before and after irradiation, respectively. No peak at Rt 6.55 min for the compound **16** was detected.

5.6.2. Triplet Quenching by Cyclohexadiene

Samples Seven sample solutions of 1-NpOH (0.030 M), NND (0.030 M) and varied concentrations of cyclohexadiene (CHDE, 0-0.009 M) in THF (5 ml) were prepared by the general procedure described below. 216 mg (1.5 mmol) 1-NpOH, 111 mg (1.5 mmol) NND and 120 mg (1.5 mmol) CHDE were each dissolved in 10-ml THF to give three stock solutions. 1.0-ml aliquots of the 1-NpOH and NND stock solutions were pipetted into each of seven 5-ml volumetric flasks, and various aliquots (33, 66, 100, 150, 200 and 300 μl) of the CHDE stock solution were injected into each of the above six flasks with a microliter syringe. After diluting with THF to 5 ml, the sample solutions were transfered into quartz tubes (1.1 x 12 cm) and degassed.

Irradiation The degassed solutions were irradiated on a merry-go-round apparatus in a Rayonet Photochemical Reactor with 300-nm lamps (21 Watt x 16) for 20 min at 31°C. The actinometer solution of benzophenone (0.050 M)-benzohydrol (0.10 M) in 5-ml benzene was irradiated under the same conditions, but for 5 min.

Analysis The light intensity of the source was determined with the actinometer of benzophenone-benzohydrol with a known quantum yield of 0.74[64]. The absorbance (A) at 342 nm of benzophenone was measured with 0.10 cm optical path cells to be 0.730 and 0.595, before and after irradiation, respectively. The light intensity (I) was calculated by absorbance change (ΔA) from Equation 5-2 to be 2.60 x 10^{-6} Einstein/(min.ml).

$$I = \Delta A/(10^3 \epsilon_{342} \Phi l t) \qquad 5\text{-}2$$

where ϵ_{342} = 140 $M^{-1}cm^{-1}$ is the extinction coefficient of benzophenone at 342 nm, t is the elapsed irradiation time in min, and l = 0.10cm.

The concentration of quinone monooxime **16** was determined by HPLC (C_{18} column, MeOH/H_2O = 70/30 by volume) with 1-nitronaphthalene as the internal standard:

$$[OX] = A_{OX}[IS]/1.08A_{IS} \qquad 5\text{-}3$$

where [OX] and [IS] are the concentrations of **16** and the standard, respectively; A_{OX} and A_{IS} are their corresponding HPLC peak areas. The value of the relative response factor, 1.08, was previously determined from the slope of the plot of A_{OX}/A_{IS} against [OX]/[IS]. Since the sample and actinometer had the same volume, the product quantum yields (Φ_{ox}) were readily calculated from Equation 5-4.

$$\Phi_{ox} = [OX]/I \cdot t \qquad 5\text{-}4$$

where t is the elapsed irradiation time (in min) of the sample solutions.

5.7 Fluorescence Studies

5.7.1 Fluorescence Spectra

Uncorrected fluorescence spectra of the phenols **9-15** and the corresponding phenolates were taken in methanol at room temperature. Stock solutions (0.001 M) of these phenols were prepared. Each sample solution of the phenol was made by pipetting a 1.0-ml aliquot of the stock solution into a 5-ml volumetric flask and diluting with methanol to 0.0002 M. Each sample solution of the phenolates was prepared by pipetting a 1.0-ml aliquot of the stock solution into an appropriate volume of alkaline

methanol solution (containing 0.002 M KOH) to get the concentration of the corresponding phenolate of 0.0002 M. The sample solution in a sealed fluorescence cell was purged with nitrogen for 10 min, and then a fluorescence spectrum was recorded. The spectra of 1-NpOH and its naphtholate are, for example, shown in Figure 5-5. The onset wavelengths of the phenols and phenolates are listed in Table 1-2.

The 77K fluorescence spectra (Figure 2-12) of 1-AnOH in the absence and presence of NND, TEA or KOH, respectively, were recorded using the same phosphorescence sample holder assembly except for removal of the "chopper". A phosphorescence sample tube containing one of above solutions was inserted in a Dewar flask filled with liquid nitrogen. The experimental conditions are described in the caption of Figure 2-12.

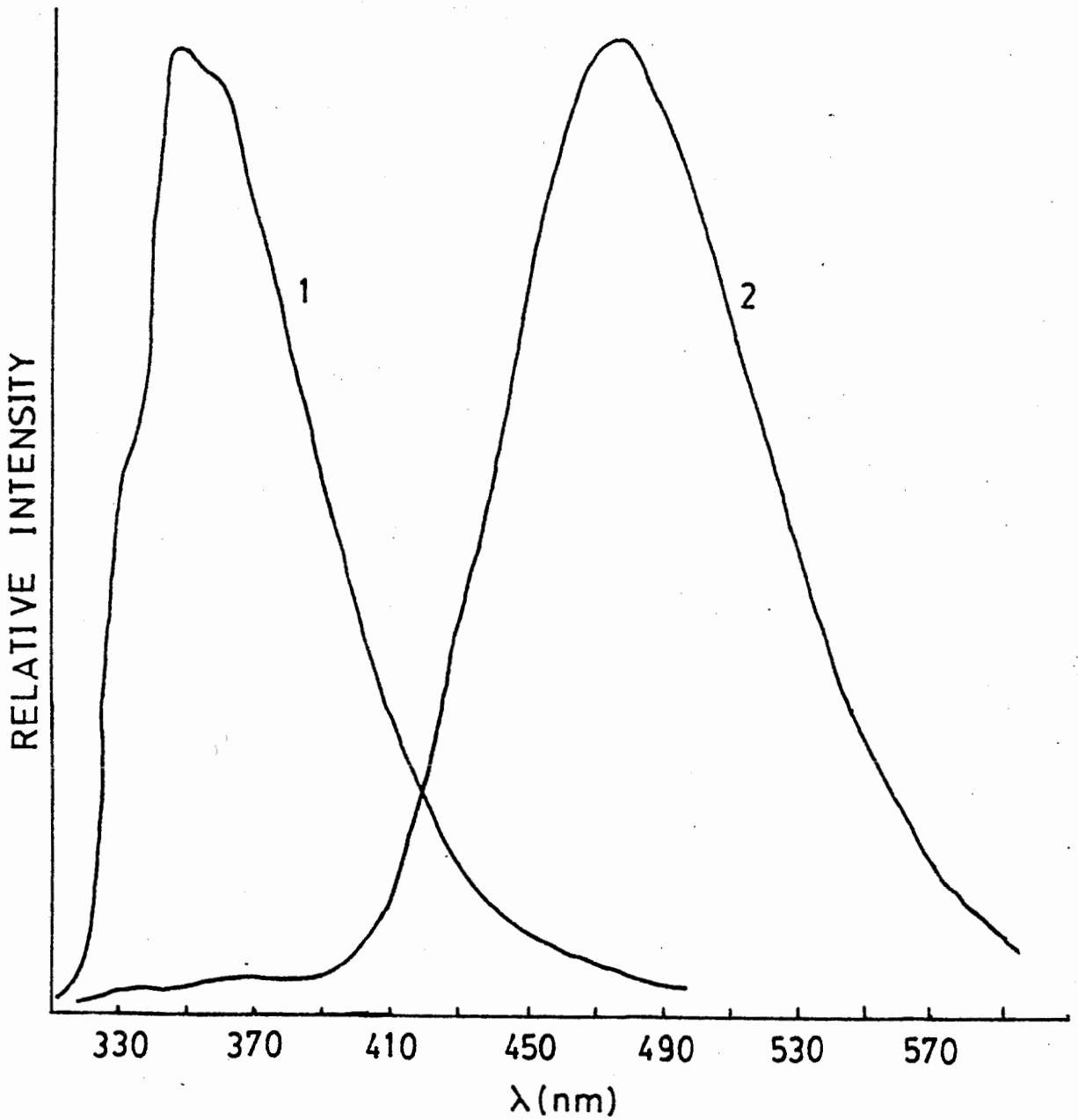

Figure 5-5 Normalized fluorescence spectra of 1-NpOH (0.0002 M) in the absence (1) and presence (2) of KOH (0.002 M) in methanol at 20°C; the excitation wavelength was at 300 nm.

5.7.2 Fluorescence Intensity Quenching

Two kinds of geometric arrangement of quartz cell for observation of fluorescence are shown in Figure 5-6.[55] Figure 5-6 **A** shows a standard geometry, i.e. a routine illumination. The front-face illumination, as shown in Figure 5-6 **B**, is performed by arranging a square cell oriented at about 45° relative to an incident beam so that only emitted light, but not reflected light, is allowed to enter the detector. In this way the emission at the incident point on the inner surface of the sample solution is detected; in another words, the effective light path length for re-absorption of emitted fluorescence by some quencher (e.g. NND) was estimated to be less than 10^{-3} cm[124] in comparison to 0.5 cm using the routine illumination technique; consequently, the reabsorption of the emission by NND is negligible.

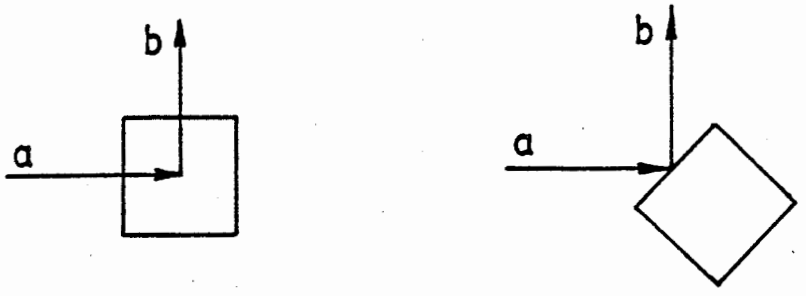

A routine illumination **B** front-face illumination

Figure 5-6 Geometric arrangements of a cell (1.0 x 1.0 cm) for measurements of fluorescence spectra, **a** is an incident beam, and **b**, an emission beam.

The fluorescence intensity ratio, I^o/I, was determined at the maximum-intensity wavelength. The Stern-Volmer correlation of I^o/I *vs* [NND], based on Equation 2-6, was calculated from the least-square analysis.

5.7.2.1 Routine Illumination

1-NpOH and NND The quenching of 1-NpOH fluorescence by NND was measured in methanol, acetonitrile and dioxane at 20°C with excitation wavelength of 300 nm (slit 3 nm). The intensity ratio was determined at about 340 nm, and linearity of I^o/I *vs* [NND] was established with a correlation coefficient of 0.996-0.999, as shown in Table 5-5.

The normalized fluorescence spectra of 1-NpOH (0.0002 M) in the presence of NND (0.01-0.10 M) in acetonitrile were recorded, as shown in Figure 2-9. The spectra show that the reabsorption of emission by NND around 340 nm seriously distorts the shape of the spectrum, causing the shift of the maximum emission band to 390 nm.

1-NpOH and H_2O Quenching of 1-NpOH fluorescence intensity by water is shown in Figure 2-29. The observed and calculated data are listed in Table 2-12.

1-NpOH and TEA Quenching of 1-NpOH fluorescence intensity by TEA is shown in Figure 2-30. The observed and calculated data are listed in Table 2-13.

1-NpOH and DMF Quenching of 1-NpOH fluorescence intensity by DMF was determined. The observed and calculated data are listed in Table 2-14.

Table 5-5 Quenching of 1-NpOH (0.0002 M) Fluorescence Intensity by NND in Various Solvents with the Routine Illumination[a]

MeOH		MeCN		Dioxane	
I^o/I (345 nm)	[NND] (M)	I^o/I (343 nm)	[NND] (M)	I^o/I (342 nm)	[NND] (M)
1.08	0.0002				
1.16	0.0004	1.13	0.0004	1.09	0.0004
1.21	0.0006	1.21	0.0006	1.22	0.0008
1.34	0.0009	1.30	0.0009	1.41	0.0012
1.48	0.0012	1.43	0.0012	1.63	0.0016
1.69	0.0016	1.72	0.0020	1.83	0.0020
$k_q\tau_o$ (M^{-1})	432		369		472
$k_q(10^{10}M^{-1}s^{-1})$	5.68		4.85		4.45
r	0.997		0.999		0.996

a. Each sample solution was excited at 300 nm.

1-NpOH and QC Quenching of 1-NpOH fluorescence intensity by QC was measured. The observed and calculated data are listed in Table 2-15.

2-NpOH and TEA Quenching of 2-NpOH fluorescence intensity by TEA was determined, as shown in Figure 5-7. The intensity ratio I°/I was measured at 355 nm.

1-AnOH and NND Fluorescence spectra of 1-AnOH in the absence and presence of increasing [NND] in various solvents were measured at 22-25°C. The observed data and the conditions of measurements are summarized in Table 5-6. The corresponding Stern-Volmer plots are shown in Figure 2-14. The spectra in THF, for example, are shown in Figure 2-13.

Fluorescence spectra of 1-AnOH in the absence and presence of increasing [NND] in dioxane at various temperature, 10-50°C, were recorded. The temperature fluctuation was kept at ± 0.3°C. The observed data and the conditions of recording the spectra are listed in Table 5-7. The Stern-Volmer plots are shown in Figure 2-15, and the quenching rate constants shown in Table 2-2.

Anthracene and NND Quenching of anthracene(0.0002M) fluorescence by NND (0.004-0.020 M) in methanol was measured at 22°C with excitation at 375 nm (slit 2.5 nm) and with emission region of 370-500 nm (slit 3 nm) (Figure 3-6). The intensity ratios, I°/I, were determined at 397 nm, and are shown in Table 3-4. Since both anthracene and NND have absorption at the excitation wavelength of 375 nm, the corrected I°/I was calculated from Equation 5-5.[124]

Table 5-6 Fluorescence Intensity Quenching of 1-AnOH by NND in Various Solvents at 22-25°C[a]

Dioxane		THF		MeCN		EtOH		MeOH	
[NND] (M)	I°/I (434 nm)	[NND] (M)	I°/I (442 nm)	[NND] (M)	I°/I (445 nm)	[NND] (M)	I°/I (446 nm)	[NND] (M)	I°/I (450 nm)
0.007	1.23	0.0075	1.14	0.0075	1.33	0.007	1.06	0.008	1.08
0.014	1.48	0.0150	1.31	0.0150	1.62	0.014	1.13	0.016	1.15
0.021	1.73	0.0225	1.50	0.0225	1.97	0.021	1.20	0.026	1.32
0.028	1.99	0.0300	1.70	0.0300	2.31	0.028	1.29	0.032	1.40
0.035	2.29	0.0375	1.92	0.0375	2.72	0.035	1.39	0.040	1.49

a. Each sample solution was excited at 400 nm (slit 2.5 nm).

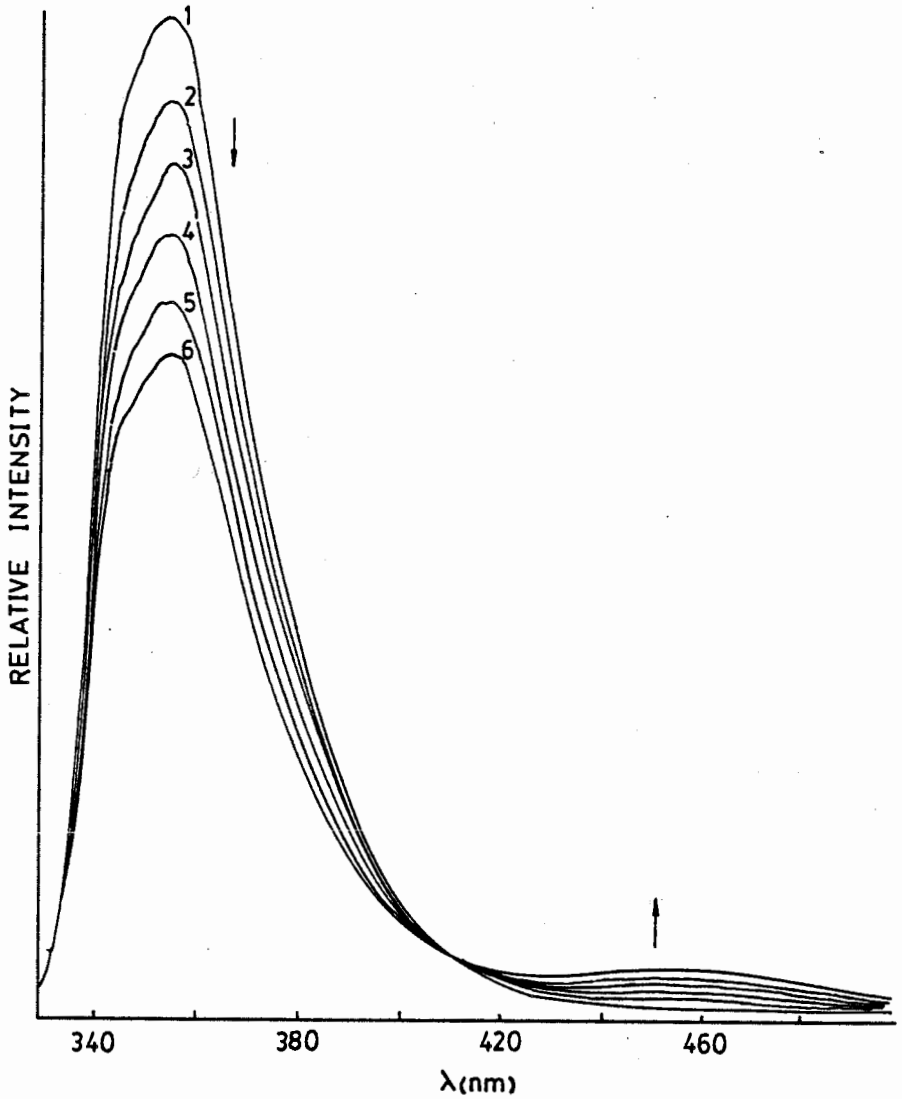

Figure 5-7 Fluorescence spectra of 2-NpOH (0.0002 M) in MeCN at 20°C in the absence and presence of TEA with excitation at 300 nm, the curve 1-6 contained [TEA] of 0, 0.0038, 0.00756, 0.0118, 0.0161 and 0.0214 M. The Stern-Volmer plot of I°/I (at 355 nm) *vs* [NND] gave $k_q\tau_o$ = 23.5 M^{-1} and r = 0.997.

$$(I°/I)_{corr} = (I°/I)_{obs} \cdot A \qquad 5\text{-}5$$

Where $A = \frac{\epsilon_D C_D}{\epsilon_D C_D + \epsilon_Q C_Q} \cdot \frac{1-10^{-(\epsilon_D C_D + \epsilon_Q C_Q)L}}{1-10^{-\epsilon_D C_D L}}$

ϵ_D and ϵ_Q are the extinction coefficients of quenchee and quencher at the excitation wavelength; C_D and C_Q are the concentrations of quenchee and quencher, respectively; L is an excitation-light path length (0.5 cm). The observed and corrected data, and the Stern-Volmer parameters are shown in Table 3-3.

9,10-Dimethylanthracene and NND

Quenching of fluorescence intensity of 9,10-dimethylanthracene (0.0002 M) by NND (0-0.0035 M) in methanol was measured at 22°C with excitation at 400 nm (Figure 3-7), and the ϵ_{400} value of 9,10-dimethylanthracene is 3500 M^{-1} cm^{-1}, but that of NND at the concentration range of 0.007-0.0035 M, about zero. The intensity ratio was determined at 425 nm, and the Stern-Volmer parameters are shown in Table 3-5.

Perylene and NND Fluorescence spectra of perylene ($7x10^{-5}$ M) in methanol at 22°C in the absence and presence of NND (0.010-0.060 M) were recorded with excitation at 430 nm (slit 2 nm), scanning from 420 to 540 nm (slit 3 nm). The intensity ratio I°/I was determined at 465 nm, as shown below:

[NND] (M):	0.010	0.020	0.030	0.040	0.050	0.060
I°/I :	1.012	1.024	1.039	1.046	1.054	1.070

The Stern-Volmer parameters are listed in Table 3-5.

Tetracene and NND Fluorescence spectra of tetracene ($6x10^{-5}$ M) in methanol at 22°C in the absence and presence of NND (0.020-0.060 M) were measured with excitation at 440 nm (slit 5 nm) and emission region of 450-620 nm (slit 3 nm). With increasing concentration of NND, the maximum intensity at 473 nm was slightly and randomly changed (Figure 3-8).

5.7.2.2 Front-Face Illumination

The front-face illumination technique was employed in the investigation of quenching of 1-NpOH fluorescence by NND. A sample-cell holder was constructed and mounted on a sample-holder turntable, as shown in Figure 5-8.

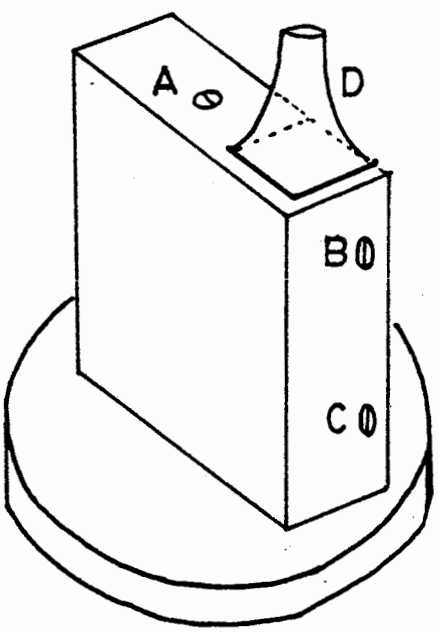

Figure 5-8 Sample-cell holder for front-face illumination technique, **A**, **B**, and **C** are screws, and **D** is a cell.

To measure the emission from the sample, contamination from the reflected-beam had to be eliminated. The entrance slit of the monochromater before the dectector was covered with a sheet of paper. Then, the reflected-light spot, which was visible on the paper, was removed from the entrance slit through the use of screw A (Figure 5-8). Fluorescence spectra of 1-NpOH (0.002 M) in the absence and presence of NND (0.0025-0.0150 M) in dioxane were measured at 22°C with excitation wavelength of 300 nm and an emission range of 310-400 nm, as shown in Figure 2-10. The intensity ratio was determined at 342 nm, and the Stern-Volmer plot with the slope of $k_q\tau_o$ = 117 M^{-1} is shown in Figure 2-11.

5.7.3 Time-Resolved Fluorimetry

Fluorescence-lifetime measurement and transient fluorescence spectroscopy of 1-NpOH, 1-NpOD and 1-AnOH in the absence and presence of NND were performed at room temperature by Dr. T.W. Steiner in the Department of Physics, Simon Fraser University, using the facilities provided by Professor M.L.W. Thewalt. The excitation source was a synchronously pumped, cavity dumped and modelocked dye laser system, operating at 600 nm with 4 MHz repetition rate and a 30 ps pulse width at 300 nm after frequency doubling.[147] The fluorescence detector was a fast photomultiplier operating in a photon counting mode.[147]

1-NpOH

Transient fluorescence spectra of 1-NpOH (0.0006 M) in acetonitrile were measured at room temperature at various delay times, 0-1, 1-3, 3-8, 8-14, 14-20 and 20-40 ns after irradiation at 300 nm with the scanning

from 320 to 521 nm. A sample solution in a fluorescence cell was sealed with a septum, and purged with nitrogen for 10 min prior to determination. The shape of the transient spectra in Figure 2-17 is not changed for different delay times. The maximum emission band is around 342-356 nm.

Transient fluorescence spectra of 1-NpOH (0.0006 M) in the presence of NND (0.006 M) in acetonitrile were measured under similar conditions. The spectra are shown in Figure 2-18 , and are similar to those in the absence of NND (Figure 2-17).

Fluorescence logarithmic decay curves of 1-NpOH (0.0002 M) in the absence and presence of NND (0.004-0.030 M) in dioxane were measured under similar conditions to those described above. For each sample solution, three decay curves were recorded at the monitoring wavelengths of 330, 345 and 400 nm, respectively. Figure 2-20 shows an example of the curves. The fluorescence lifetimes were automatically calculated by a microcomputer from the slopes of the curves, and are summarized in Table 2-3. The Stern-Volmer plots of τ_o/τ *vs* [NND] for the three runs in Table 2-3 gave straight lines, and the quenching rate constant was calculated from Equation 2-10.

Under similar conditions to those used for dioxane, fluorescence decay curves of 1-NpOH (0.0006 M) in THF in the absence and presence of NND (0.060 M) were measured by excitation at 300 nm and monitoring at 340 nm. Both decay curves are staight lines but with different slopes. The lifetimes are 9.31 and 1.33 ns for the absence and presence of NND (0.060 M), respectively. Transient fluorescence spectra of 1-NpOH (0.0006 M) in the presence of NND (0.060 M) in THF were recorded at the delay times of 0-0.5, 0.5-1.0, 1.0-2.0, 2.0-3.0, 3.0-5.0 and 5.0-10.0 ns after irradiation at 300 nm with monitoring wavelength-region of 310-496 nm. The spectra show a maximum at 390 nm and a shoulder at 344 nm (Figure 2-19).

Fluorescence decay curves of 1-NpOH (0.0002 M) in the absence and presence of EPO (0.030-0.180 M) in methanol were measured under similar conditions to those described above, except for excitation at 310 nm and monitoring at 355 nm. For each concentration of NND, three runs were performed to give an average lifetime as shown in Table 2-4, with mean deviation of 2% , The lifetime is essentially independent of the concentration of EPO.

1-NpOD

Fluorescence decay curves of 1-NpOD (0.00034 M) in the absence and presence of NND (0.005-0.025 M) in freshly dried dioxane were measured with monitoring wavelength of 345 nm under the same conditions as those used for 1-NpOH. The decay curves are straight lines, and the slopes become steeper with increasing concentration of NND. The lifetimes calculated from the slopes are tabulated in Table 2-5, together with the Stern-Volmer parameters.

Transient fluorescence spectra of 1-NpOD (0.00034 M) in the presence of NND (0.0025 M) were measured at 0-0.98, 0.98-2.94, 2.94-5.07, 5.07-8.02, 8.02-12.12 and 12.12-17.20 ns after irradiation at 300 nm with monitoring wavelength-region of 310-496 nm. The spectra are shown in Figure 2-22.

1-AnOH

Fluorescence decay curves of 1-AnOH (0.0002 M) in the absence and presence of NND (0.005-0.025 M) in dioxane were measured under similar conditions to those used for 1-NpOH, except for monitoring at 435 nm. The decay curves are straight lines, and an example is shown in Figure 2-25. The Stern-Volmer plot of τ_o/τ *vs* [NND] is a straight line, as shown in

Figure 2-26. The lifetimes and the Stern-Volmer parameters are listed in Table 2-8.

Transient fluorescence spectra of 1-AnOH (0.0002 M) in the presence of NND (0.025 M) in dioxane were measured by excitation at 300 nm with monitoring wavelength-region of 310-708 nm at various delay times of 0-1.3, 1.3-4.5, 4.5-9.0, 9.0-17.3 and 17.3-27.3 ns.

5.8 Phosphorescence Spectra

Uncorrected phosphorescence and phosphorescence excitation spectra of NND in EPA glass at 77K were measured using a Perkin-Elmer MPF 44B spectrometer. A sample solution was placed in a phosphorescence tube (quartz glass,0.4x21.0 cm), and purged with nitrogen for 4 min prior to measurement. The conditions of measurement are shown in the caption of Figure 3-5.

5.9 Quantum Yield Determination

Determination of quantum yields of oxime formation, Φ_{ox}, and NND disappearance, Φ_N, in photonitrosation was carried out in "merry-go-round" apparatus **A** or **B**. Apparatus **A** consists of a turntable which revolves around a 450 Watt Hanovia lamp inserted in a Pyrex water-cooling jacket, the whole assembly being immersed in a water-bath. Apparatus **B** is a Rayonet Photochemical Reactor equipped with RPR-300-nm lamps (21 Watt x16) and with an air- cooling system.

5.9.1 $\bar{\Phi}_{ox}$ for 1-NpOH in Various Solvents

The quantum yield for the formation of the quinone monooxime **16** was determined as a function of the concentration of NND in various solvents such as dioxane, acetonitrile, benzene, toluene and methanol. A typical

run in dioxane is described below. Stock solutions of 1-NpOH (216 mg, 1.50 mmol) and of NND (178 mg, 2.41 mmol), each in dioxane, were prepared in two 10-ml volumetric flasks. A 1.0-ml aliquot of the 1-NpOH stock solution was pipetted into each of nine 5-ml volumetric flasks, into which aliquots (0.100-0.950 ml) of the NND stock solution were injected with a microliter syringe. After diluting with dioxane to 5 ml to give nine sample solutions containing 0.030-M 1-NpOH and NND (0.00576-0.0480 M), the solutions were transferred into quartz tubes (1.1x12 cm), which were subsequently capped with septa and wired up. Nitrogen was purged through the solution for at least 10 min prior to irradiation. The actinometer solution was prepared as follows. 456 mg (2.50 mmol) benzophenone and 921 mg (5.0 mmol) benzhydrol, were respectively dissolved in 25-ml benzene. A 2.5-ml aliquot was pipetted from each of the above stock solutions into a quartz tube, then purged with nitrogen for 10 min. The actinometer solution contained 0.050-M benzophenone and 0.10-M benzohydrol. The deaerated samples and actinometer were irradiated at 19°C in "merry-go-round" **A** for 100 min (but 25 min for the actinometer). The conversion of 1-NpOH was 5-25%, and that of benzophenone was 12%. The yellow photolysates were analyzed by HPLC (C_{18} column, MeOH/H_2O = 70/30, by volume, UV detector at 254 nm) with 1-nitronaphthalene as an internal standard. The concentration of **16** was calculated from Equation 5-3, and the corresponding quantum yield, Φ_{ox}, was calculated from Equation 5-4. When the determination was performed in "merry-go-round" **A**, the correction of the incident light absorbed by 1-NpOH was made according to Equation 5-6:

$$I_c = I_o \times A_s/(A_s + A_N) \qquad 5\text{-}6$$

where I_c = light intensity absorbed by 1-NpOH, I_o = measured light

intensity, A_S = absorption area of 1-NpOH (0.03 M) from 280 to 330 nm, and A_N = absorption area of NND (0.00576-0.0480 M) from 280 to 330 nm. The I_o value was calculated from Equation 5-2 from the change in absorbance of benzophenone at 342 nm during irradiation. The Stern-Volmer plot is given in Figure 2-27. The quantum yields and the Stern-Volmer parameters are listed in Table 2-7. For other solvents, the determination was carried out in the same way as described above, and the Stern-Volmer parameters are listed in Table 2-8. The observed data are listed in Appendix II.

5.9.2 Φ_{ox} and Φ_N for 1-NpOH in Various Solvents

The quantum yields for formation of **16**, Φ_{ox}, and for NND disappearance, Φ_N, in various solvents such as dioxane, THF, acetonitrile, methanol and ethanol were determined in the presence of increasing concentration of NND in "merry-go-round" **B**. The sample and actinometer solutions were prepared in the same way as described in the previous section. The deaerated solutions were irradiated with 300-nm lamps at 31°C for 20 min, causing a 5-15% conversion of 1-NpOH (5 min for the actinometer). The Φ_{ox} value was calculated in the same way as before. After irradiation, the concentrations of NND were determined by HPLC in the same way as in the determination of [1-NpOH], and obtained from Equation 5-7:

$$[NND] = A_{NND}[IS]/0.245A_{IS} \qquad 5\text{-}7$$

where [NND] and [IS] are the concentrations of NND and 1-nitronaphthalene (an internal standard), respectively; A_{NND} and A_{IS} are the corresponding peak areas. The constant, 0.245, is a relative response factor, which was measured from the plot of A_{NND}/A_{IS} *vs* [NND]/[IS]. The Φ_N value was

calculated from Equation 5-8:

$$\Phi_N = \Delta[NND]/It \qquad 5\text{-}8$$

where Δ[NND] is the change in concentration of NND during irradiation; I is the light intensity; t is the elapsed irradiation time in minutes. It was not necessary to correct the incident light absorbed by 1-NpOH because no absorption of NND occurs at 300 nm. The Stern-Volmer correlations of $1/\Phi_{ox}$ *vs* 1/[NND] and of $1/\Phi_N$ *vs* 1/[NND] were determined by least-square calculation. The results are shown in Table 2-9. The observed data are listed in Appendix II.

5.9.3 $\bar{\Phi}_N$ for 2-NpOH, 2-Allyl-1-naphthol and Anthrols

The sample and actinometer solutions were prepared in the manner described in section **5.9.2**, and the Φ_N value was determined by the procedure described in the previous section except that a 340-nm UV detector was employed in HPLC analysis for anthrols. The Stern-Volmer parameters for these phenols are listed in Table 2-11, and their observed data are given in Appendix III.

5.9.4 Quenching of Photonitrosation

The quantum yields, Φ_{ox} and Φ_N, for the photonitrosation of 1-NpOH with NND (both at a fixed concentration) were determined as a function of the concentration of a quencher such as water, TEA, DMF, or QC. The sample solutions were prepared in the manner described in section **5.6.2**, and using the same actinometer as above.

H_2O

Deaerated sample solutions containing 1-NpOH (0.030 M) and NND (0.020 M) in the absence and presence of H_2O (0.045-0.450 M) in THF were irradiated in "merry-go-round" **B** for 20 min at 31°C. HPLC analysis (the same conditions as used in section **5.9.2**) of the yellow photolysates gave the concentration of **16** and the concentration change of NND after irradiation. The values of Φ_{ox} and Φ_N were calculated from Equations 5-3 and 5-8, respectively. The correlation of either $\Phi_{ox}^{\circ}/\Phi_{ox}$ or Φ_N°/Φ_N, *vs* $[H_2O]$ based on Equations 2-26 gave a straight line. The observed data and the Stern-Volmer parameters are listed in Table 2-12.

TEA

The conditions of the determination of Φ_{ox} as a function of [TEA] were similar to those described previously, except that the sample solutions were irradiated in "merry-go-round" **A** for 120 min at 19°C. HPLC analysis of the yellow photolysates provided the concentration of **16**, and the Φ_{ox} values were calculated from Equation 5-3. The correlation of $\Phi_{ox}^{\circ}/\Phi_{ox}$ *vs* [TEA] was obtained from the least-squares analysis. The observed data and the calculated Stern-Volmer constants are listed in Table 2-13.

DMF

The conditions of the determination of Φ_{ox} as a function of [DMF] were the same as those used for the system of 1-NpOH/NND/H_2O. The values of $\Phi_{ox}^{\circ}/\Phi_{ox}$ and the Stern-Volmer parameters are listed in Table 2-14.

QC

The conditions of the determination of Φ_N as a function of [QC] were the same as those described previously. The values of Φ_N^o/Φ_N are listed in Table 2-15.

5.10 Studies of the Ground State Complex of 1-NpOH (or 1-AnOH) with NND

5.10.1 Determination of Association Constant by UV-Vis Spectroscopy

Stock solutions of 1-NpOH (0.0006 and 0.0003 M) and stock solutions of NND (0.03, 0.05, 0.06, 0.10, 0.15 and 0.30 M) were prepared in dioxane by the volumetric method and kept in dark prior to use. Differential absorption spectra were recorded at 20°C using a pair of double-compartment cells. A typical run is shown in Figure 5-9. The OD values were determined at 398, 400 and 402 nm from the spectra shown in Figure 2-32. The association constant (K) for the complex of 1-NpOH with NND was calculated from Equation 2-28. The K values at various concentration of NND are shown in Table 2-16.

Absorption spectra of ground state complex of 1-AnOH with NND in cyclohexane at 20°C were determined using a pair of normal cells. The spectra and the calculated association constant are shown in Figure 2-33 and Table 2-17, respectively.

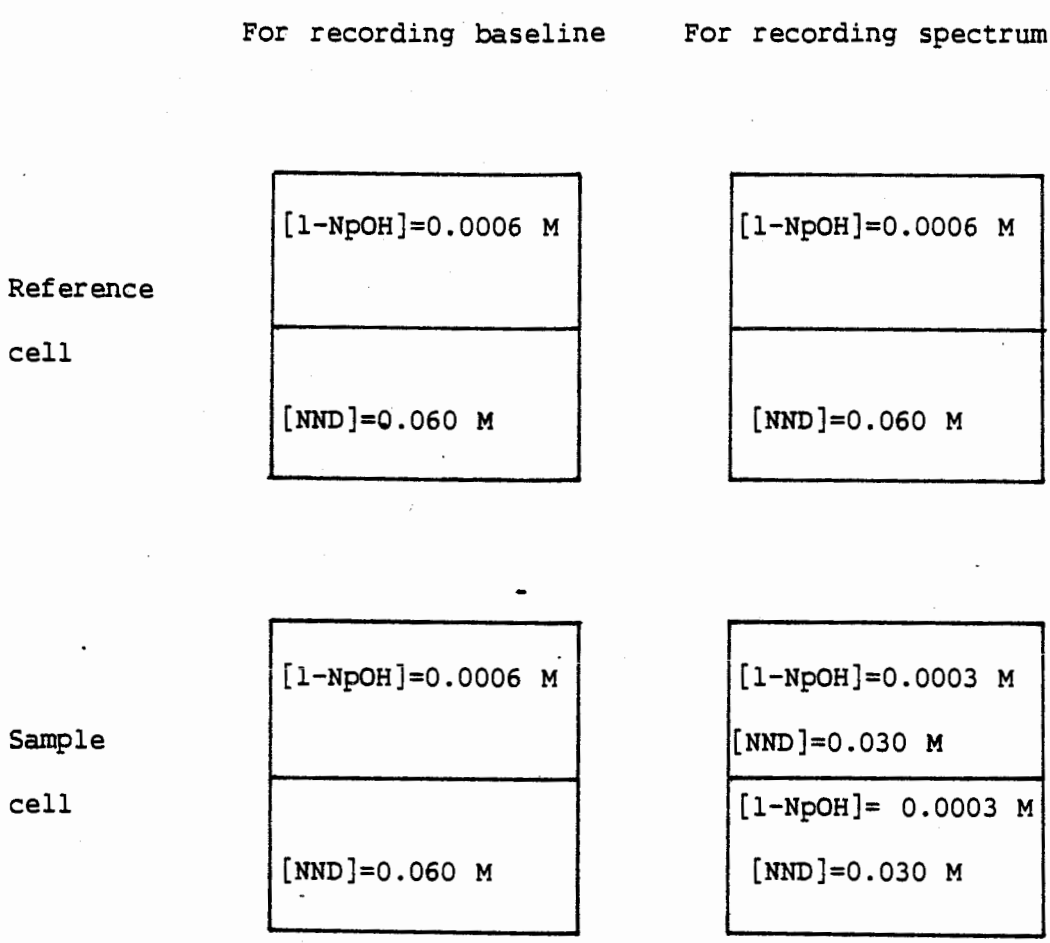

Figure 5-9 A pair of double compartment cells for the differential absorption spectra.

5.10.2 NMR Studies of the Ground State Complex

The chemical shifts of methyl groups in NND at 0.50 M in CCl_4 in the absence and presence of 1-NpOH (0.083-2.00 M) were measured at 20°C on a EM-360 spectrometer at 60 MHz. For each concentration of 1-NpOH, the determination of the chemical shift was repeated four times to get the averaged reading with a deviation of less than ±1.0 Hz. The plot of the chemical shift difference ($\Delta\delta$ defined in Equation 2-30) for each methyl group against [1-NpOH] is shown in Figure 2-34.

The NMR spectra of 1-NpOH (0.070 M) in the absence and presence of NND (0.081-0.649 M) in $CDCl_3/CCl_4$ (3/7, by volume) were measured from 9.00 to 6.00 ppm on a Bruker WM-400 spectrometer at 400 MHz at 20°C. The plots of $\Delta\delta$ *vs* [NND] and the plots of $1/\Delta\delta$ *vs* 1/[NND] are shown in Figure 2-36 and 2-37, respectively.

5.10.3 Photolysis of Ground State Complex of 1-NpOH with NND

Deaerated solutions of 1-NpOH (0.030 M) in the presence of NND (0.027 and 0.054 M) in dioxane and acetonitrile were irradiated on "merry -go-round" A through a GWV filter (cut-off < 380 nm) with a 200 Watt Hanovia lamp at 19±2°C for 31.5 h. HPLC (C_{18} column, $MeOH/H_2O$ = 70/30, by volume) analysis of the yellow photolysates gave the concentration of **16**. The quantum yield, Φ_{ox}, was determined with the actinometer of potassium ferrioxalate. The following stock solutions were prepared in re-distilled water for actinometry:

(1) 0.2% (by weight) phenanthrolin (50 mg) solution (25 ml).

(2) $NaOAc.3H_2O$ (8.2 g)-H_2SO_4 (concentrated, 1 ml) buffer solution (100 ml).

(3) $Fe_2(SO_4)_3.XH_2O$ (approximately 80% $Fe_2(SO_4)_3$, 10.03 g)-H_2SO_4

(concentrated, 5.5 ml) solution (100 ml).

(4) $K_2C_2O_4.H_2O$ (5.52 g) solution (25 ml).

The actinometer solution was prepared by pippetting 5 ml aliquots from each of $Fe_2(SO_4)_3$ and $K_2C_2O_4$ stock solutions into a 100-ml volumetric flask, and diluting to 100 ml with H_2O. A 5-ml aliquot of the green actinometer solution was pipetted into a quartz tube and purged with nitrogen for 10 min. The deaerated actinometer solution was irradiated for 20 min under the same conditions as those described previously. A 1-ml aliquot was pipetted from the irradiated actinometer solution into a 10-ml volumetric flask, followed by adding 2-ml 0.2% phenanthroline solution and 0.5-ml buffer solution and dilutting to 10 ml with H_2O, and the solution turned orange. The absorption spectrum of the orange solution was measured with 0.1-cm UV cells. The absorbance at 510 nm was determined to be OD = 0.195. A blank solution, prepared by mixing 1-ml aliquot of a un-irradiated actinometer solution with the same additives, gave OD = 0.003 at 510 nm. The light intensity was calculated from Equation 5-9 to be 3.79×10^{-4} Einstein/min.

$$I \text{ (Einstein/min)} = AV_2V_3/\epsilon l \Phi t V_1 \qquad 5\text{-}9$$

where A = corrected absorbance of irradiated actinometer solution,

V_1 = mls of irradiated actinometer solution withdrawn,

V_2 = mls of irradiated actinometer solution,

V_3 = mls of the volumetric flask used for dilution of irradiated aliquot,

$\epsilon = 1.11 \times 10^4$ $M^{-1}cm^{-1}$ at 510 nm[148]

$\Phi = 1.14$[148]

t = irradiation time in minutes.

l = optical path length of the UV cell (0.1 cm).

5.11 Photoaddition of NND to Pyrene in Acidic Medium

A yellow methanol solution (350 ml) containing pyrene (3.12 g, 15 mmol), NND (0.89 g, 12 mmol) and concentrated hydrochloric acid (2.5 ml, 29 mmol) in Apparatus III was irradiated for 3 h under nitrogen at 0-5°C. The dark photolysate was evaporated to 50 ml to give 2.545 g crude pyrpene as shown by TLC (silica gel $60GF_{254}$, toluene/ petroleum ether = 70/30, R_f = 0.80). The filtrate was evaporated to afford a dark grey solid (0.214 g), which showed two spots in TLC: the light one at R_f = 0.80 and the dark one at R_f = 0.35. The solid was recrystallized from methanol three times to give grey-yellow shining crystals (150 mg), (showing one spot at R_f at 0.35 in TLC), 1-dimethylaminopyrene hydrochloride: mp 157-159°C; IR (nujol): 3015(w) 2350 (m, br) 1600(m) 1510(w) 1480(s) 1425(m) 1405(m) 1380(s) 1150(m) 1140(m) 995(m) 920(w) 850(s) 840(s) 825(m) 800(m) 780(m) 720(m) 695(m) and 685(m) cm^{-1}; MS m/e(%): 246(20), 245(100, M^+-HCl), 230(30), 202(40) and 201(20); ^{1}H-NMR (DMSO-d_6): δ 2.50(s, $-NMe_2$, 6H), 8.12(t, 1H), 8.18(s, 2H), 8.23(d, 1H), 8.37(m, 4H) and 8.50(d, 1H); ^{13}C-NMR (DMSO-d_6): δ 45.9, 117.5, 121.8, 125.1, 125.4, 126.6, 126.8, 127.1, 127.6, 128.5, 130.3 and 130.9; anal. for $C_{18}H_{16}NCl$ (281.5) calcd.: C 76.73, H 5.68, N 4.97; found C 76.86, H 5.38, N 4.91.

A solution of 1-dimethylaminopyrene hydrochloride (30 mg) in methanol (1 ml) was adjusted to pH 10 by addition of saturated aqueous potassium carbonate solution. The dark brown aqueous solution was washed with benzene (2 x 4 ml). The washings were dried from magnesium sulfate and evaporated to afford a crude product (22 mg), which was recrystallized from benzene-petroleum ether to give 7-mg black solid **24**; ^{1}H-NMR (acetone-d_6) δ 2.08 (s, 6H, $-NMe_2$), 7.83(d, J=8.3 Hz, 1H), 8.00(AB, J=9.0 Hz 1H), 8.02(t,

J=7.5 Hz, 1H), 8.07(AB, J=9.0, 1H), 8.14(d, J=9.8 Hz, 1H), 8.18(d, J=7.5 Hz, 1H), 8.21(d, J=8.3 Hz, 1H), 8.22(d, J=7.5 Hz, 1H) and 8.48(d, J=9.8 Hz, 1H); ^{13}C-NMR (acetone-d_6) δ 45.8, 117.7, 124.5, 125.2, 125.3, 126.3, 126.5, 127.0, 128.3 and 132.4; MS m/e (%) 246(20, M^++1), 245(100, M^+), 230(25, M^+-Me) and 201(30, M^+-NMe_2).

5.12 Oxidative Photoaddition of NND to 1-Phenylpropenes in Acidic Media

5.12.1 General Procedure

^{1}H-NMR spectra of the purified arylpropenes, **26**, **29** and **32**, were measured in $CDCl_3$ with a Bruker SP-100 spectrometer. The spectra showed the coupling constants of olefinic protons: J_{13} = 16.6 (**26**), 15.7 (**29**) and 16.0 Hz (**32**). A methanol solution containing NND, an arylpropene and hydrochloric acid in Apparatus III (Pyrex filter) was irradiated under O_2 purging at 0°C using a 200 W Hanovia Lamp. The progress of the photolysis was monitored by UV spectroscopy of the samples taken at intervals. The solution was irradiated until the absorption at 330 nm for NND disappeared. The photolysate was evaporated to a small volume, diluted with 50 ml water and extracted with ether (3x20 ml). The combined ethereal solution was dried and evaporated to afford the "acidic-neutral" fraction. The aqueous phase was adjusted to pH=10 with saturated aqueous sodium hydrogen carbonate solution and then extracted with methylene chloride to give a basic fraction. Immediately, the basic fraction, taken up in dry THF, was stirred with LAH at room temperature for 24 h. After hydrolysis with sodium hydroxide solution, filtration and washing of the granular residue with THF, the combined filtrate and washings were evaporated to give the crude product, which was analyzed using IR, ^{1}H NMR and GC (OV-1 capillary column, at 140°C), and eventually chromatographed to afford pure products. Their elemental analysis and spectroscopic data are summarized in Tables 5-7 to

5-11.

5.12.2 Photoaddition to (*E*)-1(4-Methoxyphenyl)propene (26)

A solution of NND (3.55 g, 48 mmol), **26** (5.93g, 40 mmol) and concentrated hydrochloric acid (4.8 ml, *ca.* 56 mmol) in methanol (320 ml) was irradiated under O_2 for 4 h. The reddish-brown "acidic-neutral" fraction (1.82 g) showed a complex GC trace and IR absorptions (neat) at: 3400(m, br) 2840(w) 1680(s, br) 1600(s) 1550(s) 1510(s) 1460(m, br) 1250(s, br) 1170(m) 1110(m) 1030(s) and 830(s) cm^{-1}. The basic fraction (7.2 g) exhibited IR absorption at 1675(s), 1250(m) and 860(w) cm^{-1} due to a nitrate ($-ONO_2$) functional group. The basic fraction (5.0 g) was reduced with LAH (4.12 g, 110 mmol) in dried THF (120 ml) for 24 h and hydrolyzed to give a red brown oil (4.05 g) which showed the disappearance of $-ONO_2$ absorption in the IR spectrum. The GC analysis of the oil afforded the following compounds (Rt, yields calaulated from the GC peak area based on **26**): **27** (5.32 min, 24%), *threo*-isomer **28a** (7.54 min, 28%), and *erythro*-isomer **28b** (7.08 min, 15%). The crude products (300 mg) from reduction were separated on preparative TLC plates (Silica gel 60 GF_{254} / toluene/ethyl acetate/triethylamine, volume ratio, 9/3/1) to give **27** (48 mg), **28a** (74 mg), and **28b** (34 mg). The compounds of **27**, **28a** and **28b** are colorless oils.

5.12.3 Photoaddition to (*E*)-3-Phenyl-2-propenol (29)

A solution of NND (3.55 g, 48 mmol), **24** (5.37 g, 40 mmol) and concentrated hydrochloric acid (4.8 ml, *ca.* 56 mmol) in methanol (320 ml) was irradiated under O_2 for 4 h. The "acidic-neutral" fraction (0.67 g) showed a complex GC trace and IR absorptions (neat) at 3450(m,br) 1700(s) 1660(m) 1560(m) 1280(s,br) 940(w,br) and 850(m,br) cm^{-1}. The basic

fraction (7.43 g) exhibited IR absorptions at 1680(s), 1275(m) and 855(w) cm^{-1} due to $-ONO_2$. The basic fraction (5.84 g) was reduced with LAH (4.1 g, 110 mmol) in dried THF (120 ml) for 24 h, and hydrolyzed to give a brown oil (5.07 g), which showed the disappearance of the $-ONO_2$ absorptions. The GC analysis of the oil afforded the following compounds (Rt, yields calculated from GC peak area based on **29**): *threo*-isomer **30a** (10.71 min, 42%), *erythro*-isomer **30b** (10.32 min, 16%) and **31** (11.42 min, 14%). The reduced fraction (800 mg) was separated by column chromatography on neutral alumina (45 g). Elution with 0-30% ethyl acetate/toluene afforded **30a** (285 mg), **30b** (a colorless oil, 60 mg) and **31** (100 mg). The compounds **30a** and **31** were recrystallized from ether as white needles, m.p. 63.5-65.0°C and 71-72°C, respectively.

5.12.4 Photoaddition to (*E*)-1-(4-Hydroxy-3-methoxyphenyl)propene (32)

A solution of NND (1.78 g, 24 mmol), **32** (3.29 g, 20 mmol) and concentrated hydrochloric acid (3 ml, *ca.* 35 mmol) in methanol (300 ml) was irradiated under O_2 for 4.5 h. The "acidic-neutral" fraction (3.5 g) showed at least 6 GC peaks and IR absorptions at 3400(s, br) 1600(m) 1520(s) 1460(m, br) 1280(m, br) 1100(m) 1040(m) and 740(m) cm^{-1}. The basic fraction (1.04 g) exhibited the major GC peak for **33** (Rt 7.24 min). This fraction (800 mg) was purified by column chromatography on neutral alumina (50 g). Elution with 0-30% ethyl acetate/toluene provided the pure compound **33** which was recrystallized from benzene as white needles, mp 95-96°C.

Table 5-7 Elemental Analysis of Photoaddition Products

Mol. Formula (FW)	Calculated C	H	N	Compound	Found C	H	N
$C_{13}H_{21}NO$ (223)	69.96	9.42	6.28	**27**	69.77	9.33	6.60
$C_{12}H_{19}NO_2$ (209)	68.90	9.09	6.69	**28a**	69.51	9.31	6.27
				28b	69.10	9.30	6.84
$C_{11}H_{17}NO_2$ (195)	67.69	8.72	7.18	**30a**	67.75	8.99	7.16
				30b	67.56	9.00	7.41
$C_{13}H_{22}N_2O$ (222)	70.27	9.91	12.61	**31**	70.62	10.29	12.40
$C_{13}H_{21}NO_3$ (239)	65.26	8.88	5.85	**33**	65.05	8.78	5.27

Table 5-8 ^{1}H-NMR Spectral Data of Photoaddition Products

Compound	Data
27	0.62(d, J=8.0, -Me) 2.37(s, $-NMe_2$) 2.92(m, 1H) 3.13(s, -OMe) 3.82(s, -OMe) 3.95(d, J=10, 1H) 6.88-7.22(m, 4H)
28a	0.63(d, J=7.0, -Me) 2.30(s, $-NMe_2$) 2.56(m, 1H) 3.80(s, -OMe) 4.15(d, J=10, 1H) 6.88-7.25(m, 4H)
28b	0.76(d, J=7.0, -Me) 2.34(s, $-NMe_2$) 2.50(m, 1H) 3.80(s, -OMe) 4.90(d, J=3.0, 1H) 6.88-7.25(m, 4H)
30a	2.55(s, $-NMe_2$) 2.59(s, -OH, D_2O exch) 2.72(m, 1H) 3.43-3.56(m, 2H) 4.43(d, J=10, 1H) 7.25-7.42(m, 5H)
30b	2.40(s, $-NMe_2$) 2.54(s, -OH, D_2O exch) 2.58(m, 1H) 3.63-3.70(m, 2H) 5.04(d, J=3, 1H) 7.24-7.40(m, 5H)
31	2.12(s, $-NMe_2$) 2.15(s, $-NMe_2$) 3.15(m, -CHN) 3.77(d, J=11, PhCHN) 3.90(m, $-CH_2OH$) 7.15-7.30(m, 5H)
33	0.58(d, J=7.0, -Me) 2.34(s, $-NMe_2$) 2.83(m, 1H) 3.15(s, -OMe) 3.83(s, -OMe) 3.85(d, J=8.0, PhCH-) 7.75-7.83(m, 3H) 8.27(s, -OH, D_2O exch)

Table 5-9 ^{13}C-NMR Spectral Data of Photoaddition Products

Compound	Data
28a	6.21(Me) 39.9(-NMe_2) 55.2(-OMe) 66.0(-CHN) 74.4(-CHOH) 113.7-156.3(Ph)
28b	9.7(-Me) 42.9(-NMe_2) 55.2(-OMe) 65.5(-CHN) 72.1(-CHOH) 113.5-158.7(Ph)
30a	41.3(-NMe_2) 58.4(-CHN) 71.4(-CH_2OH) 71.6(PhCHOH) 127.1-141.9(Ph)
30b	42.1(-NMe_2) 58.4(-CHN) 70.2(-CH_2OH) 72.4(PhCHOH) 125.9-142.8(Ph)

Table 5-10 IR Data of Photoaddition Products

Compound	$\nu_{max}(cm^{-1})$
27 (neat)	2840(w) 2830(w) 2790(w) 1620(s) 1520(s) 1460(m, br) 1250(s) 1180(m) 1100(s) 1040(m) 840(m)
28a (neat)	3350(m, br) 1620(s) 1520(s) 1465(m) 1250(s) 1045(s) 835(s)
28b (neat)	3340(m, br) 2840(w) 2790(w) 1615(s) 1515(s) 1465(s) 1250(s) 1180(m) 1040(s) 965(m) 825(m)
30a (nujol)	3400(s, br) 2850(m) 2800(m) 1500(m) 1465(s) 1270(m, br) 1160(m) 1060(s, br) 1000(s) 755(m) 707(s)
30b (nujol)	3400(s, br) 2950(s) 2890(m) 2840(m) 2800(m) 1605(w) 1500(w) 1455(s) 1270(m, br) 1070(m, br) 1030(s) 760(m) 710(s)
31 (nujol)	3400(m, br) 2940(s) 2840(m) 2790(m) 1500(w) 1455(s) 1160(m) 1040(s) 755(m) 710(s)
33 (KBr)	3400(m, br) 1600(w) 1510(s) 1470(m, br) 1275(s) 1240(m, br) 1100(m) 1040(m) 870(w) 820(m) 750(w)

Table 5-11 MS (CI) Data of Photoaddition of Products

Compound	m/e(%, fragment)
27	224(28, M^++1) 222(25, M^+-1) 192(37, M^+-OMe) 72(100, $Me_2NCHCH_3^+$)
28a	210(100, M^++1) 192(63.4, M^+-OH) 165(11, M^+-Me_2N) 72(22.4, $Me_2NCHCH_3^+$)
28b	210(100, M^++1) 208(15, M^+-1) 192(42, M^+-OH) 165(6, M^+-Me_2N) 72(22, $Me_2NCHCH_3^+$)
30a	196(100, M^++1) 178(61.4, M^+-OH) 88(47.4, $Me_2NCHCH_2OH^+$)
30b	196(100, M^++1) 178(41, M^+-OH) 88(43.4, $Me_2NCHCH_2OH^+$)
31	223(46, M^++1) 221(27, M^+-1) 178(100, M^+-Me_2N) 134(95, M^+-Me_2NCHCH_2OH) 88(30, $Me_2NCHCH_2OH^+$)
33	240(43, M^++1) 238(30, M^+-1) 208(100, M^+-OMe) 195(6, M^+-Me_2N) 167(22, M^+-Me_2NCHCH_3)

REFERENCES

1. Y.L. Chow, in "Chemistry of Amino, Nitroso and Nitro Compounds, Supplement F", Part 1, S. Patai, Ed. John Wiley & Sons, New York, 1982, p 181.

2. Y.L. Chow, *Acc. Chem. Res.* **6**, 354, (1973).

3. R.P. Muller and J.R. Huber, *Rev. Chem. Interm.* **5**, 423, (1984).

4. Y.L. Chow, in "Reactive Intermediates", Vol. 1, R.A. Abramovitch, Ed., Plenum, New York, 1980, p. 151.

5. J. Tanaka, *J. Chem. Soc. Jap.* **78**, 1647, (1957).

6. P. Rademacher and R. Stølevik, *Acta. Chem. Scand.* **23**, 660, (1969).

7. U. Klement and A. Schmidpeter, *Angew. Chem. Intern. Ed. Engl.* **7**, 470, (1968).

8. G.J. Karabatsos and R.A. Taller, *J. Am. Chem. Soc.* **86**, 4373, (1964).

9. Y.L. Chow and C.J. Colón, *Can. J. Chem.* **46**, 2821, 1968.

10. B.G. Gowenlock, P.P. Jones and J.R. Major *Trans. Faraday. Soc.* **57**, 23, (1961).

11. W.S. Layne, H.H. Jaffé and H. Zimmer, *J. Am. Chem. Soc.* **85**, 435, 1816, (1963).

12. R. Zahradník, E. Svátek and M. Chvapil, *Chem. Listy* **51**, 2232, (1957).

13. J.B. Hendrickson, D.J. Cram and G.S. Hammond, "Organic Chemistry" 3d. edition, McGraw-Hill Book Company, New York, 1970, p.306.

14. M.P. Lau, Ph.D. Dissertation, Simon Fraser University, 1970.

15. M.P. Lau, A.J. Cessna, Y.L. Chow and R.W. Yip, *J. Am. Chem. Soc.* **93**, 3808, (1971).

16. A.J. Cessna, S.E. Sugamori, R.W. Yip, M.P. Lau, R.S. Snyder and Y.L. Chow, *J. Am. Chem. Soc.* **99**, 4044, (1977).

17. Y.L. Chow, J.N.S. Tam, C.J. Colón and K.S. Pillay, *Can. J. Chem.* **51**, 2469, (1973).

18. Y.L. Chow, J.N.S. Tam and K.S. Pillay, *Can. J. Chem.* **51**, 2477, (1973).

19. K.S. Pillay, K. Hanaya and Y.L. Chow, *Can. J. Chem.* **53**, 3022, (1975).

20. K.S. Pillay and Y.L. Chow, *J. Chem. Soc. Perkin Trans.* **2**, 93, (1977).

21. Y.L. Chow, H. Richard and R.W. Lockhart, *J. Chem. Soc. Perkin Trans.* **1**, 1419, (1982).

22. Y.L. Chow, C.J. Colón, D.W.L. Chang, K.S. Pillay, R.L. Lockhart, and T. Tezuka, *Acta Chem. Scand.* **B36**, 623, (1982).

23. S.L. Murov, "Handbook of Photochemistry", Dekker, New York, 1973.

24. E.M. Burgess and J.M. Lavanish, *Tetrahedron Lett.* 1221, (1964).

25. Y.L. Chow, *Tetrahedron Lett.* 2333, (1964).

26. L.P. Kuhn, G.G. Kleinspehn and A.C. Duckworth, *J. Am. Chem. Soc.* **89**, 3858, (1967).

27. Y.L. Chow, D.P. Horning and J. Polo, *Can. J. Chem.* **58**, 2477, (1980).

28. C.J. Michejda, N.E. Davidson and N.K. Keefer, *J. Chem. Soc. Chem. Commun.* 633, (1976).

29. A. Weller, *Prog. React. Kinet.* **1**, 189, (1961).

30. E.V. Donckt, *Prog. React. Kinet.* **5**, 273, (1970).

31. J.F. Ireland and P.A.H. Wyatt, *Adv. Phys. Org. Chem.* **12**, 131, (1976).

32. W. Klopffer, *Adv. Photochem.* **10**, 311, (1977).

33. S.C. Lahiri, *J. Sci. Ind. Res.* **38**, 492, (1979).

34. H. Shizuka, *Acc. Chem. Res.* **18**, 141, (1985).

35. Th. Förster, *Z. Elektrochem. Angew. Phys. Chem.* **54**, 42, 531, (1950).

36. A. Weller, *Ber. Bunsenges. Phys. Chem.* **56**, 662, (1952); **66**, 1144, (1956).

37. H. Beens, K.H. Grellman, M. Gurr and A. Weller, *Discuss. Faraday Soc.* **39**, 183, (1965).

38. E.L. Wehry and L.B. Rogers in " Fluorescence and Phosphorescence Analysis"; D.M. Hercules Ed., Wiley Interscience, New York, 1966, p 125.

39. S.G. Schulman in "Modern Fluorescence Spectroscopy", E.L. Wehry Ed., Plenum Press, New York, 1976, Vol. 2, p 239.

40. S.G. Schulman "Fluorescence and Phosphorescence Spectroscopy: Physicochemical Principles and Practice", Pergamon Press, New York, 1977, p 74.

41. G. Jackson and G. Porter, *Proc. R. Soc. London, Ser A* **200**, 13, (1961).

42. H. Schizuka and E. Kimura, *Can. J. Chem.* **62**, 2041, (1984).

43. J.A. Barltrop and J.D. Coyle, "Principles of Photochemistry" John Wiley & Sons, New York, 1978, p51.

44. F.D. Saeva and G.R. Olin, *J. Am. Chem. Soc.* **97**, 5631, (1975).

45. E.A. Chandross, *J. Am. Chem. Soc.* **98**, 1053, (1976).

46. M. Isaks, K. Yates and P. Kalanderopoulos, *J. Am. Chem. Soc.* **106**, 2728, (1984).

47. I.B. Berlman, "Handbook of Fluorescence Spectra of Aromatic Molecules", Academic, New York, 1965.

48. C.M. Harris and B.K. Selinger, *J. Phys. Chem.*, **84**, 1366, (1980).

49. S.A. Yamamoto, K. Kikuchi and H. Kokubun, *J. Photochem.* **5**, 469, (1976).

50. M. Swaminathan and S.K. Dogra, *J. Chem. Soc. Perkin Trans.* II, 947, (1984).

51. D. Hadži, *J. Chem. Soc.* 2725, (1956).

52. H. Baba and T. Takemura, *Tedrahedron* **24**, 4779, 5311, (1968).

53. J.C. Scaiano, C.W.B. Lee, Y.L. Chow and G.E. Buono-Core, *J. Photochem.* **20**, 327, (1980).

54. C.A. Parker, "Photoluminescence of Solution", Elsevier Publishing Company, New York, 1968, p 83, 225.

55. J.R. Lakowicz "Principles of Fluorescence Spectroscopy", Plenum Press, New york, 1983, p 43.

56. N.J. Turro, "Modern Molecular Photochemistry", Benjamin/Cummings Publishing Company, Inc., Menlo Park, California, 1978, p 298.

57. Y.L. Chow and Z.-Z. Wu, *J. Am. Chem. Soc.* **107**, 3338, (1985).

58. A. Matsuyama and H. Baba, *Bull. Chem. Soc. Jpn.* **44**, 1162, (1971).

59. Ref. 55, p 260.

60. Ref. 56, p 314.

61. Ref. 55, p 64.

62. R.W. Ware, in "Creation and Detection of the Excited State", A.A. Lamola Ed., Marcel Dekker, New York, 1971, Vol. 1, Part A, p 264.

63. Y.L. Chow, B. Marciniak and P. Mishra, *J. Org. Chem.* **49**, 1457, (1984).

64. G.S. Hammond and P.A. Leermakers, *J. Phys. Chem.* **66**, 1148, (1962).

65. S.P. Webb, S.W. Yeh, L.A. Philips, M.A. Tolbert and J.H. Clark,

J. Am. Chem. Soc. **106**, 7286, (1984).

66. K. Tsutsumi and H. Shizuka, *Z. Phys. Chem. (Wiesbaden)*, 122, 129, (1980).

67. S. Hagopian and L.A. Singer, *J. Am. Chem. Soc.* **105**, 6760, (1983).

68. *Ibid.* **107**, 1874, (1985).

69. A. Matsuzaki, S. Nagakura and K. Yoshihara, *Bull. Chem. Soc. Jap.* **47**, 1152, (1974).

70. N. Mataga and Y. Kaifu, *J. Chem. Phys.* **36**, 2804, (1962).

71. N. Mataga, Y. Kawasaki and Y. Torihashi, *Theoret. Chim. Acta.* **2**, 168, (1964).

72. J. Devaure and P.V. Huong, *Bulletin de la Societe Chimique de France* **11**, 3917, (1971).

73. S. Murov and G.S. Hammond, *J. Phys. Chem.* **72**, 3797, (1968).

74. B.S. Solomon, C. Steel and A. Weller, *J.C.S. Chem. Commun.* 927, (1969).

75. S. Nagakura and M. Gouterman, *J. Chem. Phys.* **26**, 881, (1957).

76. S. Nagakura, *J. Am. Chem. Soc.* **76**, 3070, (1954).

77. Y.Y. Shu, M.Sc. Dissertation, Simon Fraser University, 1985.

78. R. Foster and C.A. Fyfe, "Nuclear Magnetic Resonance of Organic Charge-Transfer Complex" in "Progress in NMR Spectroscopy", J.W. Emsley Ed., Vol. 4, Pergamon Press, New York, 1969, p 38.

79. R. Foster and C.A. Fyfe, *J.C.S. Chem. Commun.* 642, (1965).

80. R. Foster and C.A. Fyfe, *Trans. Faraday Soc.* **61**, 1626, (1965).

81. R. Foster and C.A. Fyfe, *J. Chem. Soc. B.* 926, (1966).

82. W. Koch and H. Zollinger, *Helv. Chim. Acta* **48**, 554, (1965).

83. Y.L. Chow and M.M. Fesser *J.C.S. Chem. Commun.* 239, (1967).

84. D.H. Williams and D.A. Wilson, *J. Chem. Soc. B* 144, (1966).

85. V. Lucchini and P.R. Wells, *Org. Magn. Reson.* **8**, 140, (1976).

86. K. Kikuchi, H. Watarai and M. Koizumi, *Bull. Chem. Soc. Jpn.* **46**, 749, (1973).

87. S.-A. Yamamoto, K. Kikuchi and H. Kokubun, *Chem. Lett.* 65, (1976).

88. S.-A. Yamamoto, K. Kikuchi and H. Kokubun, *J. Photochem.* **2**, 177, (1977).

89. H. Shizuka, H. Hagiwara and M. Fukushima, *J. Am. Chem. Soc.* **107**, 7816, (1985).

90. D. Rehm and A. Weller, *Israel J. Chem.* **8**, 259, (1970).

91. A. Weller, *Pure Appl. Chem.* **16**, 116, (1968).

92. A. Weller, in "Exciplex", M.S. Gordon and W.R. Ware Ed., Academic Press, New York, 1975, Chapter 2.

93. G.E. Buono-Core, personal communication.

94. L. Meites and P. Zuman "CRC Handbook Series in Organic Electrochemistry" Vol. I, CRC Press Inc. 1977.

95. M. Masui, K. Nose, A. Tanaka, E. Yamakawa and H. Ohmori, *Chem. Pharm. Bull.* **29**, 3758, (1981).

96. M. Eigen, *Angew. Chem. Int. Ed. Engl.* **3**, 1, (1964).

97. J.R. Murdoch, *J. Am. Chem. Soc.* **102**, 71, (1980).

98. L.E. Manring and K.S. Peters, *J. Am. Chem. Soc.* **107**, 6452, (1985).

99. *Ibid.* **105**, 5708, (1983).

100. N. Mataga, *Bull. Chem. Soc. Jpn.* **31**, 481, (1958).

101. Chi-Yu Chiang, Ph.D. Dissertation, University of Florida, 1970.

102. P. Froehlich and E.L. Wehry, Ref. 39, p 351.

103. R.S. Davidson, *Adv. Phys. Org. Chem.* **19**, 1, (1983).

104. L.M. Stephenson and G.S. Hammond, *Pure Appl. Chem.* **16**, 125, (1968).

105. P.M. Froehlich and H.A. Morrison, *J. Am. Chem. Soc.* **96**, 332, (1974).

106. T. Majima, C. Pac and H. Sakurai, *Bull. Chem. Soc. Jpn.* **51**, 1811, (1978).

107. G.N. Taylor and G.S. Hammond, *J. Am. Chem. Soc.* **94**, 3687, (1972).

108. G.N. Taylor, E.A. Chandross and A.H. Schiebel, *J. Am. Chem. Soc.* **96**, 2693, (1974).

109. Ref. 56, p 45.

110. J.V. Hatton and R.E. Richard, *Mol. Phys.* **5**, 139, (1962).

111. W.M. Vaughan and G. Weber, *Biochem.* **9**, 464, (1970).

112. J.L.G. Nilsson, H. Sievertsson and H. Selander, *Acta Chem. Scand.* **23**, 859, (1969).

113. W.A. Skinner and R.M. Parkhurst, *Lipids* **5**, 184, (1969).

114. G.B. Burton and K.U. Ingold, *Acc. Chem. Res.* **19**, 194, 1986.

115. G.W. Grams, K. Eskins and G.E. Inglett, *J. Am. Chem. Soc.* **94**, 866, (1972).

116. H. Schmid, *Helv. Chim. Acta* **50**, 255, (1967).

117. W.M. Horspool, *J.C.S. Chem. Comm.* 195, (1967).

118. S. Houry, *Israel J. Chem.* **22**, 805, (1973).

119. H. Schmid, *Helv. Chim. Acta* **60**, 768, (1977).

120. M. Kasha, *Discuss. Faraday Soc.* **9**, 14, (1959).

121. Ref. 56, p 107, 122 and 124.

122. Ref. 43, p 62.

123. K. Sandros, *Acta Chem. Scand.* **18**, 2355, (1964).

124. B. Marciniak, personal communication.

125. T. Kubota, M. Yamakawa and Y. Mizuno, *Bull. Chem. Soc. Jpn.* **45**, 3282, (1972).

126. M. Yamakawa, K. Ezumi, Y. Mizuno and T. Kubota, *Bull. Chem. Soc. Jpn.* **47**, 2982, (1974).

127. N.J. Turro, W.R. Cherry, M.J. Mirbach, M.F. Mirbach and V. Ramamurthy, *Mol. Photochem.* **9**, 111, (1978-79).

128. M. Yamakawa, T. Kubota, K. Ezumi and Y. Mizuno, *Spectrochimica Acta* **30** 2103, (1974).

129. R. Cimiraglia, M. Persico and J. Thomas, *J. Am. Chem. Soc.* **107**, 1617, (1985).

130. G. Geiger and J.R. Huber, *Helv. Chim. Acta* **64**, 989, (1981).

131. Y.L. Chow, Z.-Z. Wu, M.-P. Lau and R.W. Yip, *J. Am. Chem. Soc.* **107**, 8196, (1985).

132. C.J. Colón, Ph.D. Dissertation, Simon Fraser University, 1971.

133. Y.L. Chow, S.C. Chen and D.W.L. Chang, *Can. J. Chem.* **49**, 3069, (1971).

134. Y.L. Chow and H. Richard, *J.C.S. Perkin Trans.* I, 1405, (1982).

135. L.M. Jackman and S. Sternhell, "Applications of Nuclear Magnetic Resonance Spectroscopy in Organic Chemistry", 2nd Ed., Pergamon Press, New York, 1978, p 291.

136. J.C. Randall, R.L. Vaulx, M.E. Hobbs and C.R. Hauser, *J. Org. Chem.* **30**, 2035, (1965).

137. E.L. Eliel, N.L. Allinger, S.J. Angyal and G.A. Morrison, "Conformational Analysis", Interscience, New York, 1965, P 5.

138. D.D. Perrin, W.L.F. Armarego and D.R. Perrin "Purification of Laboratory Chemicals", Pergamon Press, New York, 1966.

139. A.I. Vogel, "A Text-Book of Pratical Organic Chemistry", Longmans Green, New York, p 426.

140. C.D. Smith *Org. Synth.* **51**, 133, 1971.

141. E.A. Walker, L. Griciute, M. Castegnaro and M. Bözrzsönyi, "N-Nitroso Compounds: Analysis, Formation and Occurrence", IARC Publicatin No. 31, Lyon, France, 1980.

142. Ref. 139, P 186.

143. C.M. Orlando,Jr., H. Mark, A.K. Bose and M.S. Manhas, *J. Org. Chem.* **33**, 2512, 1968.

144. S. Marcinkiewicz, J. Green and P. Mamalis, *Tetrahedron* **14**, 219, (1961).

145. P. Ferrero and A. Conzetti, *Helv. Chim. Acta.* **11**, 1152, (1928).

146. Ref. 139, p 345.

147. A more detailed description of the facility has been described in T.W. Steiner's Ph.D. Dissertation, Simon Fraser University, 1986.

148. C.G. Hatchard and C.A. Parker, *Proc. Roy. Soc.* (London) **A235**, 518, (1956).

149. P. Wan and K. Yates, *Rev. Chem. Inter.* **5**, 157, (1984).

150. J. B. Birks, "Photophysics of Aromatic Molecules" Wiley-Interscience, London, 1979, p 304.

151. S. Scheiner, *Acc. Chem. Res.*, **18**, 174, (1985).

152. I. Brinn, Ph.D. Dissertation, University of Pittsburgh, 1968.

APPENDIX I

1. Derivation of Equations 2-19 and 2-21 from Scheme 2-1

The steady state approximation applied to the singlet excited state 1-NpOH and to the exciplex C_1 gives

$$I = \{k_f + k_{ic} + k_{st} + k_q[NND]\}[^{1*}1\text{-NpOH}]$$

and $$k_q[NND][^{1*}1\text{-NpOH}] = (k_p + k_b + k_{p'})[C_1]$$

The quantum yield of formation of **16** (Φ_{ox}) is:

$$\Phi_{ox} = \frac{k_p[C_1]}{I}$$

Hence, the quantum yield is given by

$$\Phi_{ox} = \frac{k_p k_q[NND]}{(k_p + k_b + k_{p'})\{k_f + k_{ic} + k_{st} + k_q[NND]\}}$$

then

$$1/\Phi_{ox} = 1/\beta + 1/\{\beta\tau_o k_q[NND]\} \qquad 2\text{-}19$$

where $1/\tau_o = k_f + k_{ic} + k_{st}$

$\beta = k_p/(k_p + k_b + k_{p'})$

Similarly, the quantum yield of disappearance of NND (Φ_N) is:

$$\Phi_N = \frac{(k_p + k_{p'})[C_1]}{I}$$

Hence, this quantum yield is given by

$$\Phi_N = \frac{(k_p + k_{p'})k_q[NND]}{(k_p + k_b + k_{p'})\{k_f + k_{ic} + k_{st} + k_q[NND]\}}$$

then

$$1/\Phi_N = 1/\beta' + 1/\{\beta'\tau_o k_q[NND]\} \qquad 2\text{-}21$$

where

$$1/\tau_o = k_f + k_{ic} + k_{st}$$

$$\beta' = (k_p + k_{p'})/(k_p + k_b + k_{p'})$$

2. Derivation of Equation 2-26 from Scheme 2-1 and Equation 2-25

Similarly, the Φ_{ox} is:

$$\Phi_{ox} = \frac{k_p[C_1]}{I}$$

The steady state approximation gives

$$I = \{k_f + k_{ic} + k_{st} + k_q[NND] + k_c[B]\}[^{1*}1\text{-NpOH}]$$

and $$k_q[NND][^{1*}1\text{-NpOH}] = (k_p + k_b + k_{p'})[C_1]$$

Hence, the quantum yield is given by

$$\Phi_{ox} = \frac{k_p k_q[NND]}{(k_p + k_b + k_{p'})\{k_f + k_{ic} + k_{st} + k_q[NND] + k_c[B]\}}$$

but in the absence of a base, B, it is given by

$$\Phi_{ox}^{\circ} = \frac{k_p k_q [NND]}{(k_p + k_b + k_{p'})\{k_f + k_{ic} + k_{st} + k_q[NND]\}}$$

Hence

$$\frac{\Phi_{ox}^{\circ}}{\Phi_{ox}} = \frac{k_f + k_{ic} + k_{st} + k_q[NND] + k_c[B]}{k_f + k_{ic} + k_{st} + k_q[NND]}$$

then

$$\Phi_{ox}^{\circ}/\Phi_{ox} = 1 + k_c \tau [B] \qquad 2\text{-}26$$

where

$$1/\tau = k_f + k_{ic} + k_{st} + k_q[NND]$$

Similarly,

$$\Phi_N^{\circ}/\Phi_N = 1 + k_c \tau [B] \qquad 2\text{-}26'$$

APPENDIX II

Table II-1 Φ_{ox} in Photolysis of 1-NpOH (0.050 M) with NND in CH_3CN at 19°C[a]

$[NND]x10^3$ (M)	Φ_{ox}	1/[NND] (1/M)	$1/\Phi_{ox}$
5.76	0.0246	174	40.7
7.20	0.0313	139	31.9
9.60	0.0351	104	28.5
14.4	0.0417	69.4	24.0
19.2	0.0474	52.1	21.1
24.0	0.0536	41.7	18.7
28.8	0.0563	34.7	17.8
36.0	0.0601	27.8	16.6

$k_q\tau_o$ (M^{-1})	81±9
$k_q x10^{-9}$ ($M^{-1}s^{-1}$)	11±1
Φ_{ox}(lim)	0.080±0.004
r	0.993

a. The sample solutions were irradiated through a Pyrex filter at 19°C for 120 min to cause 8-15% conversion of 1-NpOH.

Table II-2 $\bar{\Phi}_{ox}$ in Photolysis of 1-NpOH (0.050 M) with NND in Benzene at 19°C[a]

$[NND]x10^3$ (M)	Φ_{ox}	$1/[NND]$ (1/M)	$1/\Phi_{ox}$
5.90	0.00710	169	141
7.38	0.00875	136	114
9.84	0.0110	102	91.0
12.3	0.0128	81.3	78.3
14.8	0.0143	67.8	69.9
17.2	0.0157	58.1	63.7

$k_q\tau_o$ (M^{-1})	33±4
$k_q x10^{-9}$ ($M^{-1}s^{-1}$)	3.1±0.4
Φ_{ox}(lim)	0.044±0.004
r	0.998

a. The sample solutions were irradiated through a Pyrex filter at 19°C for 120 min to cause 5-10% conversion of 1-NpOH.

Table II-3 Φ_{ox} in Photolysis of 1-NpOH (0.050 M) with NND in Toluene at 19°C[a]

$[NND]x10^3$ (M)	Φ_{ox}	1/[NND] (1/M)	$1/\Phi_{ox}$
7.38	0.00804	136	124
9.84	0.00931	102	108
12.3	0.0113	81.3	88.5
17.2	0.0143	58.1	70.0
22.1	0.0158	45.3	63.5

$k_q\tau_o$ (M^{-1})	45±9
$k_q x10^{-9}$ ($M^{-1}s^{-1}$)	4.3±0.8
Φ_{ox}(lim)	0.032±0.004
r	0.993

a. The sample solutions were irradiated through a Pyrex filter at 19°C for 120 min to cause 5-10% conversion of 1-NpOH.

Table II-4 Φ_{ox} in Photolysis of 1-NpOH (0.050 M) with NND in Methanol at 19°C[a]

$[NND]x10^3$ (M)	Φ_{ox}	1/[NND] (1/M)	$1/\Phi_{ox}$
7.87	0.00693	127	144
9.84	0.00763	102	131
14.8	0.00924	67.8	108
19.7	0.0103	50.8	97.1
24.6	0.0113	40.7	88.7
29.5	0.0125	33.9	80.1
39.4	0.0133	25.4	75.7
49.2	0.0140	20.3	71.4

$k_q\tau_o$ (M^{-1})	85±5
$k_q x10^{-9}$ ($M^{-1}s^{-1}$)	11.1±0.6
Φ_{ox}(lim)	0.017±0.001
r	0.996

a. The sample solutions were irradiated through a Pyrex filter at 19°C for 100 min to cause 3-10% conversion of 1-NpOH.

Table II-5 Φ_{ox} and Φ_N in Photolysis of 1-NpOH (0.030 M) with NND in Dioxane at 31°C[a]

$[NND]x10^3$ (M)	1/[NND] (1/M)	Φ_{ox}	$1/\Phi_{ox}$	Φ_N	$1/\Phi_N$
7.45	134	0.0276	36.3	0.0616	16.2
10.0	100	0.0340	29.5	0.0728	13.7
12.6	79.4	0.0379	26.4	0.0798	12.5
15.0	66.7	0.0402	24.9	0.0865	11.6
17.8	56.2	0.0446	22.4	0.0962	10.4

$k_q\tau_o$ (M^{-1})	74±7	93±9
$k_q x10^{-9}$ ($M^{-1}s^{-1}$)	7.0±0.7	8.7±0.9
Φ(lim)	0.08±0.01	0.15±0.01
r	0.997	0.996
$k_p:k_{p'}:k_b$	1.0:0.92:10.8	

a. The sample solutions were irradiated by RPR-300nm lamps for 30 min to cause 10-20% conversion of 1-NpOH.

Table II-6 Φ_{ox} and Φ_N in Photolysis of 1-NpOH (0.030 M) with NND in Acetonitrile at 31°C[a]

$[NND]x10^3$ (M)	1/[NND] (1/M)	Φ_{ox}	$1/\Phi_{ox}$	Φ_N	$1/\Phi_N$
8.26	121	0.0374	26.8	0.0721	13.9
11.1	90.1	0.0454	22.0	0.0816	12.3
13.8	72.5	0.0505	19.8	0.0958	10.4
16.5	60.6	0.0527	19.0	0.104	9.60
19.5	51.3	0.0558	17.9	0.110	9.07
22.2	45.1	0.0590	17.0	0.117	8.58

$k_q\tau_o$ (M^{-1})	89±9	74±9
$k_q x10^{-9}$ ($M^{-1}s^{-1}$)	12±1.2	9.7±1.0
Φ(lim)	0.089±0.005	0.19±0.01
r	0.995	0.993
$k_p:k_{p'}:k_b$	1.0:1.1:9.1	

a. The sample solutions were irradiated by RPR-300nm lamps for 22 min to cause 9-18% conversion of 1-NpOH.

Table II-7 Φ_{ox} and Φ_N in Photolysis of 1-NpOH (0.030 M) with NND in THF at 31°C[a]

$[NND]\times10^3$ (M)	1/[NND] (1/M)	Φ_{ox}	$1/\Phi_{ox}$	Φ_N	$1/\Phi_N$
8.20	122	0.0338	29.5	0.0800	12.5
11.0	90.9	0.0417	24.0	0.0966	10.4
13.7	73.0	0.0443	22.6	0.111	8.98
16.2	61.7	0.0512	19.5	-	-
18.9	52.9	0.0531	18.8	0.128	7.81
21.2	47.2	0.0558	17.9	-	-

$k_q\tau_o$ (M^{-1})	69±9	60±5
$k_q\times10^{-9}$ ($M^{-1}s^{-1}$)	7.4±1.0	6.4±0.5
Φ(lim)	0.094±0.006	0.243±0.007
r	0.993	0.999
$k_p:k_{p'}:k_b$	1.0:1.6:8.1	

a. The sample solutions were irradiated by RPR-300nm lamps for 22 min to cause 3-8% conversion of 1-NpOH.

Table II-8 Φ_{ox} in Photolysis of 1-NpOH (0.030 M) with NND in Ethanol at 31°C[a]

$[NND]x10^3$ (M)	1/[NND] (1/M)	Φ_{ox}	$1/\Phi_{ox}$
7.94	126	0.0112	89.1
10.6	94.3	0.0134	74.8
13.4	74.8	0.0151	66.2
15.6	64.1	0.0172	58.1
18.6	53.9	0.0183	54.6
21.5	46.2	0.0193	51.7

$k_q\tau_o$ (M^{-1})	60±5
$k_q x10^{-9}$ ($M^{-1}s^{-1}$)b	7.9±0.4
Φ_{ox}(lim)	0.034±0.002
r	0.997

a. The sample solutions were irradiated by RPR-300nm lamps for 33 min to cause 3-10% conversion of 1-NpOH.

b. The τ_o value is assumed to be the same as in methanol (7.7 ns).

Table II-9 Φ_{ox} in Photolysis of 1-NpOH (0.030 M) with NND in Methanol at 31°C[a]

$[NND]x10^3$ (M)	1/[NND] (1/M)	Φ_{ox}	$1/\Phi_{ox}$
7.32	139	0.00753	133
9.76	98.0	0.00865	116
14.6	64.5	0.0113	88.5
17.1	54.2	0.0120	83.1
19.5	47.6	0.0127	78.8

$k_q\tau_o$ (M^{-1})	82±13
$k_q x10^{-9}$ ($M^{-1}s^{-1}$)[b]	11±2
Φ_{ox}(lim)	0.020±0.002
r	0.991

a. The sample solutions were irradiated by RPR-300nm lamps for 26 min to cause 3-6% conversion of 1-NpOH.

b. τ_o = 7.7 ns (see Table 2-4)

APPENDIX III

Table III-1 Φ_N in Photolysis of 2-NpOH (0.030 M) with NND in Acetonitrile at 31°C[a].

$[NND]x10^3$ (M)	1/[NND] (1/M)	Φ_N	$1/\Phi_N$
10.0	100	0.0308	32.4
12.5	80.0	0.0354	28.2
15.0	66.7	0.0377	26.5
17.5	57.1	0.0419	23.9
20.0	50.0	0.0423	23.6

$k_q\tau_o$ (M^{-1})	79±10
Φ_N(lim)	0.071±0.005
$k_b/(k_p+k_{p'})$	13.2
r	0.993

a. The sample solutions were irradiated by RPR-300nm lamps for 70 min to cause 3-8% conversion of 2-NpOH.

Table III-2 Φ_N in Photolysis of 2-Allyl-1-naphthol (0.030 M) with NND in Acetonitrile at 31°C[a]

$[NND]x10^3$ (M)	1/[NND] (1/M)	Φ_N	$1/\Phi_N$
7.5	133	0.112	8.96
10.0	100	0.141	7.12
12.5	80.0	0.157	6.39
15.0	66.7	0.171	5.87
17.5	57.1	0.198	5.04

$k_q\tau_o$ (M^{-1})	59±9
Φ_N(lim)	0.35±0.04
$k_b/(k_p+k_{p'})$	1.9
r	0.994

a. The sample solutions were irradiated by RPR-300nm lamps for 18 min to cause 19-28% conversion of 2-allyl-1-naphthol.

Table III-3 Φ_N in Photolysis of 1-AnOH (0.030 M) with NND in Dioxane at 31°C[a]

$[NND]x10^3$ (M)	1/[NND] (1/M)	Φ_N	$1/\Phi_N$
7.5	133	0.0382	26.2
10.0	100	0.0453	22.2
12.5	80.0	0.0533	18.8
15.0	66.7	0.0634	15.8
17.5	57.1	0.0711	14.1

$k_q\tau_o$ (M^{-1})	34±8
Φ_N(lim)	0.19±0.04
$k_b/(k_p+k_{p'})$	4.4
r	0.993

a. The sample solutions were irradiated by RPR-300nm lamps for 20 min to cause 5-12% conversion of 1-AnOH.

Table III-4 Φ_N in Photolysis of 9-AnOH (0.030 M) with NND in Dioxane at 31°C[a]

$[NND]x10^3$ (M)	1/[NND] (1/M)	Φ_N	$1/\Phi_N$
7.8	128	0.0865	11.6
10.4	96.2	0.104	9.60
13.0	76.9	0.116	8.59
15.6	64.1	0.127	7.86
18.2	54.9	0.138	7.30
20.8	48.1	0.137	7.30

$k_q\tau_o$ (M^{-1})	79±8
Φ_N(lim)	0.23±0.01
$k_b/(k_p+k_{p'})$	3.4
r	0.996

a. The sample solutions were irradiated by RPR-300nm lamps for 21 min to cause 5-15% conversion of 9-AnOH.

Table III-5 Φ_N in Photolysis of 9-Phenanthrol (0.030 M) with NND in Dioxane at 31°C[a]

$[NND]x10^3$ (M)	1/[NND] (1/M)	Φ_N	$1/\Phi_N$
7.62	131	0.0395	25.3
10.2	98.4	0.0498	20.1
12.7	78.7	0.0589	17.0
15.2	65.6	0.0623	16.0
17.8	56.2	0.0741	13.5
20.3	49.3	0.0752	13.3

$k_q\tau_o$ (M^{-1})	38±6
Φ_N(lim)	0.18±0.02
$k_b/(k_p+k_{p'})$	4.7
r	0.996

a. The sample solutions were irradiated by RPR-300nm lamps for 20 min to cause 8-15% conversion of 9-phenanthrol.